PERFORMANCE AND DESIGN OPTIMIZATION OF STONE COLUMN IN SABKHA SOILS

BY

HASSAN ALI MOHAMAD ABAS

A Dissertation Presented to the

DEANSHIP OF GRADUATE STUDIES

KING FAHD UNIVERSITY OF PETROLEUM & MINERALS

DHAHRAN, SAUDI ARABIA

In Partial Fulfillment of the

Requirements for the Degree of

DOCTOR OF PHILOSOPHY

In

CIVIL ENGINEERING

MAY, 2015

KING FAHD UNIVERSITY OF PETROLEUM & MINERALS

DHAHRAN- 31261, SAUDI ARABIA

DEANSHIP OF GRADUATE STUDIES

This thesis, written by **HASSAN ALI MOHAMAD ABSA** under the direction his thesis advisor and approved by his thesis committee, has been presented and accepted by the Dean of Graduate Studies, in partial fulfillment of the requirements for the degree of **DOCTOR OF PHILOSOPHY IN CIVIL ENGINEERING.**

Prof. Saad A. Aiban
(Advisor)

Dr. Salah U. Al-Dulaijan
Department Chairman

Prof. Sahel N. Abduljauwad
(Member)

Prof. Salam A. Zummo
Dean of Graduate Studies

Prof. Omar S. Baghabra Al-Amoudi
(Member)

23/10/15
Date

Prof. Husain J. Al-Gahtani
(Member)

Dr. Abdullatif A.Al-Shuhail
(Member)

Dedication

This thesis is dedicated to my mother and wife for their love, patience, support and understanding have lightened up my spirit to finish this study and this thesis.

ACKNOWLEDGMENTS

All praise be to ALLAH the Most Beneficent, the Most Compassionate, and prayers and peace be upon his Messenger Mohammed.

In the name of God, the most compassionate and the most merciful. I would like to express my deep appreciation and gratitude to all the people who have advised, helped and supported me during the time I worked on this thesis.

I would like to take this opportunity to express my sincere appreciation and deep gratitude to my supervisor, Prof. Saad A. Aiban, who devoted so much time and effort to this research project. I am extremely grateful for all his support, supply of field data, encouragement and advice throughout my studies. I have learned a lot from him and have benefited greatly from his encouragement and guidance.

Thanks and appreciation are extended to all of the other committee members of this dissertation, Prof. Sahel N. Abduljauwad, Prof. Omar S. Baghabra Al-Amoudi, Prof. Husain J. Al-Gahtani and Dr. Abdullatif A. Al-Shuhail for their constructive guidance and support during this work.

I wish also to express my thanks and sincere gratitude to KFUPM for giving me the opportunity and support to finish do my PhD work and finish this research.

Finally, my last and most important acknowledgement goes to my parents and wife. I'm forever indebted to you for the never-ending support provided to me and all the sacrifices made.

TABLE OF CONTENTS

LIST OF TABLES

LIST OF FIGURES

LIST OF ABBREVIATIONS

C_c	:	Compression Index
C_s	:	Swelling Index
OCR	:	Over Consolidation Ratio
e_o	:	Initial Void Ratio
CU	:	Consolidated-Undrained Triaxial Tests
CD	:	Consolidated-Drained Triaxial Tests
c'	:	Effective Cohesion
ϕ'	:	Effective Angle of Internal Friction
q_{ult}	:	Ultimate Bearing Capacity
γ	:	The Unit Weight of Clay
Z	:	The Total Depth of the Limit of Bulge of Stone Column
K_p	:	The Coefficient of Passive Earth Pressure
q	:	Surcharge Load per Unit Area
E_c	:	Young's Modulus of the Clay
μ_c	:	Poisson's Ratio of the Clay
u	:	Pore Water Pressure
σ_{ru}	:	Radial Effective in-Situ Stress
σ_v'	:	Vertical Effective Stress

σ'_R	:	Lateral Effective Stress
c_u	:	Undrained Shear Strength of Cohesive Soil
n_o	:	Settlement Improvement Ratio
A_c	:	Stone Column Area
A	:	Unit Cell Area
K_{ac}	:	Coefficient of Active Earth Pressure for Column Material
ϕ_c	:	Friction Angle of Column Material
H_i	:	Thickness of i^{th} Layer
δ_{ri}	:	Radial Strain of i^{th} Layer
d_c	:	Diameter of the Column
F_1	:	Vertical Load Transferred to the Stone Column
F_{tot}	:	Total Vertical Load on the Area a,b
S_v	:	Vertical Settlement of the Composite Clay- Stone Column Structure
$S_{v,o}$	:	Vertical Settlement of the Original (Unimproved) Soil
E	:	Odometer Modulus of the Soft Soil
H	:	vertical Height of Stone Column Treated Ground over Which Settlements are Being Calculated

σ_0	:	Initial Vertical Effective Stress in the clay layer
σ_c	:	Change in Stress in the Clay Layer due to the Externally Applied Loading
D_e	:	Equivalent Effective Diameter of Stone Column
S	:	Spacing of Individual Stone Columns
FEM	:	Finite Element Method
SPT	:	Standard Penetration Test
CPT	:	Cone Penetration Test
Q_R	:	Tip Resistance Ratio
I_d	:	Improvement Factor
A_{after}	:	Area Under Pre- Cone Tip Resistance Profile
A_{before}	:	Area Under Post- Cone Tip Resistance Profile
D_r %	:	Relative Density
γ_i	:	Unit Weight of Individual Soil Layers
p_w	:	Initial Pore Pressures at the Stress Point
k_h	:	Horizontal Permeability Coefficient of Soil before Installation of Stone Columns

k_s : Horizontal Permeability of Soil in Smear Zones

R_{IF} : Settlement Reduction Factor

$S_{untreated}$: Settlement of Untreated Soil

$S_{treated}$: Settlement of Treated Soil with Stone Columns

F_{SL} : Settlement Reduction Factor due to Applied Pressure on Area with 0.35 (Base Case) Replacement Ratios.

$F_{Area\ Ratio}$: Effect of Variation Area Ratio between Stone Column and Surrounding Soil According to Unit Cell Idealization

F_{CPT} : Effect of Variation of CPT Value for Top Cohesionless Layer.

ABSTRACT

Full Name : Hassan Ali Mohamad Abas

Thesis Title : PERFORMANCE AND DESIGN OPTIMIZATION OF STONE COLUMN IN SABKHA SOILS

Major Field : Civil Engineering (Geotechnical Engineering)

Date of Degree : May, 2015

The use of stone columns, as one of the effective method to improve Sabkha soils, has increased in construction practice to fulfill the industry demand for transmitting larger loads through foundations. However, the ability to predict settlement of foundations resting on stone columns in Sabkha soils has not been thoroughly studied. The main objective of this work is to study all parameters, which are believed to govern/affect the performance of stone columns in Sabkha soil through field observations and numerical simulation. In addition, the study addresses the generation of design charts and procedures for stone columns in Sabkha soils and validation of these design procedures with field data.

In this research, well-documented field data of projects in Eastern Saudi Arabia that utilized stone columns for improvement of Sabkha, was studied in detail. Different methods were applied to assess the improvement of the soil layers (including Sabkha) upon the installation of stone columns. In addition, a new approach was developed and validated to predict the design parameters of cohesionless and Sabkha soils after installation of stone columns. Finite element modeling was used to investigate preferable methods for simulating the installation effects of the stone columns. The ability of these numerical models to accurately capture the performance of stone columns was validated/ verified by simulating field load tests on single and group of stone columns for three

different case studies. These studies have different stone column patterns, sabkha thickness and column spacing. In addition, the validated models were used as a powerful tool to examine the influence of different parameters on the short and long-term performance of stone columns in Sabkha.

A new simplified design method for stone columns in sabkha soils that accounts for area replacement ratio, elastic modulus of column material and soil layering has been proposed based on a series of parametric studies. The results obtained from this simplified method are producing good correlation with field data for sabkha soils. Such proposed method can be used to design stone columns in sabkha in an optimum and accurate manner.

ملخص الرسالة

الاسم الكامل: حسن علي محمد عباس

عنوان الرسالة: الاداء وتصميم الامثل للأعمدة الحصوية في التربة السبخية

التخصص: الهندسة المدنية – هندسة جيوتقنية

تاريخ الدرجة العلمية: مايو – 2015

استخدام الاعمدة الحصوية كواحدة من الطرق الفعالة لتحسين التربة السبخية في ازدياد مستمر وذلك لما توفره هذه الطريقة من القدرة على تقوية التربة و تحويل الاحمال العالية من المنشآت الصناعية عبر الاساسات، الا ان القدرة على توقع الهبوط في الاساسات المرتكزة على الاعمدة الحصوية في التربة السبخية لم تدرس بدقة. الهدف الاساسي من هذا البحث هو دراسة كل العوامل التي يعتقد انها تؤثر على اداء الاعمدة الحصوية في التربة السبخية وذلك من خلال الملاحظات الحقلية والمحاكاة العددية. بالإضافة الي ذلك، تم اقتراح طريقة ومخططات لتصميم الاعمدة الحصوية في التربة السبخية والتحقق منها بمقارنتها مع معلومات حقلية موثقة جيدا اختيرت من مشاريع التشييد من المنطقة الشرقية في المملكة العربية السعودية تم استخدام الاعمدة الحصوية في هذه المشاريع لتحسين التربة السبخية.

وقد تمت دراسة طرق مختلفة لتقيم التحسن في طبقات التربة بما في ذلك التربة السبخية الناتج من إنشاء الاعمدة الحصوية. علاوة على ذلك تم تطوير والتحقق من مقاربة جديدة تستخدم لتوقع خواص التربة الرملية والسبخية بعد إنشاء الاعمدة الحصوية. وتم استخدام طريقة العناصر المحددة لاختبار الطريقة الافضل لمحاكاة أثر تثبيت الاعمدة الحصوية على التربة المحيطة، وتمت مقارنة النتائج مع المعلومات الحقلية من ثلاثة مشاريع مختلفة وذلك للتأكد من دقة النموذج في محاكاة اداء الاعمدة الحصوية. بالإضافة الي ذلك، فان النموذج المقترح تم استخدامه لدراسة تأثير العوامل المختلفة التي تؤثر على اداء الاعمدة الحصوية على المدى القصير والمدى البعيد.

تم اقتراح طريقة جديدة لتصميم الاعمدة الحصوية في التربة السبخية اعتماداً على دراسة عميقة للعوامل المؤثرة حيث تعتمد هذه الطريقة على نسبة مساحة الابدال وخواص طبقات التربة المحيطة. النتائج المستخلصة من هذه الطريقة اظهرت توافقاً جيداً مع المعلومات الحقلية، لذلك يمكن الاعتماد على هذه الطريقة لتصميم الاعمدة الحصوية في التربة السبخية بصورة مثلى ودقيقة.

CHAPTER 1

INTRODUCTION

1.1 General

The construction of infrastructures such as residential buildings, industrial structures, railways, roads, tanks, earthen embankments, etc., on sabkha soils usually involves challenges due to stability issues and excessive settlement. The sabkha soils are known for their variability, low strength, and high compressibility. One of best alternative methods to solve or reduce the risks encountered when dealing with sabkha as a foundation material is through ground improvement using stone columns. Other ground improvement methods could be used for sabkha including densification, chemical treatments, deep mixing, preloading, and sand columns.

Stone columns referred to by other names such as granular columns or granular piles are useful for increasing the bearing capacity, reducing settlement of foundation soils, and reducing the risk of liquefaction in seismic areas (Balaam and Booker, 1981; Barksdale and Bachus, 1983; Goughnour and Bayuk, 1979; Greenwood, 1900; Mitchell and Huber, 1985). Additionally, consolidation rate in weak and less permeable soils will increase significantly due to high porosity of stone column material (Andreou et al., 2008; Balaam, 1978; Balaam and Booker, 1981; Barksdale and Bachus, 1983; Baumann and Bauer, 1974; Elshazly et al., 2008; Huang et al., 2009).

The effectiveness of stone columns technique, when used to improve/reinforce the weak ground, depends upon two main principles. The first principle is installation of stiffer material to a desired depth and the second one is the densification of the surrounding natural soil due to installation and consolidation process occurring in the soil before applying final construction load.

Many design and analysis approaches have been proposed for stone columns for its practical use, but most of them are based on simplification or heuristic rules and devolved in case of stone columns surrounded by soft clay. However, the field behavior of the stone columns in multi-layered soil condition is difficult to predict. Moreover, the analytical solutions for stone columns improved soils dealt only with a homogeneous soft clay condition. In reality, the site may be multi-layered and highly variable. In order to better understand the performance of improved soil, the numerical simulation shall account for the deformation behavior during installation and after load application.

In the present study, field data was utilized to study the performance of stone columns in Sabkha soils. A comprehensive three-dimensional finite element model is used to study all main parameters affecting both the mechanisms of load transfer from stone columns to Sabkha and the settlement performance.

Well-documented field results have been used to verify the settlement and bearing capacity values obtained from the finite element models. Design charts to estimate settlement improvement factors for stone columns reinforced sabkha are presented as a result of this parametric study.

1.2 History and Concept

Stone column installation was first utilized in 1830 by French military engineers (Barksdale and Bachus, 1983). About hundred years later, this technique was further developed by employing vibration (Baumann and Bauer, 1974). The development of depth vibrator technique began in 1937 when Keller, a German company, started its first Vibro compaction project to densify loose sand 7.5m thick. To overcome the limitation of the Vibro compaction, which is used only in cohesionless soils, continuous development and modification of equipment lead to use stone columns to reinforce the cohesive soil; this technique is called Vibro replacement or Vibro displacement. The essential equipment for the Vibro technique is a vibrator driven by electric power and high-pressure water jetting at the nozzle of the tube. Extension tubes are added as necessary for reaching the final depth and the whole assembly is suspended by a crane.

There are two beneficial effects resulting from the presence of stone columns in weak soil. First, the granular material of the stone column is stiffer and has higher frictional strength than the weak parent soil, therefore the columns act as piles to increase the bearing capacity of foundation soil. Second, the granular material has a high permeability compared to weak cohesive soils, thus the columns act as vertical drains and accelerate the rate of consolidation process of the surrounding soil (Babu et al., 2013; Castro and Sagaseta, 2009; Deb, 2008; Indraratna et al., 2012).

1.3 Significance of This Research

Structures constructed on Sabkha soil experience many problems including excessive settlements and low load carrying capacity. One of the best remedial measures for

overcoming these problems is by improving the soil with the insertion of stone or sand columns.

Many investigations have been conducted to study the behavior, bearing capacity and settlement of single and group stone columns in soft clays. However, there is no research dealing with the study the behavior of stone columns in Sabkha soils taking into consideration special properties of this problematic soil type. Certainly more research in the form of full-scale field load testing and numerical modeling is needed to develop proper understanding and knowledge about the performance of stone columns in Sabkha soils.

1.4 Objective of the Study

The objectives of this study are:

(1) To study and evaluate the design methods of stone column in sabkha soils, since all these methods were developed, generally, for soft clays.

(2) To study the performance of single and a group of stone columns in sabkha layer using finite element models and compare it with analytical results and field data.

(3) To study all parameters, which are, believed to govern/effect the performance of stone columns in sabkha soil using finite element models.

(4) To study the effect of stone column installation processes on the design and behavior of stone column in sabkha layers through filed observations and numerical simulation.

(5) Generation of design procedures for stone columns in sabkha soils taking into account the settlement of the improved ground and validating these design procedures with field data.

1.5 Methodology

Two case studies selected from the Eastern Saudi Arabia, are taken for detailed investigation of the performance behavior of ground improved with stone columns. Each study includes description of the project, the subsurface conditions, regional geology, the stone columns installations, soil characteristics, description of constructional phases and full-scale field tests on stone columns.

Different methods are used to assess the improvement of the soil layers (including Sabkha) upon installation of stone columns. Based on the Pre and Post Cone Penetration Test (CPT) contacted in improvement area, the improvement factor for cohesionless layer above sabkha soil is proposed in this study to estimate the improvement occurring in this layer due to installation of stone columns. In addition, new approach to predict the parameter of cohesionless and sabkha soils, that are affected by installation of stone columns, are developed and validated as they are important for stone columns modeling.

The characteristics of sabkha and other soils, after installation of stone columns, were used to develop series of three-dimensional finite element model for the plate load test on stone columns reinforced sabkha soils. The computations are carried out using geotechnical finite element software PLAXIS 3D -2013.The objectives of this modeling exercise are to find out the best method to simulate the installation effect of the stone columns and to examine the influence of different parameters on the short-term

performance characteristics. The ability of these numerical models to accurately capture the performance of stone columns is validated/verified by simulating field load tests on single and group stone columns at two different locations taking into account different stone column patterns, sabkha thickness and column properties. Once the modeling is validated using field data, the effect of other parameters such as the effect of stone columns and material properties are investigated.

Finite element analyses of consolidation have been conducted to assess the performance of stone columns in sabkha soils. The numerical results will be compared with the field data. The main features of stone columns, such as the reduction of surface settlement, the quick dissipation of excess pore pressures, and the stress concentration were studied.

Finally, new simplified design method of stone columns that accounts for area replacement ratio, stone column material properties and soil layers characteristics is proposed in this study based on a series of parametric studies. The results obtained from the simplified method are compared with field results. Figure 1-1 shows layout of the dissertation work.

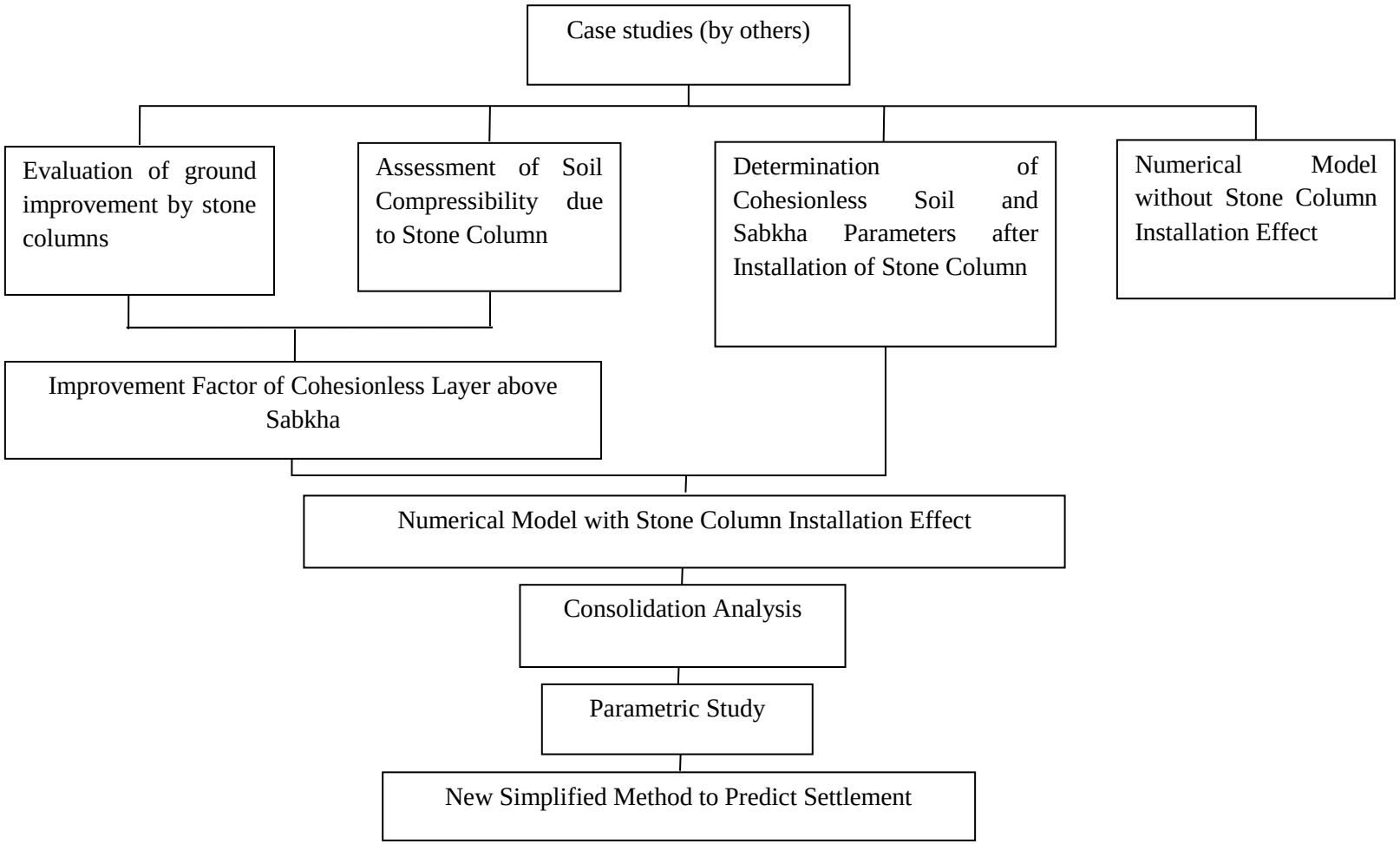

Figure 1-1: Summary of Research Program.

1.6 Scope of Study

This study is confined to the following scopes:

- The construction of stone columns has been carried out based on top feed Vibro replacement method (wet method).
- The data is collected from the eastern region of Saudi Arabia.
- The study focuses only on the performance of the end bearing stone columns resting on dense sand layer.
- A new simplified design method of stone columns is proposed in this study which depends on area replacement ratio, stone column material properties and soil layers characteristics.

1.7 Organization of Thesis

The skeleton of the dissertation is divided into eight chapters:

In the first Chapter, the reasons for the research and background details have been presented. The problem is identified and the proposed solution is outlined. Study objectives and tasks have also been delineated with the scope of this thesis.

Chapter two reviews previous studies on sabkha soil and stone columns. Geotechnical properties of sabkha soil and foundation problems caused by this type of problematic soil are discussed. Studies on stone columns installation and prediction of carrying capacity are also presented.

Chapter three describes the case studies adopted for this research. Each case history includes a description of the project, the subsurface conditions, regional geology, the

stone columns installations, soil characteristics, description of constructional phases and full-scale field tests on stone columns.

Chapter four discusses different methods which are used to assess the improvement of the soil layers (including sabkha) upon installation of stone columns. New approach is developed to predict the geotechnical parameter of cohesionless and sabkha soils after the installation of stone columns.

Chapter five describes the numerical models for the plate load test on stone columns reinforced sabkha soils. The method is used to simulate the installation effect of the stone column. New methods are suggested to simulate the installation effect.

Chapter six describes finite element analysis of consolidation conducted to assess the performance of stone columns in sabkha soils. The numerical results are compared with the field data. The main features of stone columns, such as the reduction of surface settlement, the quick dissipation of excess pore pressures, and the stress concentration are studied.

Chapter seven describes a new “proposed” simplified design method, based on a series of parametric studies of stone columns that account for area replacement ratio, stone column material properties and soil layers characteristics. The results obtained from the simplified method are compared with field results.

Chapter eight presents findings and conclusions of this study and provides recommendations for further studies.

CHAPTER 2

LITERATURE REVIEW

2.1 Sabkha

The expression sabkha is originally an Arabic name, that has been use to describe saline flats that are underlain by sand, silt or clay, and often encrusted with salt (Al-Amoudi, 1994) .Sabkha soils are widely distributed throughout Saudi Arabia, especially along the coastal areas. Typical problems encountered in foundations and structures built over Sabkha beds include excessive settlement, cracking, formation of huge potholes and rutting.

The geotechnical properties of sabkha soil show that it possesses a collapsible behavior (Aiban et al., 1998, 1995; Al-Amoudi et al., 1995). The upper surface exhibits cohesive characteristics in some seasons which will change into weak surface when inundated with water and it is impossible to construct on it (Akili, 1981). The literature reveals that there is a strong potential for sabkha soils to create a chemically aggressive environment and lead to a structurally unstable soil condition (Al-Amoudi, 1994). The main geotechnical problems in sabkha could be ascribed to one or more of the following:

- The susceptibility of sabkha soil to flooding due to low elevation and the difficulty of excavation below the water table and associated dewatering problems (Al-Amoudi, 1992; Al-Amoudi et al., 1995).

- Variation of compressibility characteristics of sabkha sediments, particularly in the uncemented layers could lead to excessive differential settlement. Sabkha deposits could vary from a very loose state to a dense state. The extreme variation in layer thickness contributes to the settlement problems. As a sequence, sabkha possesses a high collapse potential mainly as a result of dissolution of sodium chloride due to absorption of water. Collapse may also occur due to leaching of calcium ions and soil grain adjustment due to loading (Abduljauwad and Al-Amoudi, 1995).
- Problem due to low strength of the sabkha layers in their natural state. Strength will significantly decrease in the sabkha layer due to absorption of water from the humid environments (Patterson and Kinsman, 1981; Siddiqi, 2000).
- Problem of steel reinforcement corrosion due to high concentrations of chloride and sulfate salts in sabkha brine (Akili, 1981; Al-Amoudi, 1995; Robinson, 1995).

2.2 Types of Sabkha Soils

There are two main types of sabkha, namely, coastal sabkha and continental sabkha. Both types of sabkha are usually formed in hot and arid climates, and are associated with shallow groundwater tables.

2.2.1 Coastal Sabkha

Coastal sabkha is typically bordered on the seaward side by a semi-restricted lagoon and on the landward side by a desert or rock outcroppings. It is usually stark, salt–encrusted and virtually flat, except for possible scatted storm tide channels and small isolated sand dunes(Patterson and Kinsman, 1981; Sanford and Wood, 2001). Figure 2-1 shows a

generalized cross-section across a typical coastal sabkha, the figure denotes the characteristics of coastal sabkhas (Al-Amoudi, 1992): (i) the presence of a barrier from both the seaward and landward directions; (ii) a rather flat profile; and (iii) a shallowness of groundwater tables.

Since the major spectrum of sedimentation in seaward is carbonate, the main constituents of coastal sabkha are aragonite and calcite; and by virtue of their proximity to the coasts, the carbonate content decreases as the sabkha grades landward (Butler, 1969; Evamy, 1973; McKenzie, 1981; Patterson and Kinsman, 1982).

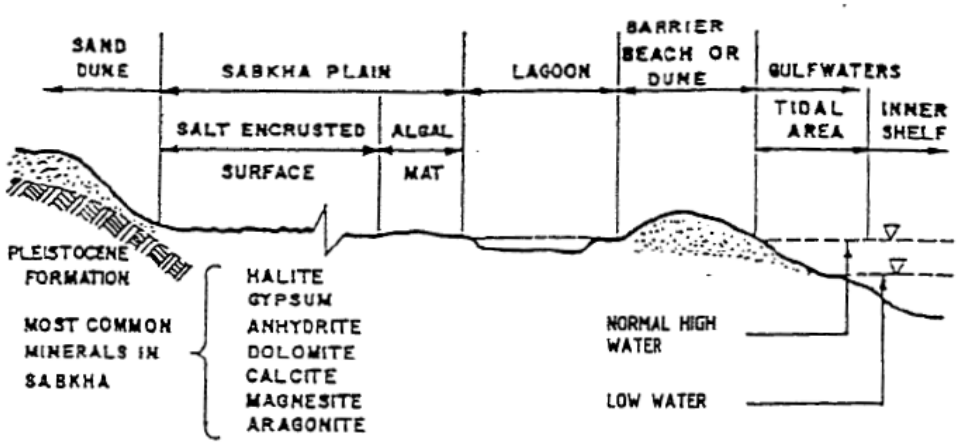

Figure 2-1: Generalized Cross Section across Coastal Sabkha with Typical Surface Features (Al-Amoudi, 1992).

2.2.2 Continental Sabkha

Continental or inland sabkha is developed without marine sedimentological association. These sabkhas are originally much older than coastal Sabkhas (Juillie and Sherwood, 1983). The rate of evaporation in inland sabkha is hypothetically higher than that of coastal ones due to more arid conditions. Consequently, the ground water table plays a far

more influential role in the development of such types of sabkha which are usually less-developed in extent and predominantly tectonically and/or topographically controlled (Al-Amoudi, 1992). The sediments of these sabkhas consist predominantly of gypsum, quartz and calcite, with halite always existing at the crust (Al-Amoudi, 1992; Al-Amoudi et al., 1995; Al-Guwaizani, 1994).

2.3 Distribution of Sabkha in Saudi Arabia

Saudi Arabia has a large area of sabkha Soils, both coastal and inland. A summary of these sabkhas in the coastal plains of the eastern province, mainly based on reconnaissance visits, has been reported by Johnson (1978). Along the western shores of Saudi Arabia, coastal sabkha also exists in Obhor, Al-lith and Yanbu; in the southwestern Saudi Arabia, near the city of Jizan. In the north, continental sabkhas are reported to exist in Wadi AsSirhan. A schematic diagram shows the distribution of sabkhas in Saudi Arabia in Figure 2-2.

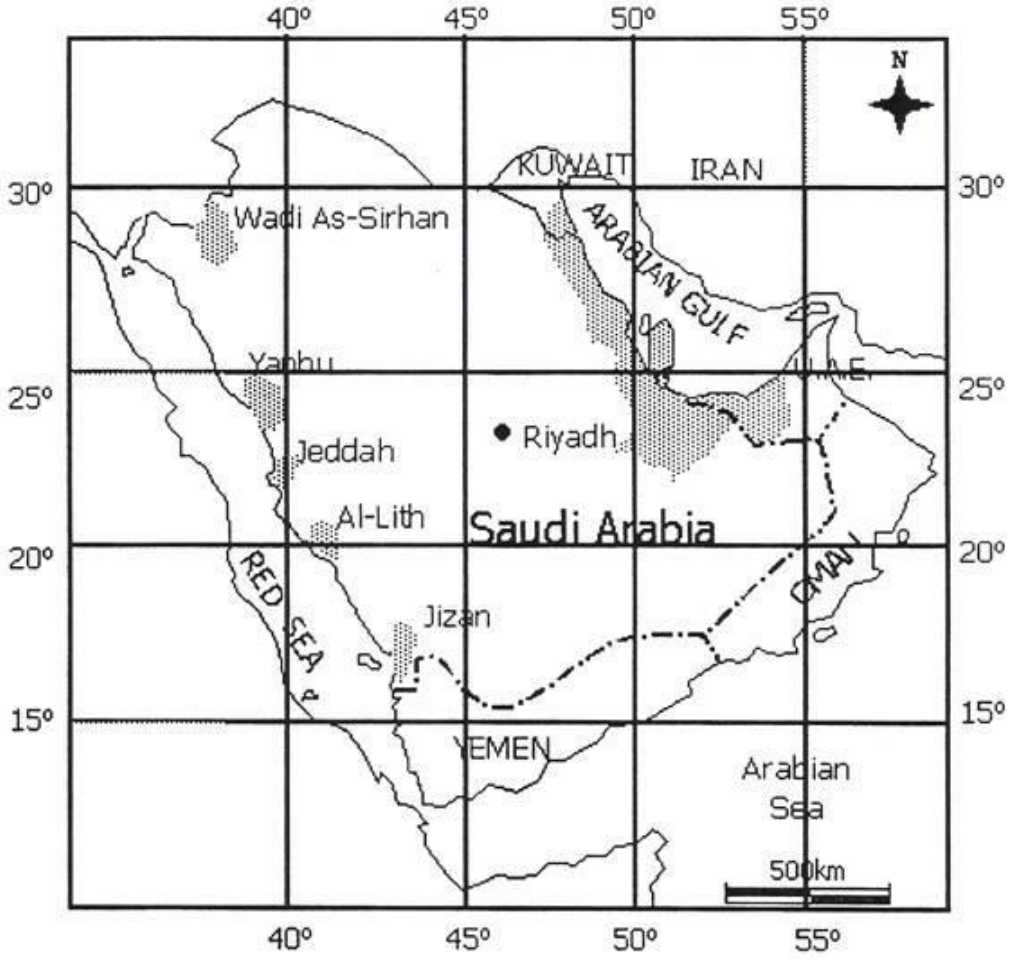

Figure 2-2: Distribution of Sabkhas in the Arabian Peninsula (Al-Amoudi, 1992).

Sabkha distribution along the southern and southwestern shores of the Arabian Gulf is well documented. Figure 2-3 gives a typical presentation of the prevalence of sabkha along the Arabian Gulf. The presence of sabkhas in Saudi Arabia and in the other Arabian Gulf States is shown to be quite extensive, especially in the well-populated cities along the Arabian Gulf and Red Sea coasts(Al-Amoudi, 1992; Al-Mousa, 2011).

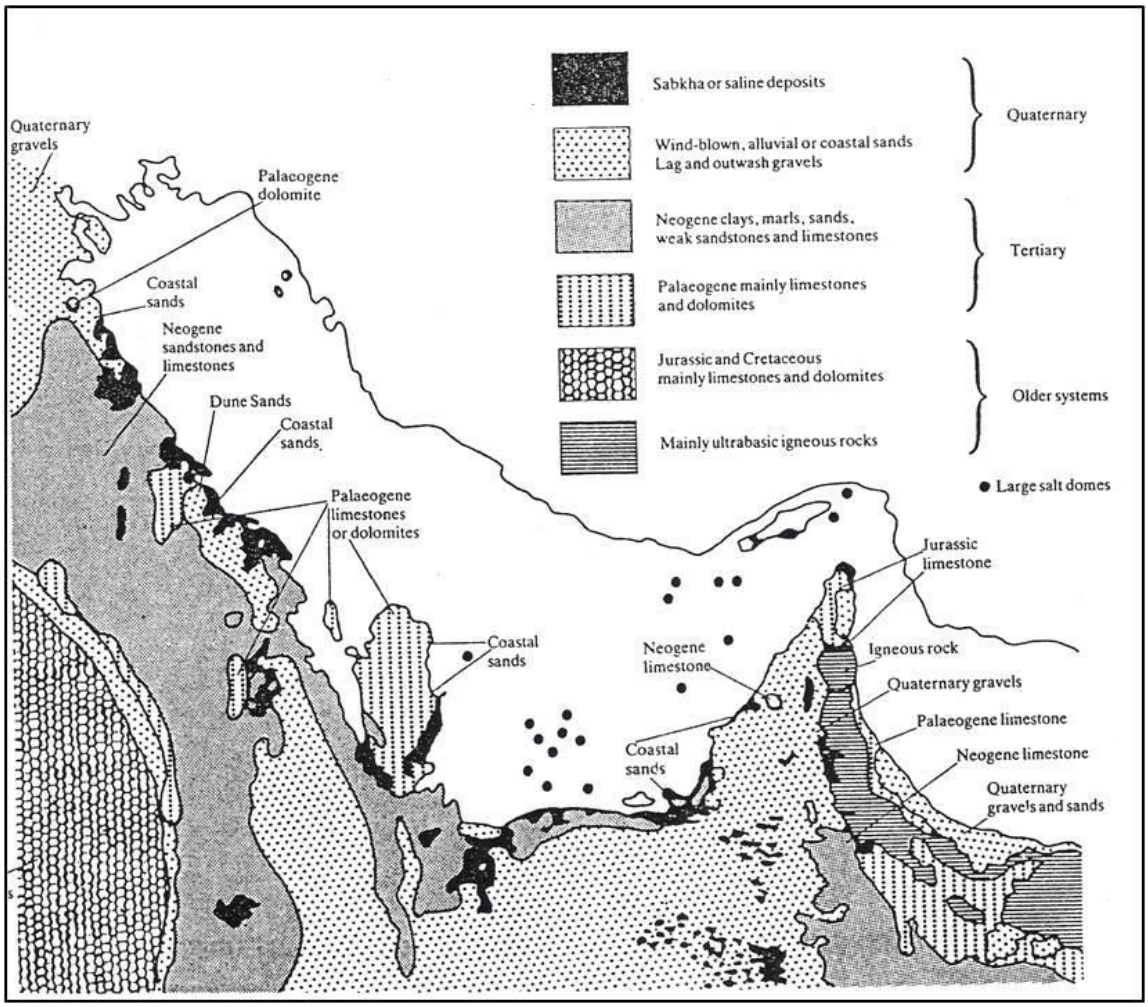

Figure 2-3: Geological Formations of Eastern Saudi Arabia and Gulf Countries (Al-Amoudi, 1992).

2.4 Geotechnical Properties of sabkha

This section is focused on the geotechnical properties of sabkha. It presents a summary of findings from several studies on sabkha soils.

Water content

Usually sabkha soil contains high levels of moisture, which is known as sabkha brine. Water content was found to be about 25% for sabkha soil in Arabian Gulf (Al-Amoudi, 1992; Al-Amoudi et al., 1995; Ismael, 1993).

Permeability

Al-Amoudi et al. (1992) evaluated the sabkha permeability considering both distilled water and sabkha brine. When using sabkha brine, the sabkha's permeability coefficient varied between $1.78x10^{-6}$ m/s and $1.35x10^{-6}$ m/s. On the other hand, the distilled water resulted in a permeability coefficient between $2.1x10^{-5}$ m/s and $3.15x10^{-5}$ m/s. Because distilled water dissolves salt in sabkha, the permeability coefficient was increased.

Compressibility

Sabkha experiences significant reduction in its void ratio when subjected to flooding and leaching. However, the conventional oedometer is unable to predict the behavior of sabkha because it is not capable of leaching the specimens. To address this issue, Al-Amoudi and Abduljauwad (1994) modified the conventional oedometer by boring two holes below the porous stone from which percolating water could be collected. Abduljauwad and Al-Amoudi (1995) tested compressibility of sabkha by using the modified oedometer; the samples were soaked and leached using both distilled water and sabkha brine. The sabkha experienced significant reduction of void ratio for both distilled water and sabkha brine, with the reduction being greater for leaching with distilled water. However, the compression (C_c) and swelling (C_s) indices remain the same in both the soaking and leaching of distilled water and sabkha brine. Table 2-1 shows the results for

soaking and leaching with both distilled water and sabkha brine. The average Over Consolidation Ratios (OCR) for sabkha is 19 and 20 for distilled water and sabkha brine, respectively (Al-Amoudi, 1992). The OCR is high which might be due to the cementations materials in the sabkha soil.

Table 2-1: Oedometer Results for Soaked and Leached Using Distilled Water and sabkha Brine (Al-Amoudi, 1992).

The characteristics	Distilled Water	Sabkha Brine
Initial void ratio (e_o)	0.93	0.94
Final void ratio	0.526	0.635
Compression index (C_c)	0.18	0.18
Swelling index (C_s)	0.016	0.016

Sabkha's Shear Strength

Sabkha, in general, has low shear strength, especially if it is exposed to water. In some cases, the foundation might collapse if the water reaches the sabkha level. However, sabkha's strength varies in both vertical and horizontal directions. Al-Amoudi and Abduljauwad (1995) assessed the shear strength of sabkhas taken from the eastern province of Saudi Arabia and conducted a number of tests to study the shear strength of sabkha. Twenty-four undisturbed samples were subjected to direct shear, unconfined compression, consolidated-undrained (CU) and consolidated-drained (CD) triaxial tests. Three moisture conditions were considered for the samples: the natural moisture condition of samples, saturated with sabkha brine or saturated with distilled water. The direct shear tests were performed according to ASTM D 3080 at a loading rate of 0.75

mm/min using 109, 218, 435 kPa as the normal stress levels. Five series of triaxial tests were conducted on sabkha specimens according to ASTM D 2850 at a loading rate of 0.5 mm/min. The first series of specimens were tested under consolidated drained (CD) conditions with their natural moisture content. The second series of specimens were tested under consolidated drained (CD) conditions after being fully saturated with distilled water. For the third series, the samples were fully saturated with distilled water and then tested under consolidated undrained (CU) conditions. For the series No.4 and No.5, the samples were tested in a similar manner to series No.2 and No.3, but the samples were tested after being fully saturated with sabkha brine instead of distilled water. The direct shear test results estimated the cohesion (C') to be 50 kPa and the angle of internal friction, (ϕ') as 36˚.

The triaxial shear strength results were divided to three groups. The first group comprises samples tested under consolidated drained (CD) conditions with natural moisture content. For this group, the cohesion (C') was 14 kPa and the angle of internal friction (ϕ') was 34.5˚. The results for the second group where the samples were fully saturated with distilled water for three days are as follows. For consolidated drained (CD) samples, the cohesion (C') was 10 kPa and the angle of internal friction (ϕ') was 27˚. However, for consolidated undrained (CU) conditions, the cohesion (C') and the angle of internal friction are 0˚ and 34˚, respectively.

The third group comprised of samples fully saturated with sabkha brine and the results were as follows. For consolidated drained (CD) samples, the cohesion (C') was 0 kPa and the angle of internal friction (ϕ') was 34˚ and for consolidated undrained (CU) samples were 16˚ and 33˚, respectively.

2.5 Foundation Problem in Sabkha Soils

Sabkha soils are extremely hostile to foundation. This is mainly due to their high natural moisture content, the close proximity of their groundwater tables to the surface, the generally loose nature of their profile, their susceptibility to settlement and/or swellings and their highly corrosive salts, amongst other factors (Aiban et al., 1998). Foundation problem in sabkha soils are summarized below.

Periodic Change in Moisture Content

The periodic changes in the moisture content of sabkhas, particularly in the capillary zones, will certainly lead to large changes in consistency, density and strength, as well as significant effect on the volume change characteristics of the soil (Abduljauwad and Al-Amoudi, 1995; Al-Amoudi, 1992; Yechieli and Wood, 2002). Such changes may result in periodic swelling and shrinkage in the soil that can cause serious damage to foundation.

Compressibility Variation

Excessive differential settlement can take place in structure built on top of sabkha soil by virtue of the inhomogeneity of its profile, the looseness of certain layers within the profile and the highly variable compressibility of its various components.

The physical composition of sabkhas can vary in classification from sand to clay within the same site (Aiban et al., 1998). Sand layers in the sabkha soil, with their high void ratios and intercalating clay and or salt lenses or pockets, can cause severe differential settlement, thereby leading to serious cracks and tilting in construction on such soils.

Shallow Ground Water

The groundwater table usually lies within a short distance of about 1 m from the sabkha surface, and fluctuates in its level, although infrequent in the short term. These rises in groundwater levels will certainly have serious geotechnical consequences on foundations built on sabkha deposits. Many study reported impacts associated with the rising subsurface water tables; these impacts are summarized as follows:

i. Development of uplift pressure, which must be resisted by the weight of the structure;
ii. Reduction in effective stresses as a consequence of increased pore-water pressure, which results in the reduction in the shear strength (Aiban et al., 1998), and
iii. Increase in lateral pressure on basement walls owing to increased hydrostatic pressures.

Presence of highly corrosive salts

The restoration of the capillary rise after excavation and refilling brings with it the additional soluble salts to the new foundations. The high concentrations of chloride and sulfate salts in sabkha brine are known to be highly corrosive and damaging to both concrete and steel reinforcement (Al-Amoudi, 1992).

2.6 Stone Columns Installation

Stone columns are extensively used to improve the bearing capacity of soft soils. The methods generally used for the stone column installation are Vibro-compaction and Vibro-replacement method. The Vibro-compaction method is commonly utilized to

improve cohesionless soils while the Vibro-replacement method is used to improve cohesive and cohesionless soils (Barksdale and Bachus, 1983). A sieve analysis chart shown in Figure 2-4 is a guide to the range of cohesionless and cohesive soils which can be improved by these two methods (Baumann and Bauer, 1974).

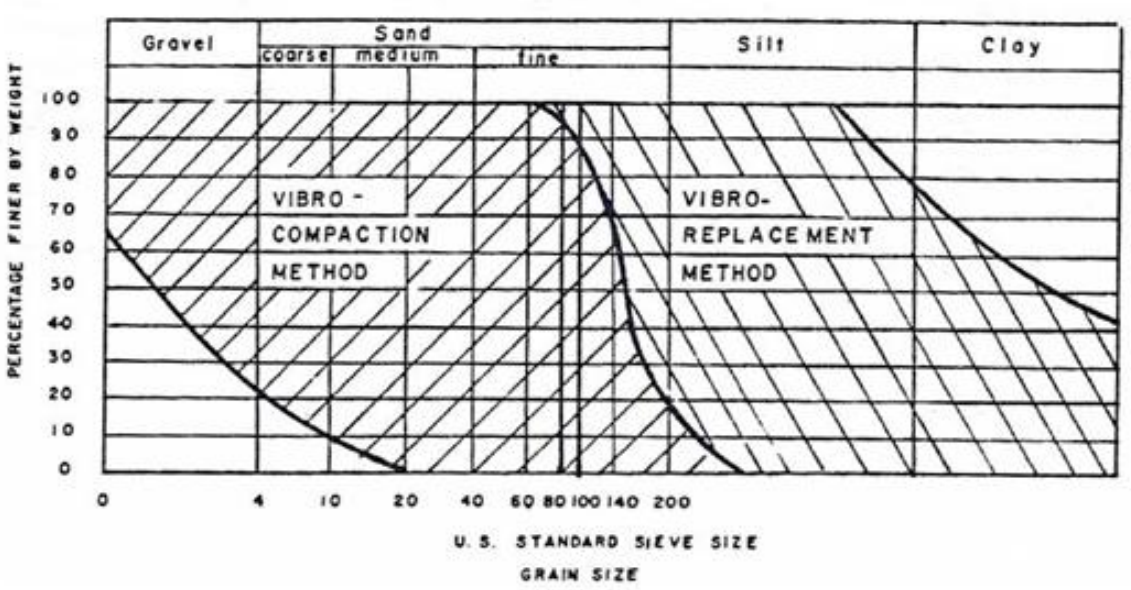

Figure 2-4: Range of Soils Suitable for Vibro-Compaction or Vibro-Replacement (Baumann and Bauer, 1974)

It is obvious that the installation of stone columns has a very significant effect on the treated ground. Two major effects that can be distinguished during the installation of Vibro-stone columns are the lateral expansion due to the inclusion of the stone column body and the ground vibration due to the vibrator (F. Kirsch, 2006). The radial effect of column installation is related to the nature of the material, to the level of compaction (workmanship) and to the technique (dry or wet) employed.

Machine characteristics play a role in the performance of a densification system. The important parameters are size, frequency, amplitude and eccentric force. It has been

found that each of these is unique to a certain soil and therefore a field trial is required to find the optimum values to achieve maximum densification (Massarsch, 1985). Various techniques of constructing stone columns are briefly described below.

2.6.1 Vibro Compaction Method

This technique is generally applied to the cohesionless soil deposit, granular soils above or below the ground water table using a vibroflot (Baumann and Bauer, 1974). The construction process, as shown in Figure 2-5, consists of forming a cavity in the ground using vibrator until the required depth is reached. After reaching the predetermined depth, the lower jets are turned off and the side jets are turned on.

The vibroflot is then gradually withdrawn from the ground and vibration is simultaneously applied at the tip to increase density of the granular backfill, which is being introduced concurrently. After the vibroflot is fully withdrawn, a well-compacted granular column is formed. The backfill material used for this technique is typically sand (Brown and Glenn, 1976; Brown, 1977).

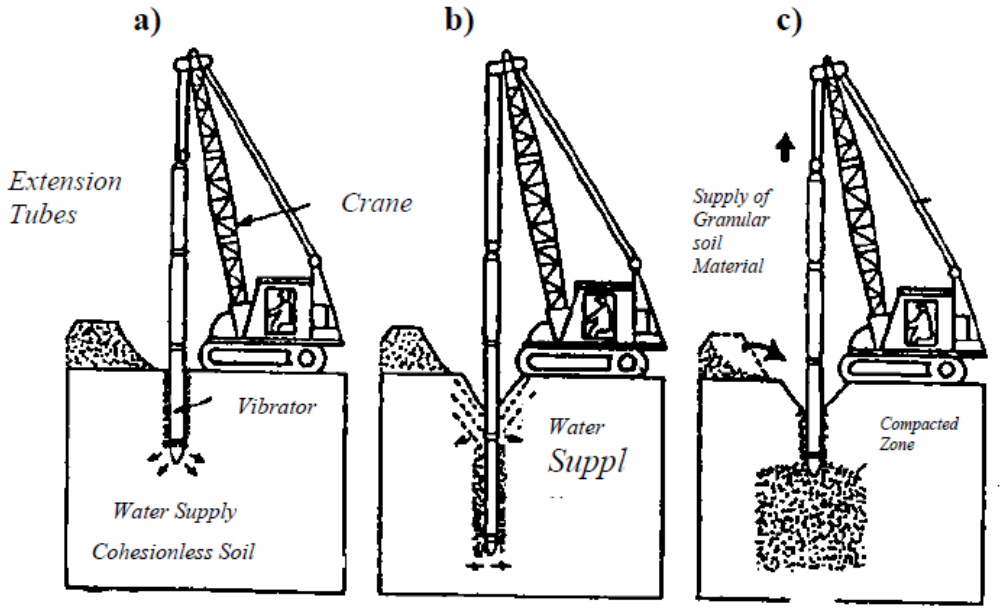

Figure 2-5: The Vibro-Compaction Method Process (Baumann and Bauer, 1974).

2.6.2 Vibro Replacement Technique

This is a deep vibratory method to improve a wide range of weak soils. In the Vibro-replacement process, vibrator displaces soil radially and flushes out the weak soil to form a cylindrical compacted zone (McCabe et al., 2007; Priebe, 1991; Raju, 1997). The Vibro-replacement stone columns are generally arranged in square and triangular grid pattern at spacing of 1.5 m to 4.0 m depending on the nature of the ground, the densification required, the equipment specification and the construction technique employed (Bell, 2004). The diameter of stone column using wet method is generally greater than dry method due to the soil extraction caused by water jetting.

Raju, 1997, reported that the wet process are having higher production rate compared to the dry method and the ability to treat grounds to depths of about 30 meters. The dry process requires no water supply and thus no disposal problem arises, and therefore it is

particularly suited for congested working areas. The wet process allows using stones grain size range from 35 mm to 75 mm, while the dry process uses a range between 15 mm to 35 mm (Castro and Karstunen, 2010; Guetif et al., 2007; Fabian Kirsch, 2006; Mitchell and Huber, 1985; Raju, 1997).

Wet process

In this method, a hole is formed in the ground by water jetting a top-feed Vibroflot down to the desired depth by vibration and high pressure water jets to avoid the remodeling of soil around the hole. Figure 2-6 shows cross-sections of typical top-feed vibrators. The vibrator's diameter ranges from 300 to 450 mm with a length about 2 to 3.5 m. Total weight ranges between 2 to 4 metric tons. Power development varies from 35 to 100 kW.

To form a stone column using wet method, the vibrator with its extension tubes is placed over the desired location by means of a crane. After starting the motor and high pressure water jet, the soil in the immediate vicinity of the vibrator, gets saturated with water causing local and temporary liquefaction under the influence of the vibrations. The oscillating vibrator with its extension tubes penetrates the soil under its own weight. When the required treatment depth is reached, the water supply is reduced in such a way that the annular space around the vibrator and its extension tubes, remain opened by hydrostatic over pressure. The coarse-grained fill material is now dropped around the vibrator which sinks to the bottom of the hole.

The constant water flow ensures that the stone fill reaches the toe of the vibrator and that the fine soil particles are continuously flushed out from the probe point by moving the vibrator slowly up and down and by the vibration of the machine itself, the supplied stone

material is pressed into the existing soil. This process is repeated in steps of about 0.5 to 1 m up to the ground level, leaving on completion a densely compacted column of stones and granular soil. The compaction by Vibro-float also enhances the density of the surrounding soil with the exception of cohesive layers, which do not respond to vibration. Hence, for a treated area, stone columns and the in-situ soil from an integrated system having low compressibility and high shear strength, the wet process is generally suited for unstable hole and a high ground water table (Paskkaran, 2004) .The wet method is the top-feed method and it can treat weak soils to depths of 30 m (Raju, 1997). The installation process of the wet method is shown in Figure 2-7.

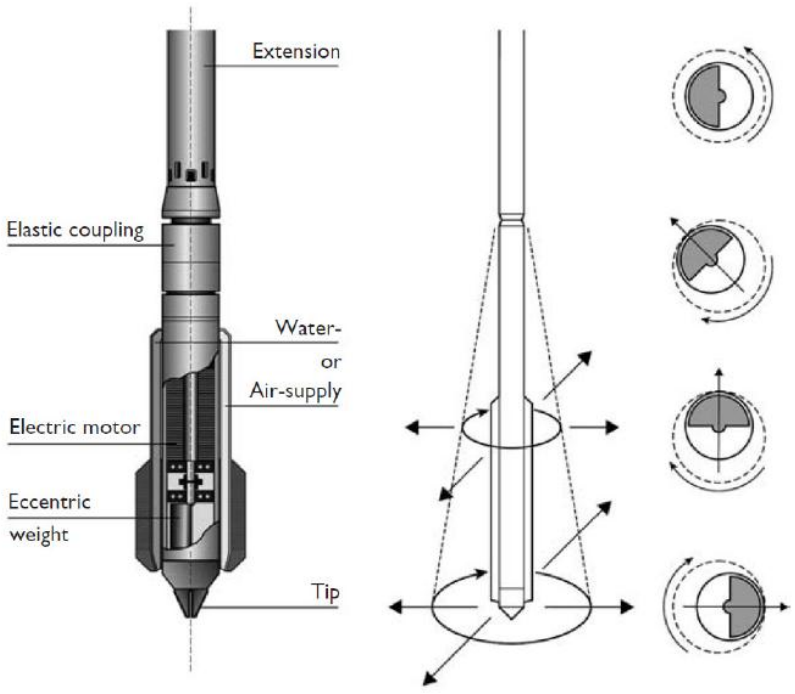

Figure 2-6: Vibrator and Principle of Vibro Compaction (Moseley and Kirsch, 2004).

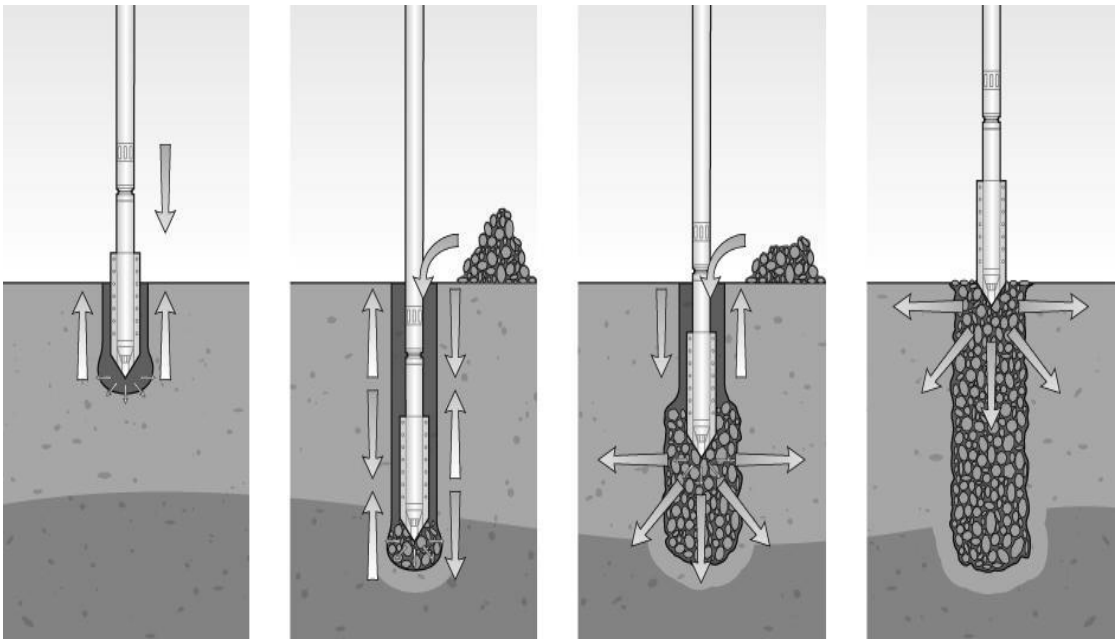

Figure 2-7 : Installation Process by the Wet Method.

Dry Process

In this method, the borehole must be able to stand opened upon extraction of the vibroflot, which requires the soil under treatment to have an undrained shear strength of more than 40 kPa and a relatively shallow ground water table depth (Paskkaran, 2004). Vibrator near the bottom of the vibroflot provides the densification. The main difference between the dry and wet process is the absence of jetting water during the initial formation of the hole in the dry process. The illustration of dry method of stone column installation is shown in Figure 2-8. In the dry method, stone feeding is done from bottom to top through the vibrator. This method has been successfully used to treat soft grounds to a depth of 20 m (Raju et al., 1997).Figure 2-9 shows cross-sections of bottom feed vibrators. Feeding tube is included in the vibrator for bottom feed and to support the sidewalls as it is left in the hole during construction. Rounded and uniform aggregate

with a maximum diameter of 38 mm to prevent clogging within the probe, is suitable for dry bottom feed method (Bachus and Barksdale, 1989).

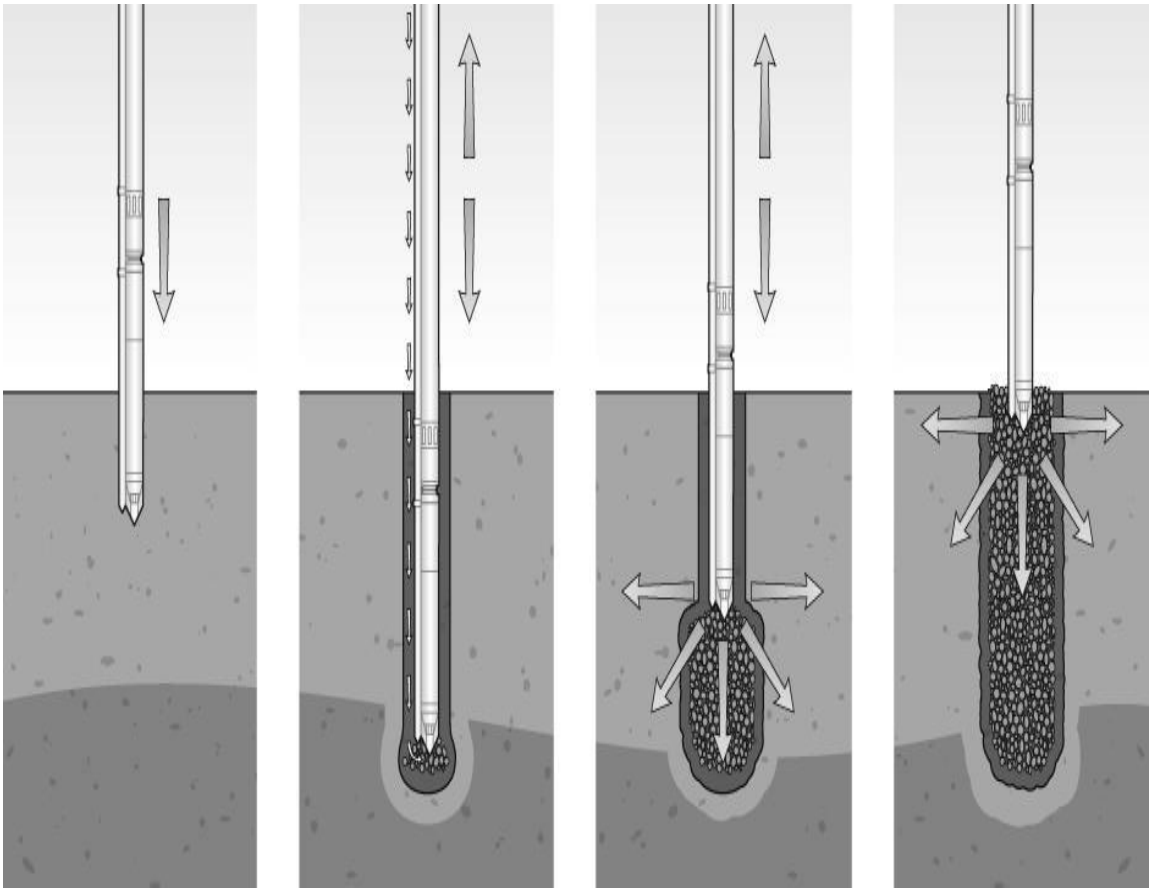

Figure 2-8: Stone Column Installation Process by the Dry Method.

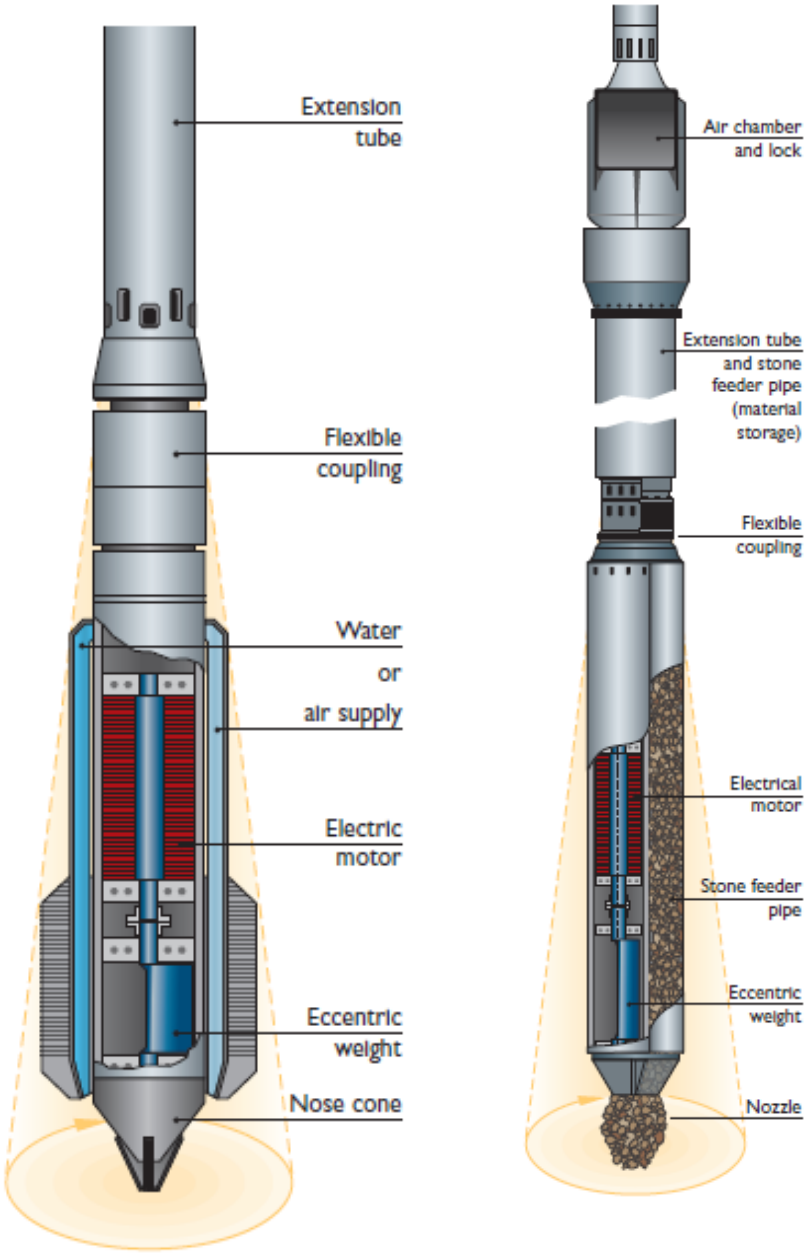

(a) (b)

Figure 2-9: Types of Vibrater Prop (a) Top and (b) Bottom Feed Vibrator.

Cased-Borehole Method

Depends on the ground to be improved; rammed stone columns are constructed by either driving an open or closed end pipe in the ground or boring a hole. The presence of casing prevents the collapse of the borehole.

In this method, a casing pipe is used to advance the hole and keep it stable, until required depth is reached, then sand or stone are constructed by ramming granular materials in increments using a heavy falling weight of usually 15 to 20 kN as illustrated in Figure 2-10 (Datye and Nagaraju, 1975; Barksdale and Bachus, 1983). The height of fall, usually 1-1.5m, is chosen considering the soil strength and project requirements. The disturbance and subsequent remolding by the ramming operation may limit its applicability to sensitive soils (Babu et al., 2013; Madhav, 2004).

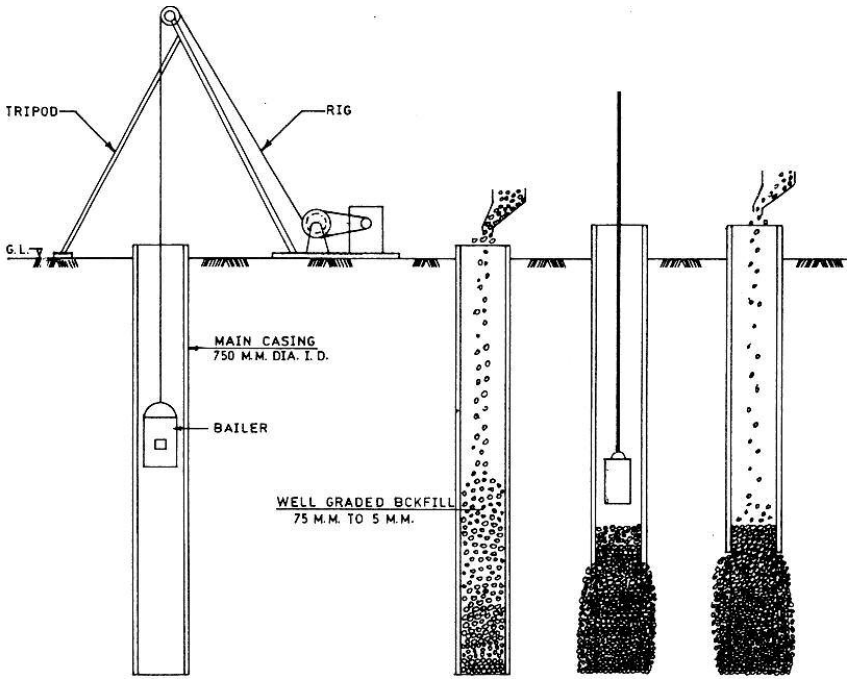

Figure 2-10: Installation of Cased Rammed Stone Column (Nayak, 1982).

2.7 Behavior of Stone Column

A proper understanding of the load transfer mechanisms in stone columns is necessary for analysis and design. The load bearing capacity of a single stone column is a complex soil-stone column interaction problem. The stone column acts as a reinforcing medium as well as drainage medium. The effectiveness of using a stone column to improve weak ground is measured by performance of the resulting composite ground, which is composed of the relatively weak soils and stronger column material. Both materials work together so that the loads are shared between the parent soils and column material (Ambily and Gandhi, 2007; Mitchell and Huber, 1985; Poorooshasb and Meyerhof, 1997; Six et al., 2012). The load bearing behavior of composite ground is thus affected by the behavior of both materials and their interactions.

Stone columns cannot be considered as completely rigid elements like pile. They are not capable of transferring high stresses to the deeper bearing stratum (Wood et al., 2000). Figure 2-11 illustrates the different mechanisms of stress transfer in pile and stone columns. The lateral stress mobilized in the stone columns will be resisted by lateral compressive strength of the soil. If the strength of the soils is less than the lateral stress in the column, then the column will fail by bulging. The passive pressure developed due to loading of treated ground offers resistance to the bulging of the stone column and thus contributes to its load carrying capacity (Greenwood, 1975). The lateral resistance of soil increases with depth for the same soil. This fact coupled with the application of the load from the top of the column means that bulging is most likely occurring in the upper part

of the column, although in the case of shorter columns bulging may be observed over the entire length of the column (Babu et al., 2013; McKelvey et al., 2004).

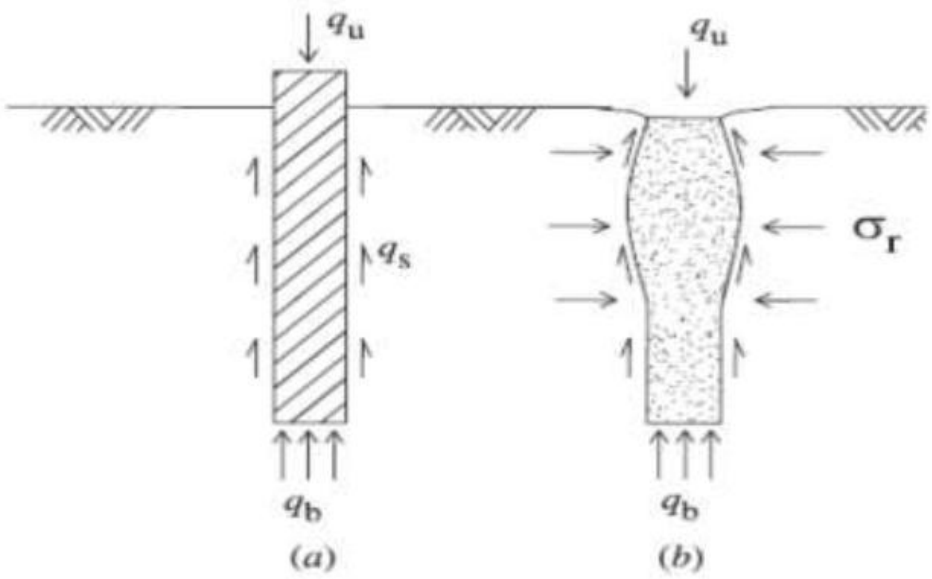

Figure 2-11 Stress Transfer for (a) a Pile and (b) a Stone Column (Hughes et al., 1975).

It is believed that depending on the column length, some degree of loading will be transmitted to the soil through end bearing and along the column interface (McCabe et al., 2007). At low length–to-diameter ratios, the short-floating stone columns may fail by punching into the underlying soft soil. The ultimate bearing capacity of a single stone column for punching failure can be determined by adding the end bearing capacity of the stone column, obtained from conventional bearing capacity theories, and the skin friction developed along the sides of the stone column (Barksdale and Bachus, 1983; Hughes et al., 1975). For longer columns, no load reaches the base of the column because friction, especially at the top parts, is enhanced and takes most of the load and thus minimal load is transferred to the base of the column (Black et al., 2007) and therefore punching will not occur.

In a cohesive soil, when stone columns are constructed, ground improvement is achived by inserting stiff material. In addition, the stone columns act as a drainage path, which would accelerate consolidation settlement (Hughes and Withers, 1974). In a cohesionless soil, when stone columns are constructed by Vibro-floatation, the ground is densified by the reduction in voids and the intrusion of gravel. Thus, the bearing capacity increases due to the addition of stiff material and densify surrounding soils (Barksdale and Bachus, 1983). The drainage and consolidation settlements are not important in such soil conditions.

2.8 Ultimate Carrying Capacity

A realistic assessment of the ultimate bearing capacity of the supporting soil is of paramount importance for safe and economic design of the foundation. The bearing capacity of stone columns depends, mainly, on configuration of columns (i.e. geometry or arrangement), stone column material properties, the characteristics of the soils surrounding the stone column, flexibility or rigidity characteristics of the structural foundation and the magnitude of lateral earth pressure developed in the surrounding soil mass (Greenwood, 1900; Vesic, 1972; Hughes and Withers, 1974; Aboshi et al., 1979; Barksdale and Bachus, 1983; Priebe, 1991; Malarvizhi and Ilamparuthi, 2004). No well-defined guidelines or codes are available to calculate the bearing capacity of the stone columns, therefore empirical equations have been used so far (Ambily and Gandhi, 2004).

The analytical methods for analysis of stone columns reinforced foundations, were mostly based on the consideration of a single stone column using unit cell concept

(Greenwood, 1975; Datye and Nagaraju, 1975; Balaam and Booker, 1981, 1981; Barksdale and Bachus, 1983; Priebe, 1995). To theoretically analyze such a complex problem, certain idealizations for the individual materials are essential.

For a single stone column in soft clay, the most probable failure mechanism is often bulging failure (Bergado et al., 1991). The lateral confining stress around the stone column is usually taken as the ultimate resistance provided by the surrounding soil, which is mobilized as the column bulges outward. Thus, most of the approaches in predicting the ultimate bearing of a single stone column have been developed based on the bulging failure mechanism. These include the passive pressure and the cavity expansion approaches. Empirical and analytical design methods to determine the ultimate bearing capacity of columns are presented in the next section.

2.8.1 Passive Pressure Approach

Greenwood (1970) has assumed, for preliminary analyses, that the lateral resistance from the surrounding soil can develop and is equal to the passive resistance mobilized behind a long retaining wall, which is laterally translated into the soil. Such an approach assumes a plane strain loading condition and hence does not realistically consider the three-dimensional geometry of a single column or group of columns. The lateral confining stress supporting the stone column is usually taken in these methods as the ultimate passive resistance, which the surrounding soil can mobilize as the stone column bulges outward against the soil. We should keep in mind that bulging is taking place at the top portion of the stone column.

In the passive pressure approach, the load from a strip footing Figure 2-12 (a) is assumed to be concentrated on the stone column, which is the stronger component of the composite foundation soil. The stone column expands laterally and exerts lateral stresses on the surrounding soils which are resisted by passive earth pressure. Greenwood (1970) proposed the following equation to estimate the ultimate bearing capacity of a stone column by considering the earth pressure theory.

$$\mathbf{q_{ult} = \gamma Z K_p + 2C_u\sqrt{K_p}} \quad (2\text{-}1)$$

Where:

$q_{ult:}$ The ultimate bearing capacity of stone column.

γ: The unit weight of clay.

Z: The total depth of the limit of bulge of stone column.

$K_{p\ :}$ The coefficient of passive earth pressure = $K_p = \frac{1+\sin\varphi_s}{1-\sin\varphi_s}$

ϕ: Angle of internal friction of the soft soil.

In the case of widespread load as shown in Figure 2-12 (b), the lateral passive restraint on the stone column away from the edge of loaded area is much larger owing to the equal all around pressure of surcharge loads. Hence, Greenwood (1970) proposed the following equation to estimate the ultimate bearing capacity of the stone column under the central areas of the wide foundation, which accounts for the development of passive pressure in the surrounding clay under loading.

$$q_{ult} = \gamma Z K_p + 2C_u\sqrt{K_p} + qK_p \quad (2\text{-}2)$$

Where:

q: Surcharge load per unit area.

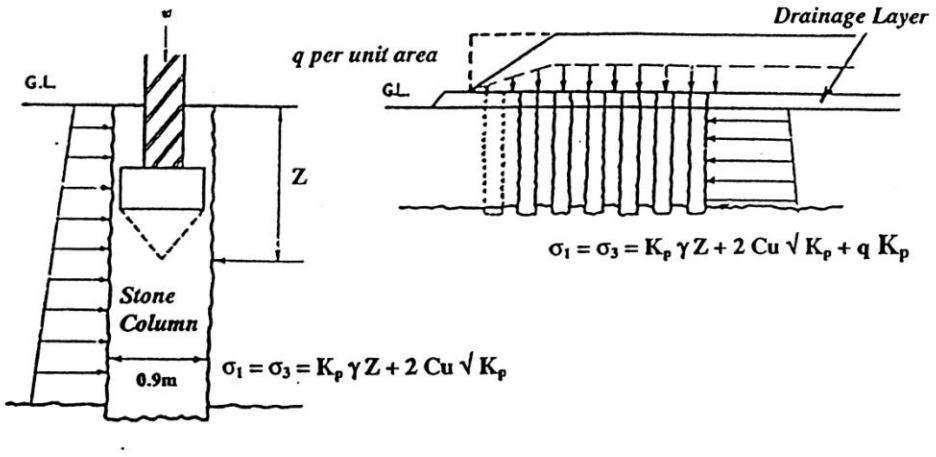

(a). Strip footing (b). Widespread loadings

Figure 2-12: Stone Columns under Strip Footing and Widespread Loadings (Greenwood, 1970).

2.8.2 Cavity Expansion Theory

The general cylindrical cavity expansion theory developed by Vesic (1972) includes both cohesive and cohesionless soils, and the behavior of the material is assumed to be elastic initially and then plastic once the stress reaches the plastic limit, as shown in Figure 2-13.

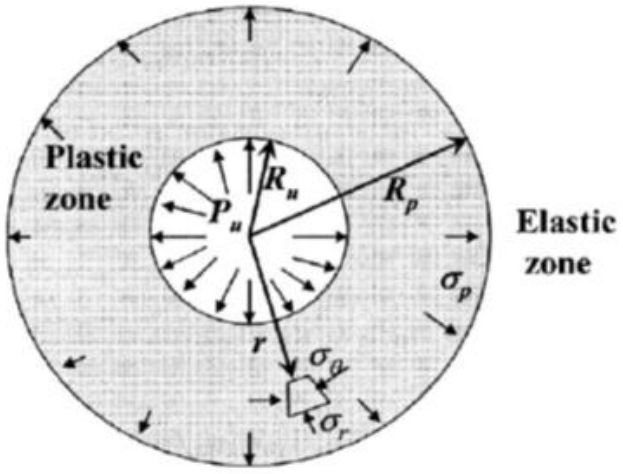

Figure 2-13: Expansion of Cylindrical Cavity (Vesic, 1972).

Hughes and Withers (1974) idealized bulging of the column like the expanding of a cylindrical gap in clay similar to the pressuremeter test. They used a model in soft normally consolidated clay and showed that bulging occurred in the columns up to depths 2 to 3 times the width of the column below the surface. In this model, 150 mm long sand columns were used with 12.5 mm to 38 mm diameters. This experimental study showed that forces acting on the column are transmitted to soil due to expanding and vertical movement of the column. It is observed that the column material pressurized the surrounding soil. Both field and laboratory investigations Figure 2-14 showed geometrically similar deformation results.

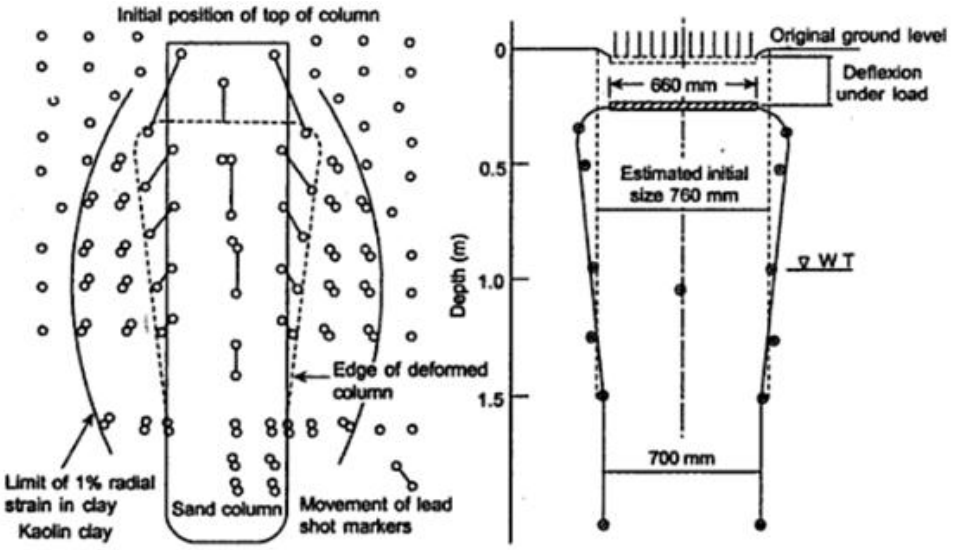

Figure 2-14: Deformation of Stone Column (Hughes and Withers, 1974).

Based on the laboratory and field test results for a single stone column, Hughes and Withers (1974) indicated that the ultimate strength of the column is governed by the maximum lateral resistance of the soil around the zone, which bulges. The shear forces associated between column and surrounding soil interface is neglected. Principal stresses are those, which act horizontally and vertically. This approach is used in developing the

method for analysis. The lateral expansion of the stone columns is idealized as a cylindrical expansion into the clay, by considering the failure condition, at which the soil deforms plastically due to expansion of the cavity. The limiting lateral pressure, σ_{rL} was found to be dependent on the total initial lateral stress, σ_{r0} and undrained shear strength C_u of soil and may be expressed as:

$$\boldsymbol{\sigma_{rL} = \sigma_{r0} + C_u \left[1 + \ln\left\{\frac{E_c}{2C_u(1+\mu_c)}\right\}\right]} \quad (2\text{-}3)$$

Where

E_c: Young's modulus of the clay.

μ_c: Poisson's ratio of the clay.

For simplicity, they further provided an approximated version of equation as:

$$\boldsymbol{\sigma_{rL} = \sigma_{ru} + 4C_u + u} \quad (2\text{-}4)$$

Where

u : Pore pressure.

σ_{ru}: Effective insitu lateral stress.

If soil in the bulged zone of the column has yielded, then:

$$\boldsymbol{\sigma'_v = \left[\frac{1+\sin\acute{\phi}}{1-\sin\acute{\phi}}\right] \sigma'_R} \quad (2\text{-}5)$$

Where

σ'_v: Vertical effective stress.

$\acute{\phi}$: Angle of internal friction.

σ'_R: Lateral effective stress.

Therefore, the ultimate vertical stress on a column can carry as it reaches its critical state (bulging laterally) can be obtained as:

$$\boldsymbol{\sigma_{ult} = \frac{1+\sin\acute{\phi}}{1-\sin\acute{\phi}}(\sigma_{ru} + 4C_u - u)} \quad (2\text{-}6)$$

In practice, columns are usually analyzed for drained conditions so that excess pore pressure u = 0, and the cohesion of a clay is not constant with depth and thus the choice of C_u for use in the equation is dependent on the location, i.e. depth.

Hansbo (1994) reported that E_c is in the range of $150C_u$ – $500C_u$ for soft clay. With this value of E_c and assuming undrained condition (μc =0.5), σrL would lie between $\sigma ru+5C_u$ and $\sigma ru +6C_u$. In practice it is often assumed that $\sigma_{rL} = \sigma_{ru} +5C_u$ (Hansbo, 1994). Hence, σ_{ult} can be obtained as:

$$\boldsymbol{\sigma_{ult} = K_p(\sigma_{ru} + 5C_u)} \quad (2\text{-}7)$$

2.8.3 Barksdale and Bachus Method

On the basis of the Vesic's cavity expansion theory, Barksdale and Bachus (1984) presented an even simpler equation for calculation of the ultimate bearing capacity of a single column in clay by introducing a bearing capacity factor $\overline{N}_c$.

$$\boldsymbol{q_{ult} = c_u \overline{N}_c} \quad (2\text{-}8)$$

Where

c_u: Undrained shear strength of the clay.

The value of $\overline{N}_c$, lie normally in the range of 10-22 depending on the compressibility of the clay(Barksdale and Bachus, 1983a). They recommended a value of $\overline{N}_c$, of 22 for soil having high initial stiffness such as non-organic soft to stiff clays and silts, and a value of

$\bar{N}_c$ is 18 for those soils having low stiffness such as organic soils and clays with plasticity index greater than 30. Datye et al. (1982) recommended using 25 to 30 for Vibro replacement columns, 45 to 50 for cased, rammed stone columns and 40 for uncased, rammed stone columns.

2.9 Settlement Theories

One of the most important design criteria for stone column is the settlement value and rate, particularly the primary consolidation settlement. Depending on the soil type, the consolidation settlement may take several months or years before the majority of the settlement is completed. By adopting Vibro stone columns, consolidation time is reduced and the indigenous soil consolidates quickly. As a result, the shear strength of the soil develops at a faster rate.

The methods used in settlement prediction range from empirical approximations to complicated analyses based on fundamental elastic and plastic soil mechanics theories. Most of these approaches for settlement analysis are based on the unit cell concept. A series of design methods, ranging from empirical to analytical, are presented in the next sections for the determination of the magnitude of stone column settlement.

2.9.1 Greenwood Method

Greenwood (1970) presented empirical curves as a function of stone column spacing and settlement reduction, for the estimation of consolidation settlements of clay reinforced by granular columns. The curves in Figure 2-15 are for a stone column having a diameter of 0.9 m, C_u = 40 kPa for the upper bound curve and a diameter of 1.07m for the C_u = 20 kPa lower bounds curve.

The shaded region represents the reductions in settlement expected when the wet process of construction is employed. The immediate settlement was neglected in this theory. In addition, the theory assumes that columns are resting on a firm stratum (end bearing).

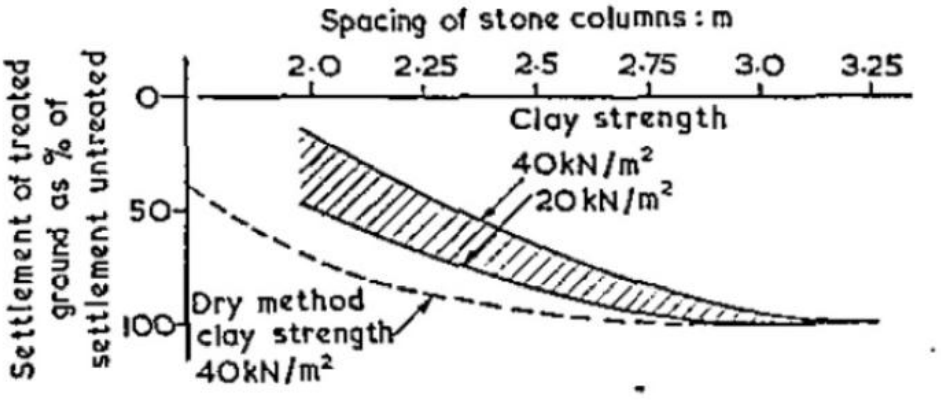

Figure 2-15: Settlement Diagram for Stone Columns in Uniform Soft Clay (Greenwood, 1970).

2.9.2 Priebe's Method

This method also uses the unit cell idealization model. The stone column is assumed to show plastic behavior while the soil within the unit cell is assumed to show elastic behavior (Priebe, 1995). The column material is assumed to be incompressible; as a result, vertical shortening of the stone column shows the change of volume within the soil, i.e. any settlement results in the bulging of the stone column. The radial deformation of the elastic soil is determined using the solution of infinitely long cylindrical cavity in an elastic medium in deforming cavity expansion. Further assumptions made in the analysis are:

- Equal settlement of stone column and soil.

- The state of stresses of the soft soil is assumed to be isotropic.
- Uniform stresses in the two materials.
- The stone column support onto a rigid layer (End Bearing).
- The bulk density of column and soil is neglected.

Taking into consideration of all above-mentioned assumptions and taking the coefficient of lateral earth pressure K=1, the results of the evaluation can be expressed as basic improvement factor n_o.

$$\boldsymbol{n_0 = 1 + \frac{A_c}{A}\left[\frac{5-\frac{A_c}{A}}{4K_{ac}\left(1-\frac{A_c}{A}\right)} - 1\right]} \tag{2-9}$$

$$\boldsymbol{K_{ac} = tan^2\left(45 - \frac{\varphi_c}{2}\right)} \tag{2-10}$$

Where

n_o : Settlement improvement ratio.

A_c : Stone column area.

A: Unit cell area.

K_{aC} : Coefficient of active earth pressure for column material.

ϕ_c: Friction angle of column material

The relationship between the improvement factor, n_o, the surrounding area ratio $\frac{A_c}{A}$ and the friction angle of the backfill material $\emptyset_c$is illustrated in Figure 2-16.

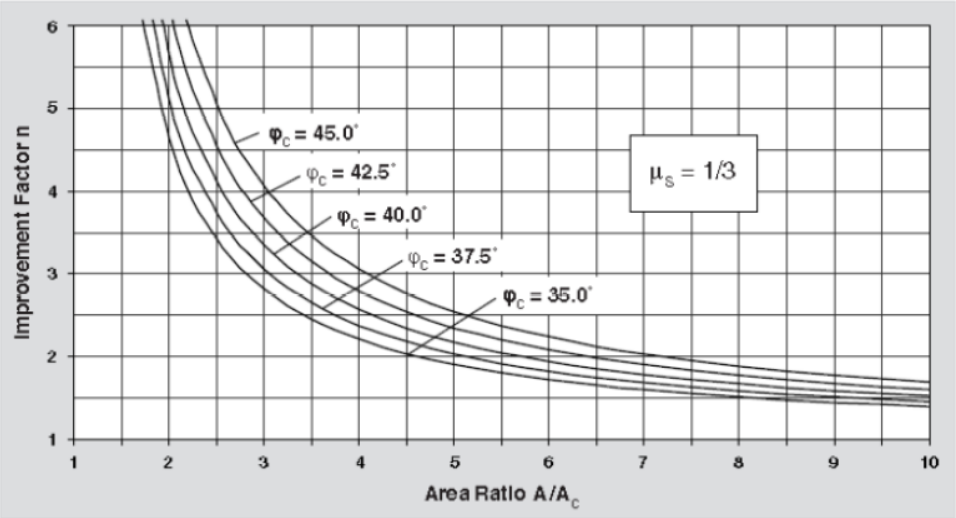

Figure 2-16: Design Chart for Vibro Replacement (Priebe, 1995).

Priebe, (1995) considered the compressibility of the backfill material and recommended the additional amount on the area ratio $\Delta(A/A_c)$ depending on the ratio of the constrained moduli D_c/D_s which can be readily taken from Figure 2-17, and the weight of the stone columns and of the soil has to be added to the external loads. While considering these additional loads (overburden), he defined the depth factor, f_d as illustrated Figure 2-18.

The improvement ratio no (corrected for consideration of the stone column compressibility) should be multiplied by fd. Due to the compressibility of the backfill material, the depth factor reaches a maximum value, which can be taken from the diagram given in Figure 2-19.

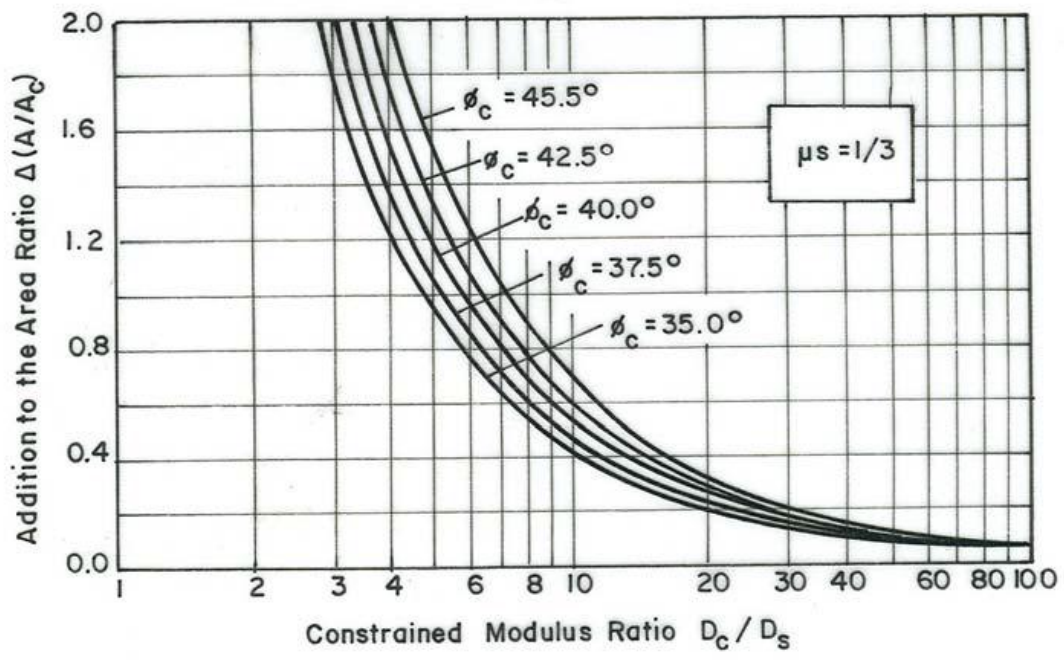

Figure 2-17: Consideration of Column Compressibility (Priebe, 1995).

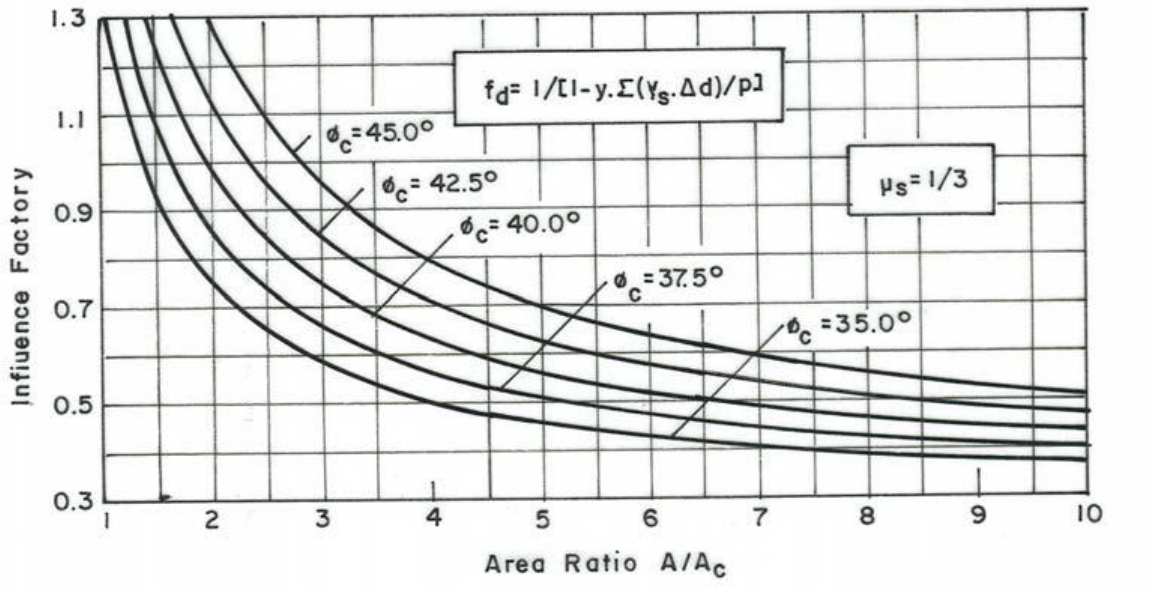

Figure 2-18: Determination of the Depth Factor (Priebe, 1995).

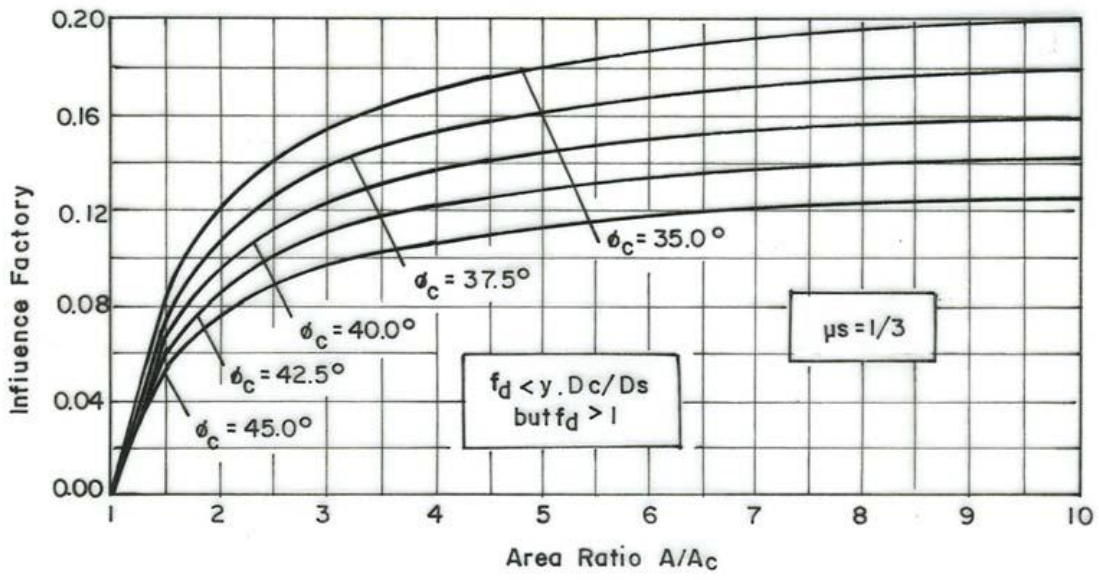

Figure 2-19: Limit Value of the Depth Factor (Priebe, 1995).

The basic system of Priebe's method discussed so far, assumes improvement by a large grid of stone columns. Accordingly, it provides the reduction in the settlement of large slab foundation. For small foundations, Priebe (1995) offers diagrams, given in Figure 2-20 (a) and (b), which allows a simple way to determine the settlement performance of isolated single footings and strip foundations from the performance of a large grid. The diagrams are valid for homogeneous conditions only.

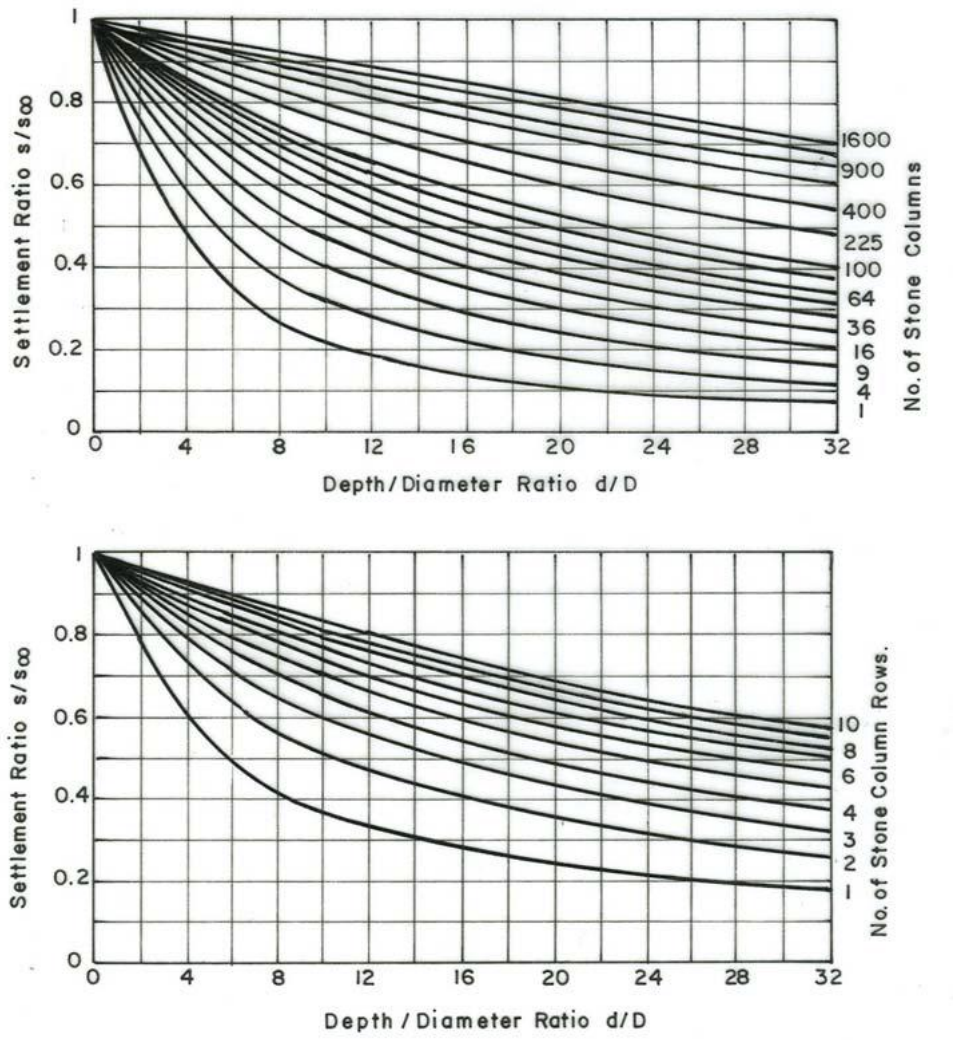

Figure 2-20: Settlement of Small Foundations (a) for Single Footings (b) for Strip Footings (Priebe, 1995).

The simplicity of Priebe's method of applying an improvement ratio to conventional consolidation calculation is attractive and makes it probably the most widely used. However, the limitation of this method is that it does not take into account the properties of the surrounding soft clay.

2.9.3 Incremental Method

Goughnour and Bayuk (1979) presented an elasto-plastic analysis of stone column, assuming that the stone column is linearly elastic initially until the completion of consolidation of the soft soil, perfectly plastic at failure and incompressible at the plastic state. The soft soil is assumed to exhibit nonlinear elastic behavior. The composite mass is considered to be elastic initially, becoming plastic as strain increases. The analysis assumes that a unit cell idealization is valid and it can be used to represent a large loaded area (Goughnour and Bayuk, 1979).

Incremental method offers a solution by dividing the unit cell into small horizontal increments, for which all variables are assumed to be constant, and the vertical strain with vertical and radial stresses, are calculated iteratively.

$$\mathbf{s} = \sum_{\mathbf{i=1}}^{\mathbf{m}} \mathbf{S_i} \tag{2-11}$$

$$\mathbf{S_i} = \mathbf{2H_i(2\delta_{ri}/d_c)} \tag{2-12}$$

Where

H_i: Thickness of i^{th} layer.

δ_{ri}: Radial strain of i^{th} layer.

d_c: Diameter of the column.

2.9.4 Granular Wall Method

Van Impe and De Beer (1983) presented a simple analytical method to estimate the reduction of settlements of soft soil reinforced by stone columns by considering deformations of the granular strip at constant volume and elastic deformation of columns

under limit of equilibrium conditions. The stone columns were replaced by stone walls with equivalent plan area in his analysis as shown in Figure 2-21.

The only parameters to be known are the geometry of the pattern of the stone columns, their diameter, the angle of shearing strength of the stone material, the oedometer modulus of the soft soil and its poisson's ratio (Van Impe, 1983). They also presented a diagram for estimating effective vertical stress in the stone material.

In order to express the improvement on the settlement behavior of the soft layer reinforced with the stone columns, the following parameters are defined:

$$\boldsymbol{m} = \frac{\boldsymbol{F_1}}{\boldsymbol{F_{tot}}} = \propto \left(\frac{\boldsymbol{\sigma'_{v,1}}}{\boldsymbol{P_0}}\right) \tag{2-13}$$

$$\boldsymbol{\beta} = \frac{\boldsymbol{S_v}}{\boldsymbol{S_{v,0}}} \tag{2-14}$$

Where

F_1: Vertical load transferred to the stone column.

F_{tot}: Total vertical load on the area a,b.

S_v: Vertical settlement of the composite clay-stone column structure.

$S_{v,o}$: Vertical settlement of the unimproved soil.

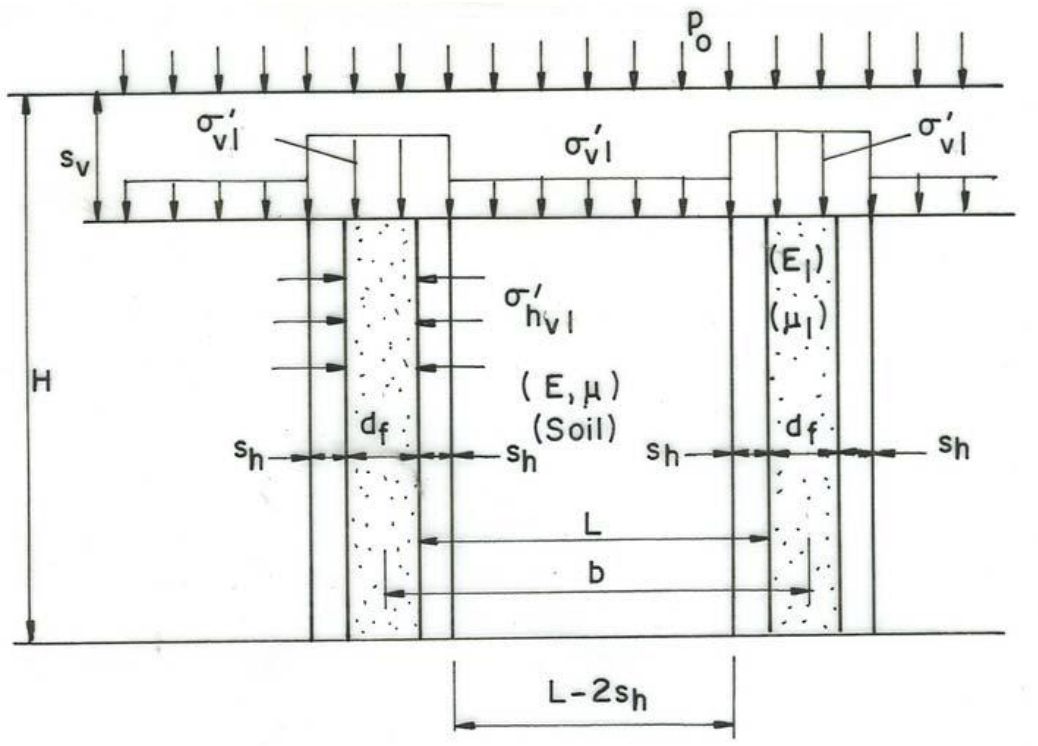

Figure 2-21: Definitions for Granular Wall Method (Van Impe, 1983).

In Figure 2-22, the relationship between m and α is given at different values of φ_1 and for chosen values of the parameters P_o/E and μ. In the Figure 2-23, the β (settlement improvement factor) values as a function of α are given for some combination of P_o/E and μ and for different φ_1 values.

The vertical settlement of the composite layer of soft cohesive soil and stone columns, S_v is expressed as:

$$\boldsymbol{S_v = \beta H(1-\mu^2)\left[1-\frac{\mu^2}{1-\mu^2}\right]\frac{P_0}{E}} \qquad (2\text{-}15)$$

Where

β : f(a, b, φs, μ, P_o/E), obtained from Figure 2-23.

μ : Poisson's ratio of the soft soil.

φ_1 : Angle of shearing strength of the stone material.

E: Odometer modulus of the soft soil.

P_o = Vertical stress.

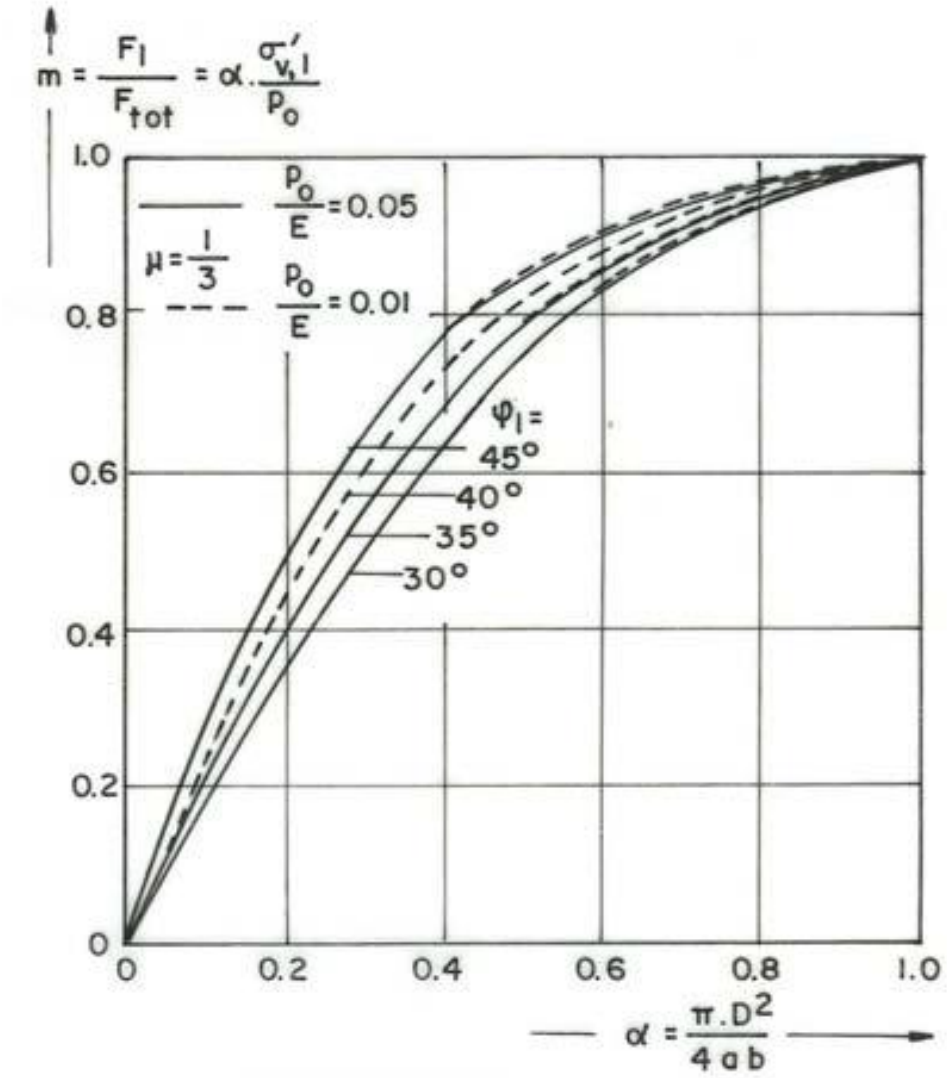

Figure 2-22: Stress Distribution of Stone Columns (Van Impe, 1983).

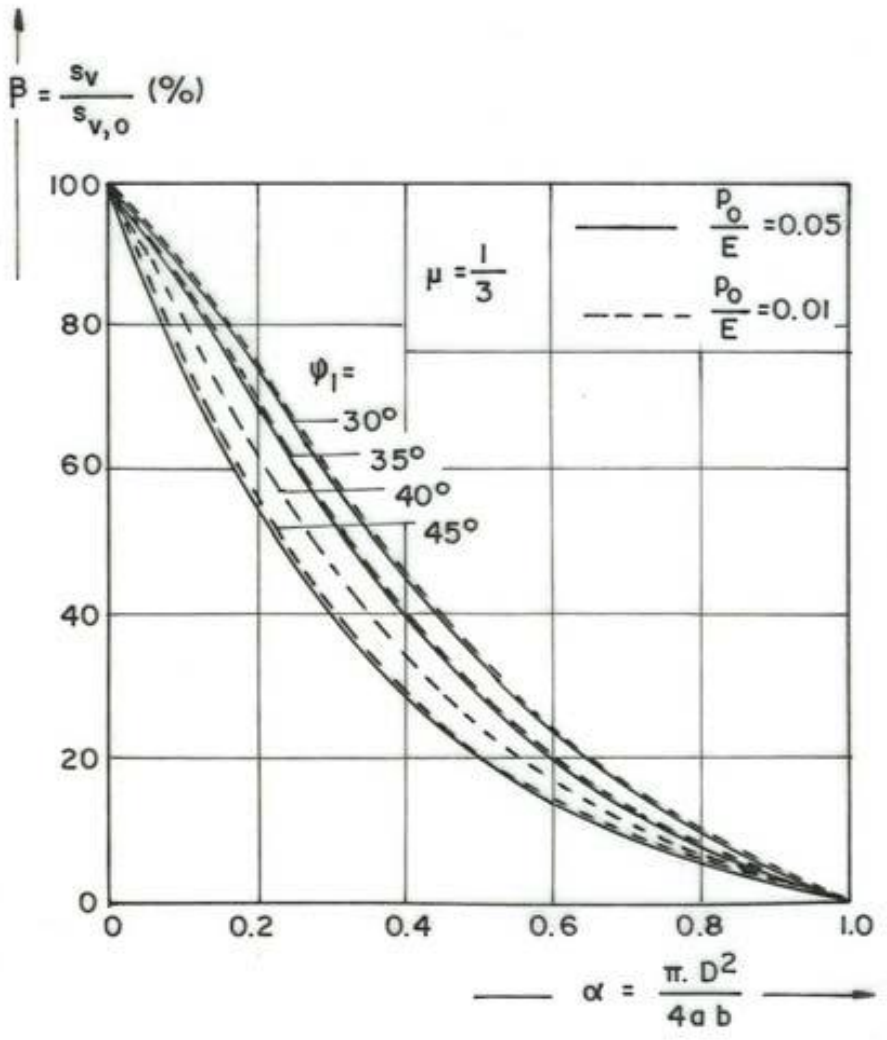

Figure 2-23: Improvement on the Settlement Behavior of the Soft Layer Reinforced with the Stone Columns (Van Impe, 1983).

2.10 Numerical Analysis of Stone Columns

In the analyses of geotechnical problems, exact solutions are applicable under limited conditions. An approximate solution can be obtained using numerical modeling. Finite element method is one of the most powerful solution methods that can be applied to solve a wide range of problems. The power of such method comes from the fact that it can easily accommodate changes in the material stiffness, which is evaluated at elemental

level. It also allows different boundary conditions to be applied in such a way that an acceptable global approximate solution to a physical problem can be achieved.

This technique provides a very useful tool for the investigation of the behavior of stone column reinforced ground. It is also served as a supplementary tool to the existing design methods especially in case of heterogeneous and anisotropic soil where current design methods normally adopt simplification and assumptions.

The stone column reinforced foundation analysis and design were mostly done using empirical methods. Although, there exist some vigorous analytical methods for analysis and design of stone columns, the field behavior of the stone column in multi layered soil condition is difficult to predict. In addition, the analytical solutions for stone column improved soil dealt, so far, with homogeneous soil condition only. In reality, the site soil conditions can be multi-layered and highly variable. In order to better understand the performance of improved soil, the numerical simulation of the deformation behavior plays an important role.

Numerical analysis of stone column reinforced ground can be modeled with different approaches:

i. Axis-symmetrical unit cell: commonly used for stone column under wide loading area and to simulate the stone column conducted in laboratory testing (Balaam, 1978; Castro and Karstunen, 2010; Domingues et al., 2007; Hird et al., 1992).
ii. Axi-symmetrical concentric ring: a single column is surrounded by converted gravel rings when columns are used under circular loads, such as tanks (Mitchell and Huber, 1985; Elshazly et al., 2006; Gäb et al., 2008) .

iii. Plane strain modeling: the cylindrical columns are converted to equivalent continuous strip (Van Impe, 1983). Suitable for long foundation, such as embankments and strip footing.

iv. Homogenization technique: composite ground treated as single material with static and kinematic constraint (Schweiger and Pande, 1986; Canetta and Nova, 1989; Lee and Pande, 1998; Wang et al., 2002; Hassen et al., 2010).

v. Three-dimensional (3D) modeling: required extensive effort and time compared to 2D analysis. Used to obtain more realistic results with better understanding of mechanics of column performance (Kirsch and Sondermann, 2003; Weber et al., 2008) .

2.11 Unit cell concept

The unit cell method considers a typical column and its tributary soil within a large group with a fixed boundary condition as shown in Figure 2-24 and Figure 2-25. Since the load and geometry are symmetrical in unit cell, the boundary conditions at the outer wall are: zero shear stress, zero radial displacement, and no water flow (Barksdale and Bachus, 1983; Castro and Karstunen, 2010). Following these assumptions, total stress applied on the top of the unit cell must remain within the unit cell although the stress distribution between the column and soil can be varied with depth (Barksdale and Bachus, 1983). Uniform loading applied over the unit cell is analogous to one dimensional (1D) consolidation test (Bergado et al., 1996).

The basic assumptions in association with the use of the unit cell idealization in analysis of settlement are:

- Vertical surcharge stresses are constant over an infinite loading so that the concept of a unit cell is theoretically valid.
- Shear stresses on the boundaries of the cell are insignificant so that boundaries can be approximated to be frictionless.
- Settlements for both the column and the soft clay are equal in the unit cell.
- The boundaries are rigid.

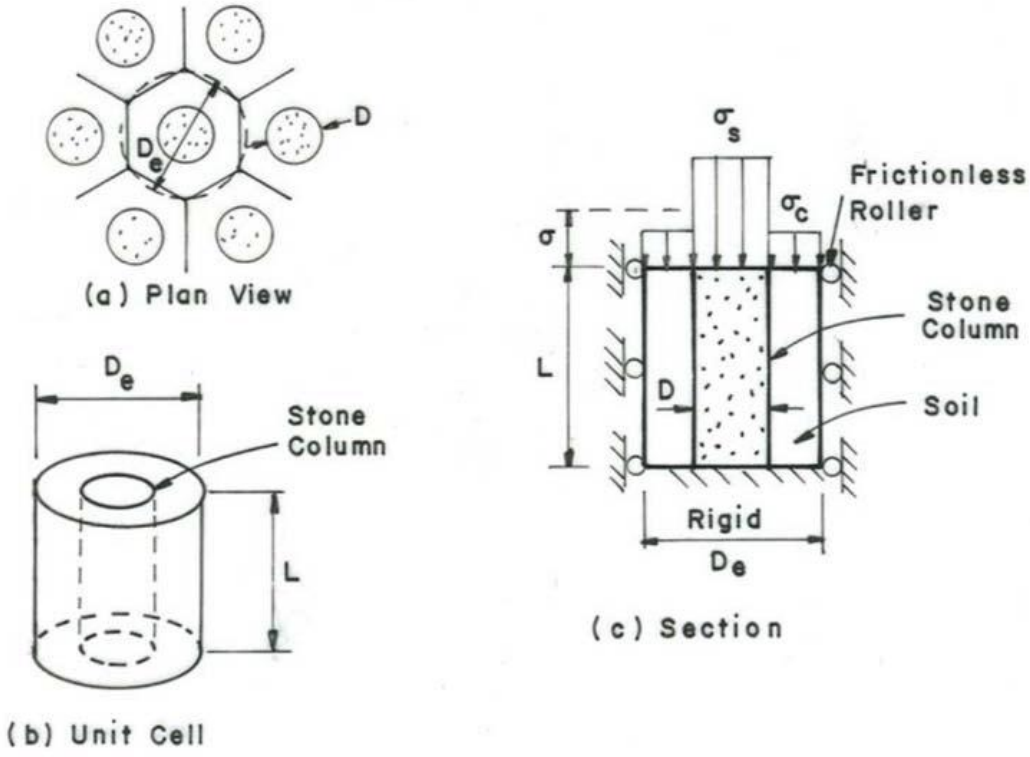

Figure 2-24:Idealization of Unit Cell: (a) Plan View (b) Unit Cell (c) Vertical Cross Section (Barksdale and Bachus, 1983).

Each column may be considered as a unit cell. According to Barksdale and Bachus, for a triangular placement of columns, the equivalent effective diameter can be calculated as follows:

$$D_e = 1.05S$$

For a square placement of columns, the equivalent effective diameter can be calculated as follows:

$$D_e = 1.13S$$

Where

D_e: Effective diameter of the column.

S: Spacing of individual columns.

Unit cell concept used in most stone column analysis suffers a few limitations due to the simplification made. The assumptions of unit cell concept are valid only for rigid raft and have severe weakness regarding the boundary conditions (Schweiger and Pande, 1986). In addition, the validity of unit cell is only restricted to uniform loading and uniform subsoil characteristics (Canetta and Nova, 1989).

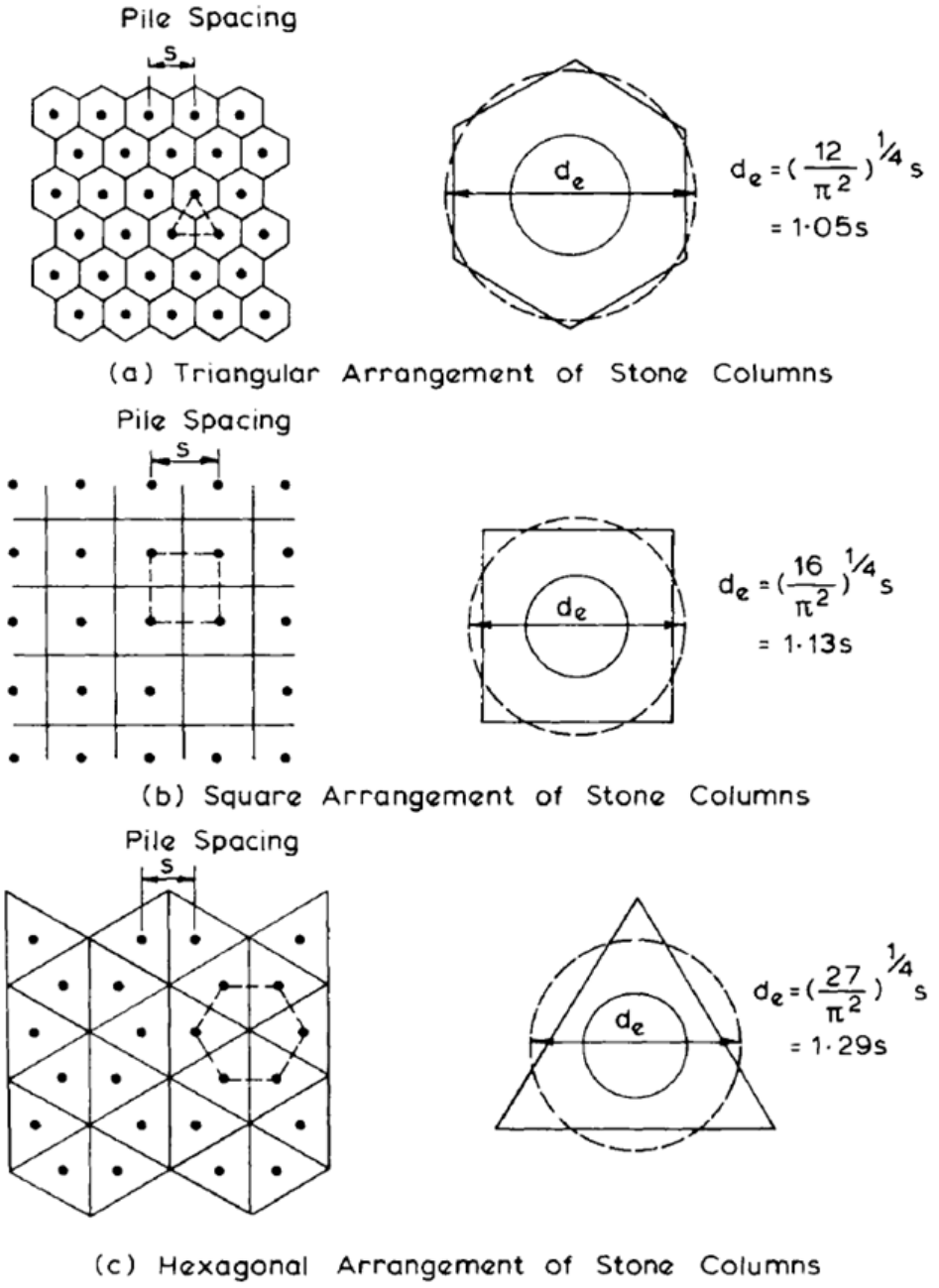

Figure 2-25: Equivalent Diameter of the Tributary Soil Treated by Stone Column (Barksdale and Bachus, 1983).

Balaam et al. (1977) is the first to adopt numerical models to examine the behavior of stone columns using the unit cell concept. Finite elements were used for settlement prediction while finite differences were employed to calculate the time rate of consolidation. The ratio of modulus of the stone to that of the clay was assumed to vary from 10 to 40, and the poisson's ratio of all material types was assumed to be 0.3. A coefficient of at rest earth pressure K_0=1 was used to simulate the effect of installation process. Only about 6% difference in settlement was found between elastic and elastic-plastic response. The authors concluded the difference in elastic and elasto-plastic modeling is very minor.

This seems to be an ambiguous finding because they used very low loading (24 kPa) in their foundation scheme and it is understood also that greater loading intensity will likely cause greater plastic deformation of the column as well as the improved ground. The amount of stone column penetration into the soft layer and the diameter of the column were found to have a significant effect on settlement as shown in Figure 2-26; the modular ratio of stone column to soil was of less importance.

Barksdale and Bachus (1983) presented some design curves for predicting primary consolidation settlement. Finite element analysis was used in their study. For a nonlinear analysis, load was applied in small increments and computation of incremental and total stresses were performed by solving a system of linear, incremental equilibrium equations for the system. Curves for predicting settlement of low compressibility soils such as stone column reinforced sands, silty sands and some silts were developed using linear elastic theory. Low compressibility soils are defined as those soils having modular ratios $E_s/E_c \leq 10$ where E_s and E_c are the average modulus of elasticity of the stone column and soil,

respectively. The settlement curves for replacement area ratios of 0.1, 0.15 and 0.25 are given in Figure 2-27.

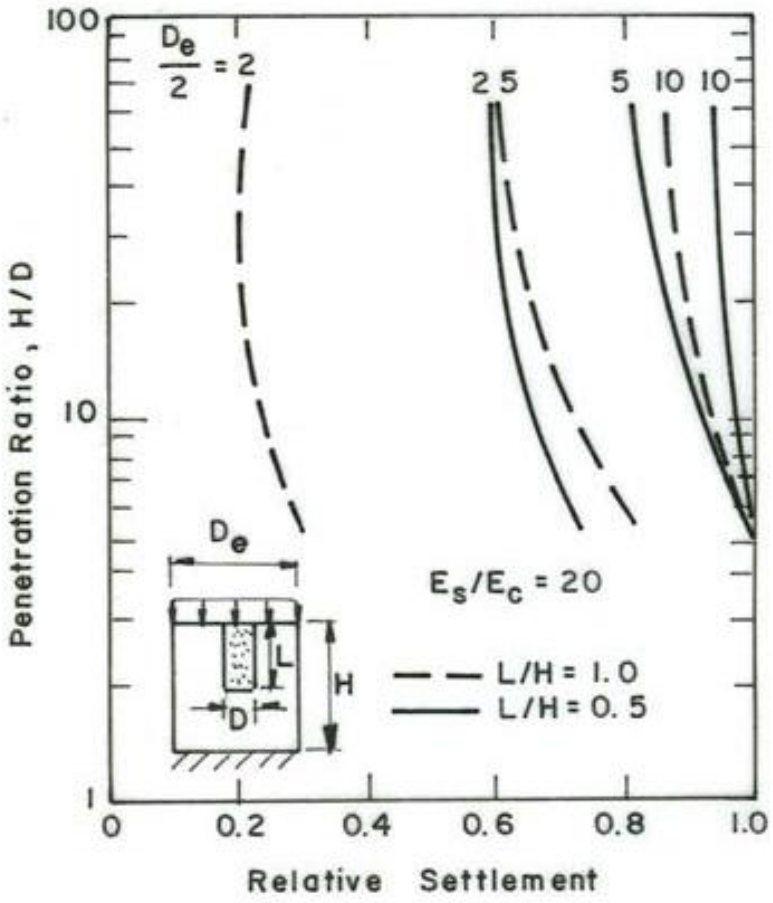

Figure 2-26: Effect of Stone Column Penetration Length on Elastic Settlement (Balaam, 1978).

Elshazly et al. (2008) adopted finite element method to access the reliability of the unit cell concept. The model incorporates the changes of stress state due to stone column installation process (Elshazly et al., 2006). They proposed settlement correction factor, f $=S/S_{uc}$, which relates the settlement, S, of foundations extending beyond the unit cell to the settlement when considering the unit cell alone, S_{uc}. It was found that the correction

factor generally depended on the foundation size and the virgin soil characteristics. It has been observed in some cases that the values of f are higher than one, which indicates the underestimation of settlement using unit cell idealization.

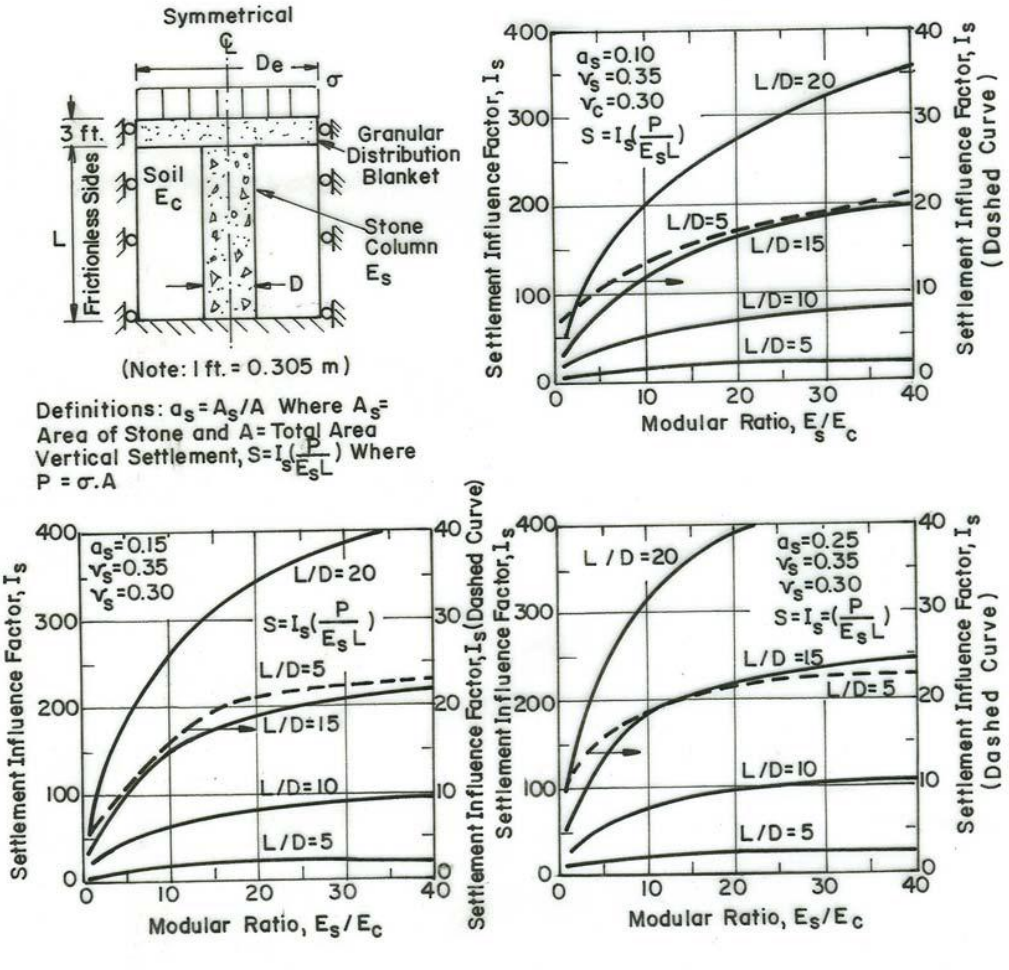

Figure 2-27: Notations Used in Unit Cell Linear Elastic Solutions and Linear Elastic Settlement Influence Factors for Area Ratios, as = 0.10, 0.15, 0.25 (Barksdale and Bachus, 1983).

Castro & Sagaseta (2009) carried out a coupled finite element analysis of the consolidation around stone columns to evaluate the accuracy of different analytical solutions using a unit cell. A uniform load is applied by means of a rigid plate and a

simple elastic or elastic-perfectly plastic (i.e. Mohr Coulomb) soil models are utilized (Castro and Sagaseta, 2009b). The numerical results showed that the analytical solution by Castro & Sagaseta (2009) which considers the immediate settlement and the horizontal displacement to have better agreement compared to previous study.

2.12 Description of Material Models

The behavior of real soil is highly non-linear, with both strength and stiffness depending on the stress and strain level (Potts et al., 2001). Furthermore, real soil often exhibits time-dependent behavior and anisotropic tendencies. The behavior of soil may be approximated to varying degrees of accuracy using material models. An overview of the material models used during the finite element modeling is given fowling section:

2.12.1 Linear Elastic Model

This is based on Hooke's law of elasticity and idealizing soil as a linear elastic material, thus precluding the development of irreversible strains. The material behavior is defined by two parameters, Young's modulus (E) and Poisson's ratio (μ). This model is too crude to, accurately, capture the complicated stress-strain behavior of soil and is only adopted to represent structural elements e.g. concrete and steel.

2.12.2 Mohr-Coulomb Model

The Mohr-Coulomb criterion is a popular model used by geotechnical engineers for a wide range of problems. It is widely understood and requires a few input parameters, which can be determined using common laboratory test.The elastic-perfectly plastic criterion is based on dividing the relationship between stress and strain into two phases:

(i) the first phase represents the elastic relationship between stress and strain, (ii) second phase starts after the curve reach the yield point; then the perfect plastic phase starts at which the strain is increasing while the stress level remains the same as the yield stress (Holtz and Kovacs, 1981). Figure 2-28 shows the relationship between stress and strain for elastic-perfectly plastic criterion.

The failure of soil is based on the Mohr-Coulomb failure criterion, which is defined, by two parameters, angle of internal friction (ϕ) and cohesion (c). This failure criterion is an extension of Coulomb's friction theory and its yield surfaces in principal stress space are shown in Figure 2-29. The model does not generate irreversible strains below the yield surfaces. However, irreversible plastic strains resulting from shearing are captured using a non-associated flow rule, which is defined by an angle of dilation (ψ) (Brinkgreve et al., 2012).

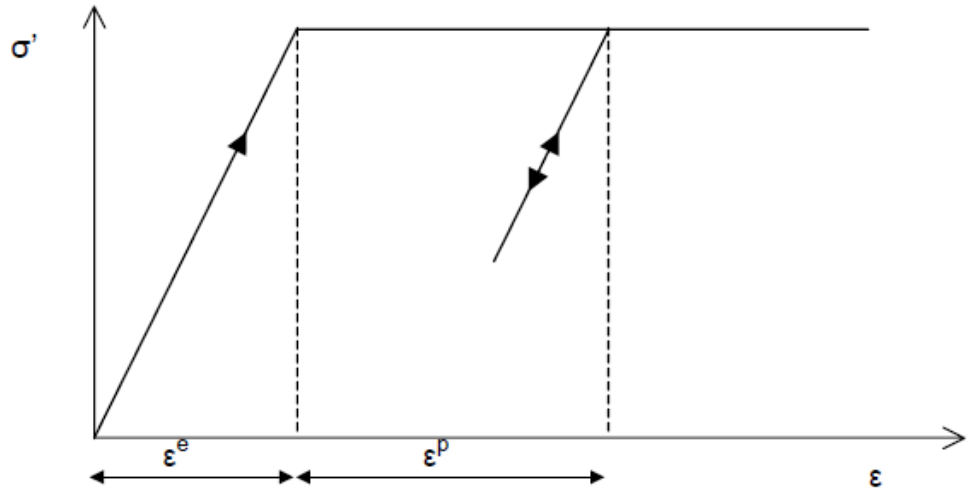

Figure 2-28: An elastic Perfectly Plastic Model (Brinkgreve et al., 2012).

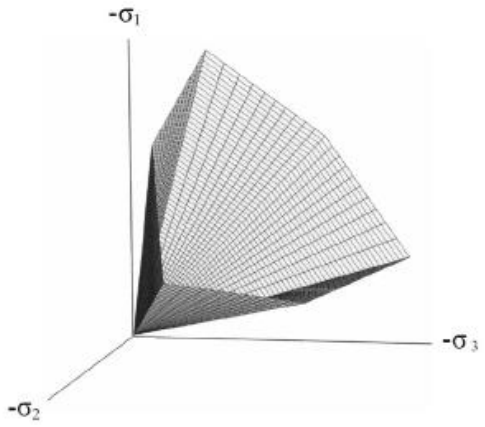

Figure 2-29: Mohr-Coulomb Yield Surface in Principal Stress Space (c = 0 kPa) (Brinkgreve et al., 2012).

A constant Young's modulus defines the behavior of soil before failure and it is important to choose an appropriate value which reflects the stress path and stress level experienced by the soil. A drawback to the Mohr-Coulomb model is that it fails to accurately capture the stiffness response of soils due to the simplistic assumption of linear elasticity before failure and is only used as a first approximation of soil behavior (Brinkgreve et al., 2011).

The angle of dilation controls the amount of plastic volumetric strain developed during plastic shearing and is assumed constant during plastic yielding. The value of $\psi=0$ corresponds to the volume preserving deformation while in shear. Clays (regardless of over-consolidated layers) are characterized by a very low amount of dilation ($\psi\approx0$). However, for sands, the angle of dilation depends on the angle of internal friction. For non-cohesive soils (sand, gravel) with the angle of internal friction $\phi > 30°$ the value of dilation angle can be estimated as $\psi = \phi - 30°$(Bolton, 1986). A negative value of dilation

angle is acceptable only for rather loose sands. In most cases, however, the assumption of $\psi = 0$, can be adopted.

2.13 Interface Element

In numerical study, an interface element is normally used to simulate the interaction between structure and soil. Without interface, there will be no slipping and gapping between the structure and soil. During the installation of stone columns, the granular materials are interlocked with the surrounding soil creating a mixed (smear) zone where the shear strength properties and the thickness of remolded annular zone varied depending on the method of installation. As this is not incisive, an interface element is not used (Ambily and Gandhi, 2007b).In addition, the deformation of the column is mainly by bulging and no significant shearing and slippage is expected, thus modeling using interface elements could over predict the punching of the stone columns in the soil.

2.14 Effect of Smear Zone and the Clogged

Remolding of the soil around the probe during installation of stone columns developed smear zone in the soil adjacent to interface between soil and stone column. The smear zone between soil and stone columns cause an important reduction in the horizontal permeability of the soil surrounding the stone column and hence, ultimately around the stone column (Casagrande and Poulos, 1969). Also, because of the migration of sabkha and fine cohesionless particles into the voids between stone column, a clogged zone may be formed within the stone column in the closeness of the soil-column interface (Adalier and Elgamal, 2004) .

2.15 Failure Mechanisms

A proper understanding of the load transfer and failure mechanisms for stone column is necessary for analysis and design. Failure mechanisms of stone column are dependent on the confining effect of the surrounding soil as well as the soil beneath the layer where columns are resting. The failure mechanisms of stone columns can be study under two categories:

2.15.1 Single Stone Column

Stone columns may be constructed as either end bearing on a firm stratum underlying weak soil, or as floating columns with the tip of the column embedded within the soft layer (Barksdale and Bachus, 1983b). In practice stone columns are commonly constructed as end bearing (Bergado et al., 1991). The possible failure modes for a single stone column are bulging, general shear and punching failures (Aboshi et al., 1979; Hughes and Withers, 1974; Madhav and Vitkar, 1978) as shown in Figure 2-30.

Either end bearing or floating stone columns greater than about three diameters in length fail in bulging (Hughes and Withers, 1974) as illustrated in Figure 2-30 (a). The bulging failure of the stone column takes place when the applied load is higher than the confining stress. The surrounding soil provides some lateral support to prevent further expansion of the stone column. The confining stress increases with depth, so the bulging failure occurs in the upper part of the stone column. The increase of horizontal stress in the surrounding soil leads to subsequent consolidation and provides further resistance to bulging (Madhav and Van Impe, 1994). In practice, end-bearing stone columns usually

have lengths greater than three diameters, thus bulging failure usually becomes the controlling factor in design. However, there is numerical and experimental evidence indicating that even bulging can occur in shallower depth less than 2-3D (Murugesan and Rajagopal, 2006).

A very short column bearing on a firm support will undergo either by general or local bearing capacity type failure at the surface Figure 2-30 (b). The Local or general shear failure mechanism is similar to shallow foundation failures in unreinforced soils. Punching failure or shearing below the short stone column support in the weakest layer, is a failure mechanism that occurs when the applied load is greater than the skin friction that develops along the surface of the stone column, end bearing resistance, or a combination of both as shown in Figure 2-30 (c). Finally, a floating stone column less than about 2 to 3 diameters in length may fail in end bearing by Punching failure in the weak underlying layer before a bulging failure can develop Figure 2-30 (c).

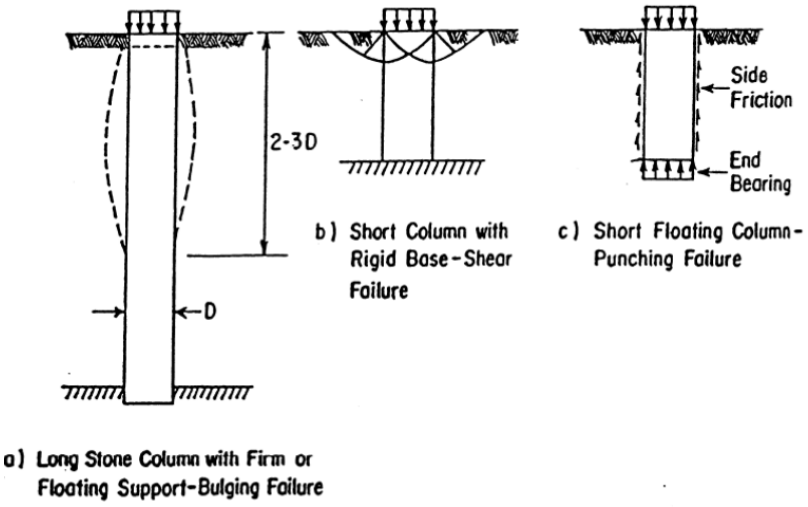

Figure 2-30: Failure mechanisms of a Single Granular Pile in a Homogeneous Soft Layer (a) Bulging, (b) General or Local Shear (c) Punching (Barksdale and Bachus, 1983).

2.15.2 Group Stone Columns

Barksdale and Bachus (1983) reported that, under a rigid foundation, an isolated single stone column has a smaller ultimate load capacity per column than a stone columns group. They attributed the increase to the fact that the interior columns are confined by the surrounding soil and the neighboring stone columns.

Barksdale and Bachus, (1983) investigate the interaction effect between two adjacent columns based on series laboratory tests Figure 2-31, it was noted that the presence of adjacent columns provides some confinement for the column, furthermore, bulging was restrained in the interior side of the columns.

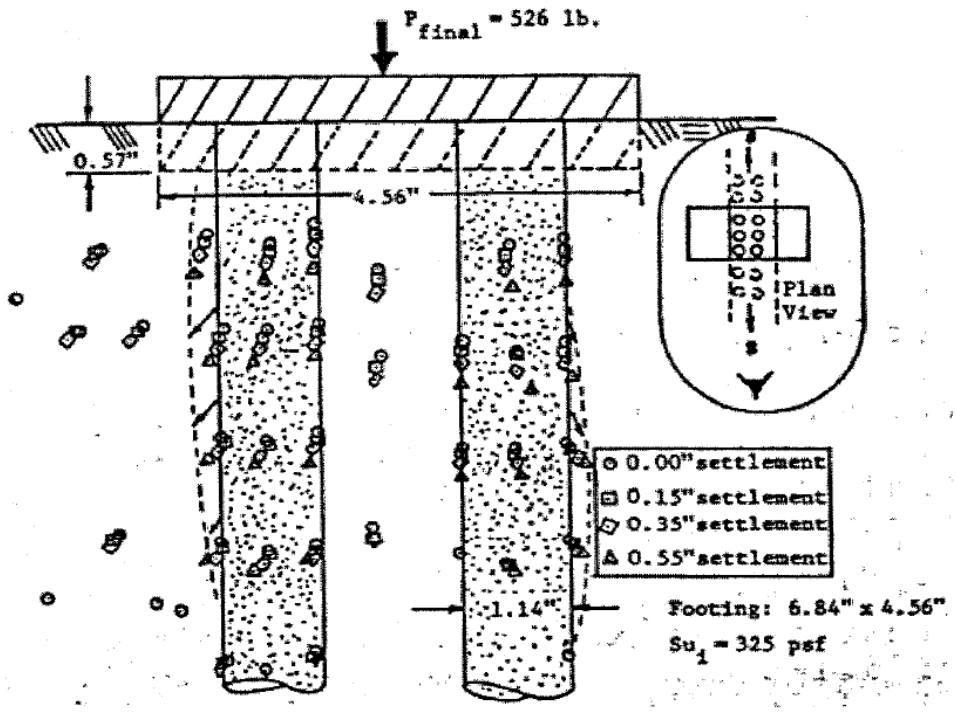

Figure 2-31 Displacements of Two Adjacent Stone Columns (Barksdale and Bachus, 1983).

The failure modes of the stone column group are shown in Figure 2-32. Lateral spreading and circular slip failure are two common modes of failure under embankments and both can result in more settlement than expected (Barksdale and Bachus, 1983a). Spreading reduces the lateral confining stress acting on the stone column and thus increases the degree of bulging as illustrated in Figure 2-32 (a) and (b).

A group of stone columns in a soft soil probably undergoes a combined bulging and local bearing, type failure as illustrated in Figure 2-32 (c). A local bearing failure is the punching of a relatively rigid stone column (or group) into the surrounding soft soil. Stone column groups having short column lengths can fail in end bearing Figure 2-32 (d) or perhaps undergo a bearing capacity failure of individual stone columns similar to the failure mode of short, single stone columns.

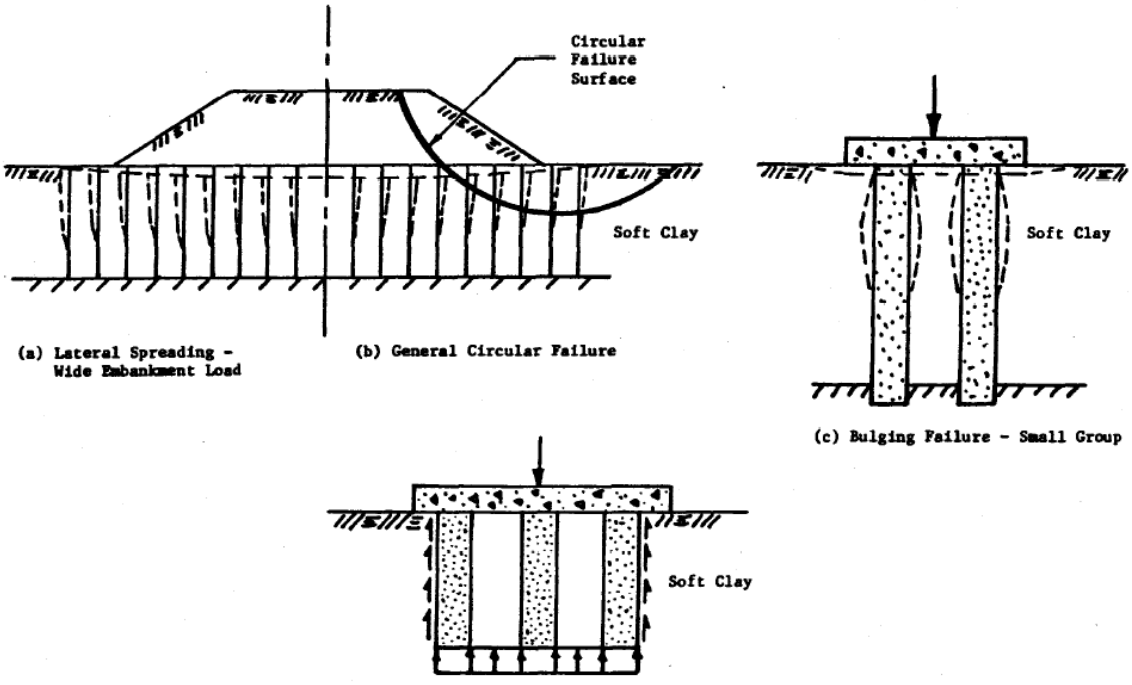

Figure 2-32: Failure Modes of Stone Column Groups (Barksdale and Bachus, 1983).

Hu, (1995) reported from experimental work that group interaction plays a major rule in understating the behavior of group of stone columns. He reported that deformation of stone columns under footing is that a wedge shaped body is displaced vertically in connection with bulging and buckling of the columns as shown in Figure 2-33. Buckling was observed near the edges of the footing close to the ground surface and bulging occurred under the center of the footing in deeper region (Hu, 1995). The columns adjacent to the footing showed only a small amount of bending.

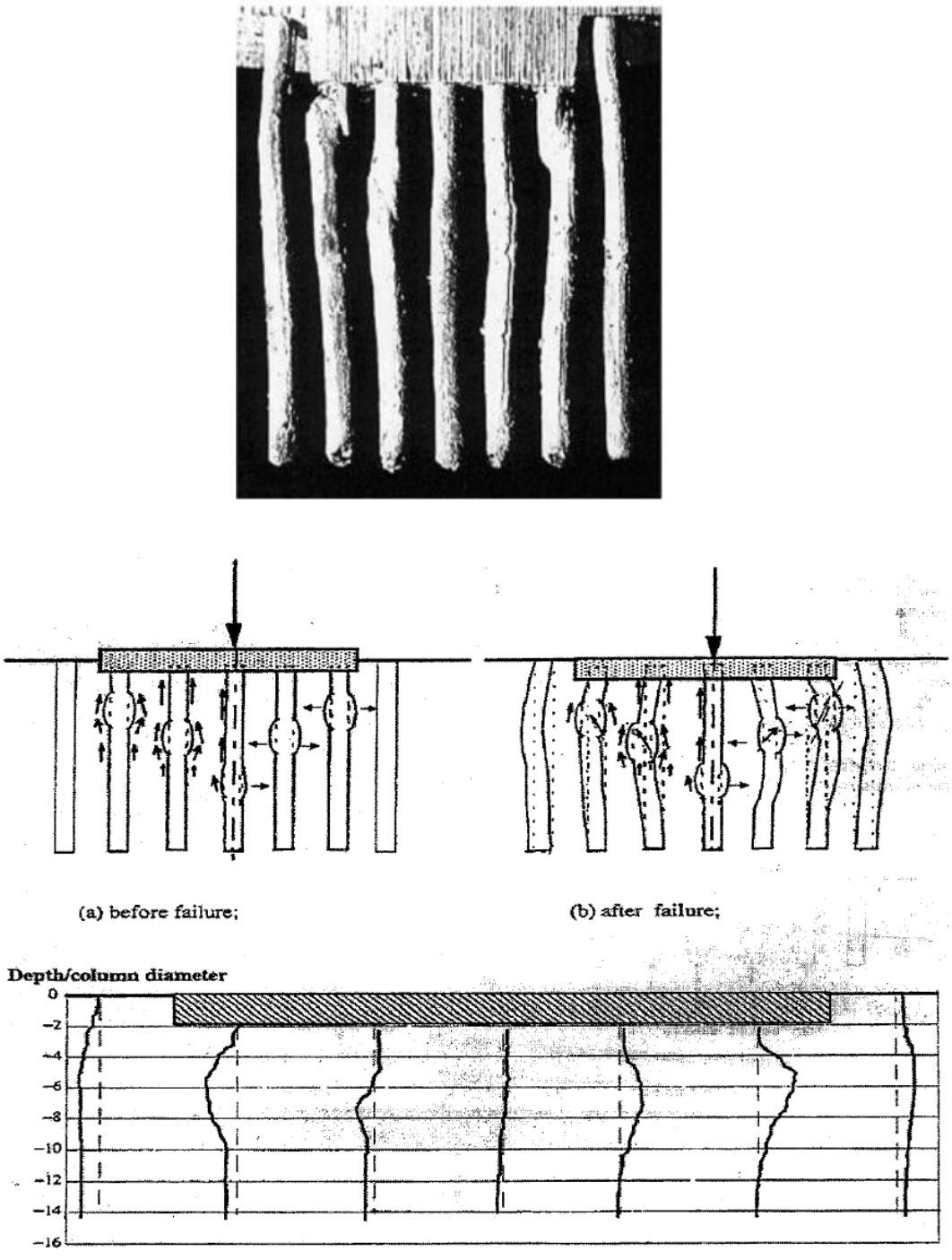

Figure 2-33: Suggested Mode of Failure for Long Group Columns (Hu, 1995).

CHAPTER 3

FIELD TESTING AND FULL SCALE LOAD TEST

3.1 Introduction

In this chapter two case study chosen from the Eastern Saudi Arabia are studied in detail to investigate the performance behavior of ground improved with stone columns. Each case history includes a description of the project, the subsurface conditions, regional geology, the stone columns installations, soil characteristics, description of constructional phases and full-scale field tests on stone columns.

3.2 Case study 1: A Petrochemical Company, Jubail Industrial City

Well-documented case study, which was intended to optimize the design of stone columns for a lightly loaded structure, such as a product warehouse. The case belongs to Polypropylene (PP) plant and a Warehouse area (WHA). The project is located on the coast of Arabian Sea in the eastern region of Saudi Arabia at Jubail. The two facilities are constructed on two adjacent areas. Plan area of plant (Polypropylene plant) is 301.5m x 154m while that of warehouse for storage facilities is 770mx284m.

3.2.1 Subsoil condition

The project site is located within the region of coastal Aeolian dunes. In this region, sand deposits mixed with silt and/or clay in loose conditions, commonly known as “Inland Sabkha", are the common features. At the entire project site, Sabkha formation exists

with thickness of up to 6.50m. The sub-surface conditions were investigated at the project site covering plant area and the warehouse facilities by drilling and sampling sixty-five boreholes up to 26.00 m depth. Based on the field investigation and laboratory analysis of representative soil samples, subsurface stratigraphy & design parameters are evaluated up to the maximum drilled depth.

The sub-soil can be generally classified into five (5) layers system based on the density and soil type. These layers exist with different thickness and characteristics. The layers encountered and their engineering properties are summarized below:

Layer 1: A recent light brown backfill, loose to medium dense, fine to medium-grained granular non-cohesive poorly graded SAND (SP/SP-SM). This layer is the top layer and has a thickness ranging from 2.0 to 2.8m. It is generally in loose to medium dense condition with Standard Penetration Test (SPT) values in the range of 4 to 38.

Layer II: Light brown to light gray, very soft lean CLAY interbedded with layers of poorly graded SAND (CL/SP). It is very soft with SPT values in the range of 1 to 2 (Sabkha). This layer exists below the sand backfill and has a thickness of about 5.0 to 6.5m.

Layer III: Light gray, with localized dark zones, medium dense poorly graded, fine to medium SAND with varied silt content. This layer was encountered below Sabkha formation up to about 15.0 m depth in most of the locations. The range of SPT values in this layer generally varied in 19 to refusal (N > 50).

Layer IV: Gray, hard, fat CLAY (CH) the thickness of this layer is also varying from 2 to 11.5m. This layer is very stiff to hard condition with SPT value in the range of 20 to refusal (N > 50).

Layer V: Fine to medium grained, very dense, brown, and fine to medium silty SAND to SAND with silt (SM/SP-SM). The SPT values were generally refusal (N > 50) and in very dense condition.

3.2.2 Optimization of stone column design in Warehouse Area

To optimize the design of stone columns in this area, the project team selected three stone column groups at square grids of 1.65m×1.65m, 2m×2m and 2.5m×2.5m and the stone columns are 10 m deep as shown in Figure 3-1. This work was done before the installation of more than 53000 stone columns. The soil conditions under this area are shown in

Figure 3-4 and Table 3-1. Finally after field full load testing, the grid spacing of 2x2 m was selected. The discussion here will be limited to the test related to the 2x2 m grid spacing.

Three large plate load tests were conducted at the site as follows:

1. The first load test was performed on four stone columns with grid spacing 2x2 m, as shown in Figure 3-1. The test was intended to be a short term test (few days). The top 1.5 m of sand backfill was removed to simulate the footing level and minimize the effect of sand layer on the settlement and thus reduces the amount of load required during testing.

2. The second load test was done by loading on one stone column with static load imposing a pressure of 137KN/m^2 using concrete block for a period of 73 days, as shown in Figure 3-2 .
3. The third load test was performed on group of stone columns but the concrete footing was resting directly on the Sabkha soil (the sand backfill was removed), as shown in Figure 3-3 .

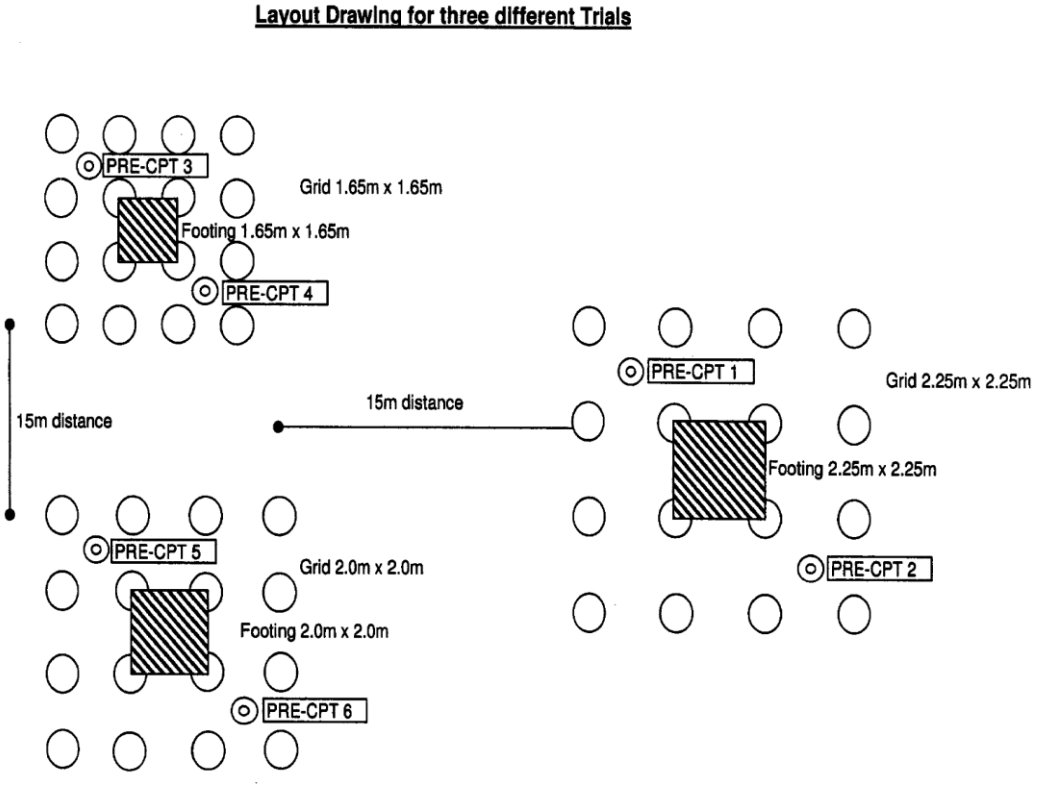

Figure 3-1: Layout of Three Different Trails (Aiban, 2009).

The soil conditions "representative" within this area is shown in Figure 3-4. Result of full-scale test and theoretical analysis of short term tests are summarized in Table 3-2. The long-term plate load test is shown in Figure 3-5. The test was conducted at the working level of stone columns in accordance with ASTM D1194.

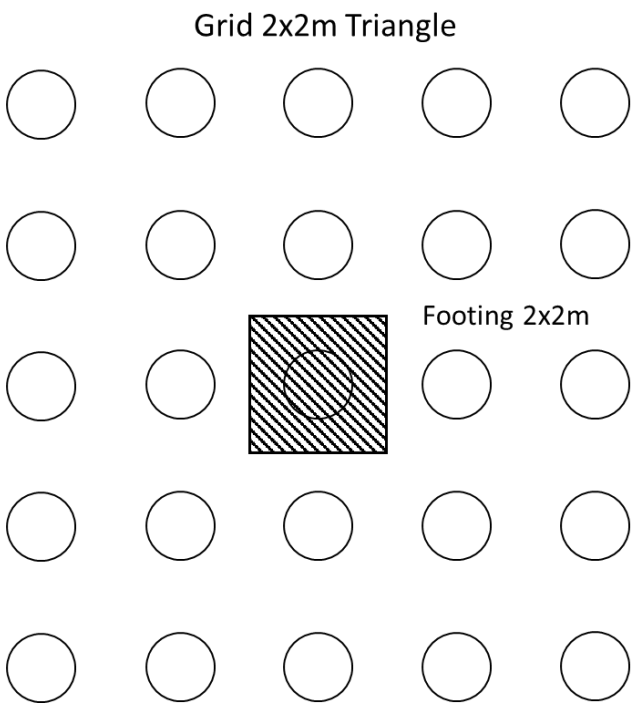

Figure 3-2: Plate Load Test on one Stone Column for a Period of 73 Days (Aiban et al., 2010).

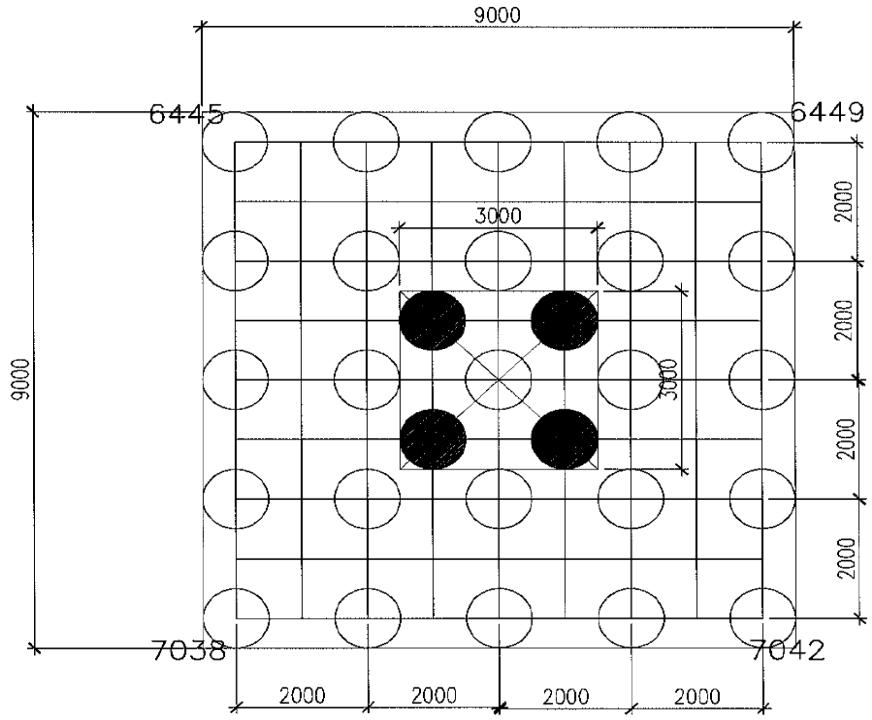

Figure 3-3: Layout for Plate Load Test on 3m×3m Footing Size Directly on Sabkha Soil (Aiban et al., 2010).

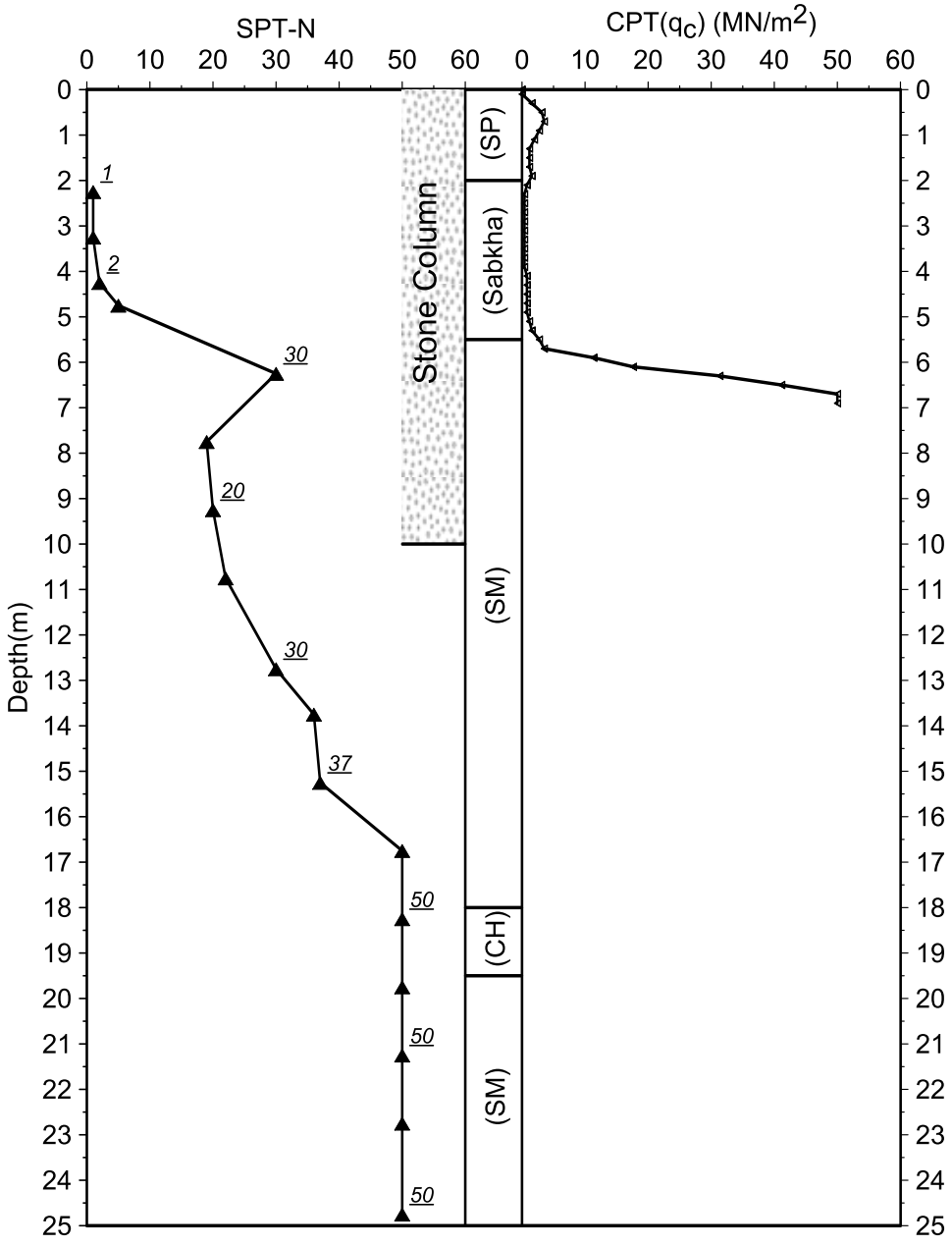

Figure 3-4: The Soil Profile around Trails Stone Columns (data from Aiban, 2009).

Table 3-1: Summary of Laboratory Test Results of Borehole around Trail Stone Columns (data from Aiban, 2009).

Depth(m)	Moisture Content (%)	Particle size analysis Percentage Passing through Sieve No				Atterberg Limits		Soil Classification
		#4	#10	#40	#200	LL%	PI%	
2.25-2.7	36	87	79	62	48	49	29	SC
4.5-4.95	21	97	96	75	32	NP	NP	SM
18-18.45	18	85	77	68	44	97	65	CH
22.5-22.95	20	-	-	99	18	NP	NP	SM

Table 3-2: Field Test Result and calculated settlement values for Different Stone Column Configurations (data from Aiban, 2009).

Grid		1.65m×1.65m	2m×2m	2m×2m	2.25m×2.25m
Stone Column No under the Plate		1	1	4	1
Field Settlement(mm)	60 kPa	0.97	3.244	1.836	2.454
	120 kPa	3.11	6.792	3.67	5.878
Settlement by (mm) using Pierbe Method	60 kPa	7.1	13.1	13.1	17.8

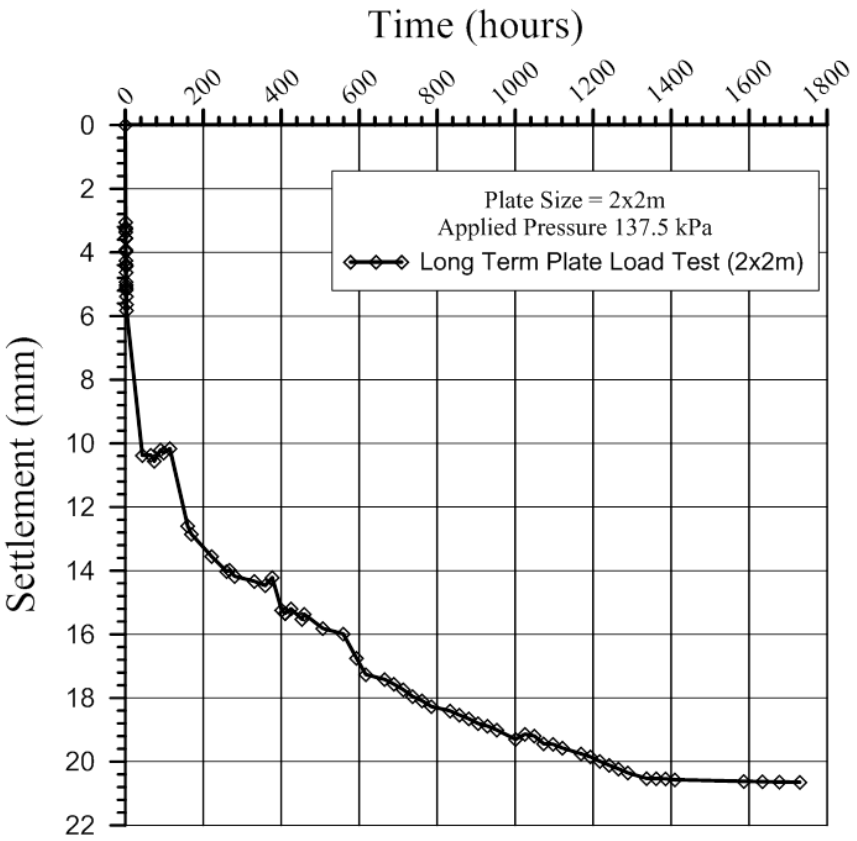

Figure 3-5: Long Term Plate Load Test in the WHA (Aiban et al., 2010).

3.2.3 Plate Load Test on Group of Stone columns Direct in Sabkha soils

Due to the overshadowing effect of the 2.5 m sand recent backfilling on the results of full-scale load tests on stone columns, a full scale plate load test was performed directly on Sabkha surface using the proposed grid configuration of stone column 2m×1m. The soil conditions in this area are shown in Figure 3-6. The plate measures 3m×3m×0.6m and was placed on e five stone columns including one stone column in the center. The location and the layout are presented in Figure 3-3. The foundation was made more rigid by placing another footing of 0.4 m thickness over the 3m×3m footing.

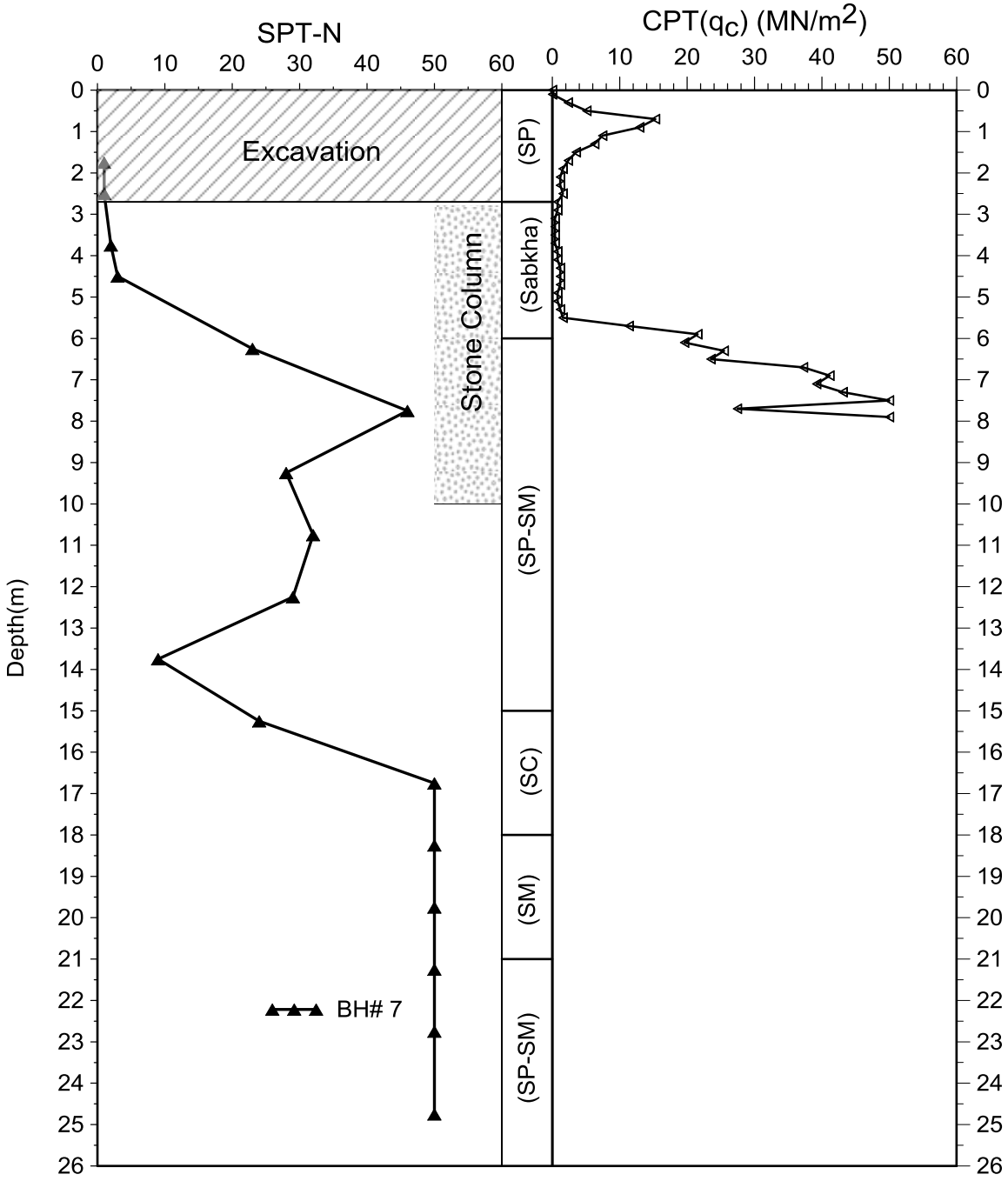

Figure 3-6: The Soil Profile around Plate Load on Sabkha Surface (data from Aiban, 2009).

Two Pre- CPT were conducted to verify the top level of Sabkha surface and to confirm the treatment depth of stone columns. The top of Sabkha was found at EL. 2.80m. The footing was placed at the surface of Sabkha soil as shown in Figure 3-7. The load was applied using two hydraulic jacks 200Ton capacity each. The two jacks were reacting against the concrete blocks Kentledge platform, as shown in Figure 3-3.

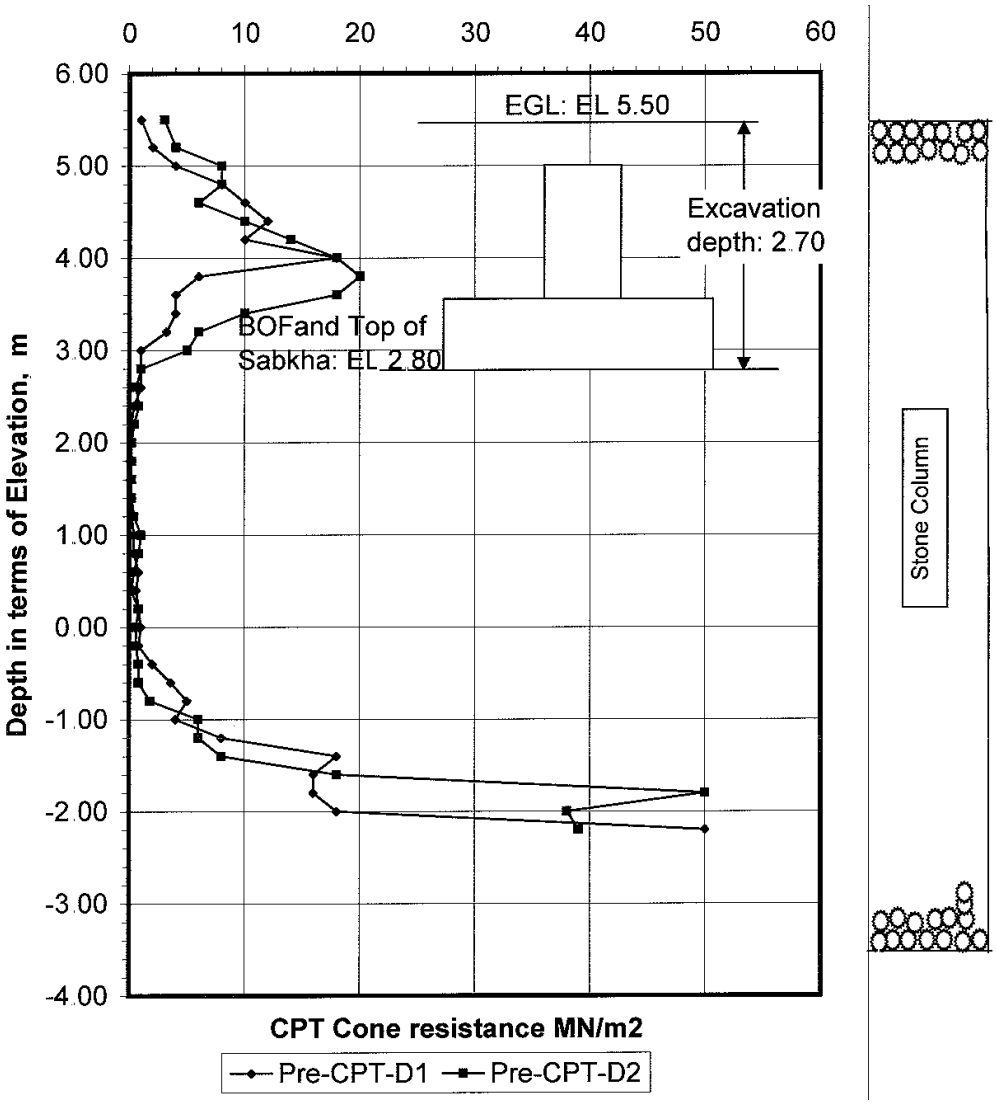

Figure 3-7: Pre-Cone Penetration Test in Trial Area to Verify the Top Level of Sabkha Surface (Aiban et al., 2010).

Settlement calculations were made for the improved soil condition for the 3m×3m footing placed at Sabkha level and using 2m×1m stone column grid for the improved soil condition. The depth of settlement analysis was taken up to 2.5 times the width of foundation i.e. 7.5m below the bottom level of foundation. Pierbe method was used to calculate theoretical settlement and result of theoretical and filed test settlement are summarized in Table 3-3. The results of the load tests are plotted in forms of load/settlement graphs as shown in Figure 3-8.

Table 3-3: Theoretical and Filed Test Settlement Result for Plate Load Test Directly on Sabkha Surface (data from Aiban, 2009).

Applied Stress (kPa)	Filed test Settlement (mm)	Theoretical Calculated Settlement (mm)
80	22.025	19.8
120	46.71	29.6
135	60.6075	33.3
202.5	N/A	49.7

3.2.4 Soil Improvement by Stone Columns in WHA

From the result of theoretical design and trail tests, the project team adopted the use of stone columns up to 9 m below the working level at a square grid of 2m×2m. The number of stone columns amount to almost 34,000 (thirty four thousand columns. Thirteen large-scale plate load tests were performed on working column in order to confirm the achievement of the required bearing capacity of the improved ground. In this study, four-plate load tests have been selected for validations.

Those tests were selected near boreholes and Pre-CPT in order to identify the soil profile before and after installation of stone columns and assess the degree of improvement. Soil profile and Pre-CPT near plate load test No.1, 2, 3 and 4 are shown in Figure 3-9 and Figure 3-10. In all tests, the stone columns layout and Post CPT positions were similar to the layout shown in Figure 3-11.

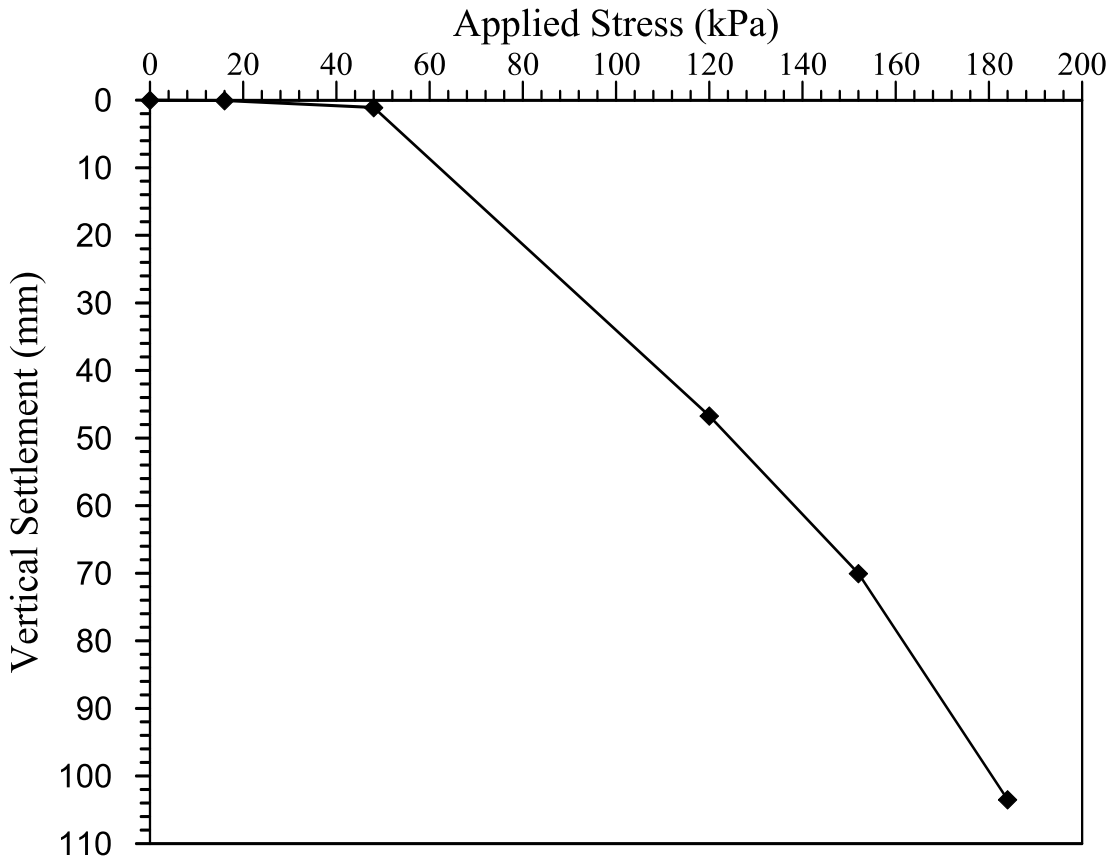

Figure 3-8: Load - Settlement for 3m×3m Footing Directly on Sabkha Surface (data from Aiban, 2009).

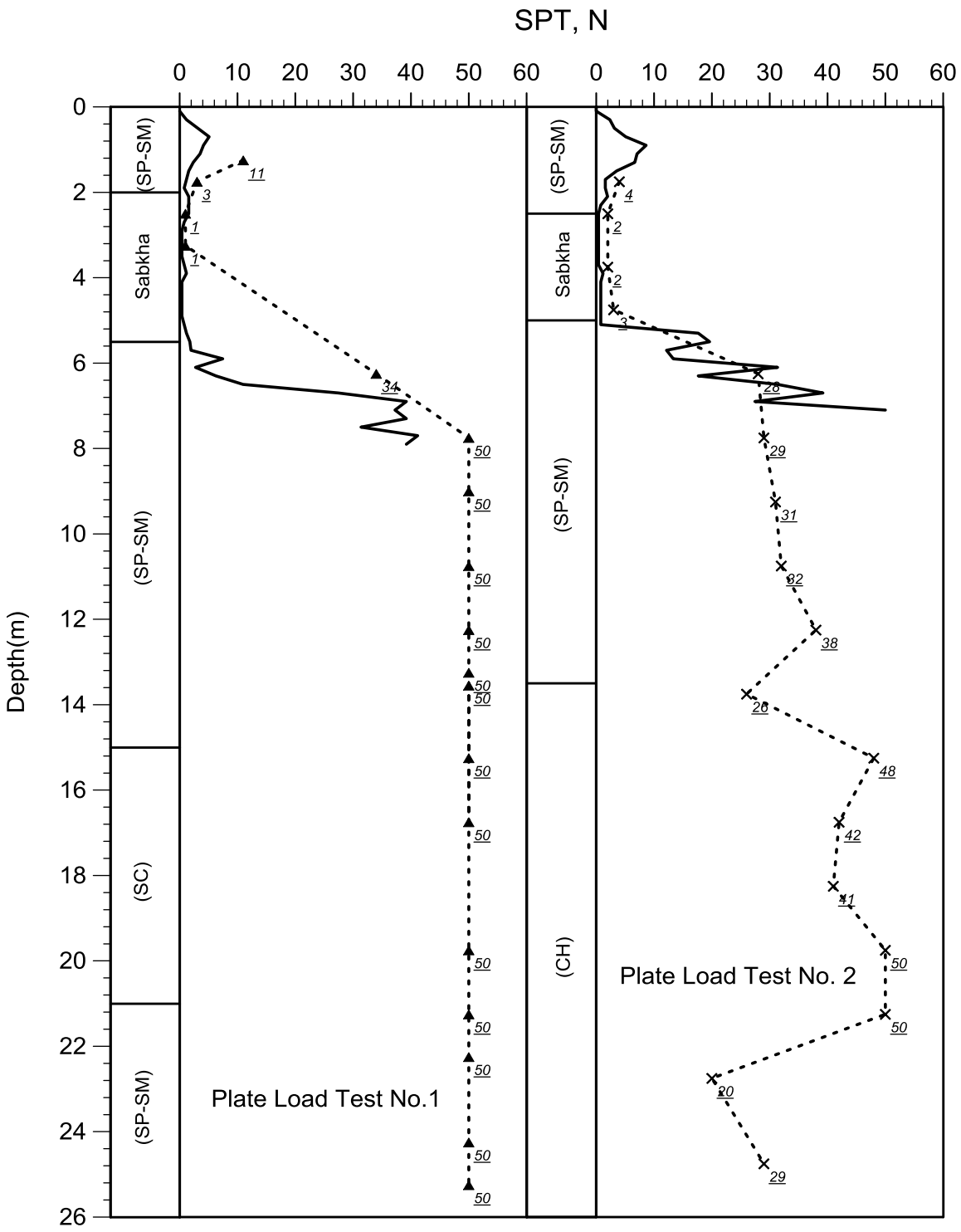

Figure 3-9: Soil Profile near Plate Load Test No.1 and 2 in the WHA (data from Aiban, 2009).

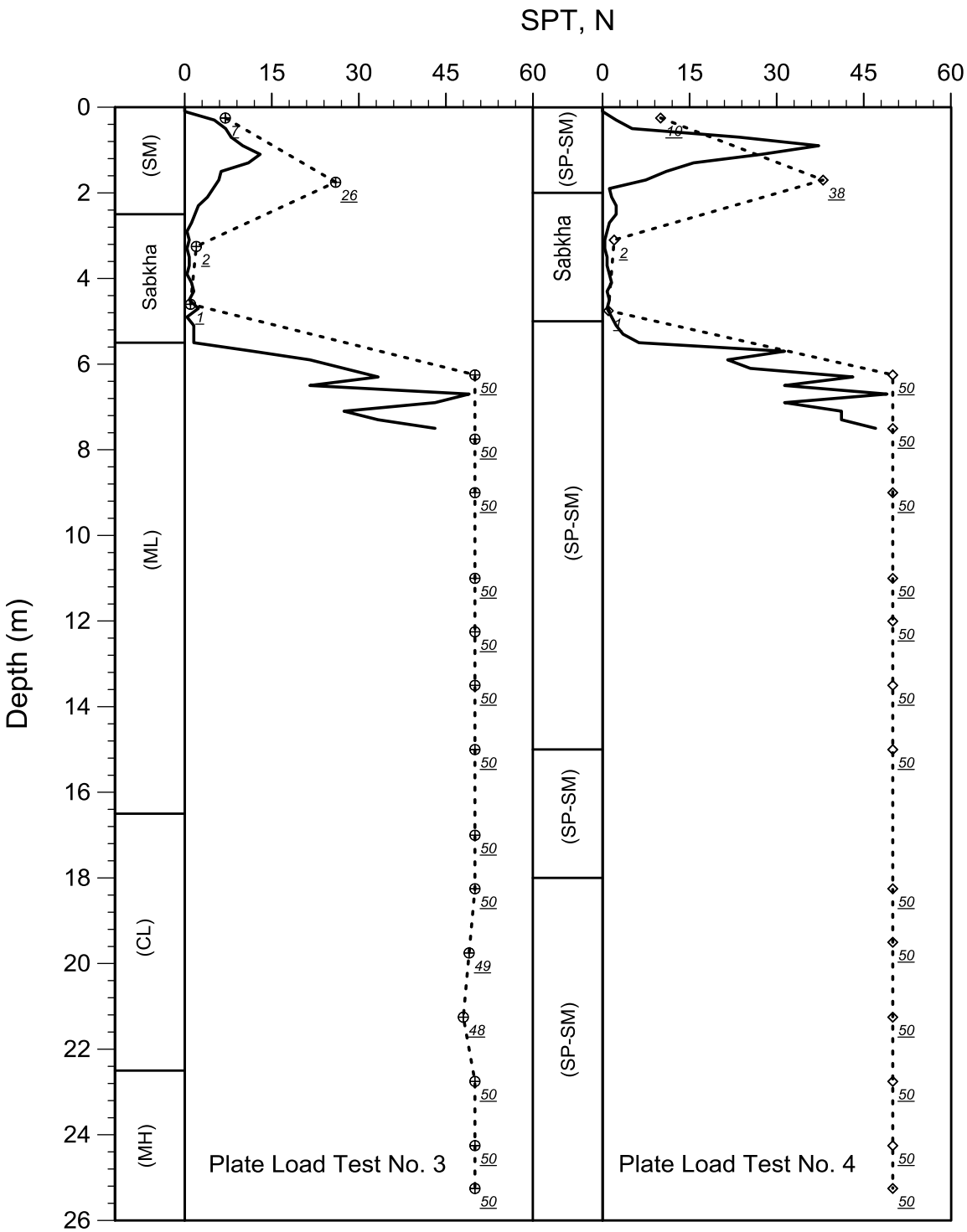

Figure 3-10: Soil Profile near Plate Load Test No.3 and 4 in the WHA (data from Aiban, 2009).

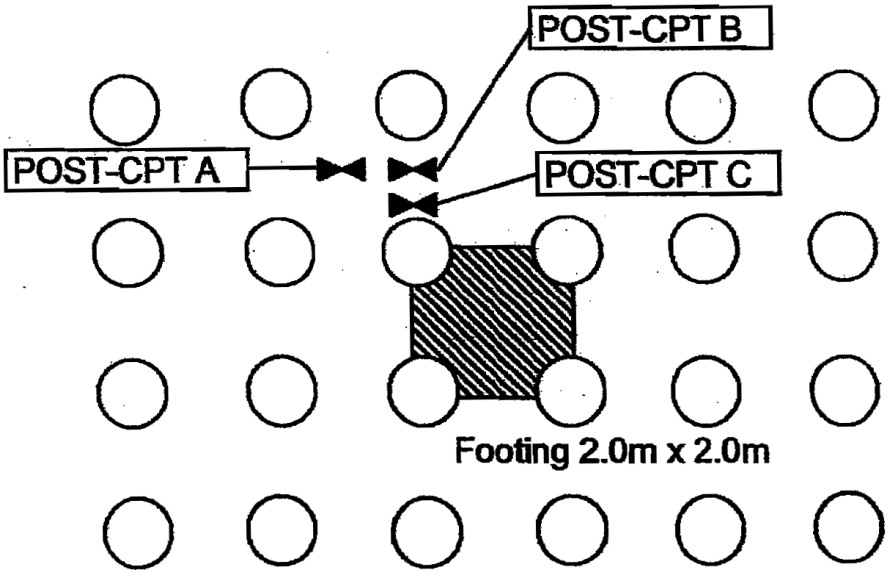

Figure 3-11: Layout for Plate Load Test and Post-CPT's in the WHA (Aiban, 2009).

The vertical settlement versus applied load curves are plotted in Figure 3-12. The stone columns were tested by applied loading using a hydraulic jack of 90 ton capacity reacting against a concrete block kentledge platform. The size of the concrete loading plate was 2.0m x 2.0m.Three Post-CPT's for every test were carried out as shown in Figure 3-13 to Figure 3-16. One CPT in the center of four stone columns, one CPT in the center between two stone adjacent columns, and one CPT is very close to the stone column (only 60 cm away from the center of stone column).

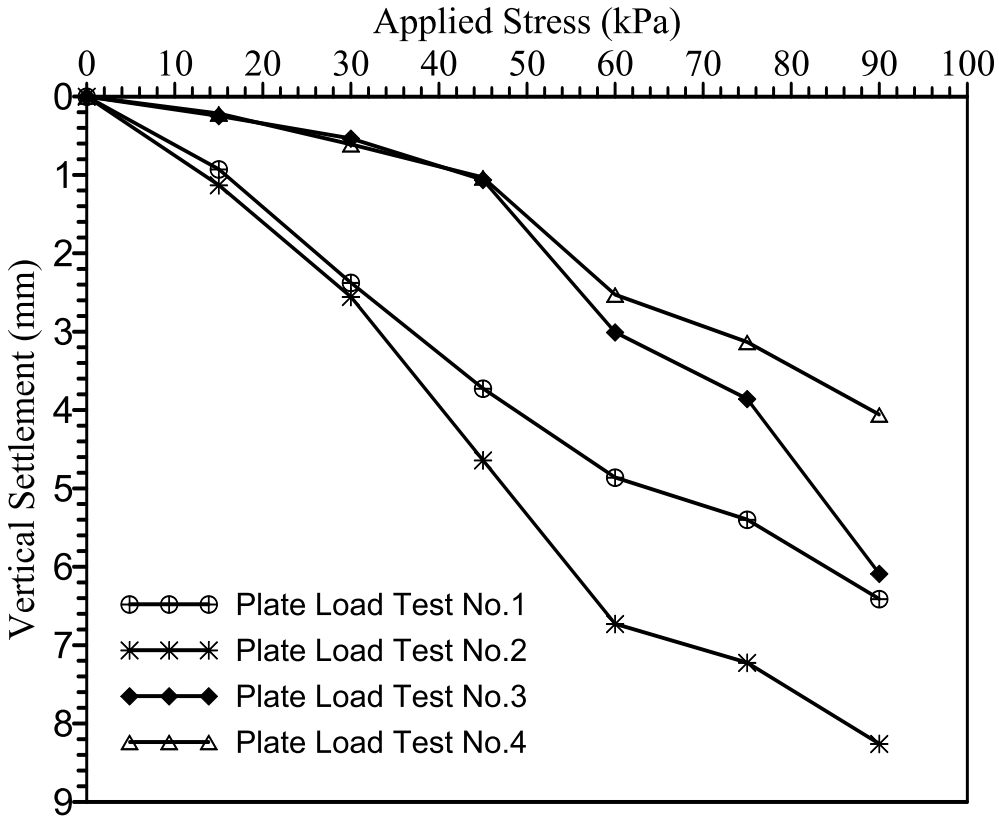

Figure 3-12: Full Scale Plate Load Tests in WHA for 2x2m plates resting on four Columns (data from Aiban, 2009).

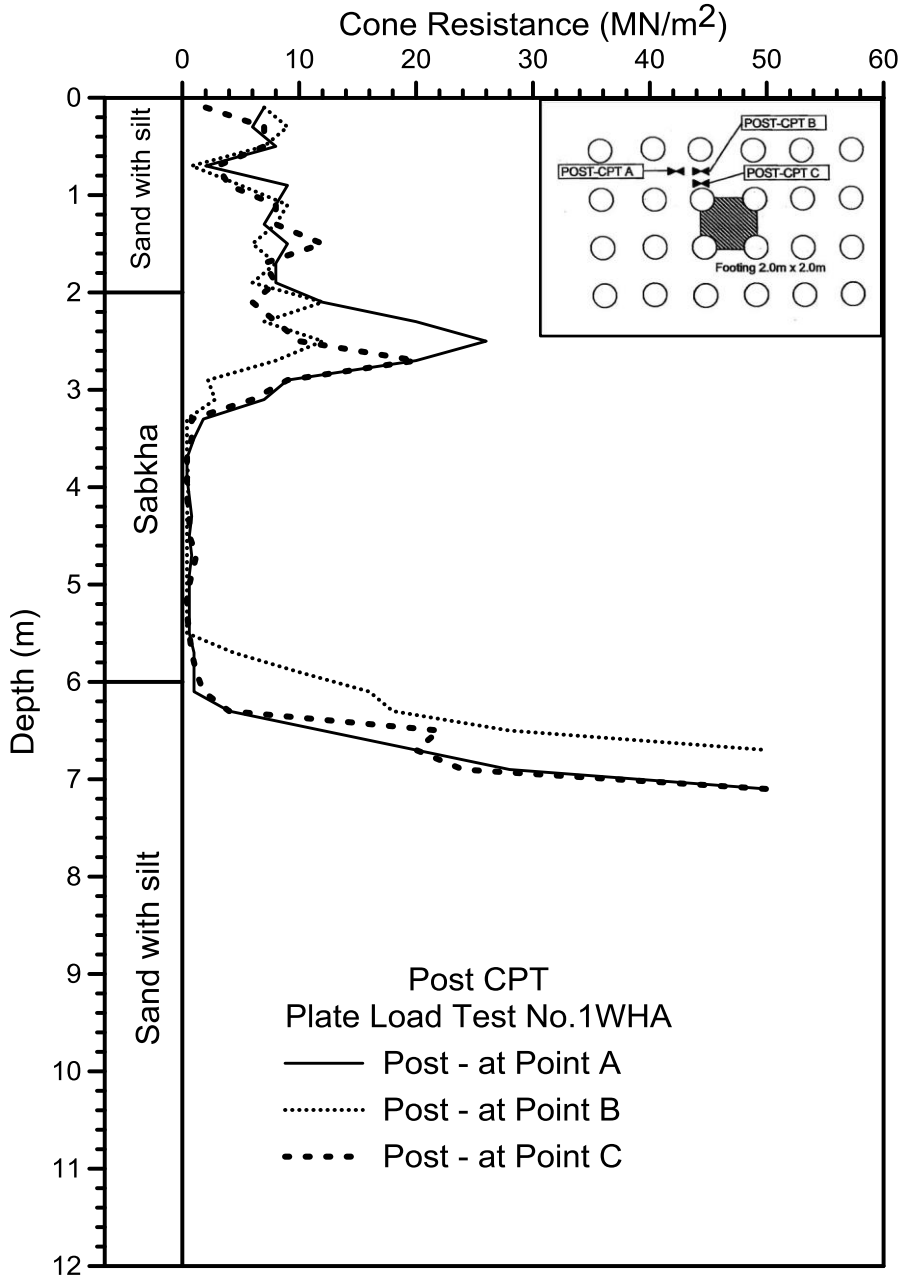

Figure 3-13: Post-CPT Cone Resistance around Plate Load Test No.1 (data from Aiban, 2009).

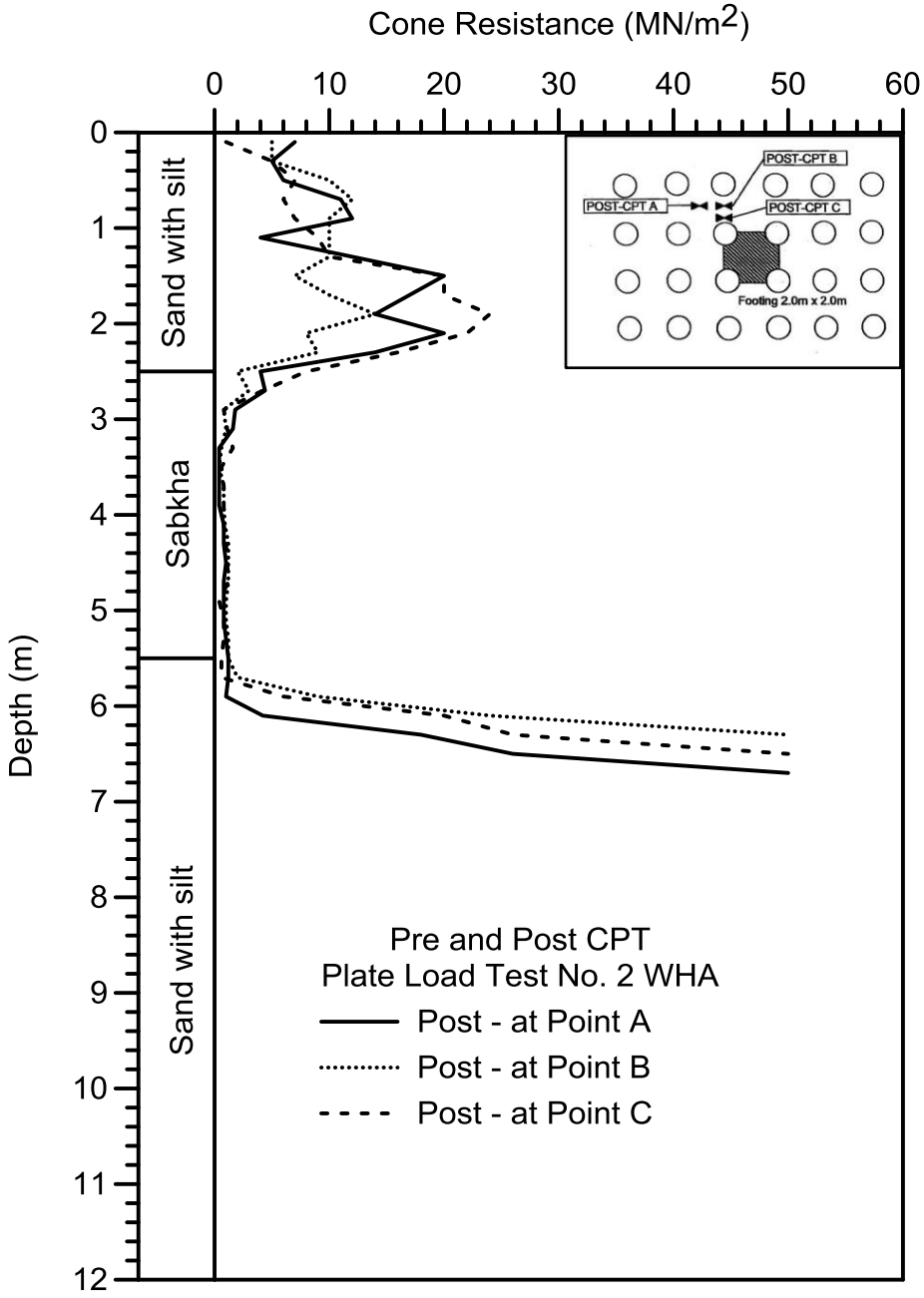

Figure 3-14: Post-CPT Cone Resistance around Plate Load Test No.2 (data from Aiban, 2009).

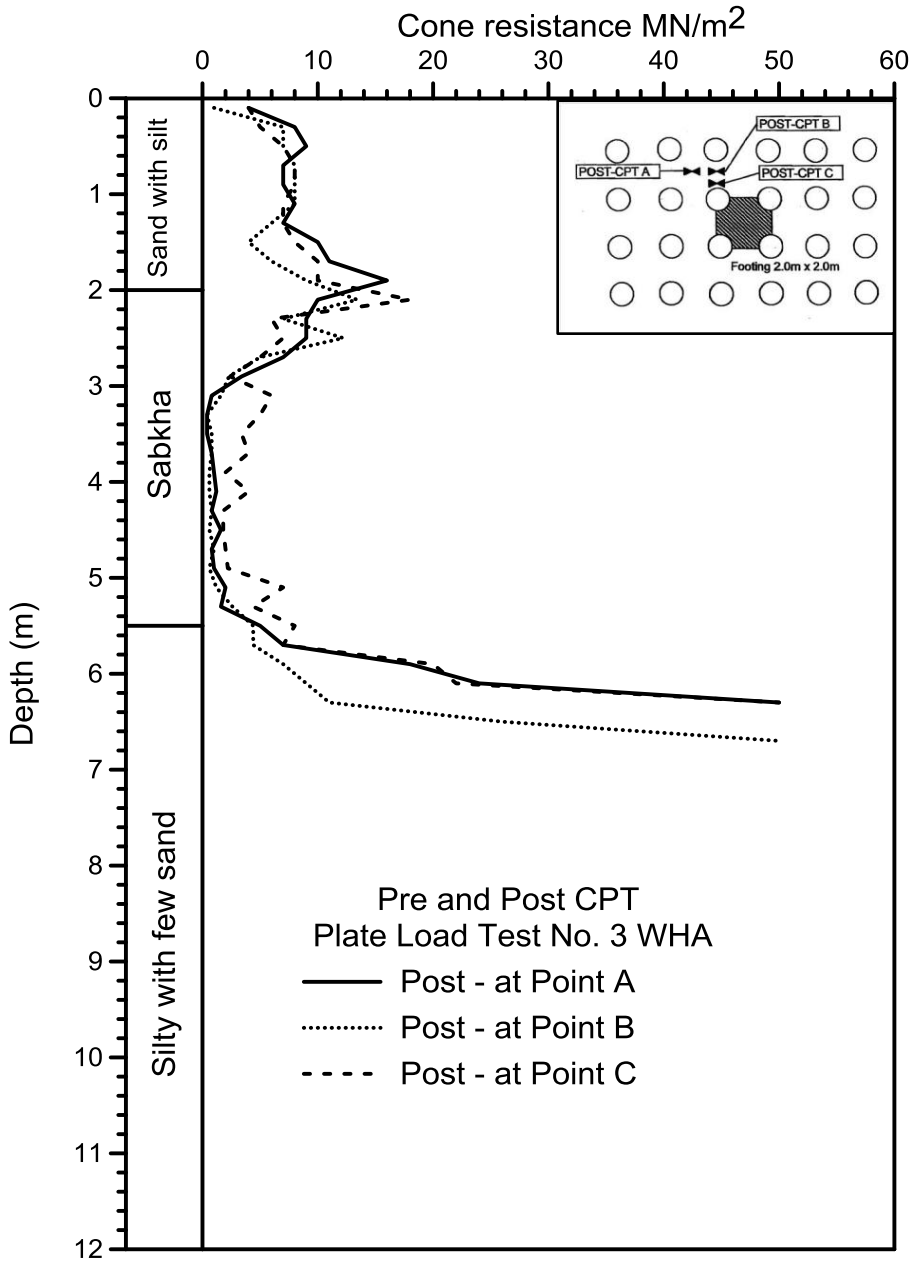

Figure 3-15: Post-CPT Cone Resistance around Plate Load Test No.3 (data from Aiban, 2009).

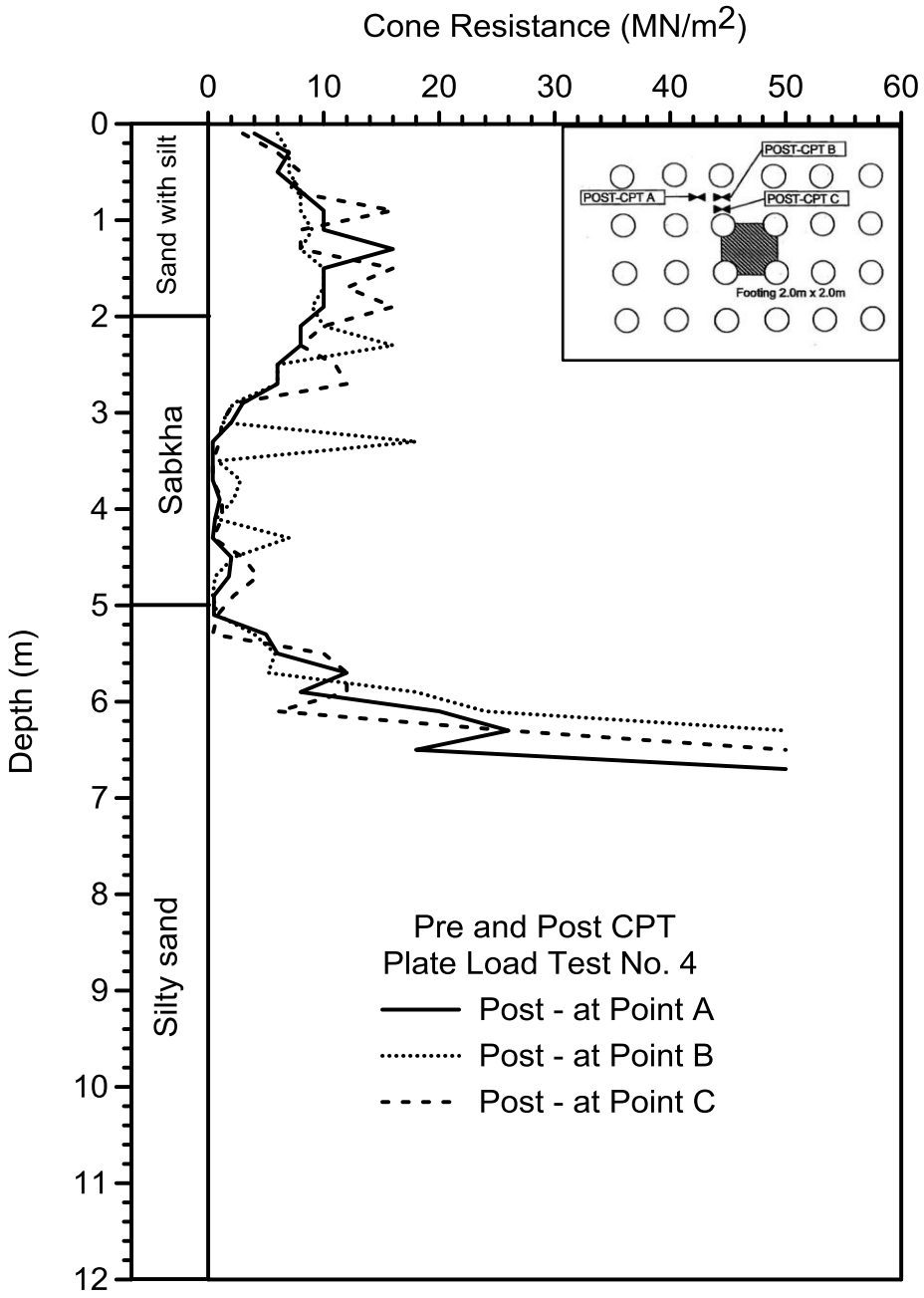

Figure 3-16: Post-CPT Cone Resistance around Plate Load Test No.4 (data from Aiban, 2009).

3.3 Case Study 2: Early Water Tank Project, Jubail Industrial City

Soil improvement by means of Vibro - replacement was used to improve the soil below the Early Water Tanks (EWT) in a Petrochemical Company Project – Jubail industrial city, in order to limit total and differential settlement, and to achieve the required bearing capacity. The tanks is 72m in diameter and 20m high and consists of steel shell. The tank is intended for firewater and drinking water for the entire plant.

3.3.1 Subsoil condition

A soil investigation program had been carried out in the area of the proposed plant; the stratigraphy observed from borings generally indicates the presence of top 2.5m loose to medium dense sand layer (recent backfill) followed by very soft compressible strata (Sabkha) up to 6m depths. The strata below Sabkha layer is comprised of medium to very dense sand up to the maximum depth of exploration. The soil condition under tank is summarized in Figure 3-17. The Ground water level is at an elevation of about EL= -1. 5m.

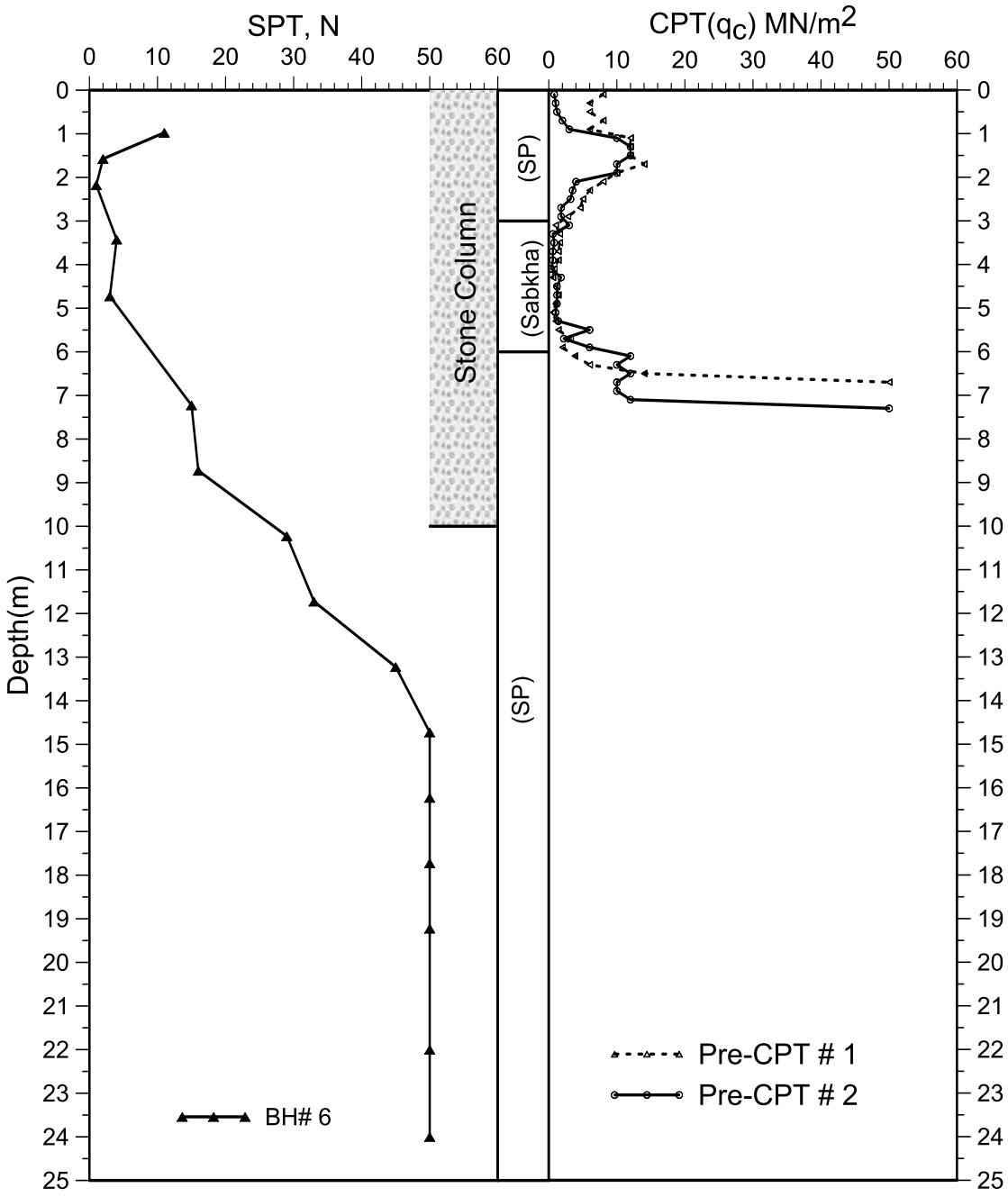

Figure 3-17: Soil Profile, SPT and Pre-CPT in EWT (data from Aiban, 2009).

3.3.2 Soil Improvement Work and Full-Scale Plate Load Test

The original soil conditions underneath the foundation was improved by the installing stone columns using wet method in a regular triangular grid 1.7x1.7m, which extends from existing ground level to the load bearing, medium dense sand layer at an approximate depth of 10 m.

In order to confirm the required design capacity of the 10 m working, stone column, plate load tests were performed. The size of the test footing was 2m×2m×0.6m. The footing was loaded as per loading schedule presented in Table 3-4. The load was applied using a hydraulic jack reacting against 120 tons kentledge platform of concrete blocks. The test was conducted in accordance with ASTM D1194. The results of the load tests are plotted in forms of load/settlement as shown in Figure 3-18.

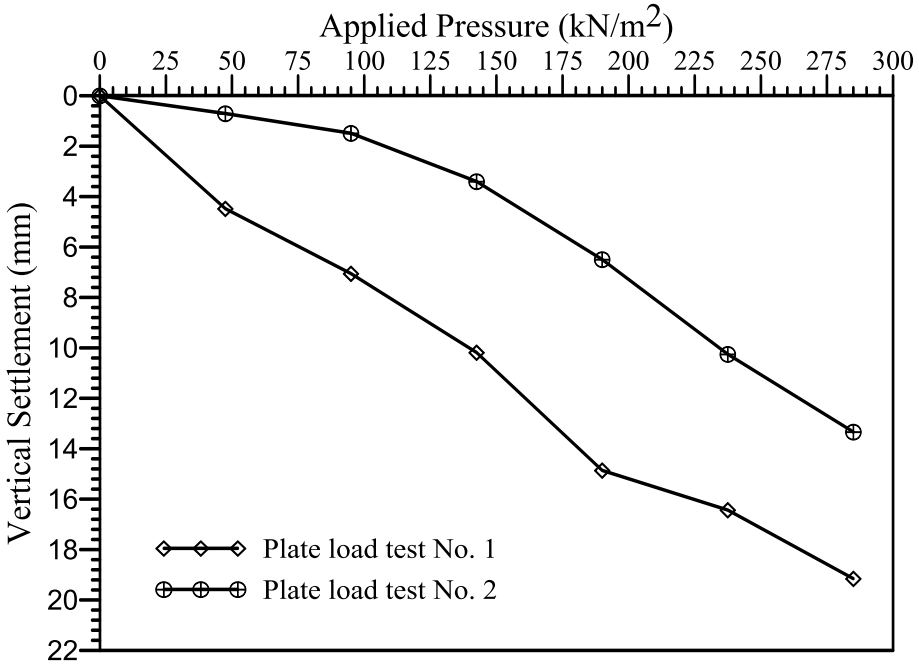

Figure 3-18: Plate Load Test No. 1 and 2 in Early Needs Tank (data from Aiban, 2009).

Three post-CPTs were carried out as shown in Figure 3-19 and Figure 3-20. The first was in the center of the group of stone columns, the second in the center of two stone columns, and third was 60 cm away from the center of stone column.

Table 3-4: The Loading Schedule for the Load Test in Early Needs Tank (data from Aiban, 2009).

Load %	Applied pressure (kPa)	Min-Time duration (Hr:min)
0	0	0
25	47.5	00:15
50	95	00:15
75	142.5	00:15
100	190	12:00
125	237.5	00:15
150	285	2:00
100	190	00:15
50	95	00:15
0	0	01:00

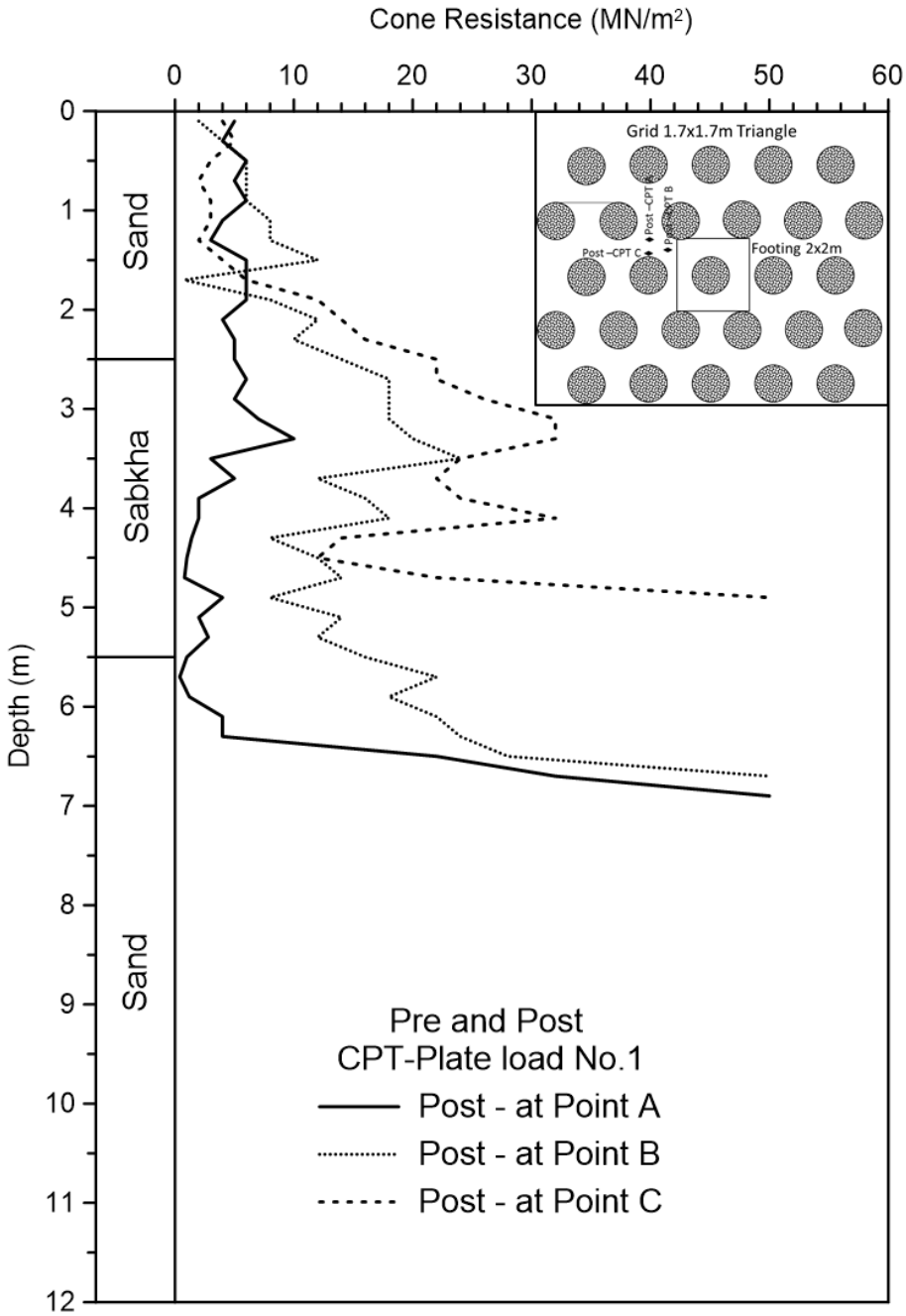

Figure 3-19: Post- CPT around Plate Load Test No. 1 in Early Water Tank (data from Aiban, 2009).

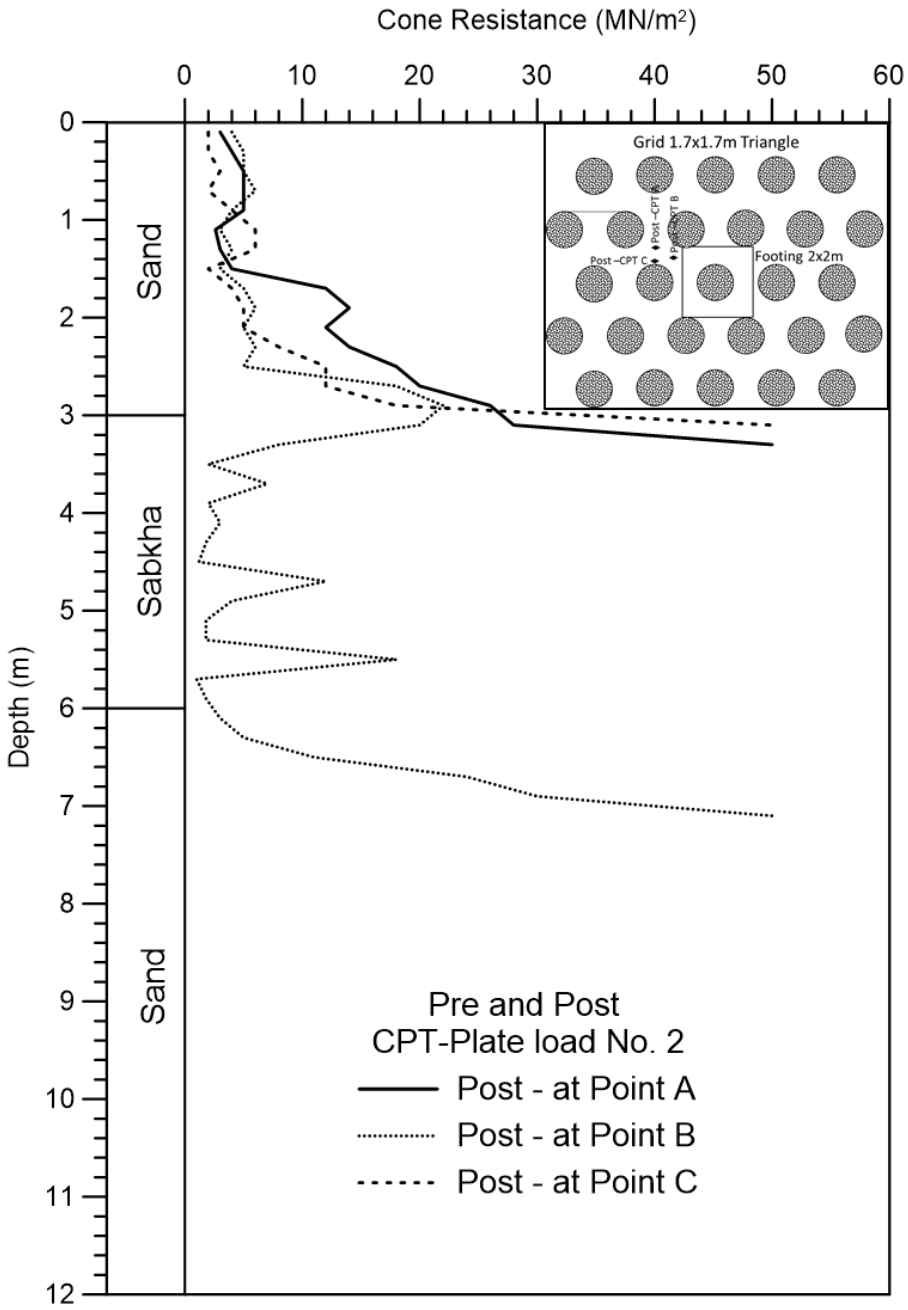

Figure 3-20: Post- CPT around Plate Load Test No. 2 in Early Water Tank (data from Aiban, 2009).

CHAPTER 4

EVALUATION OF SOIL IMPROVEMENT AFTER INSTALLATION OF STONE COLUMN

4.1 Introduction

Site characterization, in terms of geotechnical properties, can be the single most important task for geotechnical engineering investigations. Once a site has been realistically characterized in terms of geotechnical property taking into account the needs of a project, the foundation design or foundation performance evaluation can be achieved with greater economy and reliability. Stone columns improvement has been used on many construction sites to reinforce and densify weak soil layers by inserting stiff material and improve surrounding soils properties. Considering the changes that are occurring in the soil parameters will lead to better understanding of the performance of stone columns.

The goal of this Chapter is to discuss different methods that are used to assess the improvement of the soil layers (including Sabkha) upon installation of stone columns. Another objective is to develop new approach to predict the parameter of cohesionless and Sabkha soils that are affected by installation of stone columns, as these are of importance for stone column modeling. The study depends on published and field data collected from different locations in eastern Saudi Arabia.

4.2 Evaluation of Ground Improvement by Stone Columns

The performance of the stone column reinforced ground is evaluated through the changes achieved in the values of density, void ratio, and constrained modulus of the ground after installation (Massarsch and Fellenius, 2014, 2002; Murugaiah, 2004) . The most important tool for quality assurance and quality testing of ground improvement works through installation of stone columns, Cone Penetration Test (CPT) are more suitable and more preferable than normal Standard Penetration Test (SPT) (Mayne, 2007).

The Cone resistance value is governed by many factors including soil density, in-situ stresses, stress history, soil type and soil compressibility (Jacobs, 2004). Therefore Changes in shear strength, stiffness and density can be documented with changes in measured cone resistance (Massarsch and Broms, 2001). These tests generate full depth profiles against the design depth of stone columns and hence give a comparison of unimproved and improved ground conditions for the full depth.

In this study, a Comparison between Pre- and Post - CPT was conducted for three projects with different sabkha thickness and properties. The top layers above sabkha is classified as cohesionless soils with different conditions and properties. The stone columns were constructed using the wet method with different lengths and configurations.

The influence of stone column installation is represented by the ratio of tip resistance (Q_R) between the post-installation data and pre-installation data, given by:

$$\text{Tip resistance ratio, } Q_R = \frac{q_{t\_post\_installation}}{q_{t\_pre\_installation}} \quad (4\text{-}1)$$

Dove, (2000) suggested an improvement factor (I_d) to evaluate the improvement of soil after installation of stone columns using Vibrofloatation. The improvement factor (I_d) is calculated using the following equation:

$$I_d = \frac{A_{after}}{A_{before}} - 1 \quad (4\text{-}2)$$

$$A = \frac{\Delta x}{2}(q_{c1} + q_{c2}) \quad (4\text{-}3)$$

Where:

A_{after}: Area under Pre- cone tip resistance profile/curve.

A_{before}: Area under Post- cone tip resistance profile/curve.

q_{c1} and q_{c2}: Adjacent values of CPT profile, as illustrated in Figure 4-1.

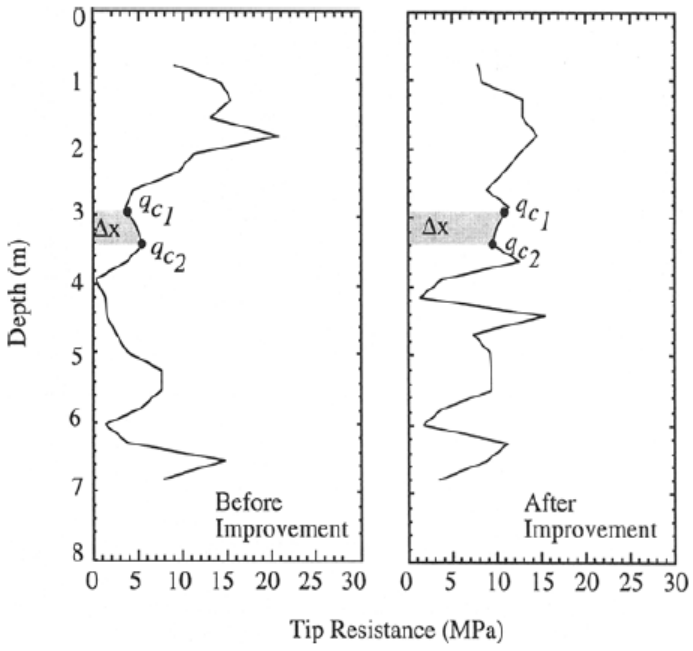

Figure 4-1: Determination of Areas Under Cone Tip Resistance Profiles (Dove et al., 2000).

Schaefer, (2004) discussed this method and reported that it could be used as quality control measurement technique (Schaefer and White, 2004). The use of this method requires CPT data before and after installation of stone columns. It is necessary that the pre and post CPT data are within the same area of improvement to minimize the effects of soil conditions' variations (Dove et al., 2000). In this study, the improvement index and tip resistance ratios are used to evaluate the improvement in the soil layers resulting from installation of stone columns in two projects.

4.2.1 Evaluation of Ground Improvement in EWT

Comparison between pre and post-improvement CPT tests and improvement factors in the EWT are presented in Figure 4-2 to Figure 4-5. Relationships between tip resistance ratio and depth of soil layers in EWT are illustrated in Figure 4-6. In general, there are slight improvements occurring in the top sand layer. There are several possible explanations for the non-improvement occurring in some points including lack of confinement on the surface and presence of some cemented materials in the sand before installation of stone columns.

This cementation will break down as a result of vibrations accompanying the stone columns installation. Massarsch and Fellenius, (2014) reported that increase in sleeve friction, as a result of Vibro stone column compaction, must be caused by an increase in horizontal stress (Massarsch and Fellenius, 2014).

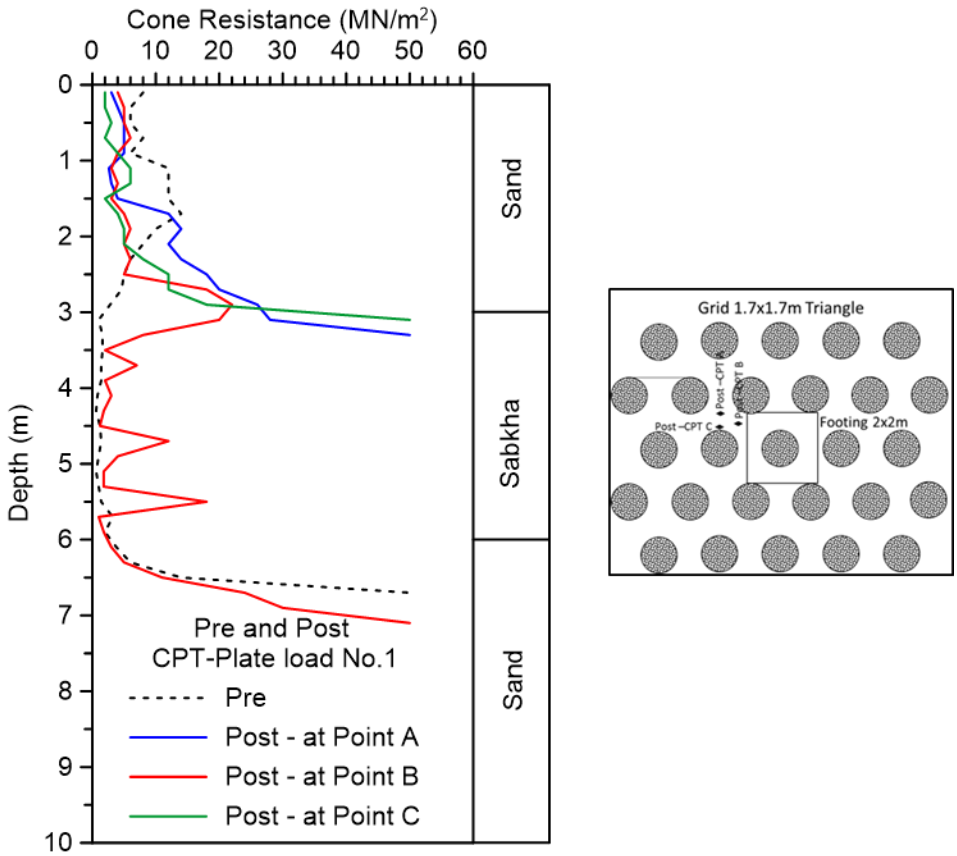

Figure 4-2: Pre and Post- CPT within Plate Load Test No. 1, the EWT.

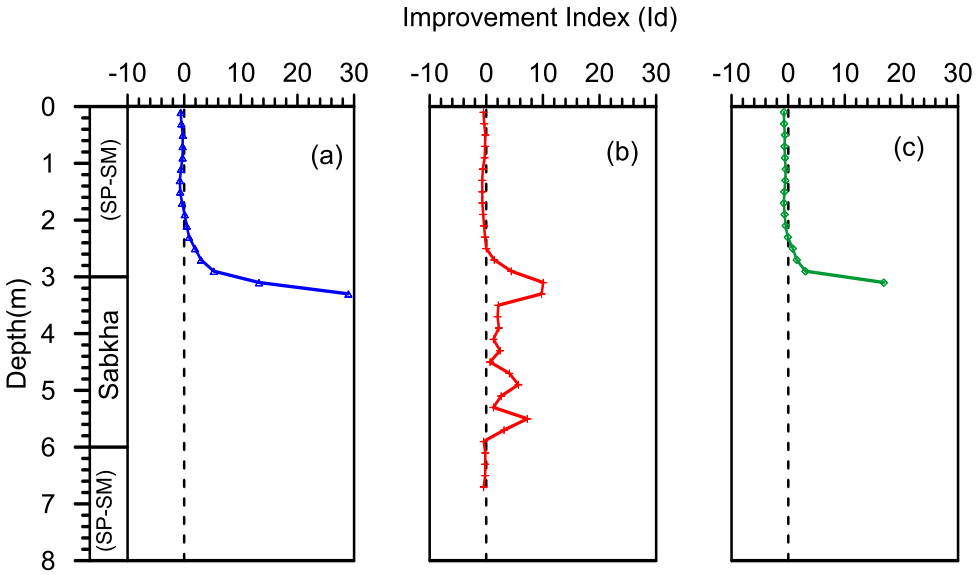

Figure 4-3: Improvement Index at Plate Load Test No.1, the EWT.

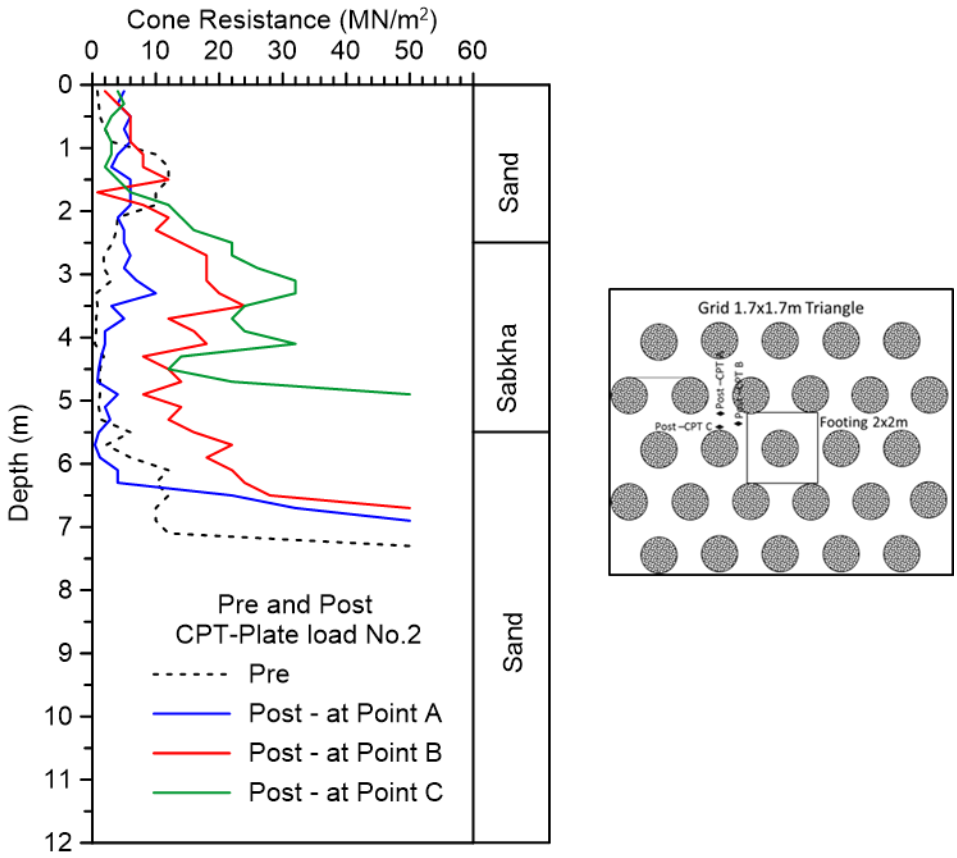

Figure 4-4: Pre and Post- CPT within Plate Load Test No. 2, the EWT.

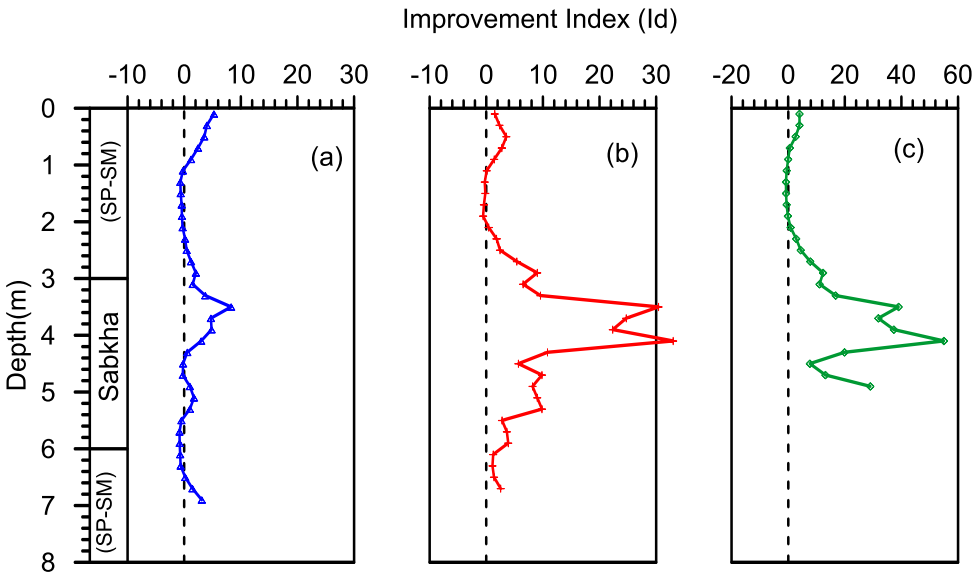

Figure 4-5: Improvement Index at Plate Load Test No.2, the EWT.

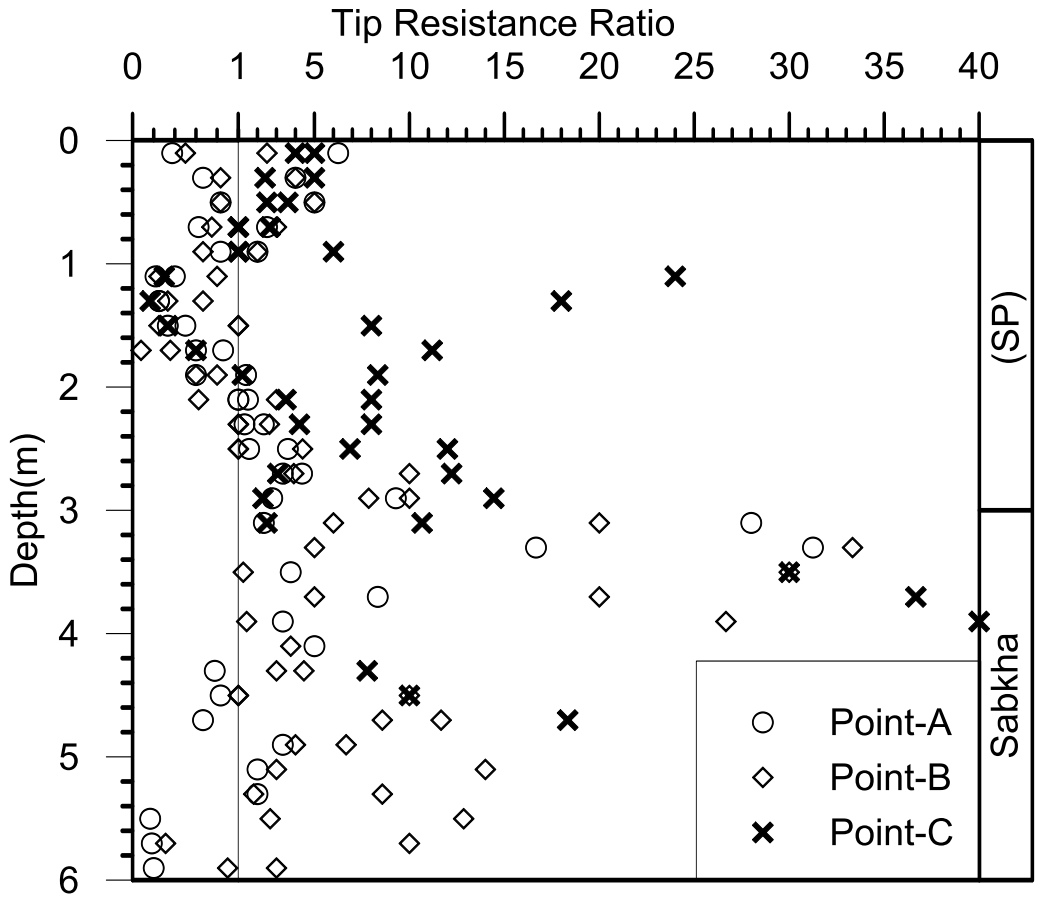

Figure 4-6: Tip Resistance Ratio Versus Depth for DCP tests within Plate Load Test 1 and 2 in the EWT.

Significant improvement occurred in the Sabkha layer especially at the top 1 to 1.5m. The explanations for the improvement occurring in the Sabkha may be due to its sandy clayey nature with shell fragments mixed with sand from top layers.

The value of CPT tip resistance and sleeve friction in the sand layer below Sabkha (to a depth of 15m) is approximately the same in pre and post installation of stone columns. The strength of this layer before inserting the stone columns is high. The Pre-CPT 20 MN/m^2 is at 6m depth and refusal is at 7m. Therefore, the vibration accompanying the installation of stone columns may not cause significant improvement in this layer; assessment with CPT refusal is not possible.

4.2.2 Evaluation of Ground Improvement in WHA

Comparison between pre and post-improvement CPT in the WHA is presented in Figure 4-7 to Figure 4-16. Variations of tip resistance ratios with depth of soil layers are illustrated in Figure 4-17. Slight improvement occurred in the cohesionless layers above sabkha where clean sand or sand with silt is present. There are some points where the Pre-CPT values are higher than the Post-CPT. This is due to the reduction in density of the top layer upon vibration and the lack of confinement at the surface of the cohesionless material layer.

The Post-CPT tests show good improvement in the upper part of the sabkha to depth of 1m from its top. No significant change was noticed in the remaining sabkha depth. The possible explanation for improvement of the top portion of sabkha is the consolidation resulting from the 2.7 m recent backfill and the fact that this part of the Sabkha is somehow sandy. Full consolidation is taking longer time for Sabkha but this is relatively quick near the sand top layer. Dry sieve analysis presented in Chapter 3 shows that sabkha under 4 m depth contains very fine materials (70% <0.075mm). Field observations have shown that Vibro compaction methods are generally ineffective when the percentage (by weight) of fines exceeds 20% (Brown, 1989). Hussin, (1987) and Mackiewicz, (2007) reported that no significant enhancement was obtained with Vibro-stone column method when the fine materials exceeded 12% and the degree of enhancement is more critical to the quantity of the clay content than to the silt content (Hussin and Ali, 1987; Mackiewicz and Camp, 2007).

The soil under sabkha was classified mainly as sand and has high Pre-CPT value (more than 20 MN/m^2). This high CPT value increases with depth and reaches refusal at a depth

of about 8 m. Table 4-1 shows refusal for pre and post-CPT. The decrease in refusal depth indicates that there are slight enhancements in this layer due to installation process of stone columns.

Table 4-1: Compare between Pre and Post- CPT Refusal Point in the WHA.

Plate Load Test, #	Pre-CPT Refusal (m)	Post-CPT Refusal (m)		
		Point A	Point B	Point C
1	7.9	7.1	6.7	7.1
2	7.7	6.5	6.7	6.3
3	7.5	6.3	6.7	6.3
4	7.5	6.7	6.3	6.5
5	7.7	7.7	7.3	-

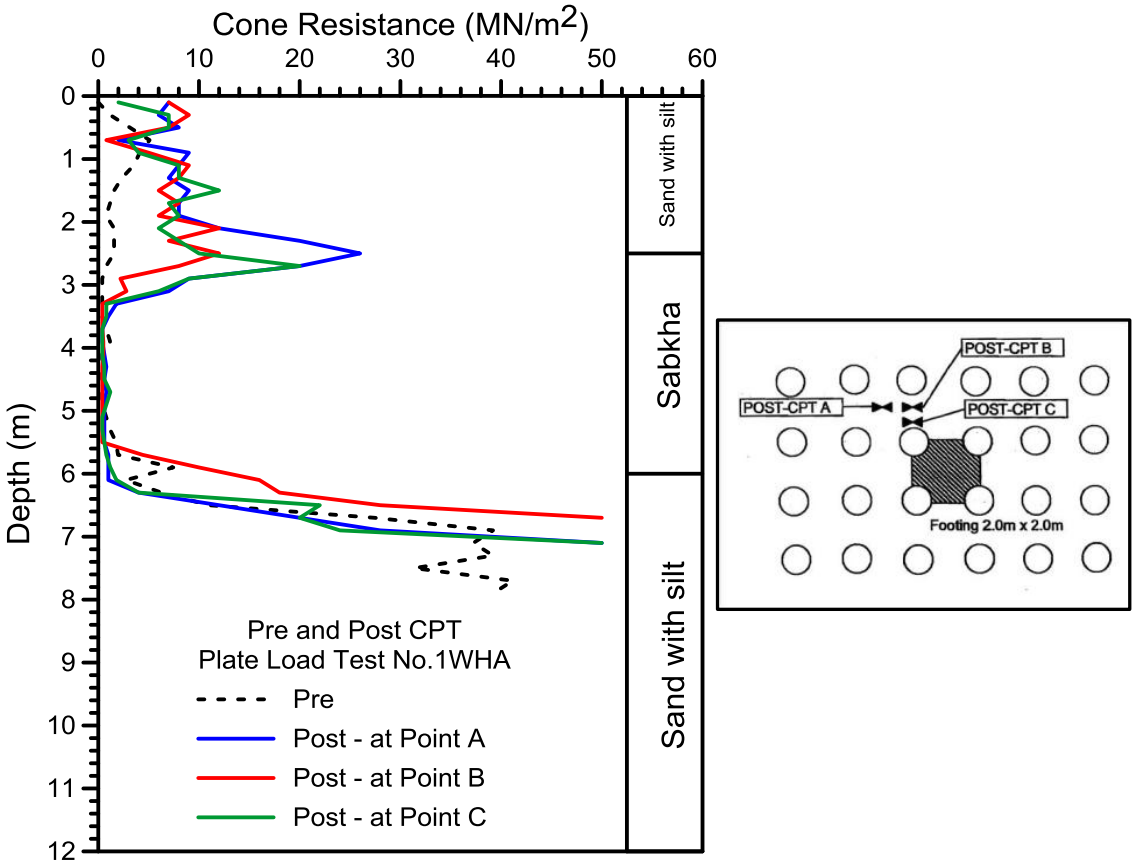

Figure 4-7: Pre and Post- CPT within Plate Load Test No. 1, the WHA

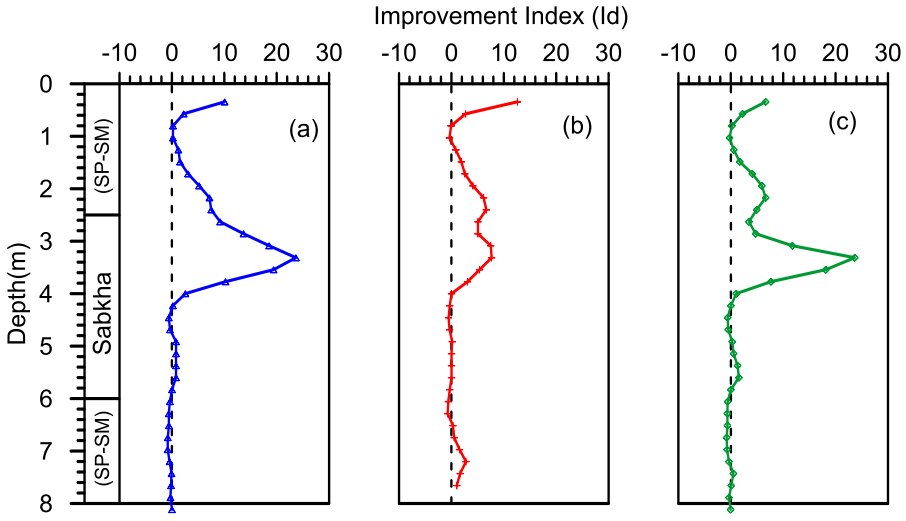

Figure 4-8: Improvement Index within Plate Load Test No.1, the WHA

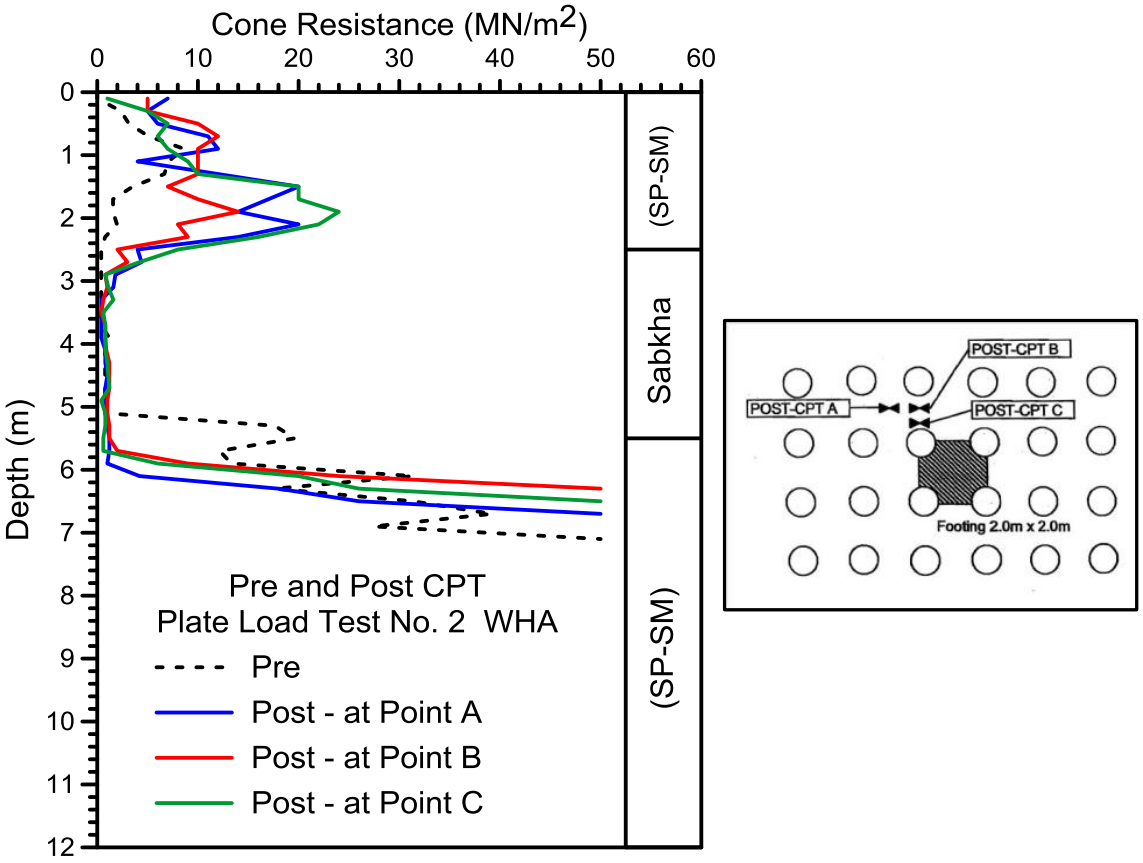

Figure 4-9: Pre and Post- CPT within Plate Load Test No. 2, the WHA

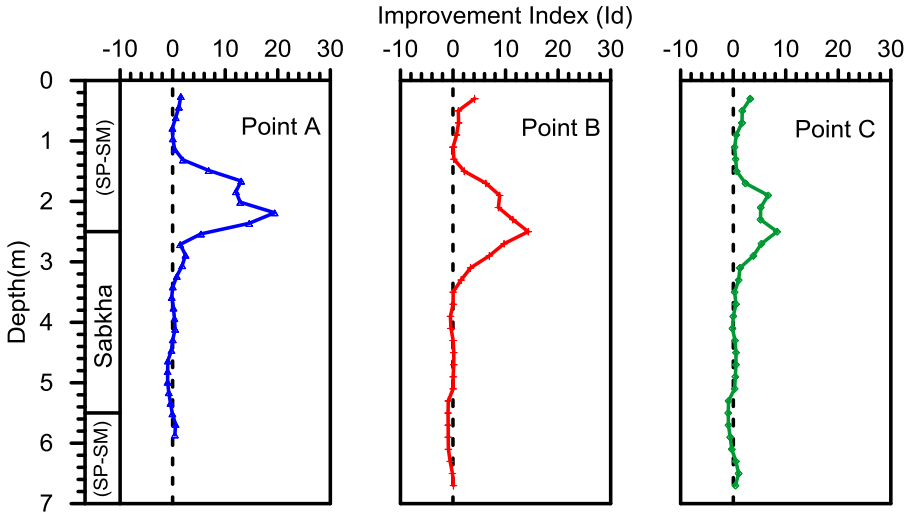

Figure 4-10: Improvement Index within Plate Load Test No.2, the WHA

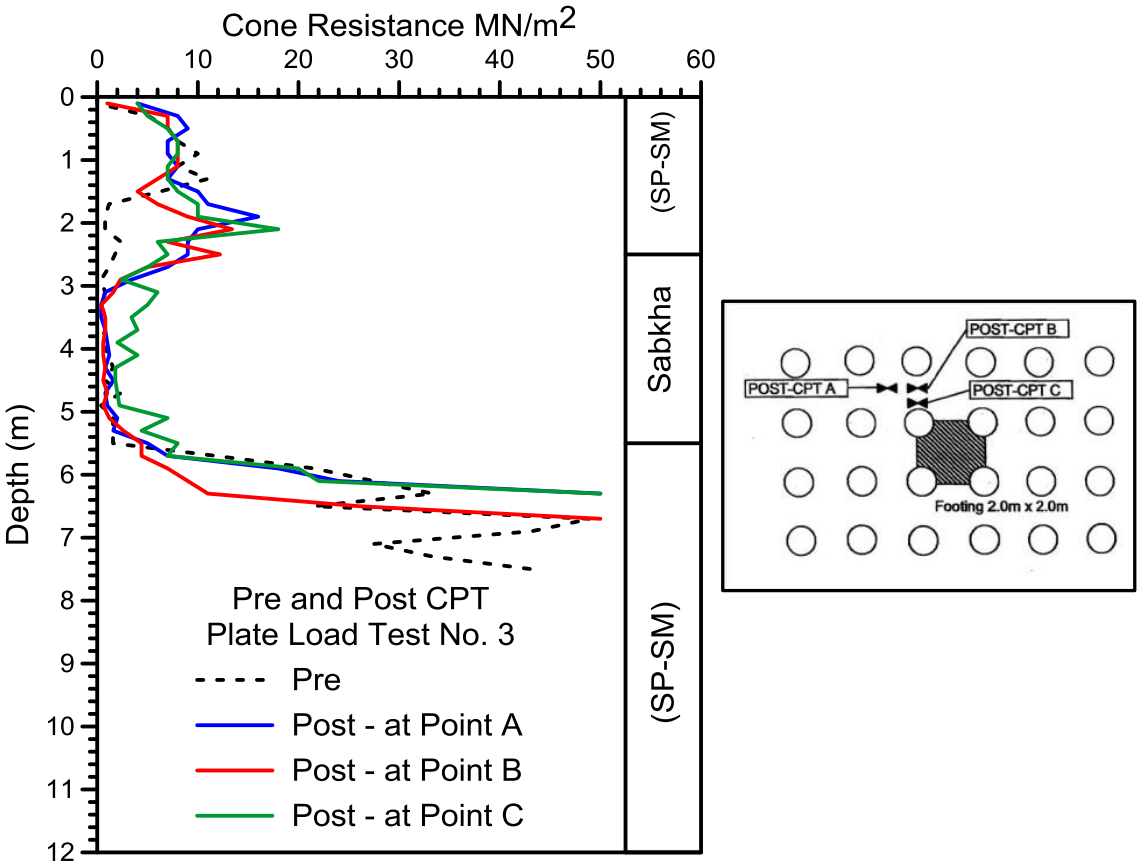

Figure 4-11: Improvement Index within Plate Load Test No.3, the WHA

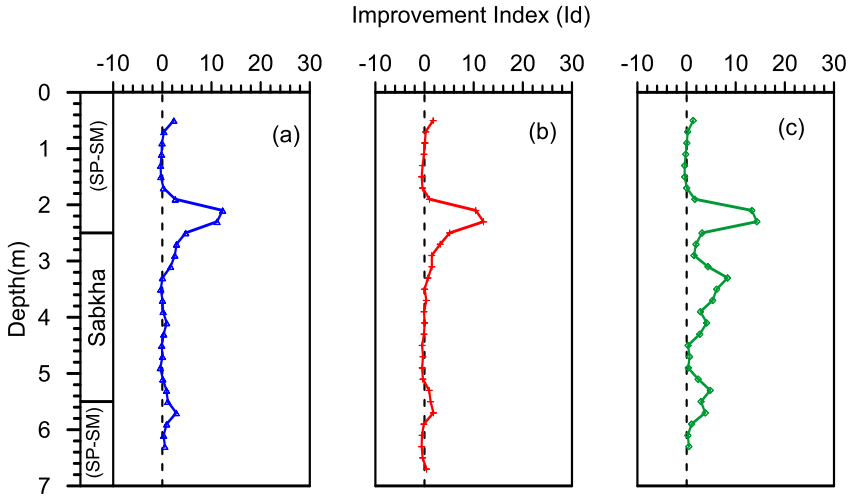

Figure 4-12: Improvement Index within Plate Load Test No.3, the WHA

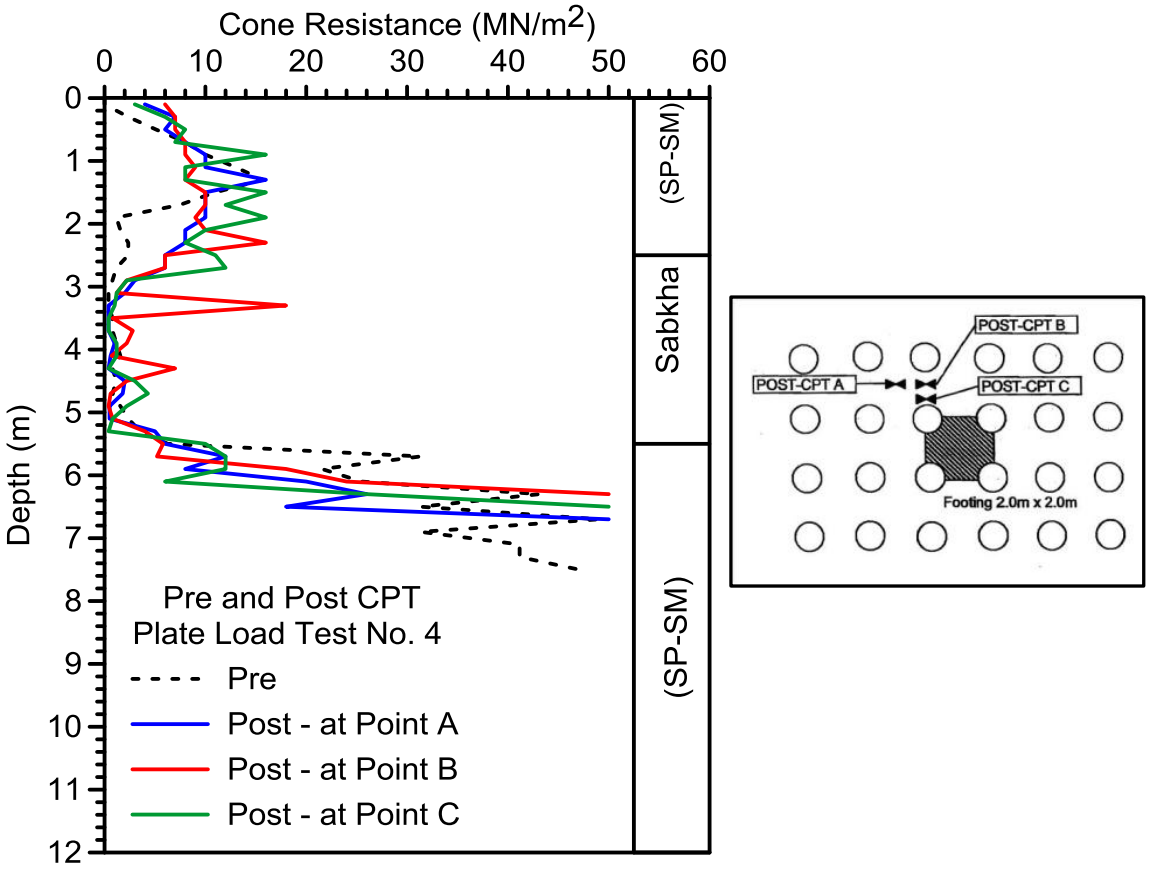

Figure 4-13: Pre and Post-CPT within Plate Load Test No. 4, the WHA.

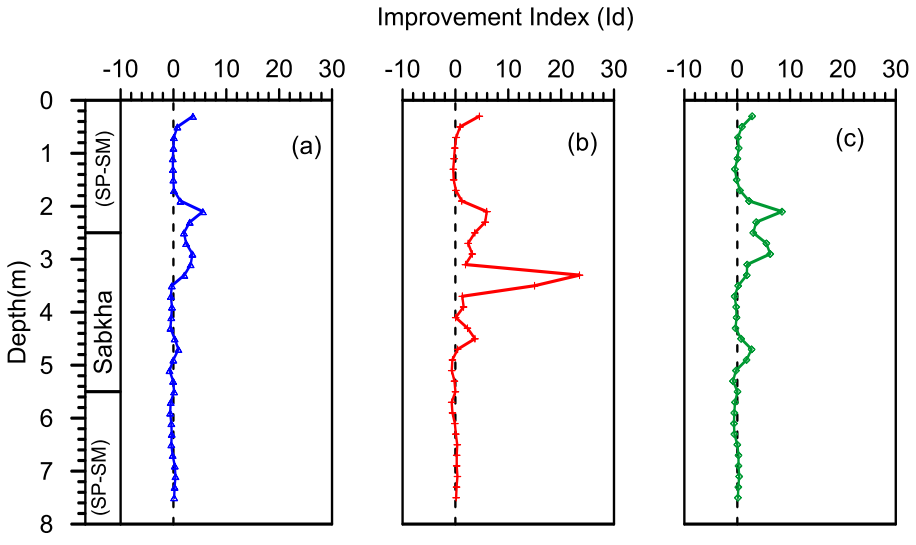

Figure 4-14: Improvement Index within Plate Load Test No.4, the WHA.

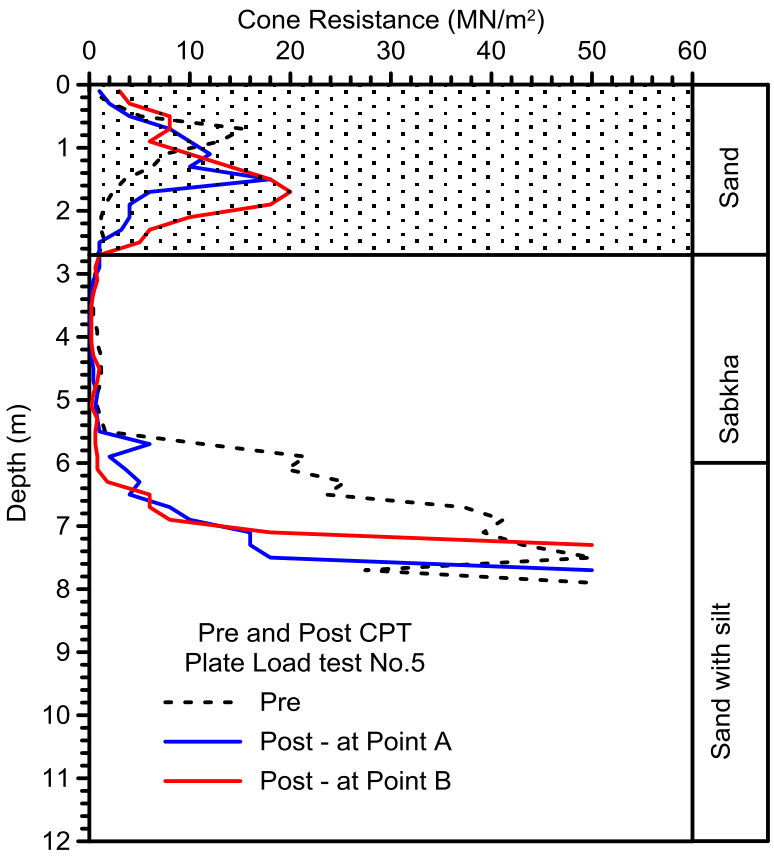

Figure 4-15: Pre and Post-CPT within Plate Load Test No.5, the WHA.

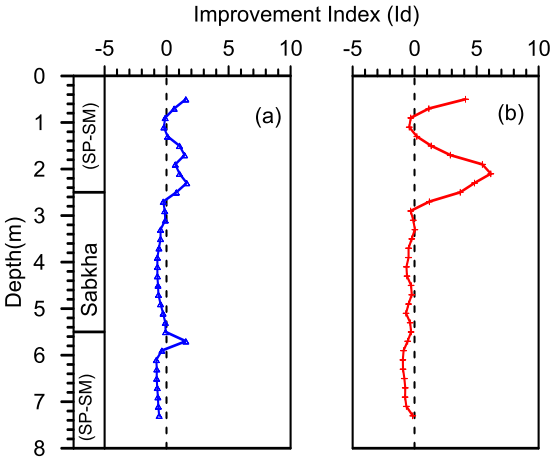

Figure 4-16: Improvement Index within Plate Load Test No.5, the WHA.

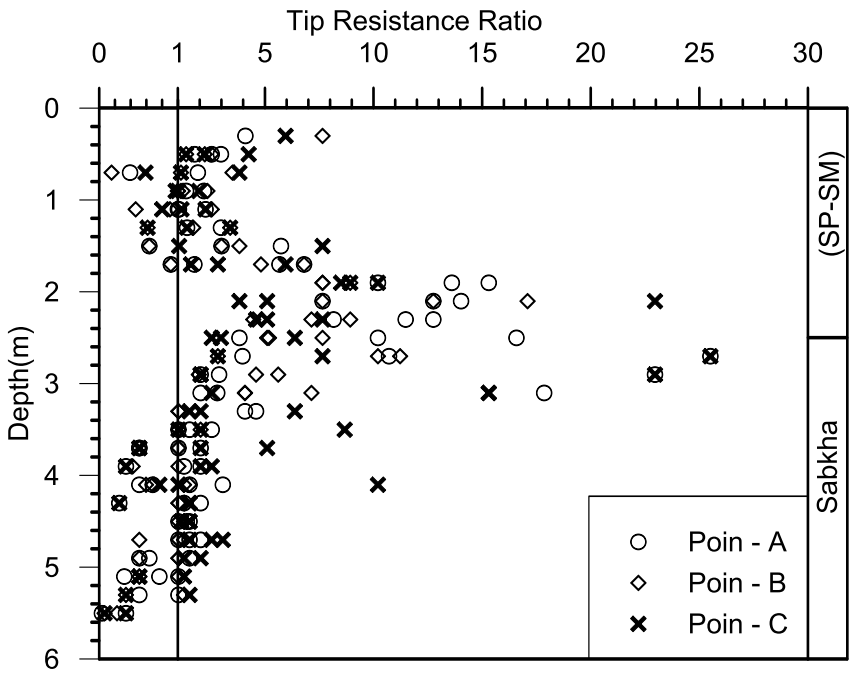

Figure 4-17: Tip Resistance Ratio versus Depth in Plate Load Test 1, 2, 3, and 4 in the WHA.

4.3 Assessment of Soil Compressibility Due to Stone Column

By assessing soil compressibility prior to the compaction work it is possible to determine whether, and to which degree, soil compaction will be required (Massarsch, 2002, 1991; Massarsch and Broms, 2001; Massarsch and Fellenius, 2014, 2002). Massarsch, (1991) developed compactability criteria which depends on the CPT to evaluate the ability of soil to be compactable or not after vibration compaction. Massarsch (1991), suggested that soils subjected to Vibro compaction can be categorized as "compactable", "marginally compactable", and "not compactable" as shown in Figure 4-18. This approach is based on the cone tip resistance and friction ratio (Massarsch, 1991). Such

method is used in this study to assess the ability of cohesionless and Sabkha soils to improve density after installation of stone columns.

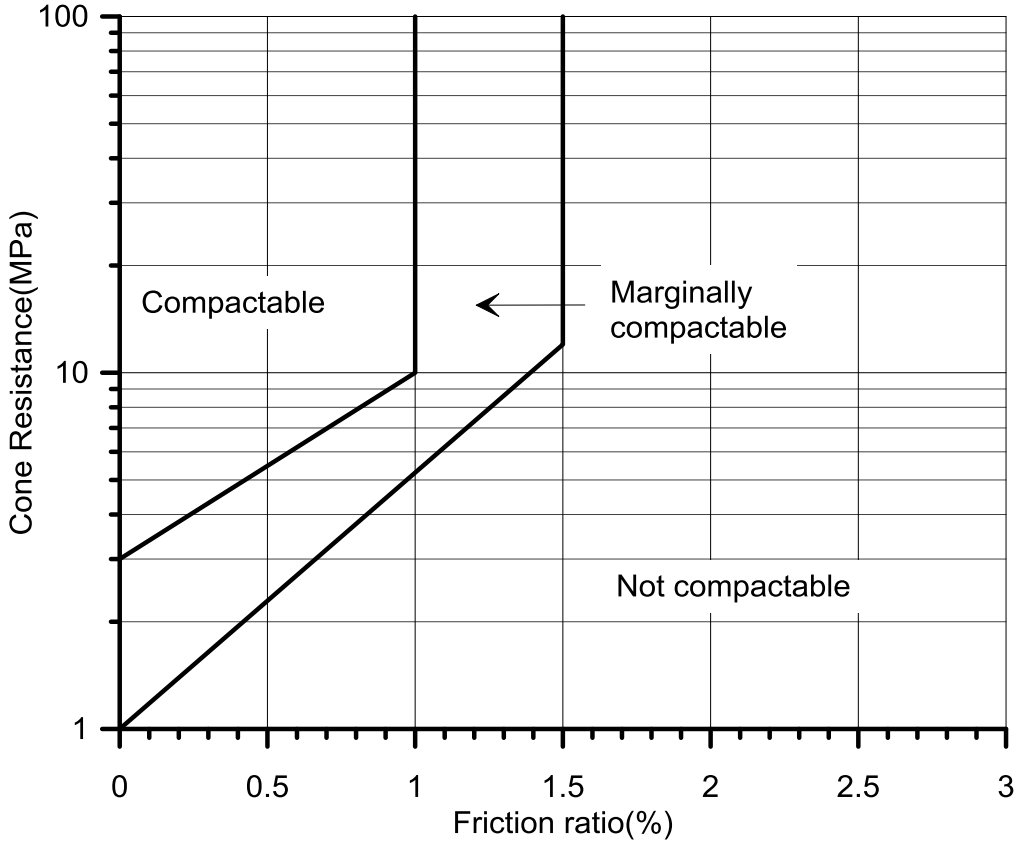

Figure 4-18: Soil Classification for Vibratory Compaction after Massarsch, (1991).

Relationships between friction ratio and cone resistance in EWT are shown in Figure 4-19 and Figure 4-20. A visual review of the data points in the two figures indicates that the upper sand layer is located in all ranges, namely “compactable”, “marginally compactable” and “not compactable”. However, sabkha soil points concentrated in “marginally compactable” to the “not compactable” categories, and the sand with silt under sabkha exhibited compactable category.

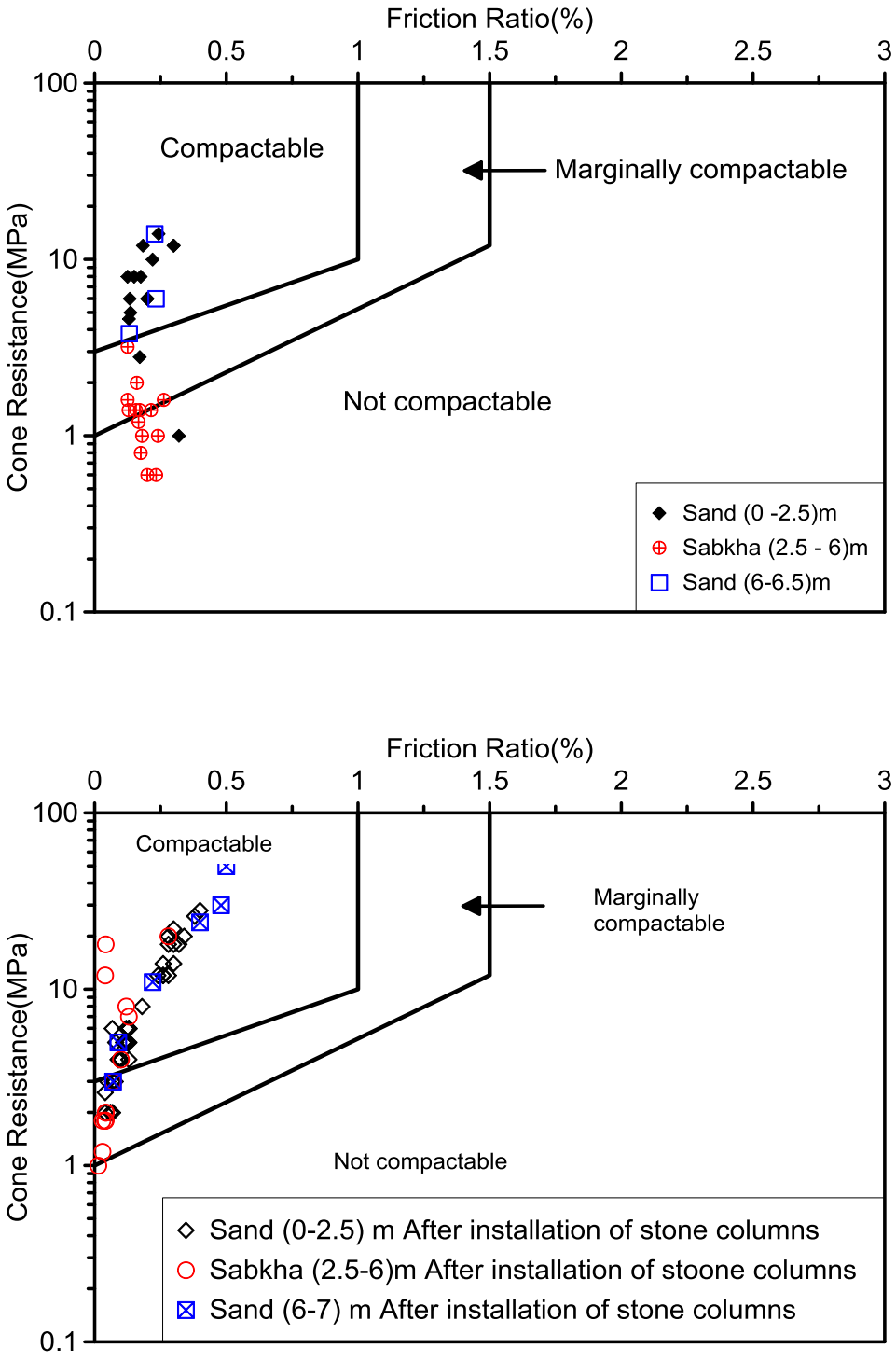

Figure 4-19: Evaluation of Vibratory Compaction at Plate Load Test No.1 in the EWT based on the work of Massarch, (1991).

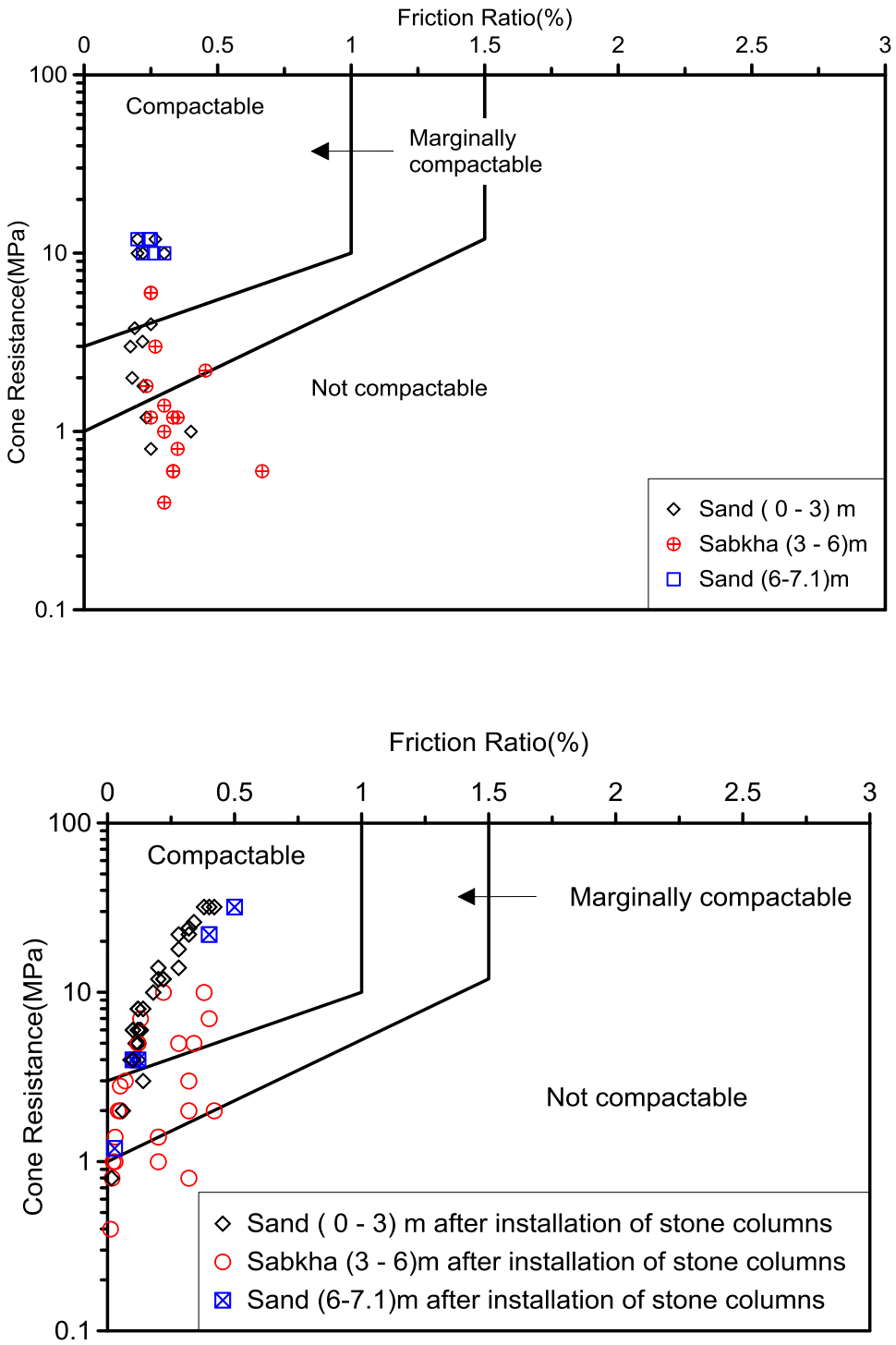

Figure 4-20: Evaluation of Vibratory Compaction within Plate Load Test No.2 in the EWT after Massarch, (1991).

Figure 4-21 to Figure 4-24 show relations between the friction ratio and cone tip resistance in WHA. A visual review of the data in the four figures indicates that the upper layers is located in the range of compactable to the marginally compactable and few points are in compactable category. The Sabkha soils depth in this area range is from 5 to 6 m from the surface. The upper part from this layer (about 1 m) exhibited marginally compactable while the remaining layer points concentrated in "not compactable" category.

The layer under Sabkha in this case is classified as sand with silt to depth range from 15 to 18 m from the surface. The refusal point in these layers is not more than 7.9 m deep, so the data plotted in the figures represents only the upper part of these layers. The points are concentrated in the compactable to the marginally compactable and few points are in "not compactable" category.

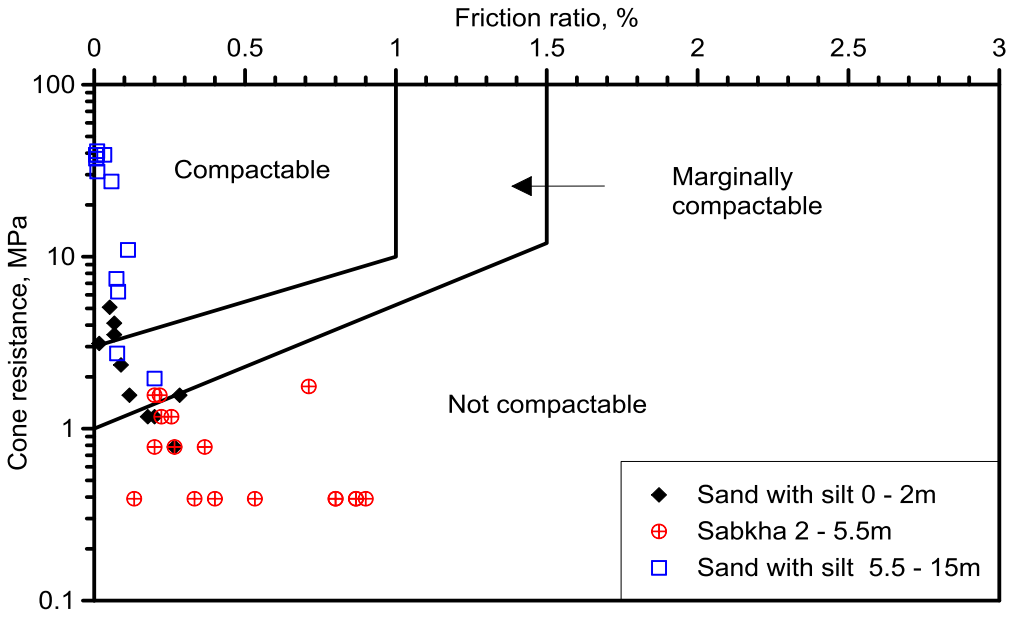

Figure 4-21: Evaluation of Vibratory Compaction at Plate Load Test No.1 in the WHA after Massarch, (1991).

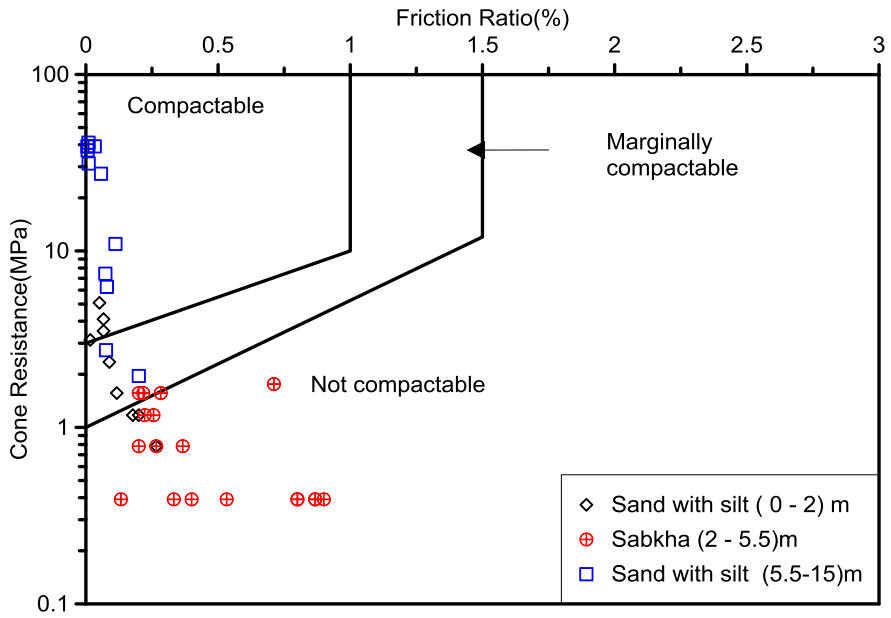

Figure 4-22: Evaluation of Vibratory Compaction at Plate Load Test No.2 in the WHA (After Massarch, 1991).

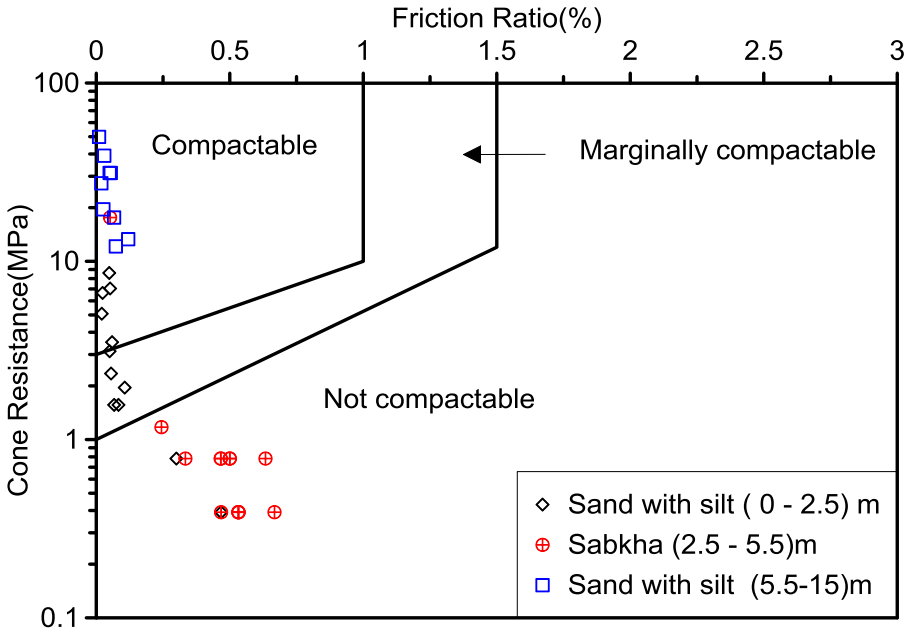

Figure 4-23: Evaluation of Vibratory Compaction at Plate Load Test No.3 in WHA (after Massarch, 1991).

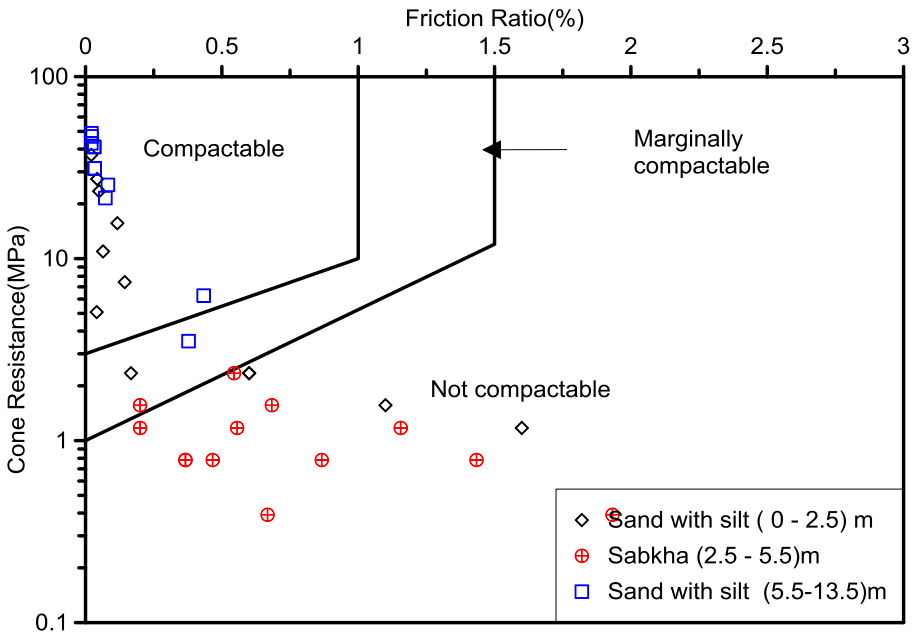

Figure 4-24: Evaluation of Vibratory Compaction at Plate Load Test No.4 in WHA (after Massarch, 1991).

4.4 Improvement Factor of Cohesionless Layer above Sabkha

Based on the above case study data, the improvement factor for cohesionless layer above sabkha soil is proposed to estimate the improvement occurring in this layer due to installation of stone columns. The improvement degree achieved within the case study areas are listed in Table 4-2 and Table 4-3. Values presented in this table were obtained from the comparison of pre-treatment and post-treatment soil properties with depth. The compaction effects are most pronounced in soils with a low initial density.

Table 4-2: The Improvement Degree Achieved in Upper Layers in EWT.

Plate Load Test	Layer thickness, m	Ave, Pre-CPT	Ave, Post-CPT		Change, %
1	3	8.03	Point A	10.98	36.74
			Point B	7.56	-5.85
			Point C	8.81	9.71
2	2.5	4.98	Point A	5.19	4.22
			Point B	9.43	89.36
			Point C	11	120.88

Table 4-3: The improvement Degree Achieved in Upper Layers in WHA.

Plate Load Test	Layer Depth, m	Ave, Pre-CPT	Ave, Post-CPT		Change, %
1	2	2.2	Point A	7.6	245.45
			Point B	7.1	222.73
			Point C	5.5	150.00
2	2.5	3.1	Point A	11.92	284.52
			Point B	11.23	262.26
			Point C	8.62	178.06
3	2.5	4.8	Point A	8.85	84.38
			Point B	7.66	59.58
			Point C	8.08	68.33
4	2.5	6.15	Point A	8.69	41.30
			Point B	8.77	42.60
			Point C	9.92	61.30

Average pre and post-CPT values versus depth, are presented in Figure 4-25 for the ground improvements by Vibro-stone columns. In case of very loose conditions, (Pre-CPT< 4 MN/m^2) significant improvement must have occurred due to the installation

effect of Vibro-stone columns and the relative density conditions changed to medium (Post-CPT between 4 to 12 MN/m^2). In case of medium relative density condition (Pre-CPT from 4 to 12 MN/m^2), data shows slight increase in the majority of points and decrease in few points.

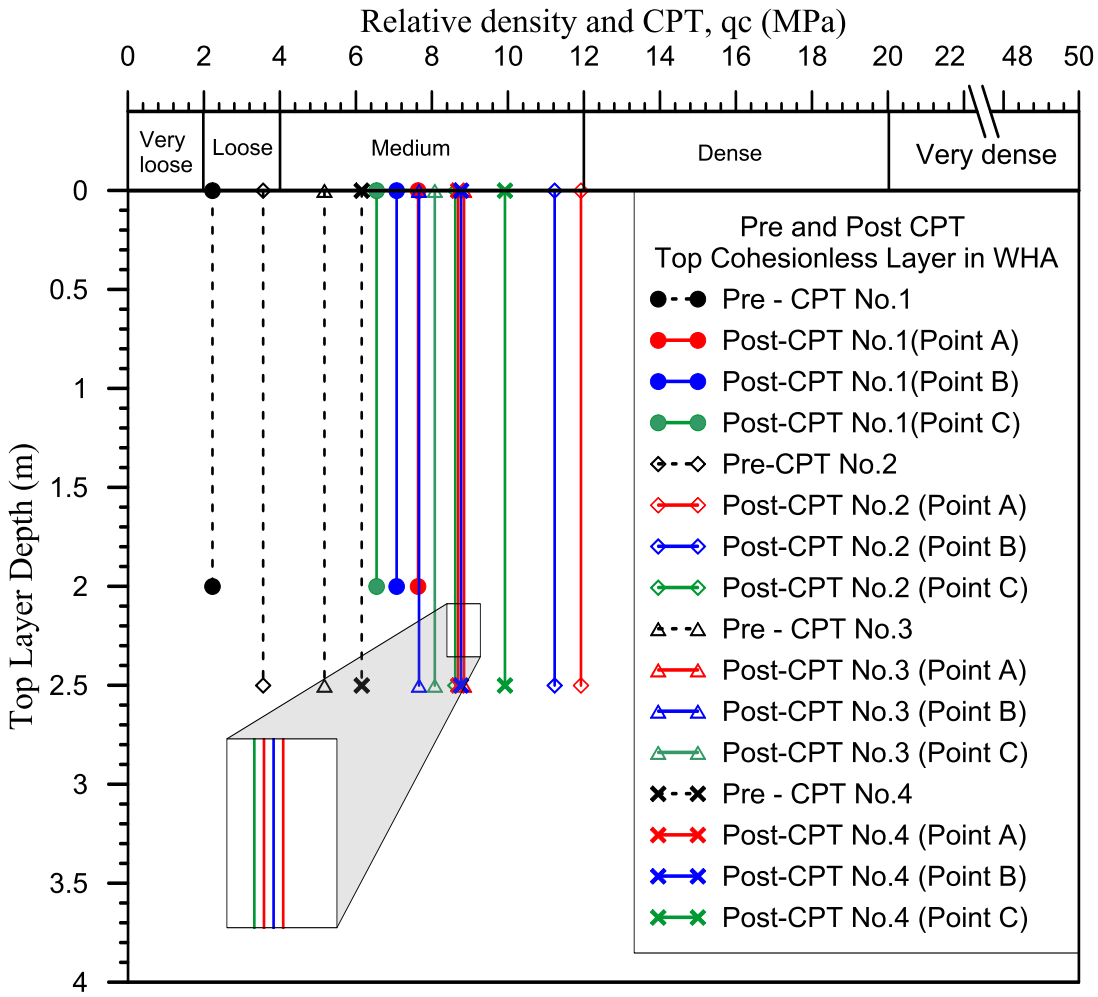

Figure 4-25: Average Pre and Post-CPT Values Versus Depth in Top Layers in WHA.

According to the behavior of the top (3m thick) cohesionless soil layer, the improvement factor can be used to predict the Post-CPT as shown in Figure 4-26. This factor is limited only to the case of cohesionless layer above sabkha soils and can be used as one of the quality control tools after installation of Vibro stone columns.

The value of Post-CPT can be predicted as:

$$\text{Average Post\_CPT} = \text{Improvement factor} \times \text{Average Pre\_CPT} \qquad 4\text{-}4$$

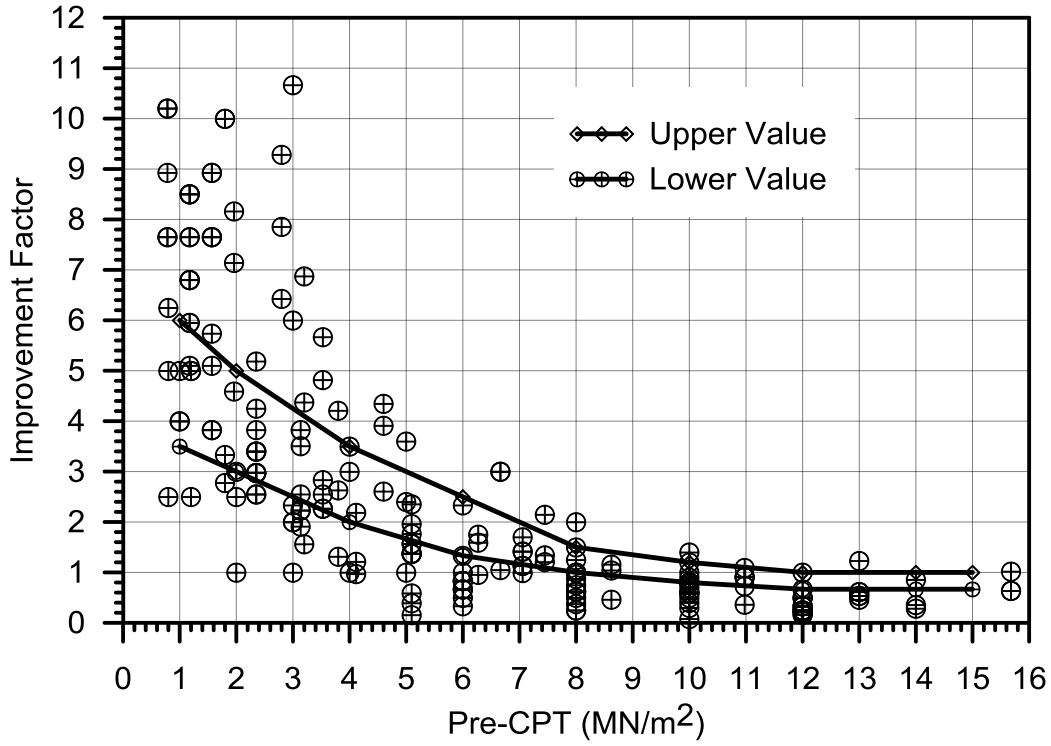

Figure 4-26: Upper Layer Improvement Factor.

4.5 Determination of Cohesionless Soil Parameters after Installation of Stone Columns

An important requirement of many Vibro-stone column projects is to assess the densification occurring in the soil surrounding the stone columns due to the installation process. This section presents how to obtain the cohesionless soil parameters after installation of Vibro-stone columns. The densification effect depends on several factors: (1) soil type; (2) degree of saturation and water table location; (3) initial relative density;

(4) soil structure including the effect of aging, sedimentation etc.; (5) installation machine characteristics.

An innovative procedure for assessing the degree of compaction of cohesionless soil surrounding stone columns is developed and evaluated. The method depends on the relationship between CPT and relative density for cohesionless soil that was developed by many researchers (Terzaghi and Peck, 1968; Schmertmann, 1978; Lamb and Whitman, 1979). This relationship is presented in Table 4-4 and has been redrawn in Figure 4-27. Therefore, by using Post-CPT, it is possible to estimate the relative density of soils after installation of stone columns. Post-relative density and cohesionless soil type can be used to assess the angle of internal friction and dry unit weight from Figure 4-28 as suggested by (Navfac, 1982). Saturated unit weight can be obtained from relation between dry and saturated unit weight with soil type presented by (Navfac, 1982), as shown in Table 4-5. In this study and to make the relation simpler, the relationship has been redrawn in Figure 4-29.

Table 4-4: Relative Density of Cohesionless Soils Based on SPT (N) and CPT.

Relative density	SPT, N, Blows*	(Tip Resistance), ** MPa	Relative density (Dr %)
Very loose	0-4	0-2	0-20
Loose	4-10	2-4	20-40
Medium	10-30	4-12	40-60
Dense	30-50	12-20	60-80
Very dense	Over 50	Over 20	80-100

(Terzaghi and Peck, 1968) **(Schmertmann, 1978; Lamb and Whitman, 1979).

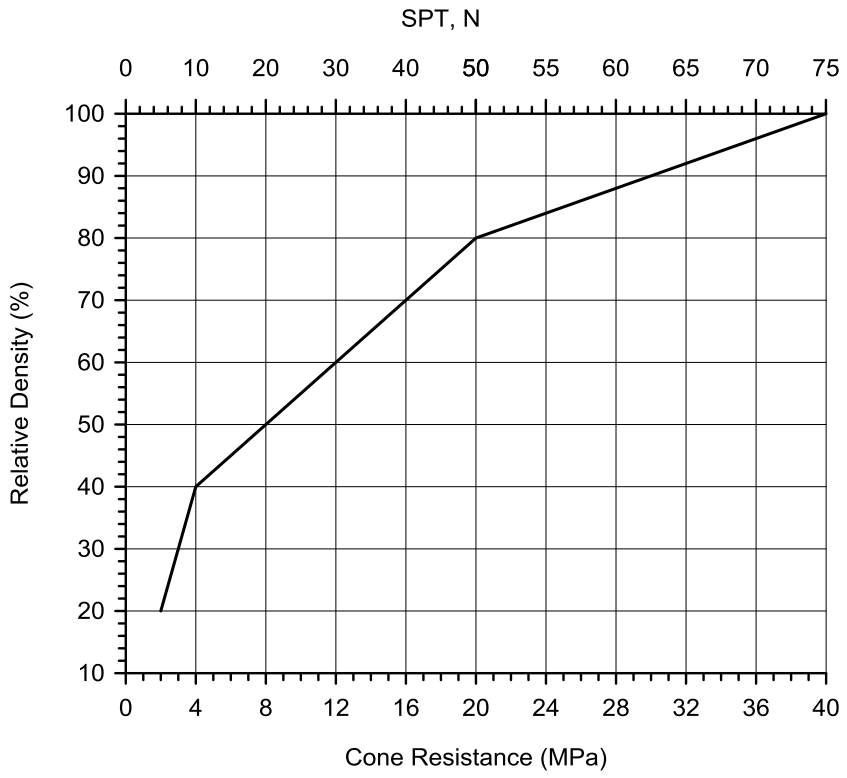

Figure 4-27: Relative Density Versus q_c and SPT (N) for Cohesionless Soils (Terzaghi and Peck, 1968; Schmertmann, 1978; Lamb and Whitman, 1979)

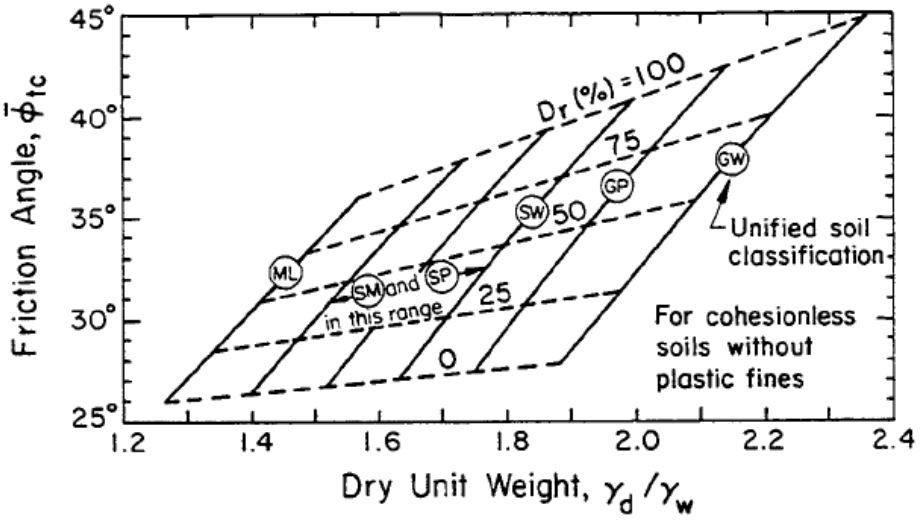

Figure 4-28: Angle of Internal Friction Versus Relative Density and Unit Weight for different granular material (Navfac, 1982).

Table 4-5: Typical Values of Soil Index Properties (Navfac, 1982).

Soil Type	γ (kN/m^3)		γ_{sat} (kN/m^3)	
Sand; clean, uniform, fine or medium	13.19	21.35	17.97	21.27
Silt; uniform, inorganic	12.72	21.35	17.82	21.27
Silty Sand	13.82	22.29	18.29	22.21
Sand; Well-graded	13.50	23.24	18.13	23.31
Silty Sand and Gravel	14.13	24.34	18.60	24.25
Sandy or Silty Clay	15.70	23.08	15.78	23.16

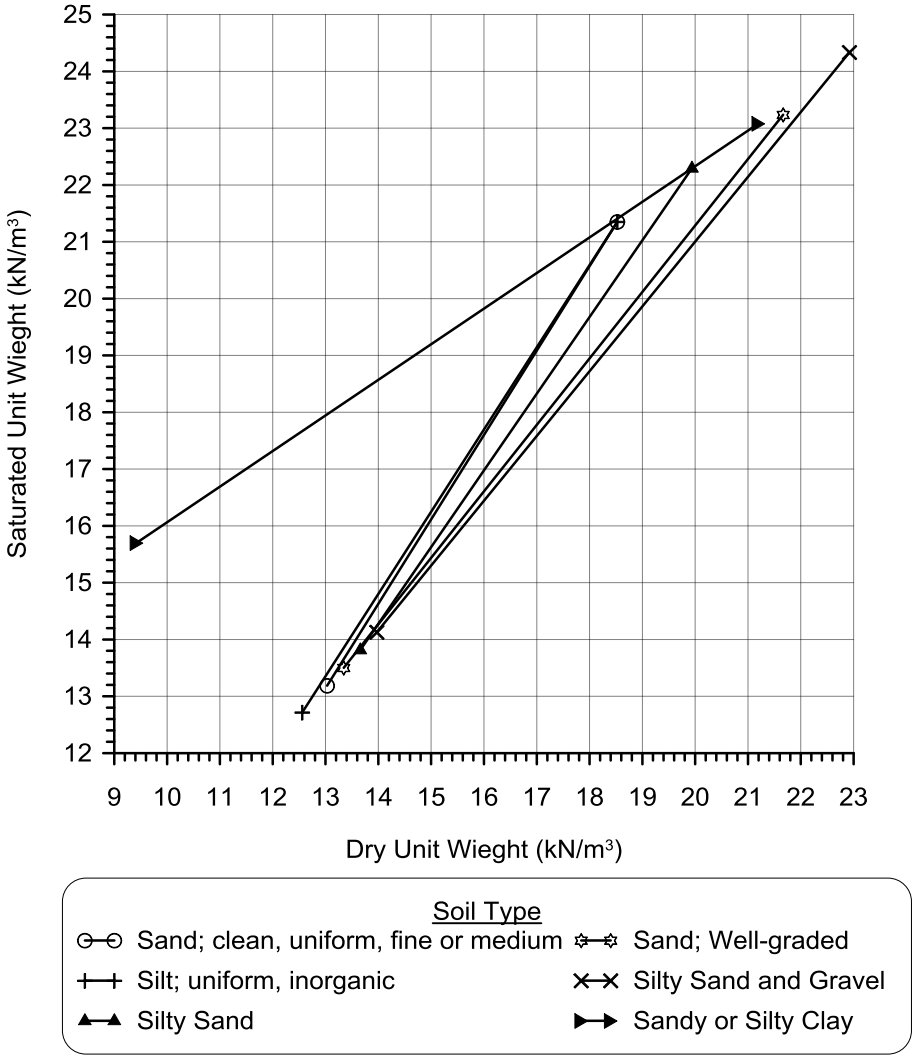

Figure 4-29: Relation between Dry and Saturated Unit Weight (Navfac, 1982).

4.6 Determination of Sabkha Parameters after Installation of Stone Column

In this section, a procedure is presented to assess sabkha parameters before and after installation of Vibro-stone columns. The method is based on linking field and laboratory values from geotechnical report and published Sabkha data. Table 4-6 shows the relationship between Sabkha properties reported by many researchers. In this study, the data has been redrawn by relating the density, cohesion and friction angle values to the CPT values, as shown in Figure 4-30 and Figure 4-31. By using this method and through Pre-CPT or Post-CPT, one can determine the in-situ density, cohesion and angle of internal friction of sabkha before and after installation of stone columns.

Table 4-6: Mechanical Properties of an Eastern Saudi Sabkha

Properties	(Juillie and Sherwood, 1983)		(Abu-Taleb and Egeli, 1981)
	Muddy sabkhas	Sandy sabkhas	Muddy sabkhas
Percentage fines, %	25 to 95	5 to 25	18 to 97 Passing sieve No.75
Salt content (%)	2 to 18	2 to 15	-
Water content (%)	25 to 90	4 to 40	10 to 84.6
Specific gravity	-	-	2.51 to 2.82
In-situ density	1.0 to 1.35	1.3 to 1.85	1.34 to 1.89
Internal friction	0 to 22	20 to 35	0 to 22
Percentage of CaCo3 (%)	20 to 90	>30	-
Liquid limit, %	-	-	30 to 84
Plasticity index	0 to 40	NP	0 to 39
Cohesion (kN/m2)	0 to 55	Zero	0 to 0.54(kg/cm2)
Compression index	0.4 to 0.95	Zero	0.39 to 0.95
Initial void ration	-	-	1.08 to 2.16
S.P.T values (blows)	0 to 4	2 to 10	0 to 6
Static cone resistance (MN/m2)	0.2 to 2.0	1 to 6	-
Bearing capacity (kN/m2)	15 to 30	30 to 60	-

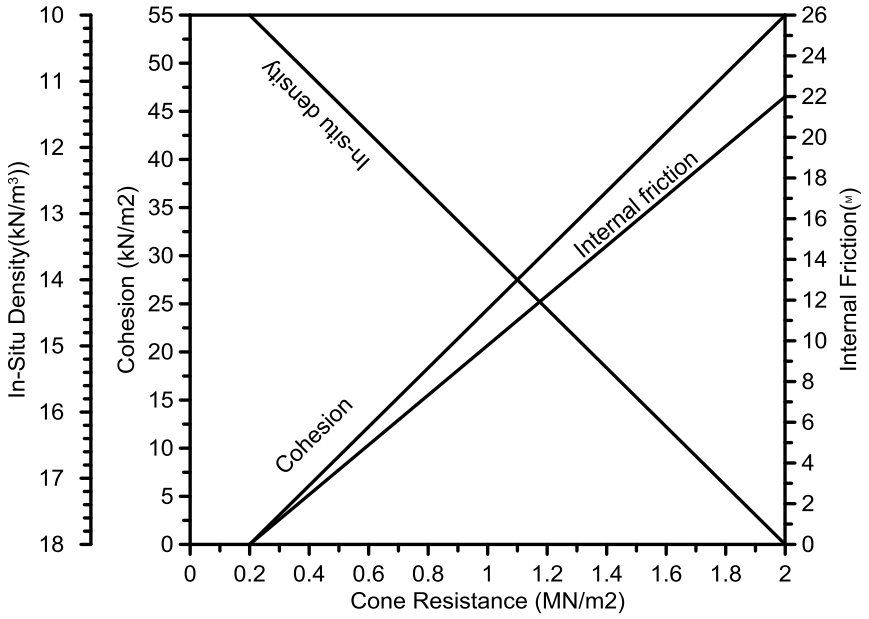

Figure 4-30: Evaluation of Muddy Sabkha Soils after Installation of Stone Column Using CPT Data.

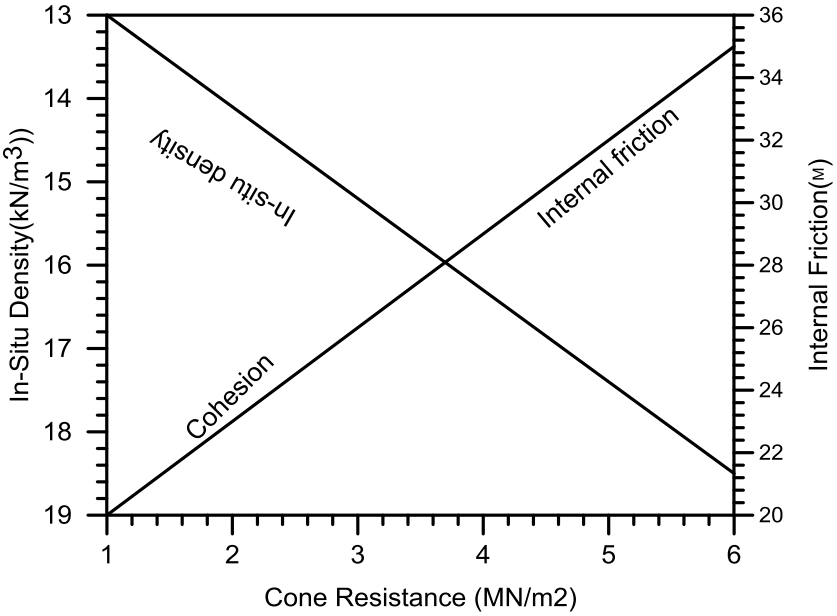

Figure 4-31: Evaluation of Sandy Sabkha Soils after Installation of Stone Column Using CPT Data.

CHAPTER 5

NUMERICAL MODEL OF STONE COLUMN INSTALLATION EFFECT

5.1 Introduction

To carry out an analysis of the soil-structure stone-column interaction under various types of loading and boundary conditions, a finite element model is required to simulate the real problem as close as possible. The utilization of FEM in geotechnical problems is still an approximate technique, which idealizes real-life situations into a set of continuum components and adopts constitutive models to simulate soil behavior. As a result, it is necessary to validate the output of the FEM to ensure that the real-life situation is accurately modeled.

For the current investigation, the characteristics of Sabkha were obtained from the field data at three different locations. The characteristics of sabkha and other soils have been used in this Chapter to develop numerical models for the plate load test on stone columns reinforced sabkha soils. The computations are carried out using geotechnical finite element software PLAXIS 3D-2013.

The aim of this modeling exercise is to find out the best method to simulate the installation effects of the stone columns and to examine the influence of different parameters on the short-term performance characteristics. The ability of these numerical

models to accurately capture the performance of stone columns is validated/verified by simulating field load tests on a single and a group of stone columns in the three different locations taking into account different stone column patterns, sabkha thickness and stone column materials properties. Once the modeling is validated using field data, the effect of other parameters will be investigated.

5.2 Materials Properties

The selection of the appropriate and accurate material properties is essential in a numerical analysis to simulate the system accurately. The model parameters were based on the data collected from the geotechnical reports, which were discussed in Chapter 3. Mohr-Coulomb failure criterion considering the elasto-plastic behavior is utilized to model soil layers and stone column material. Such procedure describes the soil using its modulus of elasticity, Poisson's ratio, cohesion and angle of internal friction. A drained condition was used for the cohesionless materials and undrained condition was used for Sabkha and cohesive material. A linear elastic model was selected for the precast concrete footings.

5.2.1 Modeling Soil Behavior

The model parameters were based on the data collected from the geotechnical investigation reports, pre-improvement, post-improvement testing and well-documented correlations from the literature. The approach presented in Chapter 4 was intended to define the design parameters of cohesionless and sabkha soils taking into account the installation effects of Vibro stone column. The soil parameters for layers below 10 m correlate well with the nearest SPT data, as presented in Chapter 3. A drained condition

was used for the cohesionless materials, and undrained condition was used for Sabkha and cohesive material.

The Young's modulus (E) for cohesionless soil above the sabkha, usually recent backfill, was obtained from the CPT soundings using the relationship between cone bearing and Young's modulus for normally consolidated, uncommented sands ($E=2q_c$) given by (Robertson and Campanella, 1983; Bowles, 1988).The E-Modulus values for sabkha and soil layers below sabkha were obtained using the correlations proposed by many authors utilizing CPT and SPT values (Bowles, 1988; Robertson and Campanella, 1983), as presented in Table 5-1. The angle of dilatancy is determined from the empirical relationship $\psi = \phi - 30°$, developed by Bolton, 1986.

Table 5-1: Elastic Modulus Relations Based on CPT and SPT Data.

Soil Type	E-Modulus Formula	Reference
Sand with silt above sabkha layer (recent backfill)	$2q_c$	Robertson and Campanella, (1983) and Bowles (1988)
Sabkha	$2q_c$	(Aiban, 2009)
Sand with silt below sabkha soils	500(N+15)	Bowles, (1988)
Clayey sand	320(N+15)	Bowles, (1988)
Silt, sandy silt	300(N+15)	Bowles, (1988)

5.2.2 Stone Columns

The stone columns were installed in all cases using the wet top feed method. The final diameter of stone columns ranged from 0.9–1.1 m. The stone columns material is modeled as drained material. The properties of stone column material was estimated from the literature and geotechnical design report. These parameters are presented in Table 5-2.

Barksdale and Bachus (1983) report that Young's modules (E) for stone columns in soft clay, back-calculated from measured settlements range from E_c=(10~20) E_s for design purpose (E_c = Young' s modulus of column, E_s = Young's modulus of soil). Schweiger, (2008) used E_c=70MN/m^2 while performing a numerical investigation of stone columns supporting an embankment in loose-medium compacted sand over weak clayey silty soils which are somehow similar to cases presented in this investigation (Gäb et al., 2008). The angle of internal friction adopted in the current study for stone columns is 42°. The angle of dilatancy is determined from the empirical relationship $\psi=\phi - 30°$ (Bolton, 1986) .

Table 5-2: Parameters for the Vibro Stone Column Material.

Parameter	Value Adopted for FEM
Elastic modulus E (MPa)	60 to 70
Dry Unit Weight (kN/m^3)	18
Sat. Unit Weight (kN/m^3)	20
Poisson's ratio	0.3
Internal friction angle (°)	42
Dilatancy angle (°)	12

5.2.3 Concrete Footing

Pre-cast concrete footing was modeled as a rigid plate and the loading was applied as a uniformly distributed vertical load on the surface according to the loading scheme used during the actual field test. A linear elastic constitutive model was used for the concrete. This constitutive model utilizes the modulus of elasticity and the passion's ratio to describe the material. The concrete properties used in this study are shown in Table 5-3. There are no interface elements between the rigid precast concrete footing and the surface soil layer because no slippage occurs between the plate and the soil underneath the plate (Zahmatkesh and Choobbasti, 2010).

Table 5-3 Material Properties of Precast Concrete Footing.

Material	Constitutive Model	Parameter	Value
Concrete Footing	Linear-Elastic	Elastic modulus E (MPa)	31×10^3
		Dry Unit Weight (kN/m^3)	24
		Poisson's ratio	0.2

5.3 Model Geometry and Boundary Conditions

Three dimension finite element models were established using ten-node tetrahedral elements as shown in Figure 5-1. The depth and width of the model were selected to extend far beyond the study portion to simulate the real behavior of the model. This size ensured that the boundaries are placed at a distance greater than 9 times the stone column diameter to eliminate any boundary condition effect on the analysis. The height of the finite element model was selected as 30 meters.

It is important that a suitable mesh size is selected that is fine enough to capture the real behavior of the model while the analysis time is kept minimum, as practical as possible. The coarseness of the global mesh was generated to be fine; however, it was refined for the stone column and the top sand layer area. This was done since the stresses and deformations are higher in this area compared to other regions. The geometry of the model and the generated mesh used in analyses for plate load test in EWT are presented in Figure 5-2.

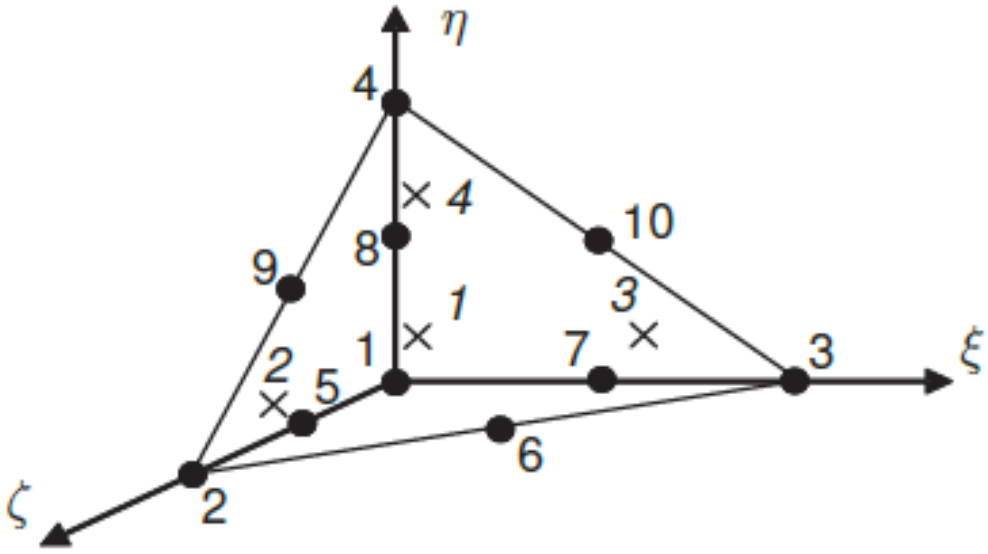

Figure 5-1: Local Numbering and Positioning of Nodes and Integration Points of Ten-Node Tetrahedral Element (Brinkgreve et al., 2011)

For the case of WHA due to symmetry of loading condition and material model, only quarter of the stone columns and its surrounding soil were modeled for the analysis, which helps in saving/optimizing computational time. An isometric view of the 3D model is given in Figure 5-3.

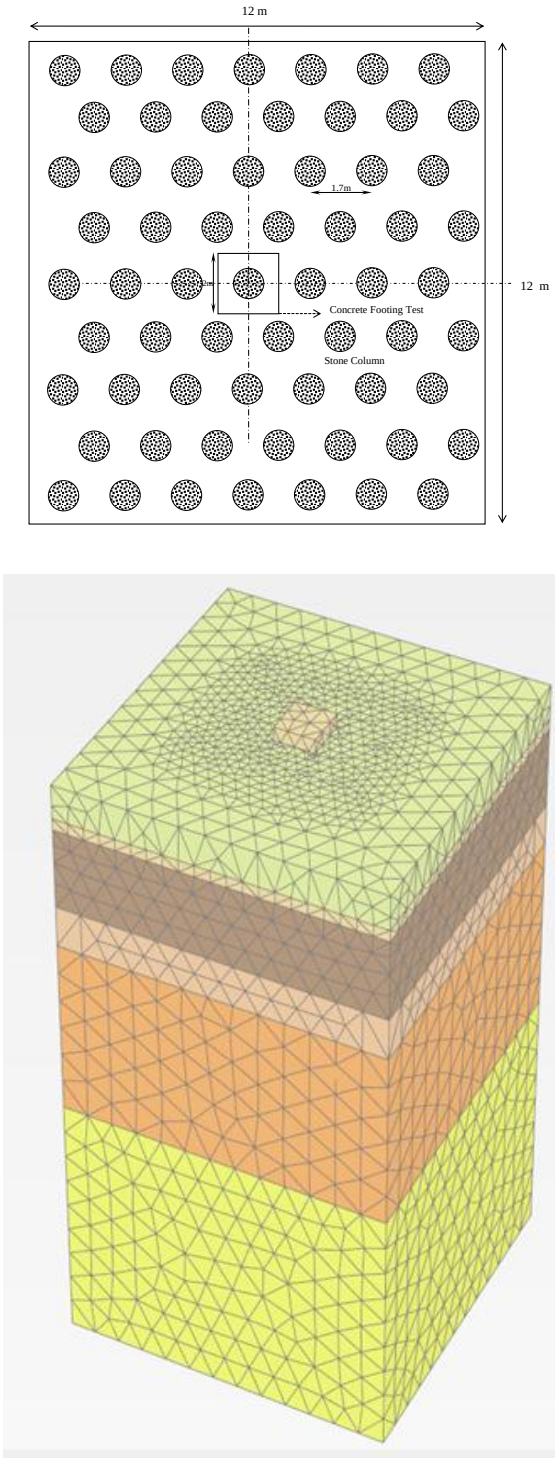

Figure 5-2 : Geometry for FEM model and Elements Discretization for Plate Load Test in the EWT.

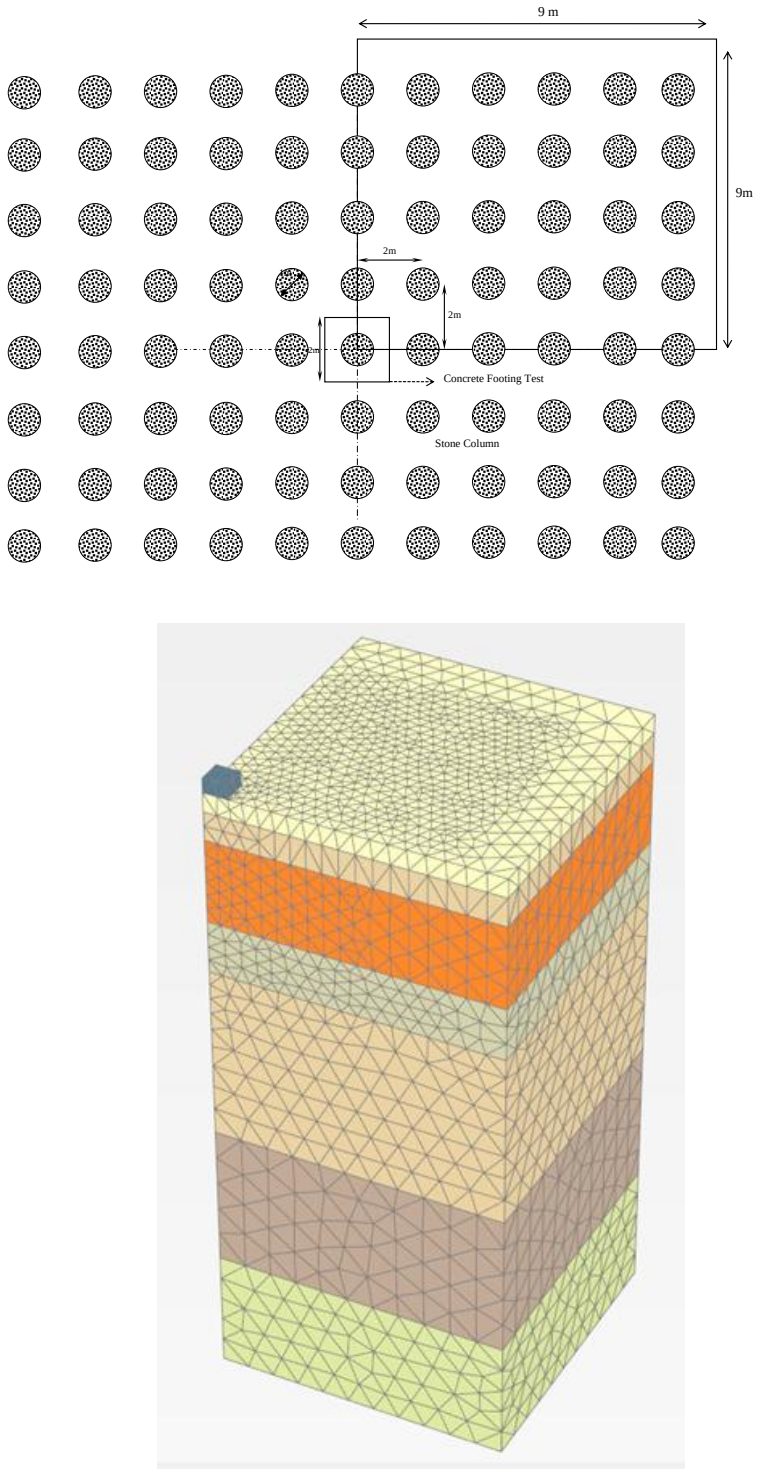

Figure 5-3: Geometry for FEM Model and Elements Discretization for Plate Load Test in the WHA.

No interface elements were defined around the stone columns since no significant shear occurs between the stone column and the surrounding soil layers, and the deformation and the failure of the column is generally due to bulging especially for end-bearing long stone column (Murugesan and Rajagopal, 2006b; Ambily and Gandhi, 2007b; Etezad-Borojerdi, 2007; Lo et al., 2010; Pulko et al., 2011). This was confirmed by Guetif et al. (2007) who reported that the stone columns are tightly interlocked with the surrounding soil and a perfect bond exists along the column-soil interface. These results have been validated after the exposure of one stone column in the WHA where the soil and gravel are totally integrated at the surface of the column, as shown in Figure 5-4.

Figure 5-4: Vertical Section of Stone Column in the WHA.

5.4 Construction Stags

The construction stages were simulated during modeling to simulate the actual sequence of construction activities. This option enabled activation and deactivation of different members, changing geometry configuration, and changing soil properties. Figure 5-5 illustrates the calculation stages implemented in the finite element modeling. The calculation type selected is plastic calculation utilizing an elastic-plastic deformation analysis.

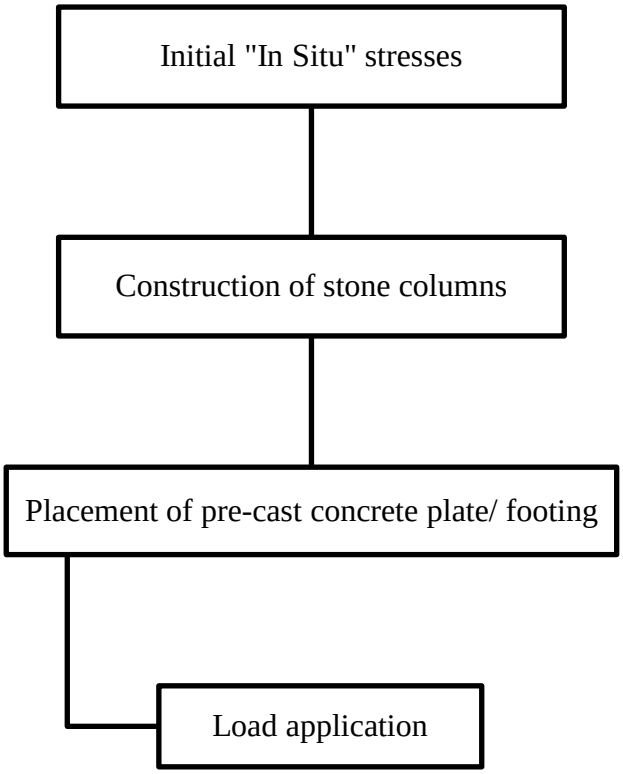

Figure 5-5: Analysis Stages for Full-Scale Plate Load Test.

5.4.1 Initial Stresses

The initial effective stresses in a soil body are caused by the self-weight of different layers. The elements that are not active in the initial situation can be deactivated. The stress state is characterized by an initial vertical effective stress $\sigma'_{v,o}$, and by an effective horizontal stress $\sigma'_{h,o}$. The initial vertical effective stress is calculated using:

$$\sigma_{v,0} = \sum_i^n \gamma_i \times h_i - p_w \quad (5\text{-}1)$$

Where

γ_i : Unit weight of individual soil layers,

h_i: Layer depth and

p_w : Initial pore pressures at the stress point.

The initial horizontal effective stress is related to vertical effective stress by the coefficient of lateral earth pressure, K_0 and is calculated using the following relation:

$$\sigma_{h,0} = K_0 \times \sigma'_{v,0} \quad (5\text{-}2)$$

Where the default K_o value is based on the (Jaky, 1944) formula;

$$K_0 = 1 - \sin\phi \quad (5\text{-}3)$$

The pore pressure variation is assumed to be fully hydrostatic i.e. the water pressure will increase linearly with depth according to the specified water weight. The highest pore pressures will therefore be seen in the lower parts. This phase will model the self-stress of soil i.e. the in-situ stresses.

5.4.2 Construction of Stone Columns

In this phase, the stone columns are generated by replacing the soil element that becomes now the stone columns with the corresponding strength and stiffness parameter as shown in Figure 5-5. It should be noted that the analysis were performed for a limited number of

stone columns (5x5) due to the meshing and computational limitations of the FE software. The selection of 5x5 stone columns is very representative of the situation for plate load testing. However, it may not represent the load from the entire structure such as circular tank; for example, due to the extent and magnitude of applied stresses.

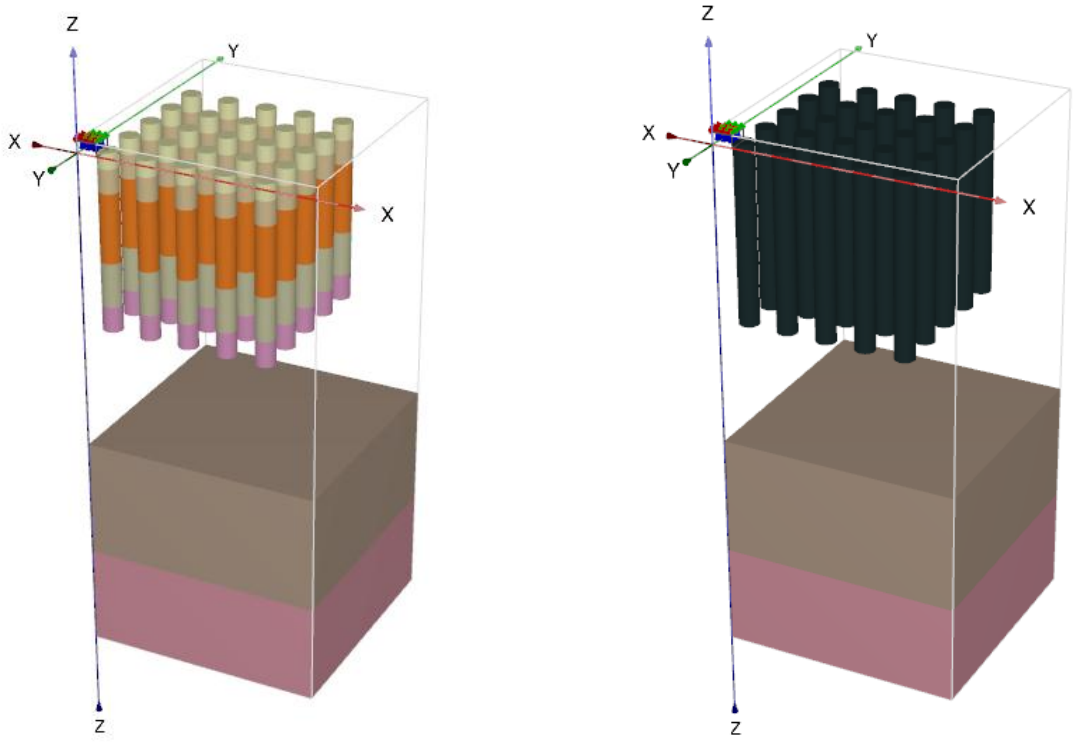

(a) (b)

Figure 5-6: Activated Stone Columns Element (a) Initial Phase Simulating the Original Soil Layering and (b) After Stone Columns Construction Phase.

5.4.3 Placing Concrete Footing

In this step, the precast concrete footing is placed on top of the stone columns. In order to eliminate unrealistic deformations caused by construction of stone column and placing concrete footing, displacement was set to zero.

5.4.4 Plate Loading Stages

The material model for calculations was selected to enable an elastic-plastic deformation analysis. An updated mesh analysis was applied due to large deformations expected in case of reinforced weak soils. Loading was applied as a uniformly distributed vertical load on the precast concrete footing according to the loading scheme followed during the actual field test, as shown in Table 5-4 for plate test in EWT and Table 5-5 and Table 5-6 for the WHA.

Table 5-4: Loading Schedule for the Plate Load Test in the EWT.

Load %	Applied Pressure (kPa)	Duration of Applied Pressure (Hr:Min)
0	0	0
25	47.5	00:15
50	95	00:15
75	142.5	00:15
100	190	12:00
125	237.5	00:15
150	285	2:00

Table 5-5: Loading Schedule for Trial Load Test Size of 3mx3m Plate Placed at Sabkha Elevation.

Load %	Applied Pressure, kPa	Duration of Applied Pressure (Hr:Min)
20	16	00:15
40	32	00:15
60	48	00:15
80	64	00:15
100	80	48:00
120	96	00:15
140	112	00:15
150	120	48:00
170	135	48:00
190	152	00: 15
210	168	00: 15
220	179	00: 15
230	184	00: 15
240	192	00: 15
250	202	48:00
270	216	00: 15
290	232	00: 15
310	248	00: 15
330	264	00: 15
340	270	00: 15

Table 5-6: Loading Schedule for the Plate Load Test in the WHA.

Load %	Applied Pressure (kPa)	Duration of Applied Pressure (Hr:Min)
0	0	0
25	15	00:15
50	30	00:15
75	45	00:15
100	60	12:00
125	75	00:15
150	90	2:00

5.5 Numerical Model without Stone Column Installation Effect

The numerical model was built to represent the entire site and the actual stone columns system that was subjected to full-scale plate load tests. The Vibro stone column installation effect on surrounding soils was ignored in this section. The soil profile and characteristics of the layers adopted for EWT model are presented in Figure 5-7 and Figure 5-8. The adopted soil parameters for the different layers are presented in Table 5-7 and Table 5-8.The soil layers parameters adopted for WHA cases are presented in Figure 5-9 to Figure 5-12. The soil parameters for these cases are presented in Table 5-9 to Table 5-12.

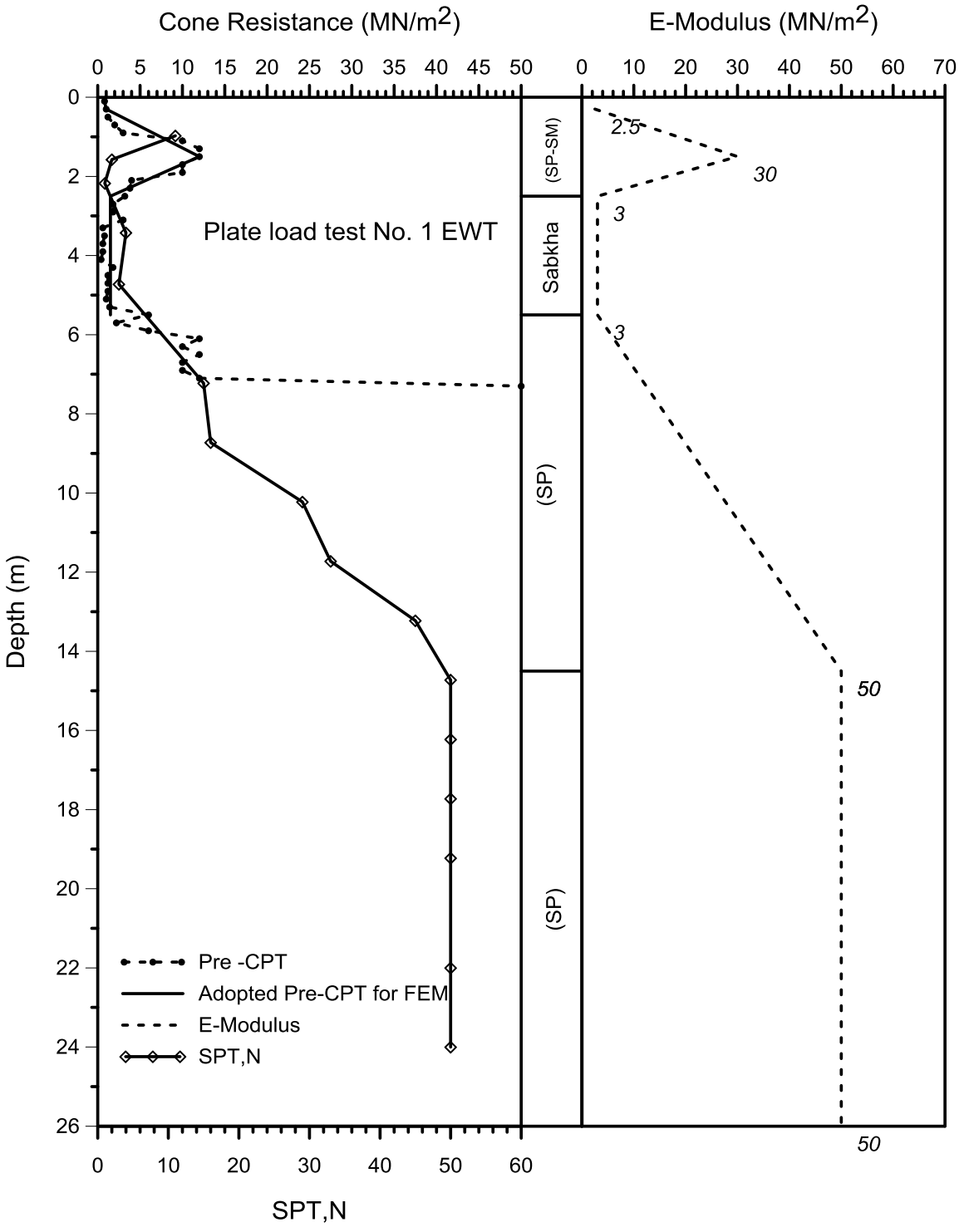

Figure 5-7: Soil Profile and Elastic Modules Adopted to Model Plate Load Test No. 1, the EWT.

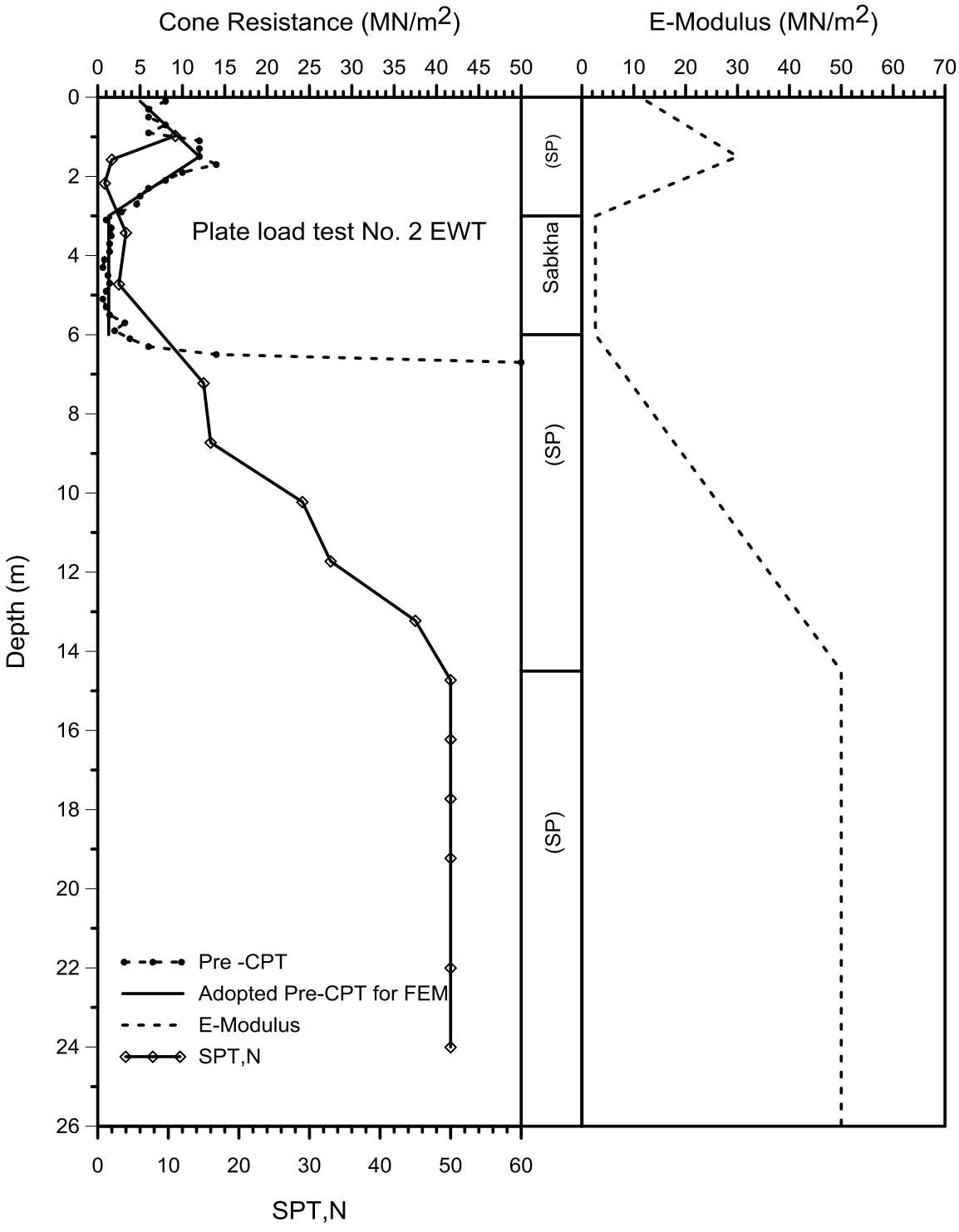

Figure 5-8: Soil Profile and Elastic Modules Adopted to Model Plate Load Test No. 2, the EWT.

Table 5-7: Soil Layer Properties for Plate Load Test No.1, the EWT.

Layer	Depth (m)	Dry/Saturated Unit Weight (kN/m^3)	Cohesion (kPa)	Friction Angle (°)	Dilatancy Angle (°)
Layer1: Sand	0-2	17/18.5	1	33	3
Layer2: Sabkha	3-6	14 (saturated)	24	10	0
Layer3: Sand Top	6-14.5	19 (saturated)	1	35	5
Layer4: Sand Bottom	14.5-30	20 (saturated)	1	37	7

Table 5-8: Soil Layer Properties for Plate Load Test No. 2, the EWT.

Layer	Depth (m)	Dry/Sat. Unit Weight (kN/m^3)	Cohesion (kPa)	Friction Angle (°)	Dilatancy Angle (°)
Layer1: Sand	0-3	17.5/18.5	1	34	4
Layer2: Sabkha	3-6	14 (saturated)	24	10	0
Layer3: Sand Top	6-14.5	19 (saturated)	1	35	5
Layer4: Sand Bottom	14.5-30	20 (saturated)	1	37	7

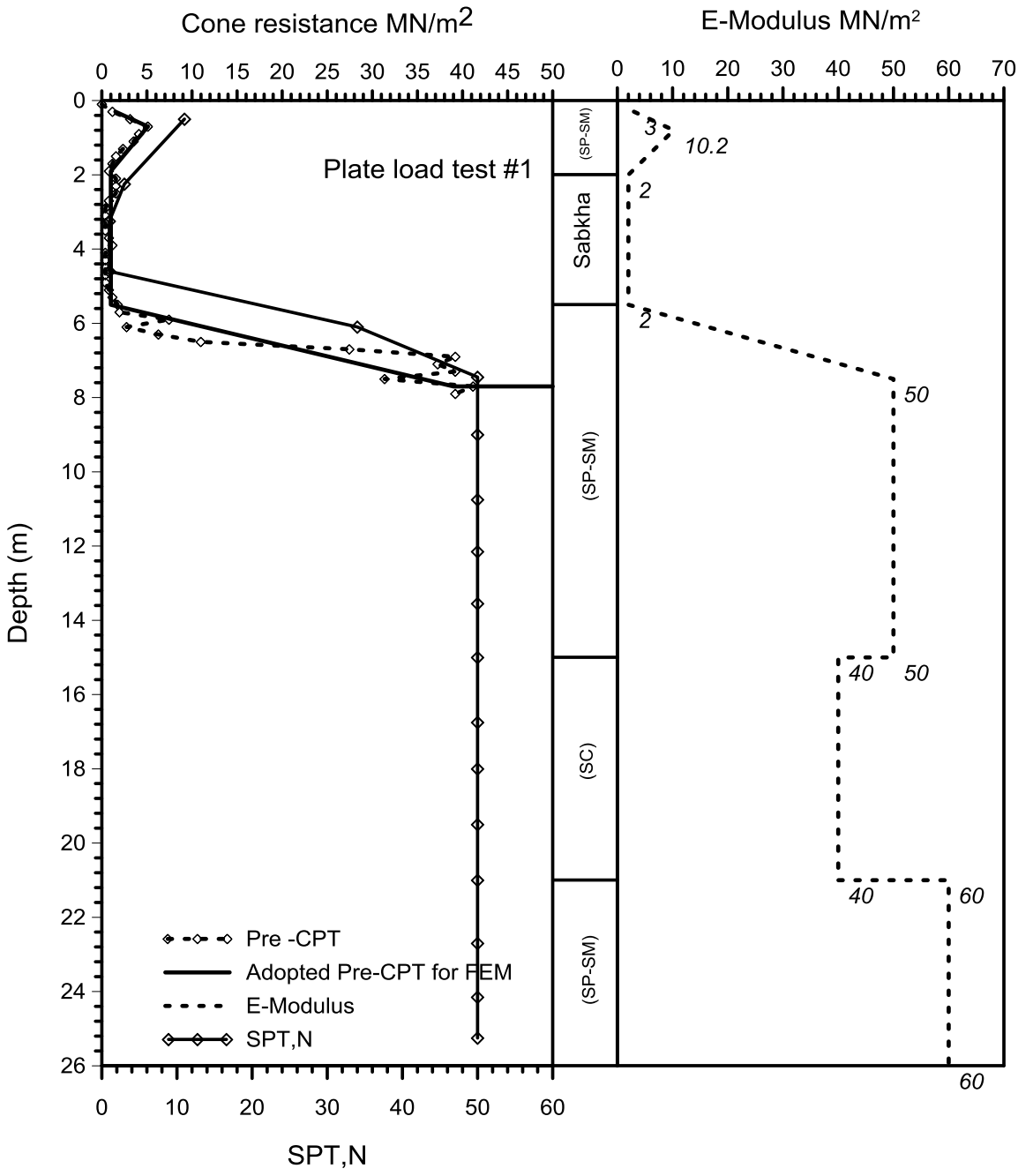

Figure 5-9: Soil Profile and Elastic Modules Adopted to Model Plate Load test No. 1, the WHA.

Table 5-9: Soil Layer Properties for Plate Load Test No.1, the WHA.

Layer	Depth (m)	Dry/Sat. Unit Weight (kN/m^3)	Cohesion (kPa)	Friction Angle (°)	Dilatancy Angle (°)
Layer1:Sand with silt (Top and Bottom)	0-2	15.5/17.5	1	28	0
Layer2: Sabkha	2-5.5	14 (Saturated)	20	10	0
Layer3: Sand with silt	5.5-15	20 (Saturated)	1	36	6
Layer3: Clayey sand	7-21	17 (Saturated)	150	15	0
Layer4: Sand with silt	21-26	21 (Saturated)	1	38	8

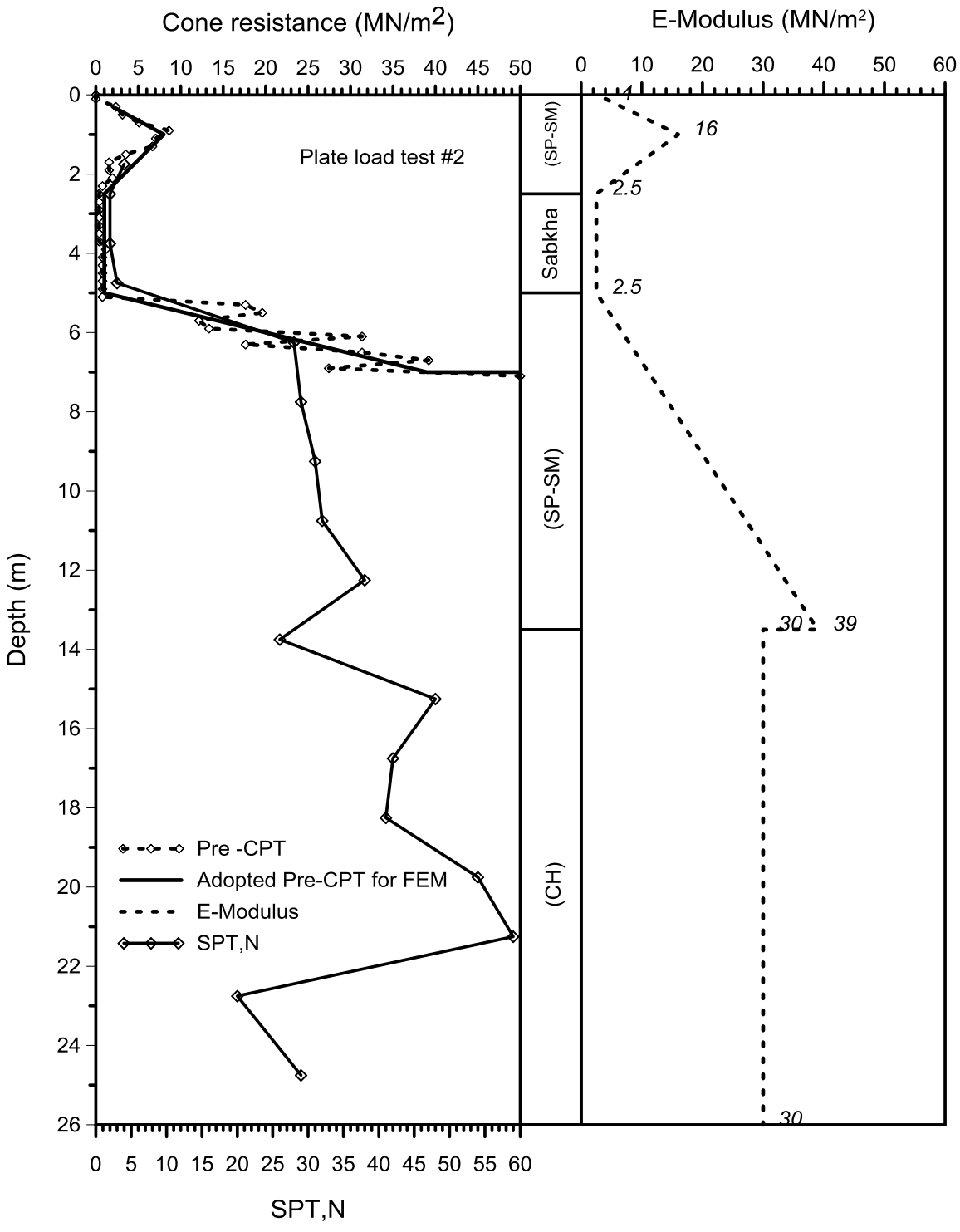

Figure 5-10: Soil Profile and Elastic Modules Adopted to Model Plate Load Test No. 2, the WHA.

Table 5-10: Soil Layer Properties for Plate Load Test No. 2, the WHA.

Layer	Depth (m)	Dry/Sat. Unit Weight (kN/m^3)	Cohesion (kPa)	Friction Angle (°)	Dilatancy Angle (°)
Layer1: Sand with silt (Top and Bottom)	0-2.5	15.5/17.5	1	30	0
Layer2:Sabkha	2.5-5.5	14 (saturated)	20	10	0
Layer3: Sand with silt	5.5-13.5	20 (saturated)	5	35	5
Layer4: Fat clayey	13.5-26	18 (saturated)	250	0	0

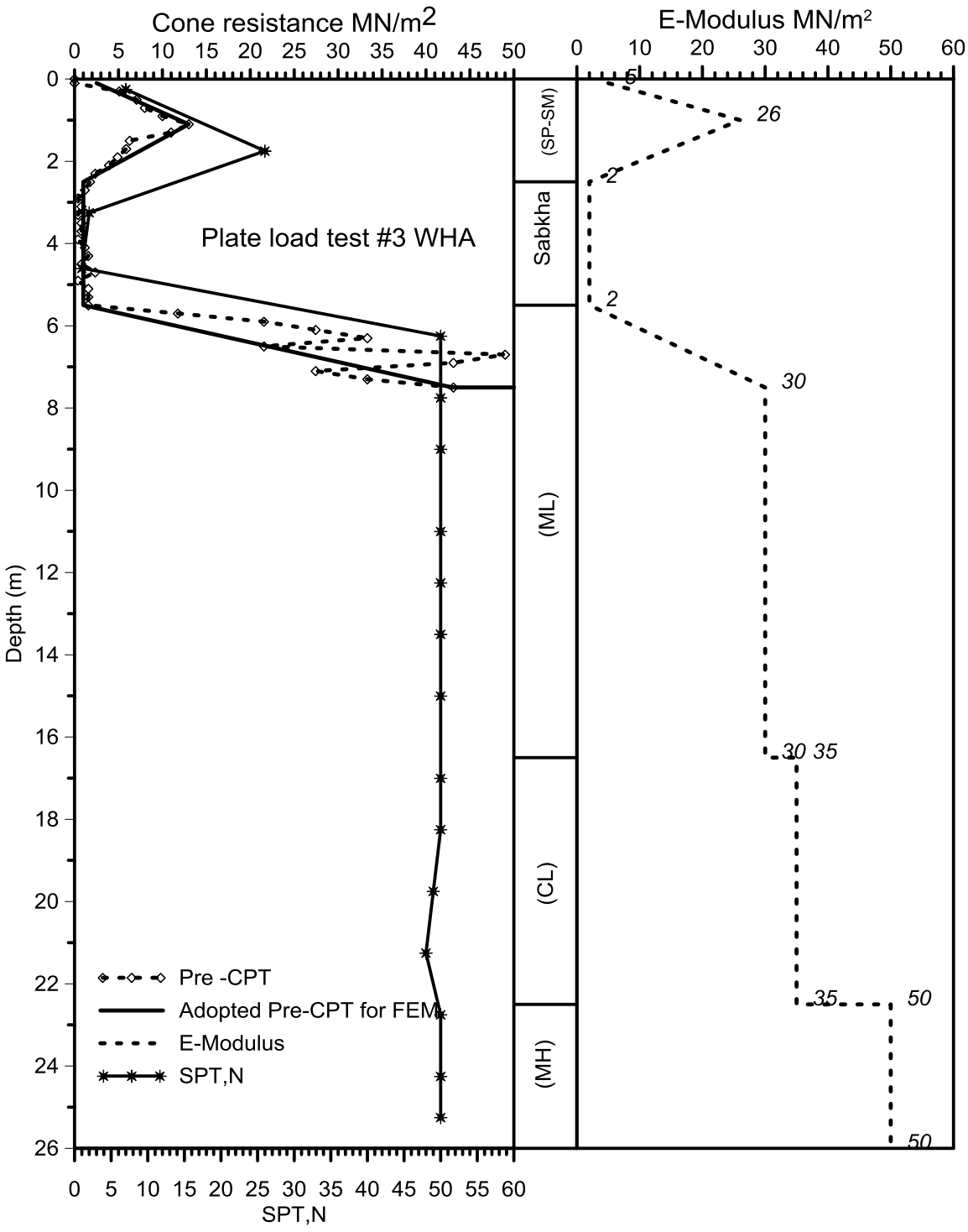

Figure 5-11: Soil Profile and Elastic Modules Adopted to Model Plate Load Test No. 3, the WHA.

Table 5-11: Soil Layer Properties for Plate Load Test No. 3, the WHA.

Layer	Depth (m)	Dry/Sat. Unit Weight (kN/m^3)	Cohesion (kPa)	Friction Angle (°)	Dilatancy Angle (°)
Layer1: Sand with silt (Top and Bottom)	0-2.5	15.8/17	1	32	2
Layer2: Sabkha	2-5.5	14 (saturated)	20	12	0
Layer3: Silt with few gravel	5-16.5	18 (saturated)	1	36	6
Layer4: Clayey sand	16.5-22.5	18 (saturated)	150	15	0
Layer4: Sandy silt	22.5-26	21 (saturated)	10	37	7

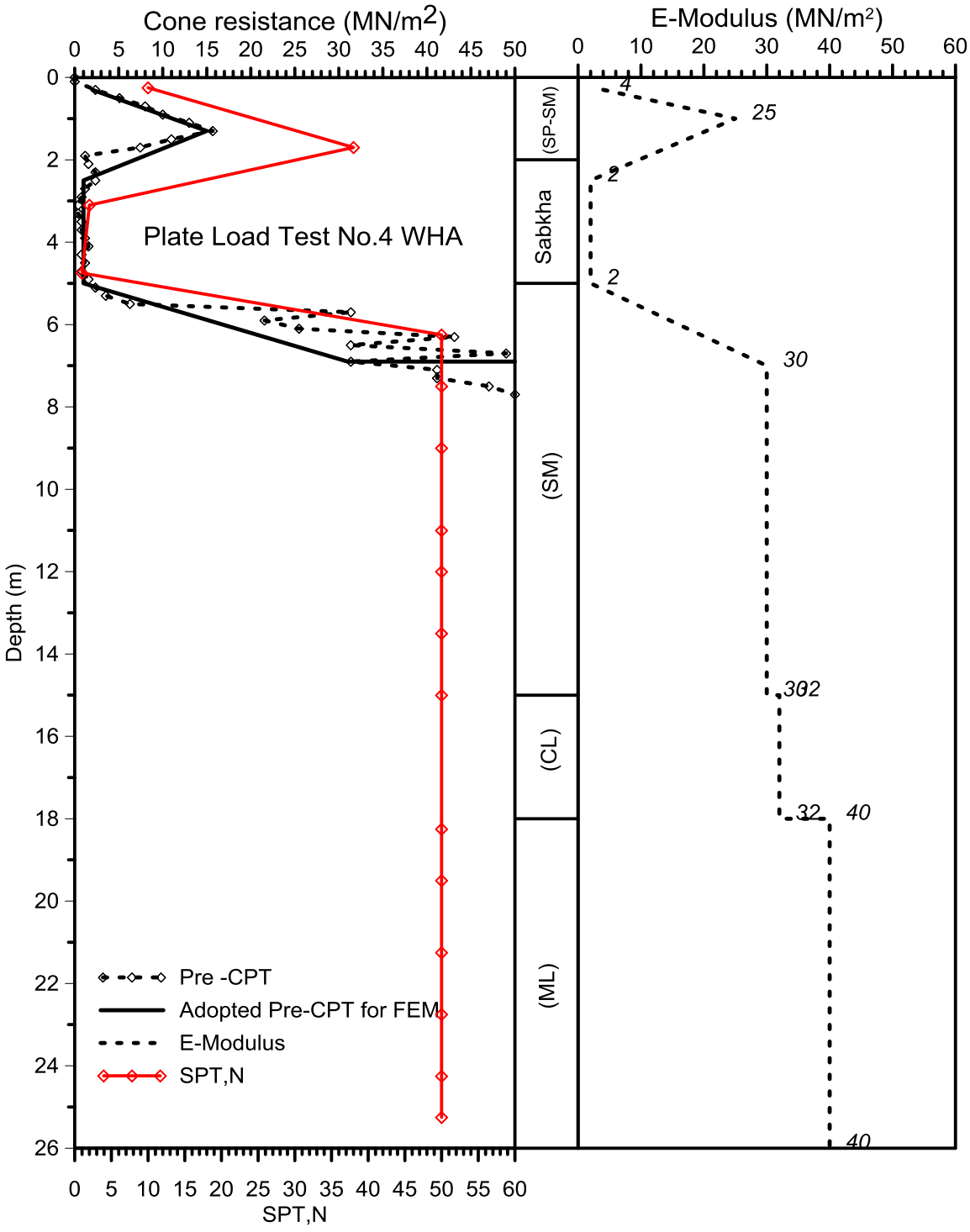

Figure 5-12: Soil Profile and Elastic Modules Adopted to Model Plate Load Test No. 4, the WHA.

Table 5-12: Soil Layer Properties for Plate Load Test No. 4, the WHA.

Layer	Depth (m)	Dry/Sat. Unit Weight (kN/m^3)	Cohesion (kPa)	Friction Angle (°)	Dilatancy Angle (°)
Layer1: Sand with silt (Top and Bottom)	0-2	16.5/18	1	32	2
Layer2: Sabkha	2-5	12.5 (saturated)	20	12	0
Layer3: Silt with few gravel	5-15	18 (saturated)	1	36	6
Layer4: lean Clayey	15-18	17 (saturated)	150	10	0
Layer4: Sandy silt	18-26	21 (saturated)	10	37	7

The initial model was calibrated using the load-settlement curves obtained from the full-scale stone columns. Calculated surface pressure-settlement curves for each case are compared with the field measurements in Figure 5-13 to Figure 5-18.

Despite the fact that the finite element model and the full-scale stone column load test curves have the same pattern, it is obvious that the calculated surface settlements from FEM are larger than the measured settlements for all cases and this becomes more pronounced as sabkha layer thickness increases. These results show clearly the importance of considering installation effect of stone columns for these cases.

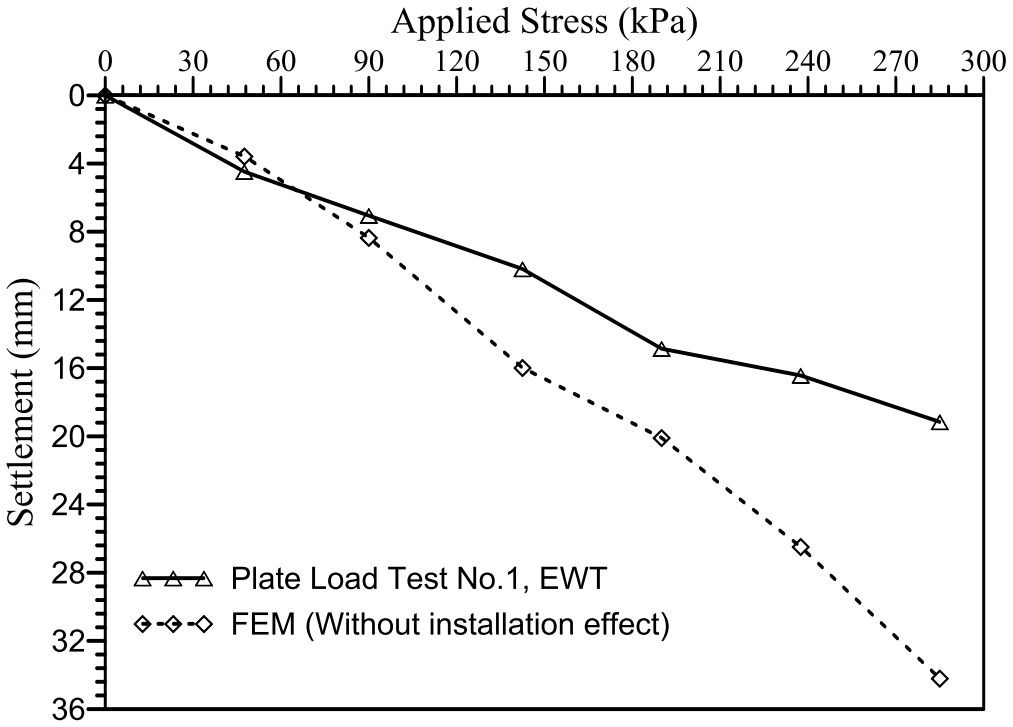

Figure 5-13: Comparison between Filed and Numerical Load-Settlement Curves for Plate Load Test No. 1, the EWT.

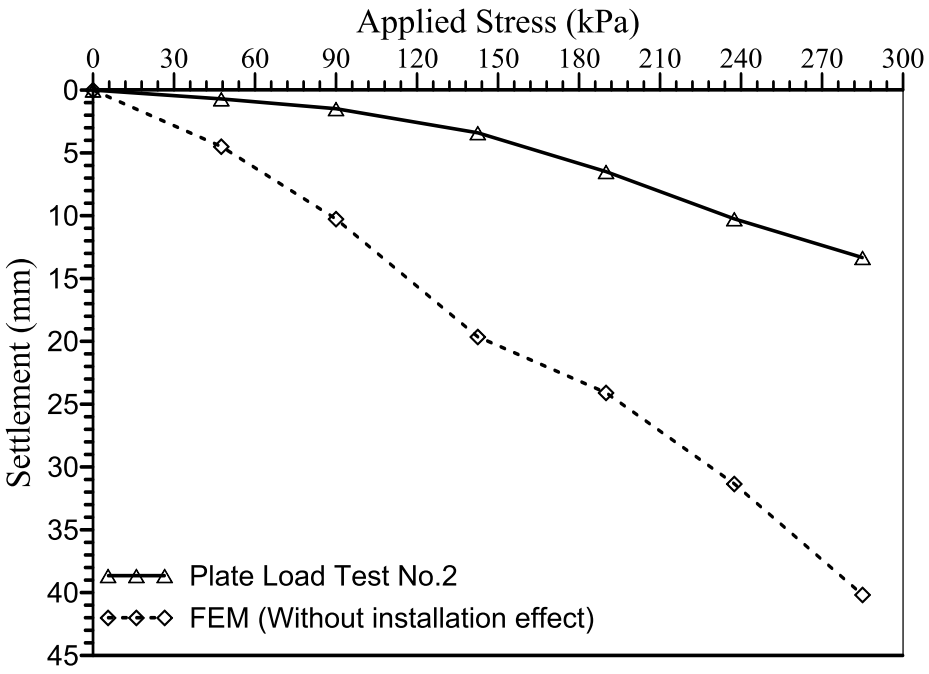

Figure 5-14: Comparison between Filed and Numerical Load-Settlement Curves for Plate Load Test No. 2, the EWT.

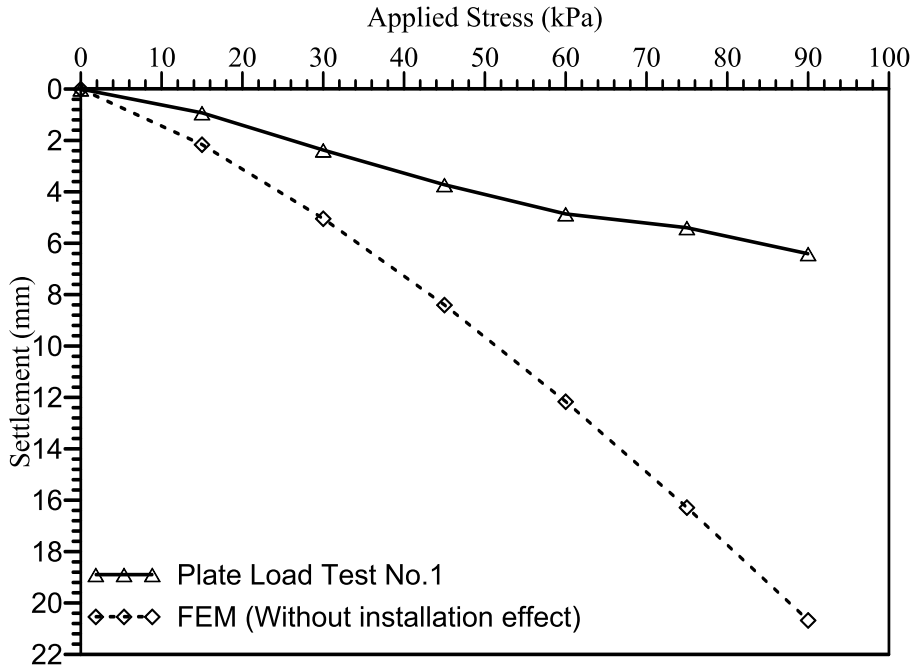

Figure 5-15: Comparison between Filed and Numerical Load-Settlement Curves for Plate Load Test No. 1, the WHA.

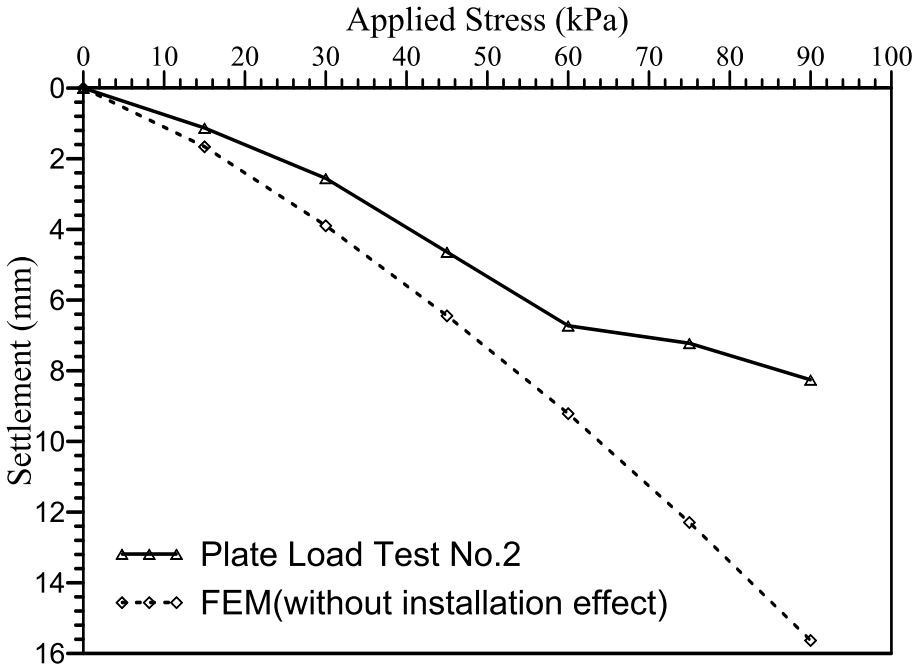

Figure 5-16: Comparison between Filed and Numerical Load-Settlement Curves for Plate Load Test No. 2, the WHA.

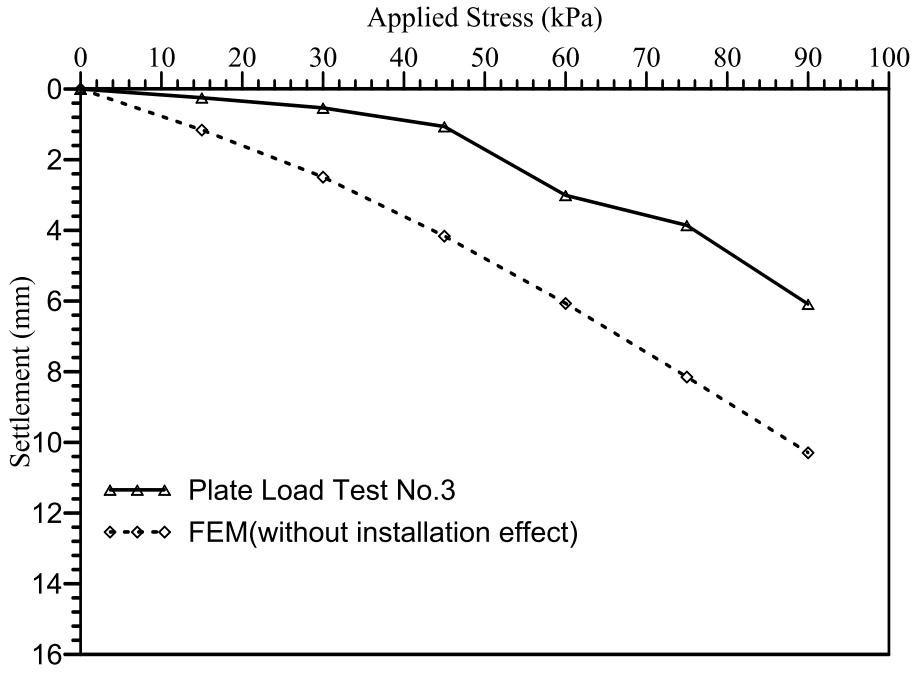

Figure 5-17: Comparison between Filed and Numerical Load-Settlement Curves for Plate Load Test No. 3, the WHA.

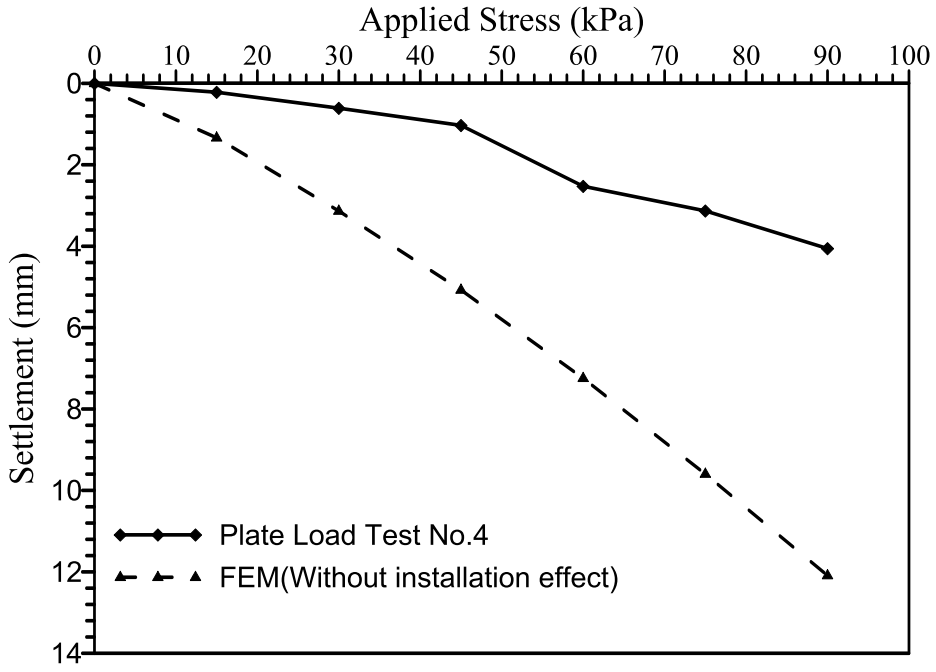

Figure 5-18: Comparison between Filed and Numerical Load-Settlement Curves for Plate Load Test No. 4, the WHA

5.6 Plate Load Test Resting Directly on Group of Stone Columns on Sabkha Surface

Due to the overshadowing effect of the 2.8 m sand recent backfilling on the results of full-scale load tests on stone columns, a full scale plate load test was performed directly on sabkha surface using the proposed grid configuration, 2m×1m, of stone column. The plate measures 3m×3m×0.6m and was placed on five stone columns including one stone column in the center as shown in Figure 5-19. The elastic modules adopted for FEM is shown in Figure 5-20. The soil characteristics are presented in Table 5-13.

In this case, the model was performed without stone column installation effect simulation because the layer affected by installation process (2.8 m sand backfill) was removed. The

Pre and Post-CPT data for sabkha at that location were not affected by stone columns installation process. Load-displacement curves for plate load test with numerical results are shown in Figure 5-21. The numerical curves show good match with the field data curves.

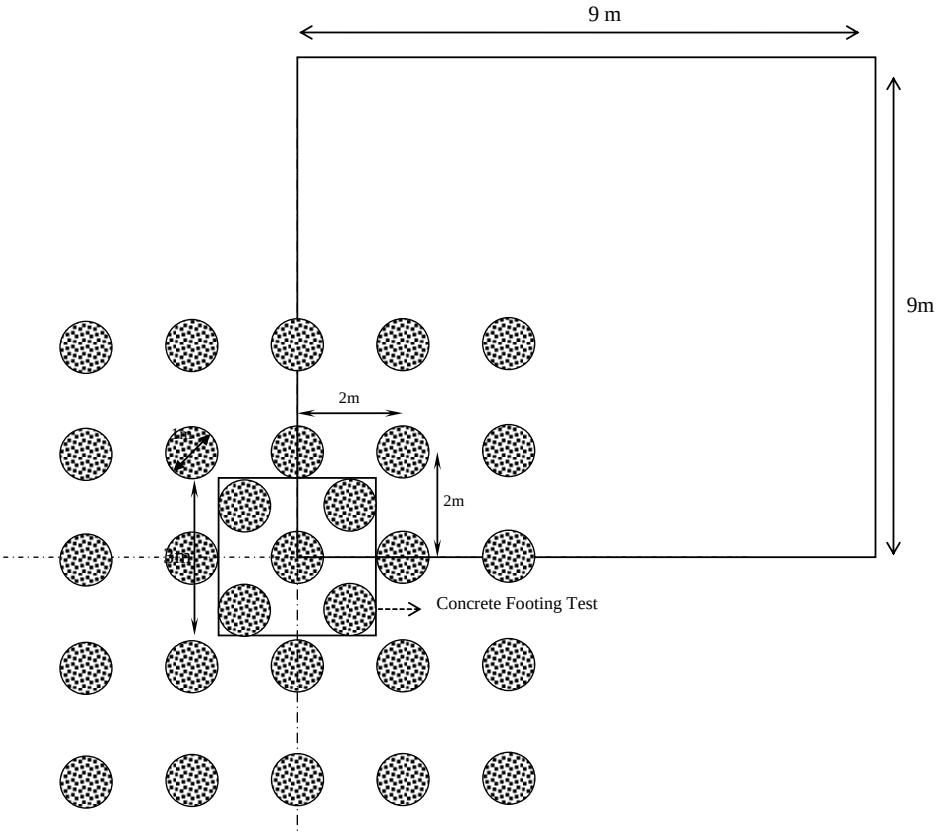

Figure 5-19: Layout of the Plate Load Test on 3m×3m Footing Size Resting on Stone Columns (plate is at the surface of the sabkha), the WHA.

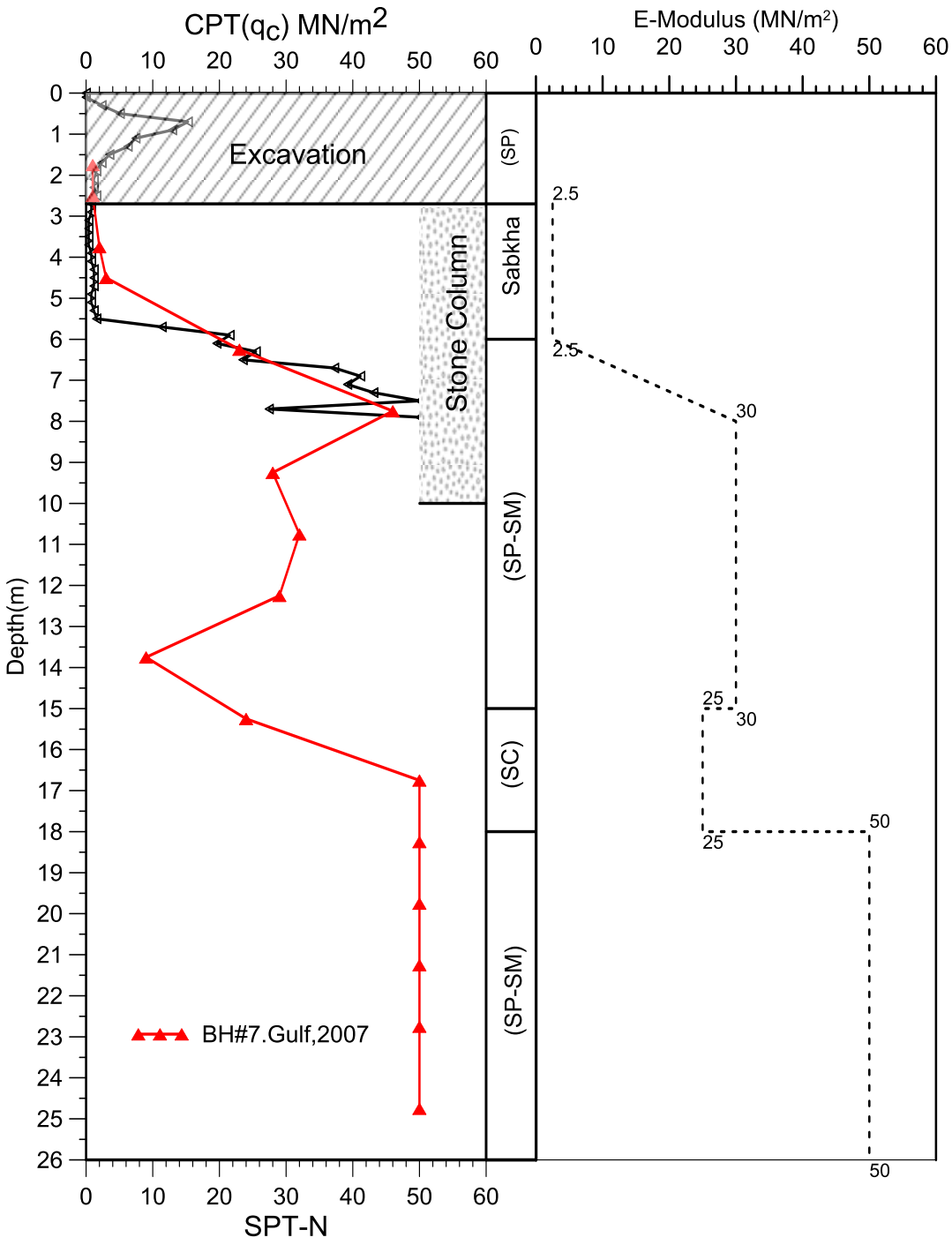

Figure 5-20: Soil Profile and Elastic Modules Adopt to Model Plate Load Test No. 5, the WHA.

Table 5-13: Soil Layer Properties for Plate Load Test No. 5 Direct on Sabkha Surface, the WHA.

Layer	Depth (m)	Dry/Sat. Unit Weight (kN/m^3)	Cohesion (kPa)	Friction Angle (°)
Layer1:Sabkha	0-3.2	11.5	10	10
Layer2:Sand with silt (Top)	3.2-5.2	17.5	1	33
Layer2:Sand with silt (Bottom)	5.2-12.2	18	1	35
Layer3:Clayey sand	12.2-15.2	18	150	10
Layer4: Sand with silt	15.2-40	20	1	37

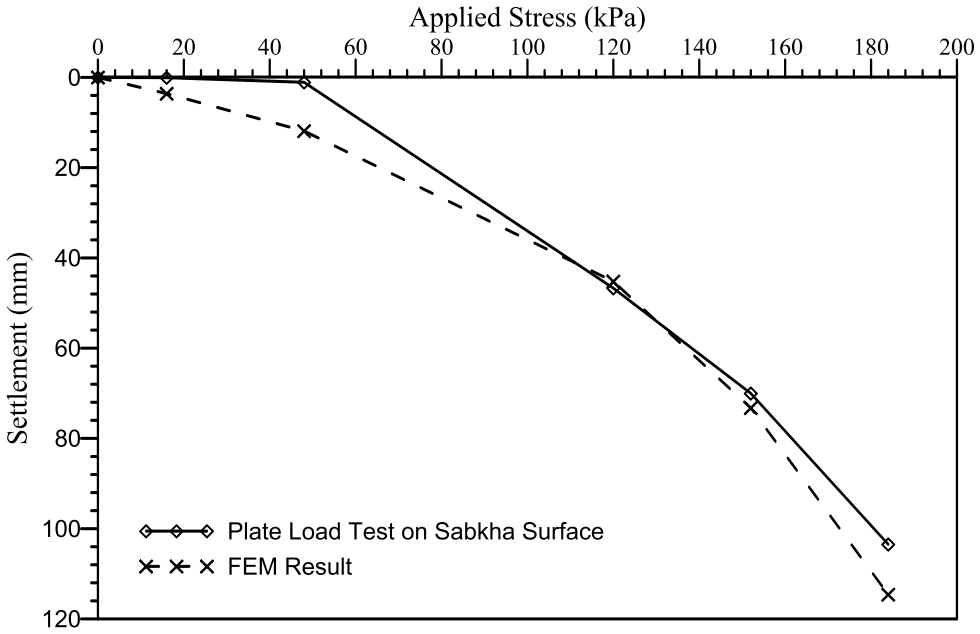

Figure 5-21: Comparison between Filed and Numerical Load-Settlement Curve for Plate Load Test No. 5 on Sabkha Surface, the WHA.

5.7 Modeling of Stone Column with Installation Effects

As discussed in the previous section that the settlement curves from the numerical modeling without installation effect are greater than the field recorded values. Therefore, it is important to consider the stone column installation densification which is occurring in the soil layers surrounding stone column.

It was shown in the literature review that stone column installation increases the horizontal stress and strength parameters in the surrounding soil. Field and laboratory studies suggest that the effects of stone column installation in soft clay can be accurately modeled by increasing the coefficient of lateral earth stress (K_o). In this study, method of increasing the coefficient of horizontal stress is examined and a new method is suggested by upgrading soil layers' parameter surrounding stone column using post-CPT data.

5.7.1 Increasing the Coefficient of Lateral Earth Stress (Ko)

Initial stresses play an essential role in the reinforced ground numerical modeling since installation of stone columns into weak ground increases lateral stresses (Balaam, 1978). The stone columns installation effects may be accounted for by increasing the coefficient of lateral earth pressure (K_o) in the surrounding soil in a way simulating the differences between the pre- and post-CPT or SPT data.

To simulate the installation effect using increased lateral earth pressure approach, the K_o values of the soil layer around the stone columns are examined for ranges between active and passive earth pressure coefficients. Increase in K_o will apply only to soils/layers affected by vibration, as presented in Chapter 4. Figure 5-22 to Figure 5-24 illustrate comparison between field and numerical results using increased values of the coefficient

of lateral earth pressure (K_o) method. This comparison clearly demonstrates that there is no constant value for (K_o) that can be adopted to obtain settlement values that are close to settlement obtained from the field testing.

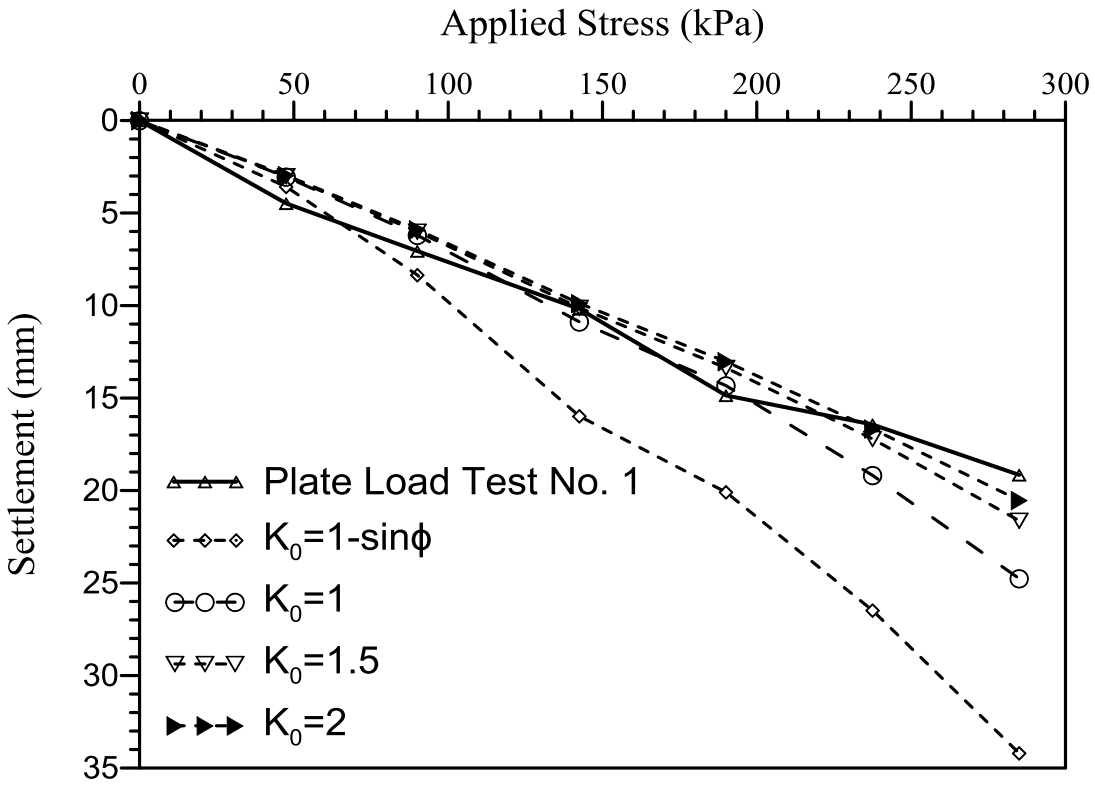

Figure 5-22: Simulation of Stone Columns Installation Effect by Increasing K_0 for Plate Load Test No. 1, the EWT.

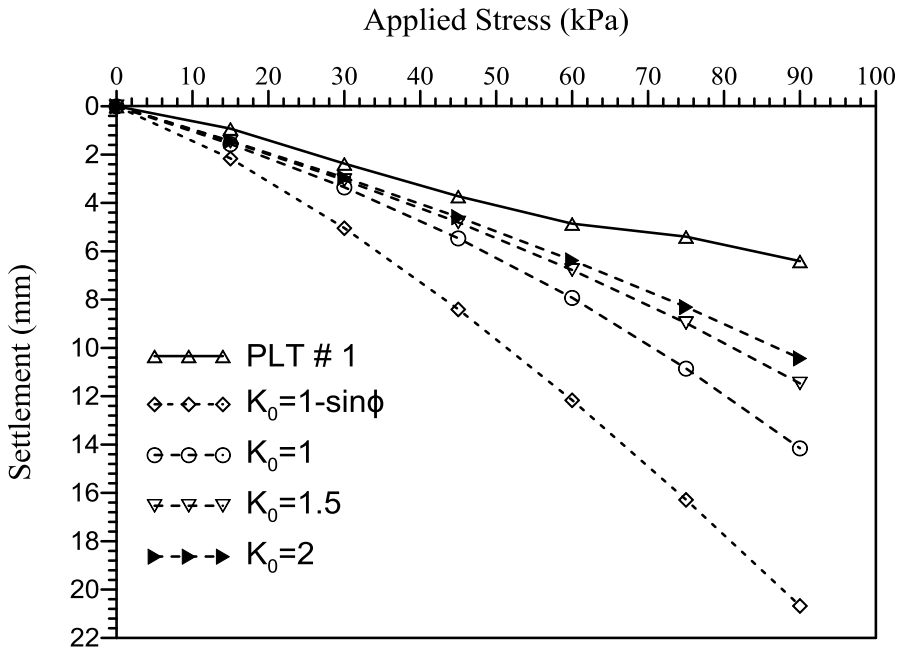

Figure 5-23: Simulation of Stone Columns Installation Effect by Increasing K_0 for Plate Load Test No.1, the WHA.

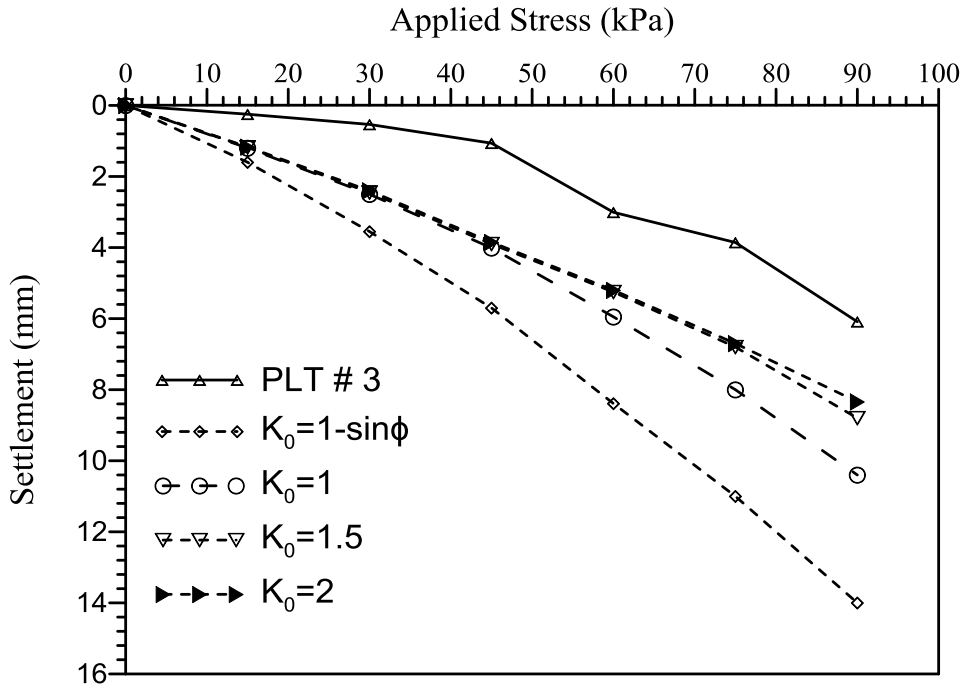

Figure 5-24: Simulation of Stone Columns Installation Effect by Increasing K_0 for Plate Load Test No. 3, the EWT.

Figure 5-25 shows an increase in the horizontal stress in soil layer due to manual increase of the coefficient of horizontal stress in the model. The increase in horizontal stress makes the stone columns more confined, and therefore reduces the vertical settlement.

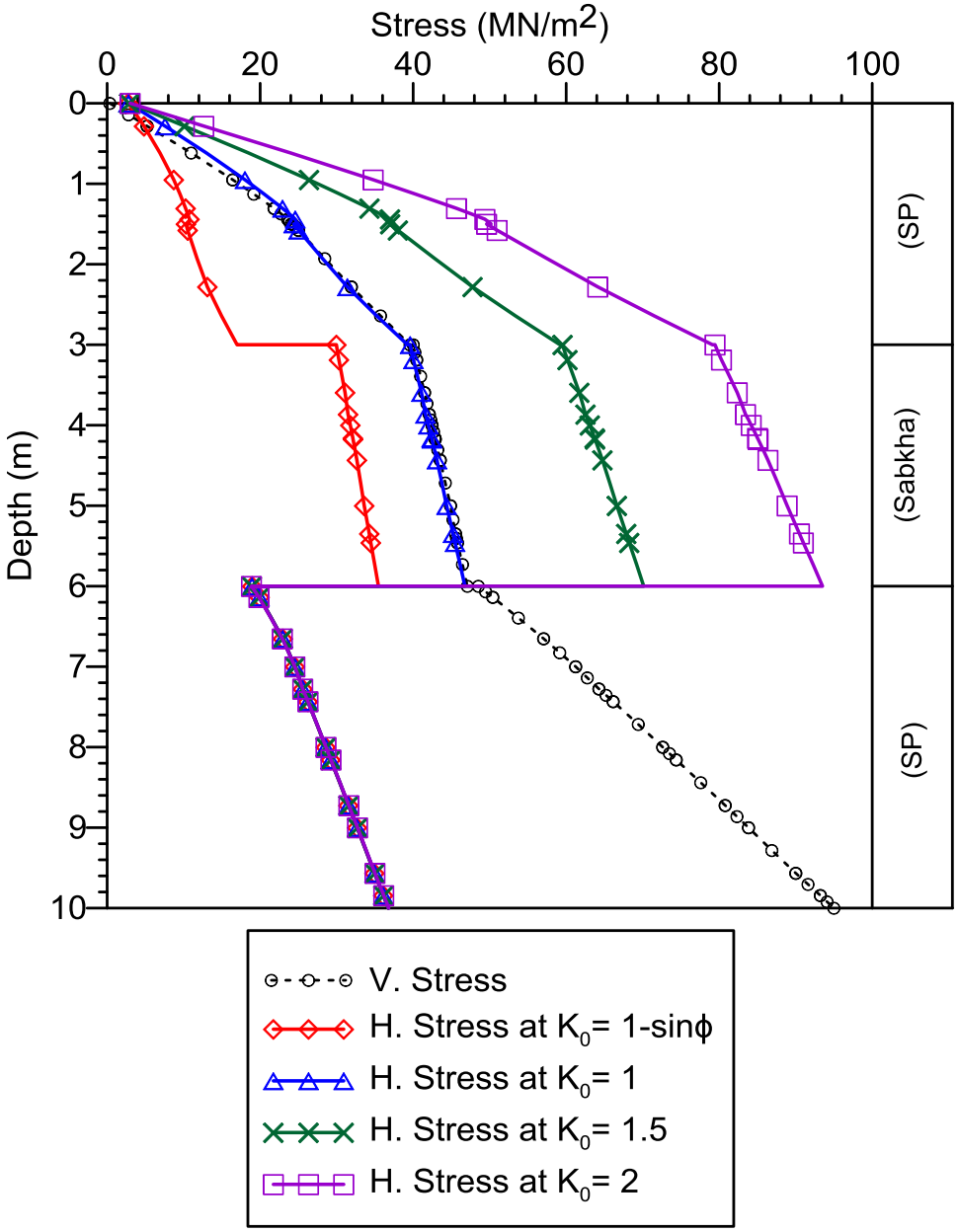

Figure 5-25 : Comparison between Horizontal Stress Using K_0 Increase Method for Plate Load Test No.1, the EWT.

5.7.2 Upgrade of Soil Layers Surrounding Stone Column

It was shown in the field data, presented in Chapter 4 that the stone column installation process significantly increases the CPT in the soil layer above sabkha but only a slight increase occurred in the upper part of sabkha. Consequently, the resistance to penetration of the soil above sabkha, surrounding the stone columns, were much higher than those measured before inserting stone columns.

In this proposed method, soils affected by stone columns installation, where the strength increased, are replaced by a material with higher strength and stiffness parameters. This is the case after the installation of the stone columns compared to the initial parameters before installing the stone columns. The approach presented in Chapter 4 uses post-CPT data to define new parameters for cohesionless soils and sabkha soils that are affected by Vibro – stone columns installation. It is possible to use the improvement factors proposed in Chapter 4 to simulate the increase in pre-CPT after installation of stone columns.

The design values for post-CPT and elastic modules after installation of stone columns are presented for each case in Figure 5-26 to Figure 5-31. The soil elastic modules and cohesion increase and decrease with depth according to the design line. The properties of soil layers after installation of stone columns are given in Table 5-14 to Table 5-19.

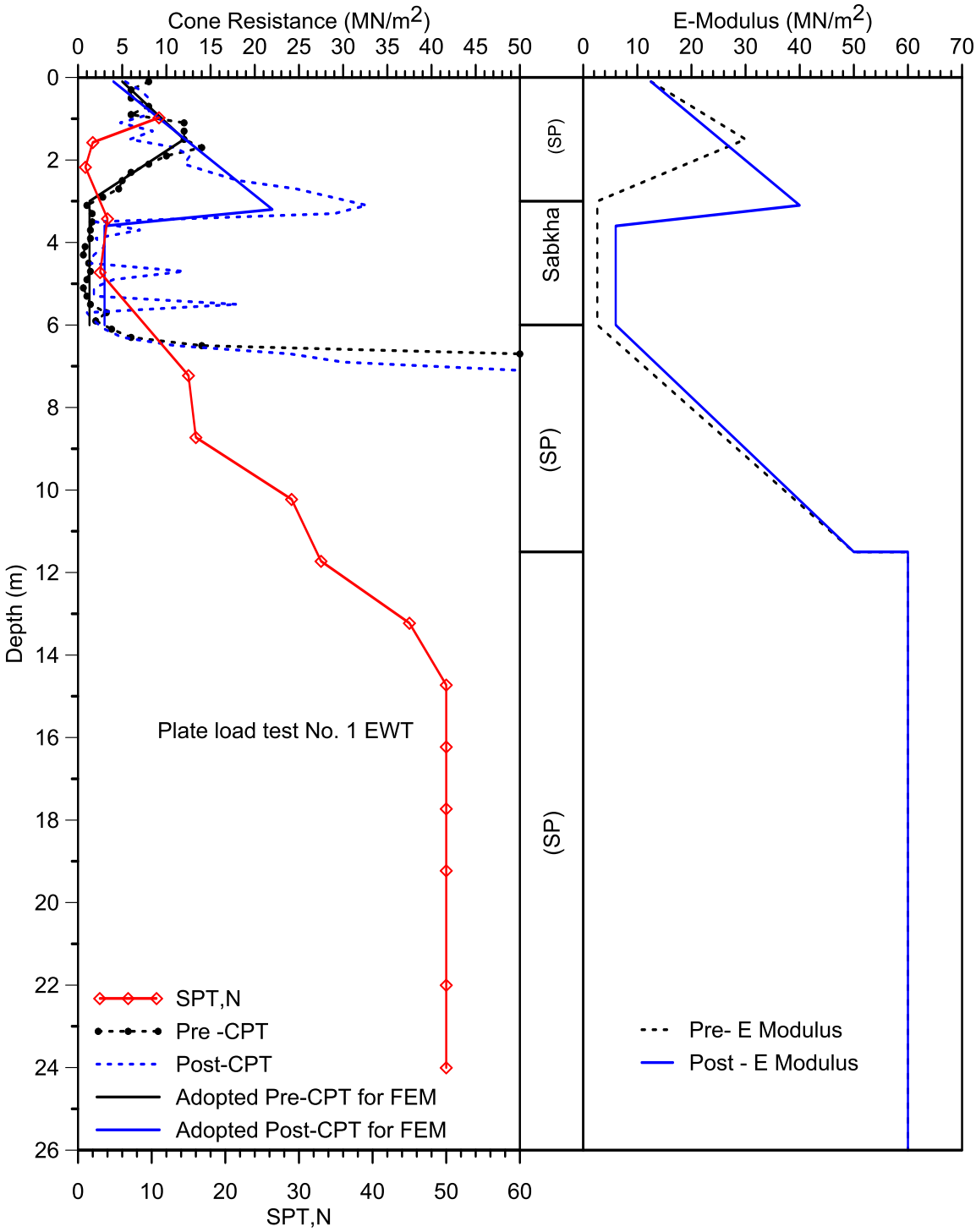

Figure 5-26: Pre- and Post-CPT Design Values Adopted for FEM, Plate Load Test No.1, the EWT.

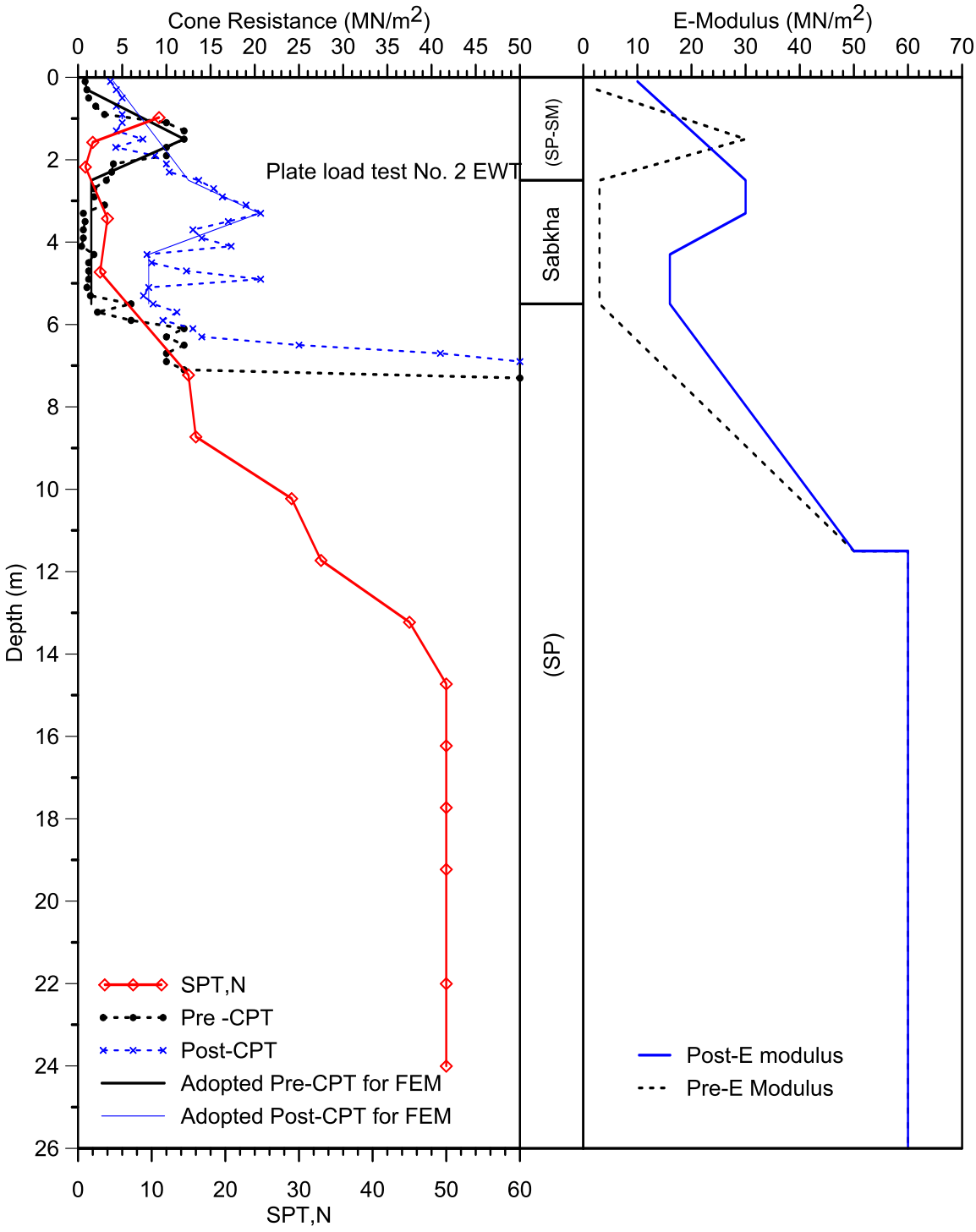

Figure 5-27: Pre- and Post- CPT Design Line Adopted for FEM in Plate Load Test No.2, the EWT.

Table 5-14: Upgraded Soil Layer Properties for Plate Load Test No.1 in EWT after Installation of Stone Columns.

Layer	Depth (m)	Dry/Sat. Unit Weight (kN/m^3)	Cohesion (kPa)	Friction Angle (°)	Dilatancy Angle (°)	Poisson Ratio
Layer1: Sand	0-3	18/21	1	35	5	0.3
Layer2: Sabkha	3-3.6	18 (saturated)	55	22	0	0.3
The other layers are not affected by stone column installation.						

Table 5-15: Upgrade Soil Layer Properties in Plate Load Test No. 2 in the EWT after Installation of Stone Columns.

Layer	Depth (m)	Dry/Sat. Unit Weight (kN/m^3)	Cohesion (kPa)	Friction Angle (°)	Dilatancy Angle (°)	Poisson Ratio
Layer1: Sand	0-2.5	18/21	1	34	4	0.3
Layer2: Sabkha (Top portion only)	3-3.6	18 (saturated)	55	22	0	0.3
The other layers are not affected by stone column installation.						

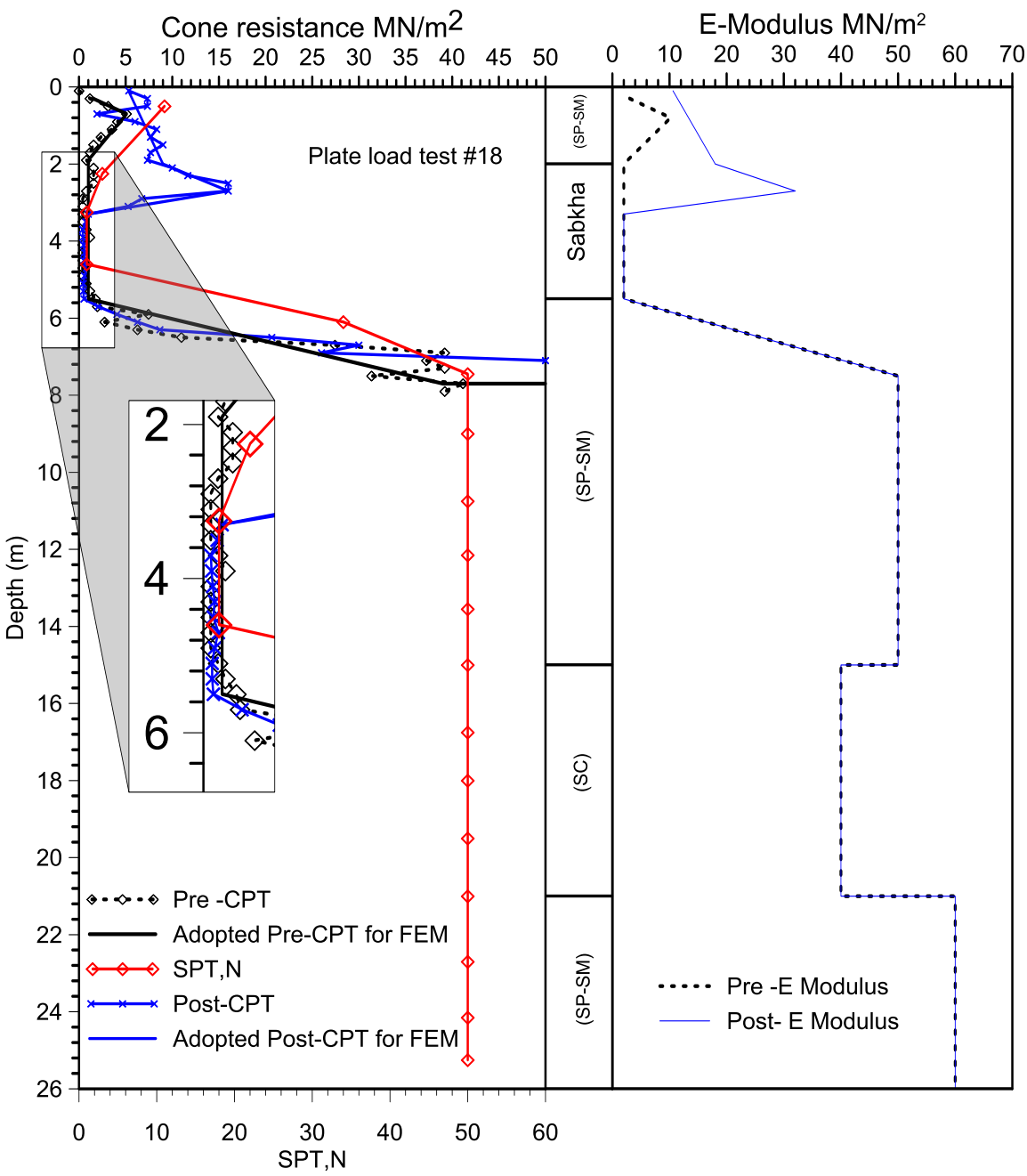

Figure 5-28: Pre and Post-CPT Design Line Adopted for FEM in Plate Load Test No.1, the WHA.

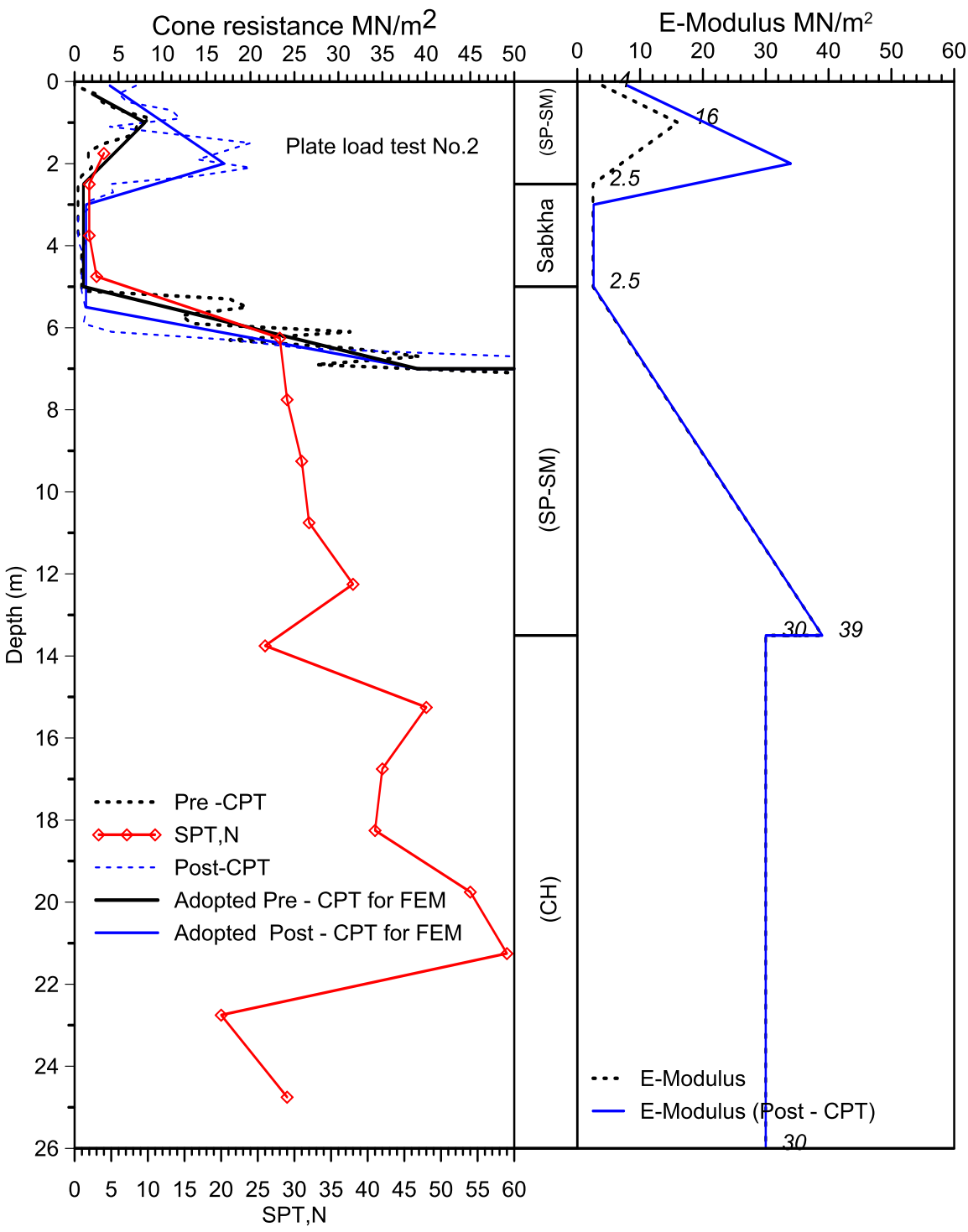

Figure 5-29: Pre and Post CPT Design Line Adopted for FEM in Plate Load Test No.2, the WHA.

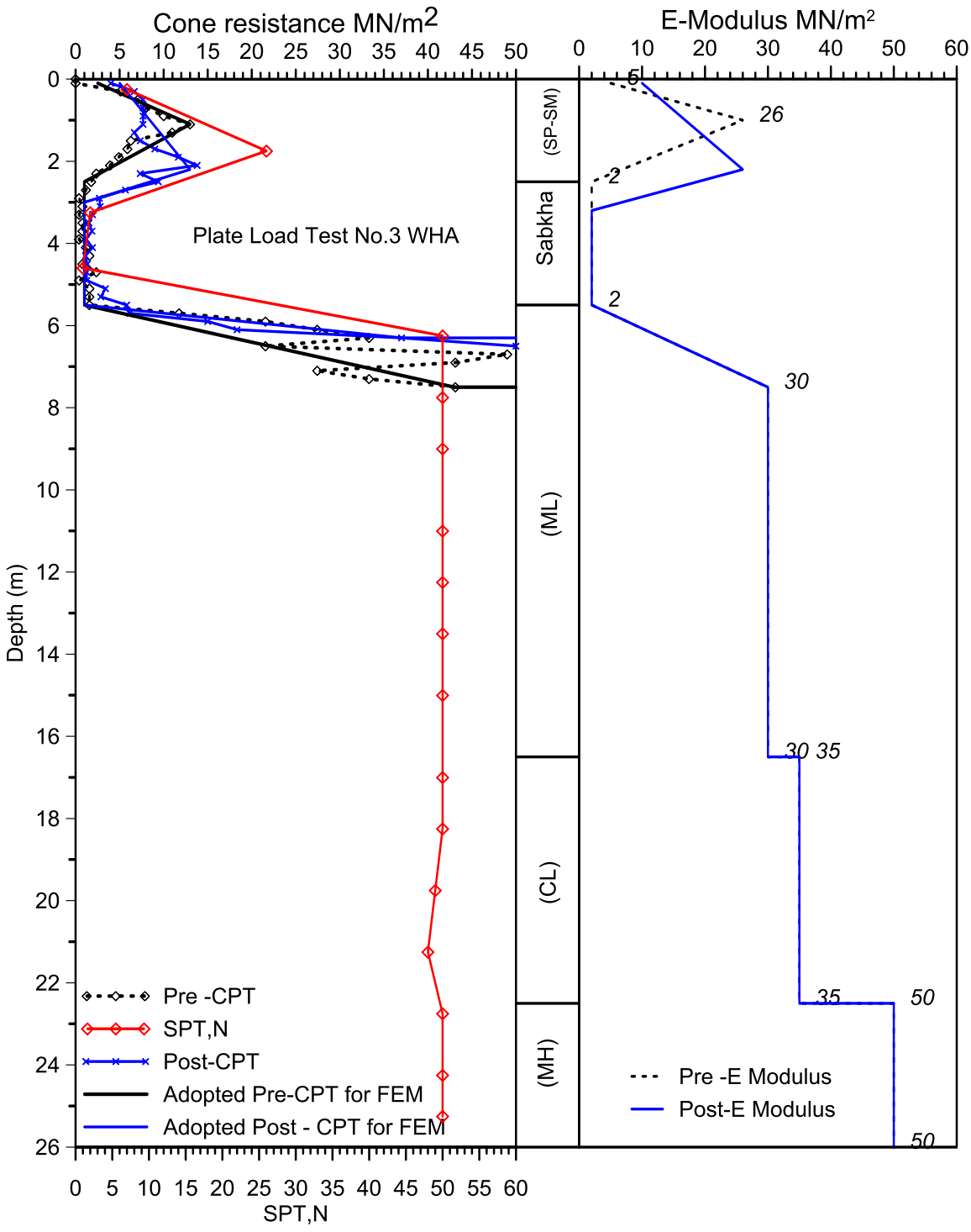

Figure 5-30: Pre and Post-CPT Design Line Adopted for FEM in Plate Load Test No.3, the WHA.

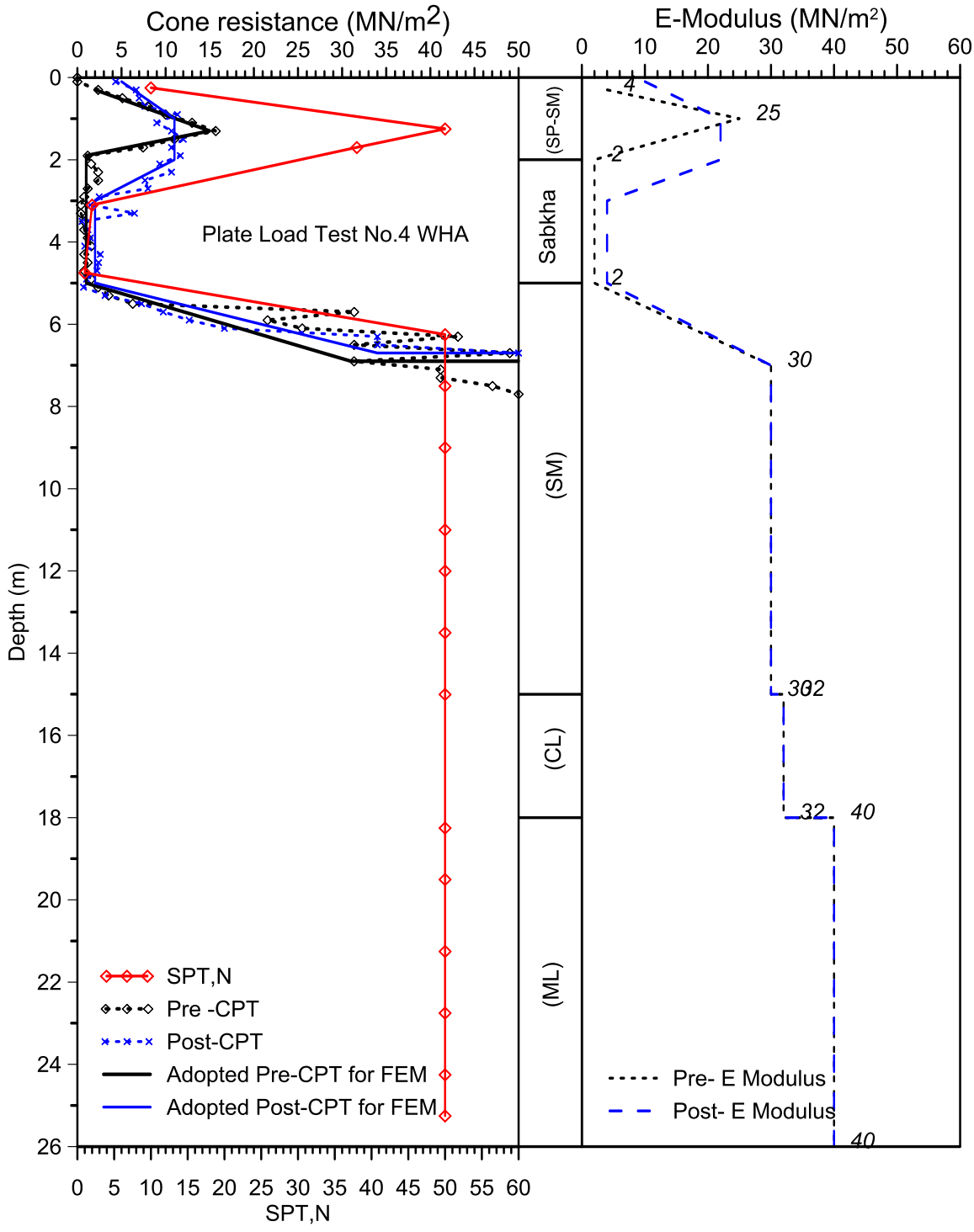

Figure 5-31: Pre and Post-CPT Design Value Adopted for FEM in Plate Load Test No. 4, the WHA.

Table 5-16: Upgraded Soil Layer Properties for Plate Load Test No.1 in WHA after Stone Columns Installation.

Layer	Depth (m)	Dry/Sat. Unit Weight (kN/m^3)	Cohesion (kPa)	Friction Angle (°)	Dilatancy Angle (°)	Poisson Ratio
Layer1:Sand with silt Upgraded)	0-2	17.5/20	1	34	4	0.3
Layer2: Sabkha (Upgraded top portion)	2-3.3	18	55	22	0	0.3
The other layers are not affected by stone column installation.						

Table 5-17: Upgraded Soil Layer Properties in Plate Load Test No.2 in WHA after Installation of Stone Columns

Layer	Depth (m)	Dry/Sat. unit weight (kN/m^3)	Cohesion (kPa)	Friction angle (°)	Dilatancy Angle (°)	Poisson Ratio
Layer1: Sand with silt (Upgrade)	0-2	17.5/20	1	33	3	0.3
Layer2: Sabkha (Upgrade)	2-3.2	18	55	22	0	0.3
The other layers are not affected by stone column installation.						

Table 5-18 : Upgraded Soil Layer Properties for Plate Load Test No. 3 in the WHA after Installation of Stone Columns.

Layer	Depth (m)	Dry/Sat. unit weight (kN/m^3)	Cohesion (kPa)	Friction angle (°)	Dilatancy Angle (°)	Poisson Ratio
Layer1:Sand with silt (Upgrade)	0-2	17.5/20	1	34	4	0.3
Layer2: Sabkha (Upgrade)	2.5-3.3	18	55	22	0	0.3
The other layers are not affected by stone column installation.						

Table 5-19 : Upgrade Soil Layer Properties in Plate Load Test No.4 in WHA after Installation of Stone Columns.

Layer	Depth (m)	Dry/Sat. unit weight (kPa)	Cohesion (kPa)	Friction Angle (°)	Dilatancy Angle (°)	Poisson Ratio
Layer1:Sand with silt (Upgrade)	0-2	18.5/20	1	35	5	0.3
Layer2: Sabkha (Upgrade)	2.5-3.3	18	55	22	0	0.3
The other layers are not affected by stone column installation.						

Typical Load-displacement curves for plate load test with numerical result using upgraded parameters method are shown in Figure 5-32 to Figure 5-34. All numerical settlement curves show good match with field data curves.

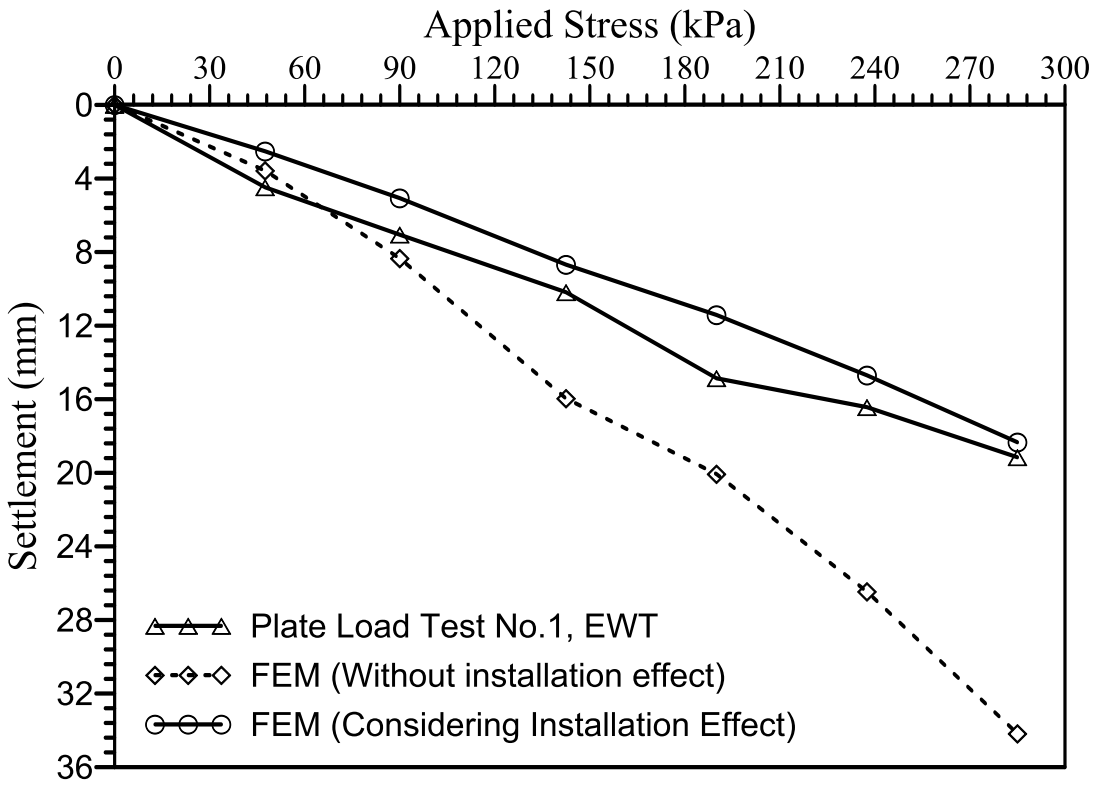

Figure 5-32: Comparison between Field and Numerical Result Using Upgraded soil Parameters Method for Plate Load Test No. 1, the EWT.

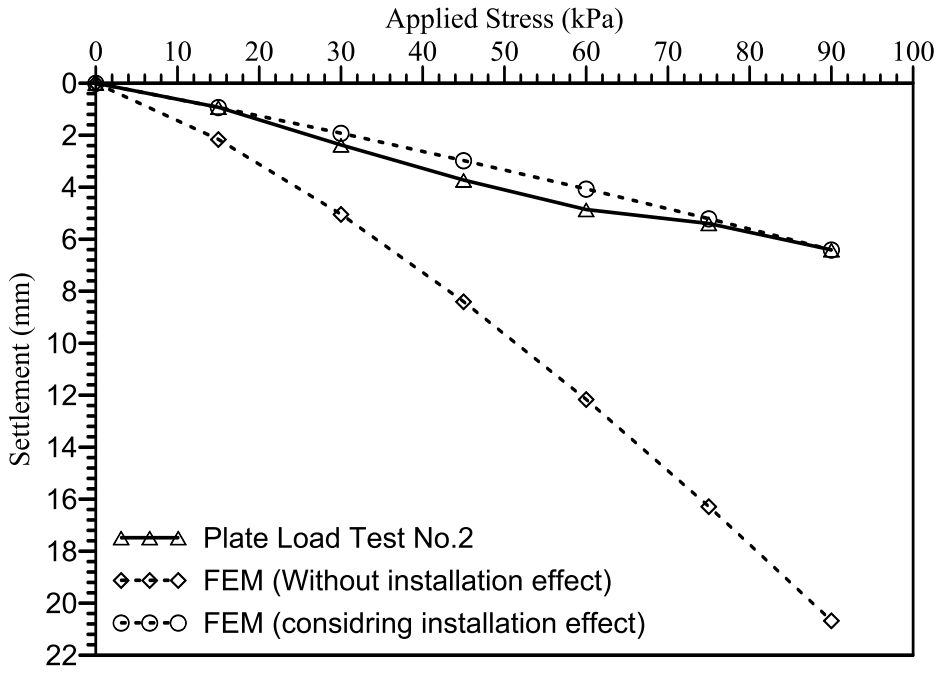

Figure 5-33: Comparison between Field and Numerical Result Using Upgraded Soil Parameters Method for Plate Load Test No.1, the WHA.

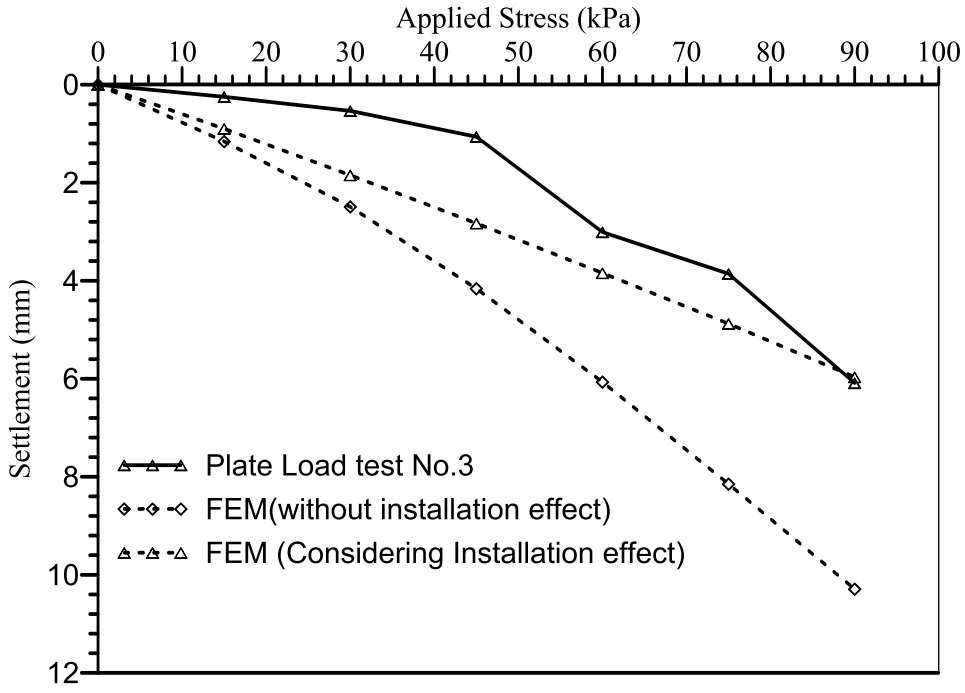

Figure 5-34: Comparison between Field and Numerical Result Using Upgrade Soil Parameters Method at Plate Load Test No.3, the WHA.

5.8 Results of Finite Element Analyses

After validation of the full scale plate load test on stone columns in sabkha soils by comparing numerical result with field data and adapting the method of upgraded soil parameters method to simulate installation effect, the main influence design parameters were examined using series of FEM models. This was intended to examine the effects on the settlement predictions, stress concentration and deformational behavior of the full-scale plate load test on stone columns in sabkha soils. A parametric study was carried out for this purpose.

5.8.1 Settlement versus Stone Column Depth

Relationship between vertical settlement and stone columns depth for plate load No. 1 in the EWT clearly shows a reduction is settlement with the increase in depth, as illustrated in Figure 5-35. The maximum settlement occurs at ground level and reduces gradually with depth to the extent that it becomes less than 5mm at depth of 5.5m, i.e. at the end of sabkha layer. The largest reduction in settlement can be seen in the upper layer, especially at ground surface, whereas, at lower depths, there is no significant difference in settlement as the depth increases. The same phenomenon appears in plate load test No. 5, which was performed directly on sabkha surface, as shown in Figure 5-36. The biggest reduction in vertical settlement can be seen in the sabkha layer, and there is no significant difference in settlement with depth increase for deeper sabkha levels.

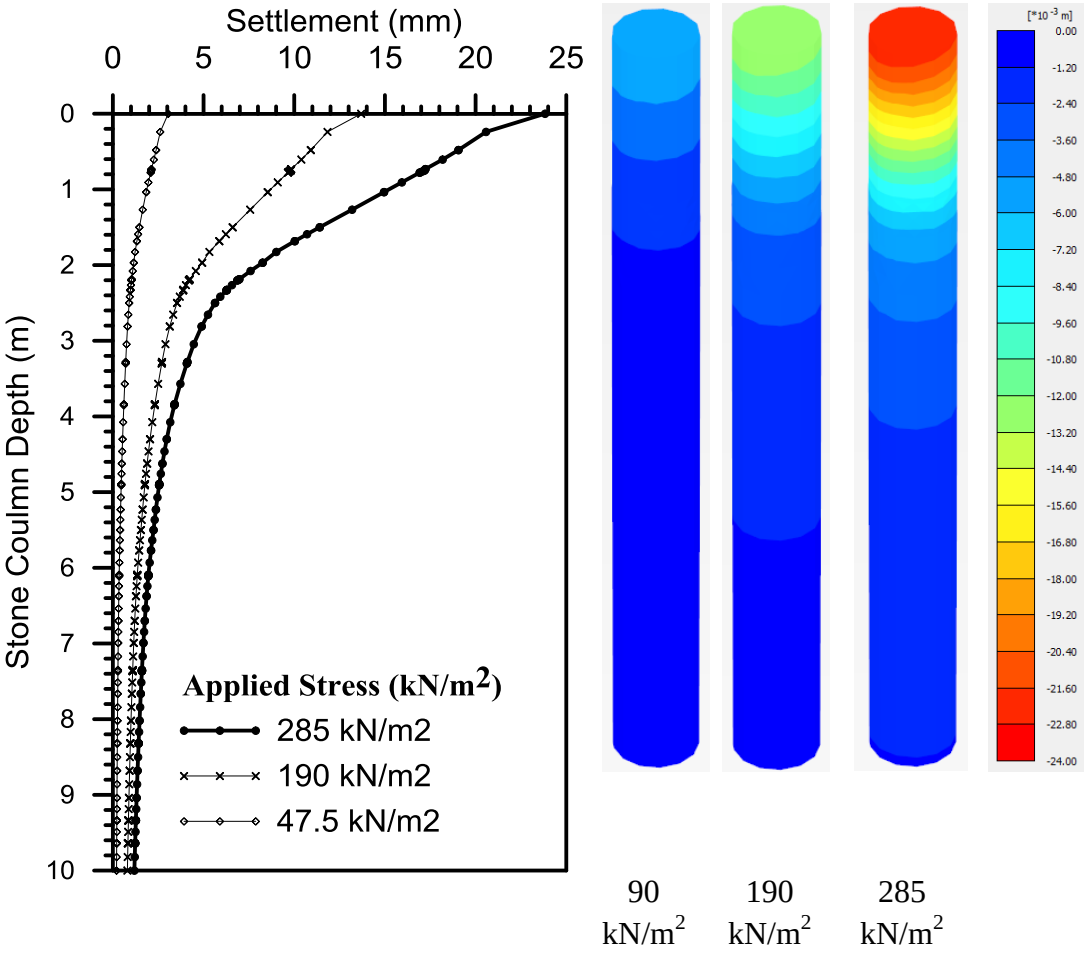

Figure 5-35: Variations of Vertical Settlement, from numerical simulation, with Stone Column Depth for Plate Load Test No. 1, the EWT.

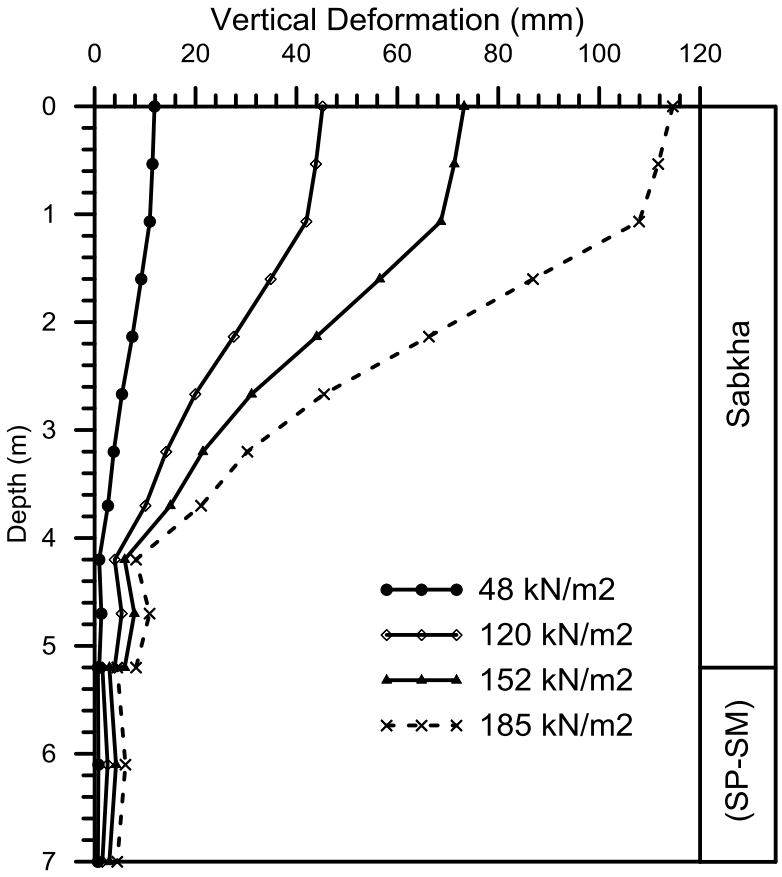

Figure 5-36: Variation of Vertical Settlement with Stone Column Depth for Plate Load Test No. 5 in EWT and Plate is Directly on Sabkha Surface.

5.8.2 Stress Distribution

Two approaches were utilized to assess the stress distribution within the columns and the soil surrounding the columns: (1) stress distribution on the surface directly under concrete plate and (2) vertical stress versus stone column depth. The results obtained from stress distribution on the surface are presented in Figure 5-37. It is obvious that the stresses on stone columns are much higher than those on the surrounding soil due to the relative stiffness of the two materials.

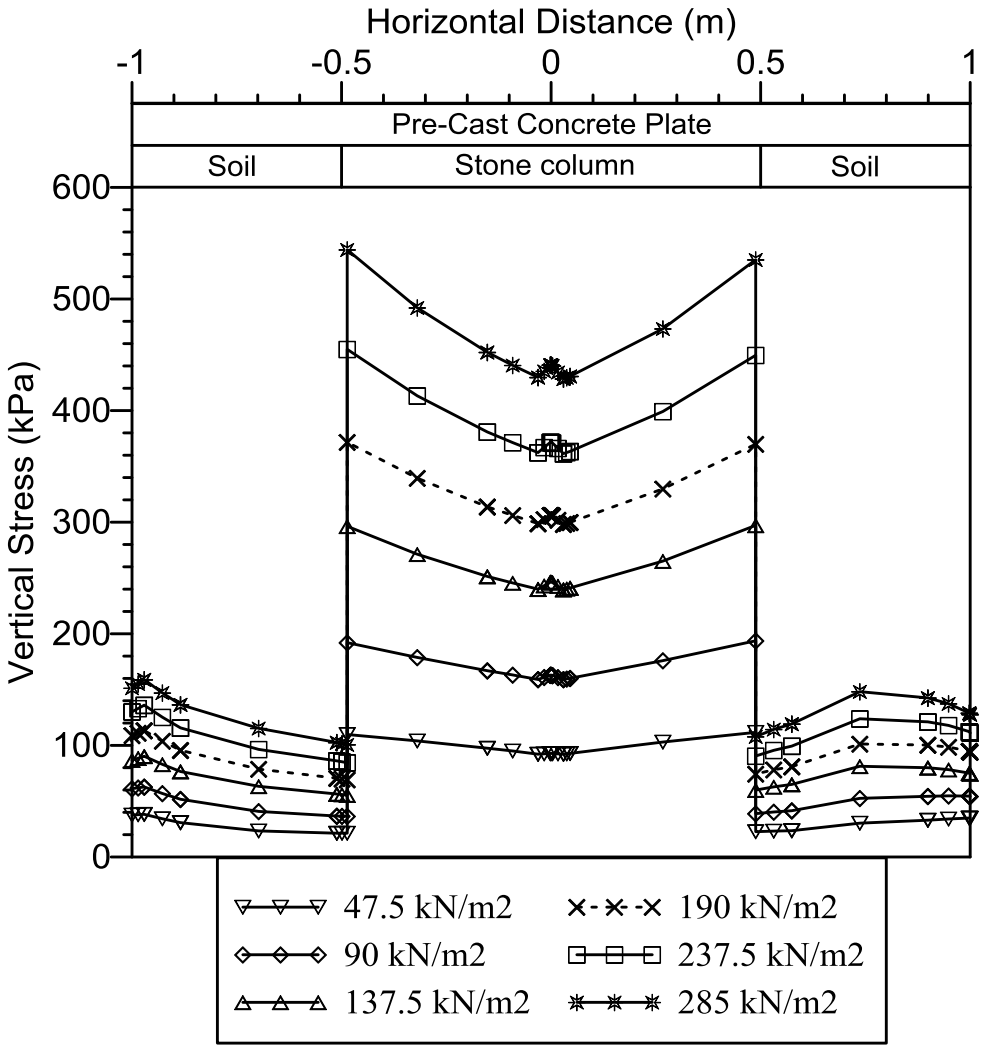

Figure 5-37: Stress Distribution over Stone Columns and Surrounding Soil for Plate Load Test No. 1, the EWT.

When a load is applied over stone columns and surrounding soils, the material tends to deform and stiffer the stone columns material, compared to soil, will take more load than the soil. The concentration of stress in the columns is mainly due to the stone columns being considerably stiffer than the surrounding soil. The deformation of the two materials, stone columns and soil, has to be approximately the same (compatibility of deformation), and therefore the stress on the stiffer stone column material will be greater than those in the surrounding soil.

Figure 5-38 shows the distribution of vertical stress in stone columns with depth. The curves show vertical stress that is high in the upper part but will decrease rapidly before reaching the depth of about 2.5m; the stresses below this level are those due to self-weight of soil, i.e. is not affected by loading.

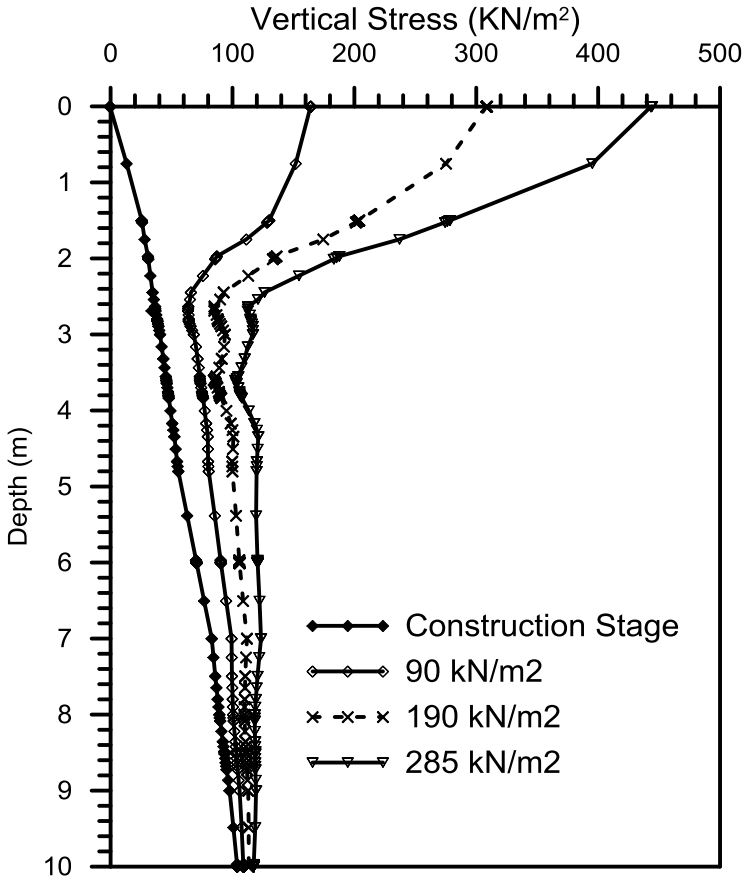

Figure 5-38: Distribution of Vertical Effective Stress with Depth in Center of Stone Column for Plate Load Test No. 1 in EWT.

Figure 5-39 shows the distribution of vertical stress at the bottom of stone column. There is no substantial increase (increase within 15% only) in stress in the stone column, compared to adjacent soil, due to load application. This proves that stress is not transmitted through stone column to end bearing stratum.

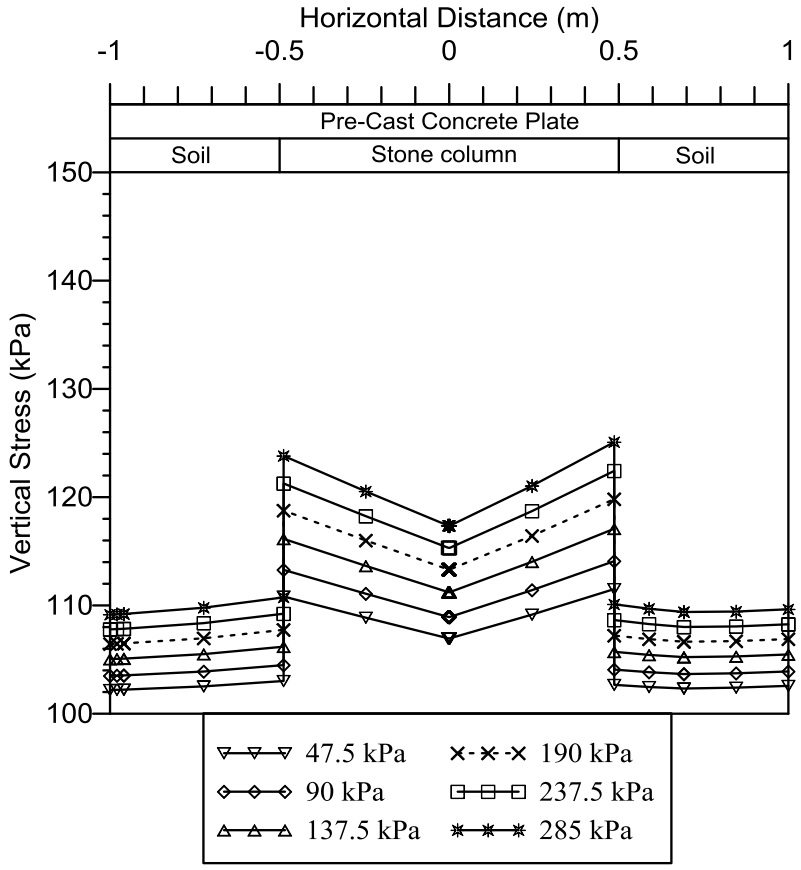

Figure 5-39: Stress Distribution at the Bottom of Stone Column in Plate Load Test No. 1 in EWT.

The stress concentration ratio is used to evaluate the relationship between stress in stone column and surrounding soils. The stress concentration ratios are calculated using the following relationship:

$$\text{Stress concentration ratio (n)} = \frac{\text{Stress on stone column}}{\text{Stress on surrounding soil}} = \frac{\sigma_c}{\sigma_s}$$

Area considered in calculating the stress in stone columns and surrounding soil is shown in Figure 5-40.

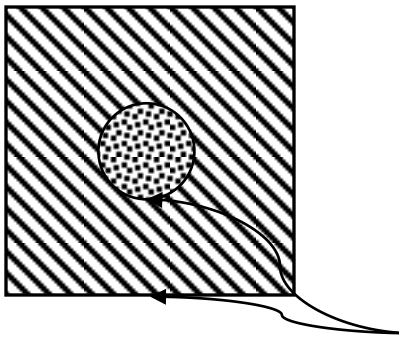

Figure 5-40: Methodology of Determination of Stress Concentration Ratios for Numerical Studies.

The stress concentration ratio shows slight increase with increased loading, as shown in Figure 5-41 .

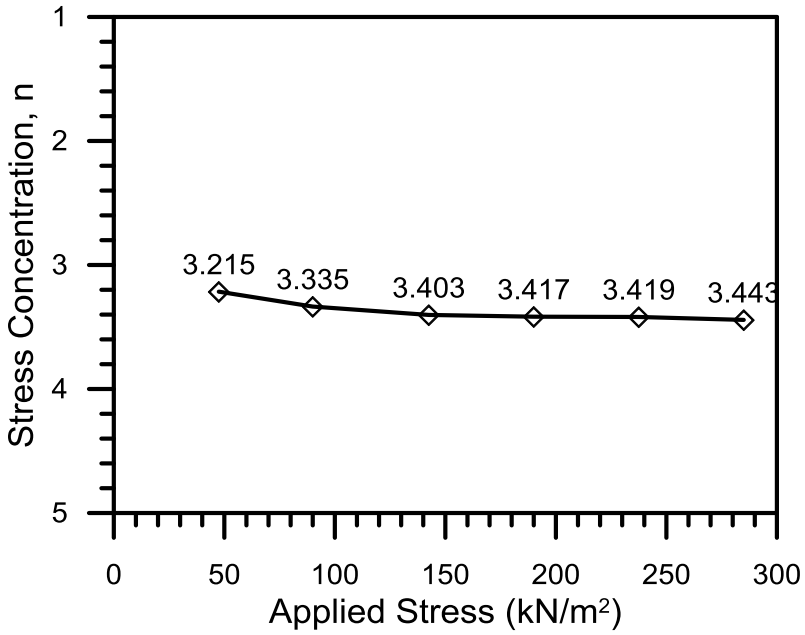

Figure 5-41: Stress Concentration Ratio at Surface in Plate Load Test No.1 in EWT.

5.8.3 Effect of Elastic Modules of Stone Column

One of parameters controlling the behavior of stone columns is the elastic modulus of the stone column material. Figure 5-42 shows the effect of stone column elastic modules values on the vertical settlement of composite area. It is observed that by keeping other

parameters constant, the change of column elastic modules did not have a major influence on the vertical settlement values. Increasing the elastic modules of columns from 50 to 80 MPa produced a reduction of settlement that did not exceed 13% at a stress of 90 kPa. This clearly indicates that the settlement is not very sensitive to the elastic modulus of the stone column material.

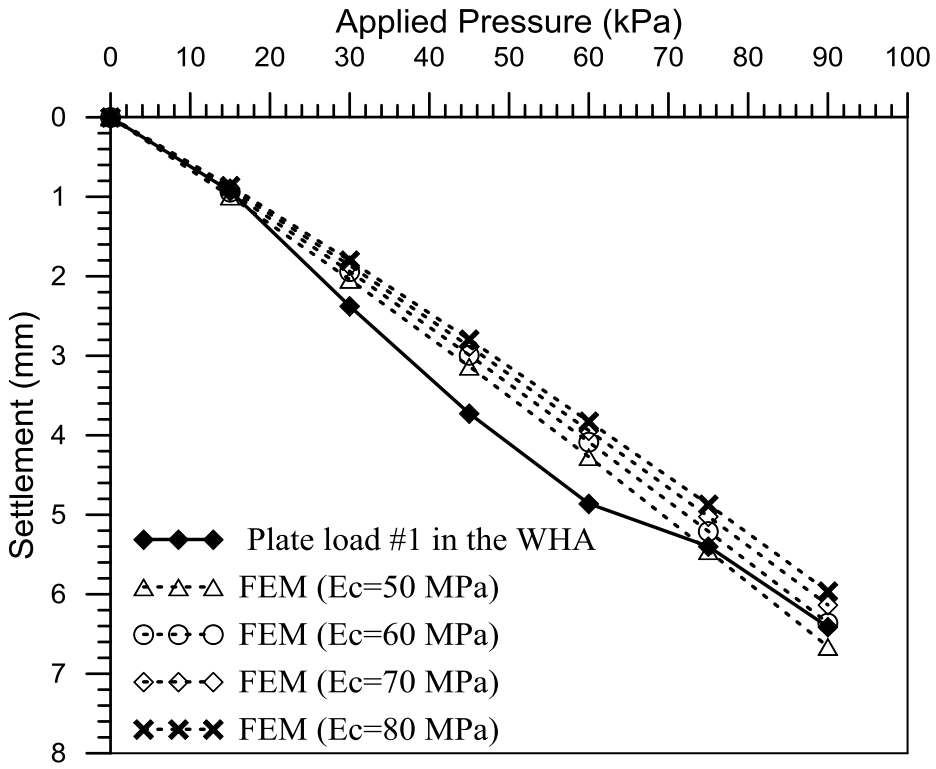

Figure 5-42: Effect of Stone Column Elastic Modules on Surface Settlement.

5.8.4 Effect of Angle Friction of the Stone Column

In addition to the elastic modulus, another parameters controlling the behavior of stone columns is the angle of internal friction of the stone column material. Figure 5-43 shows the variations of vertical settlement with the angle of friction of the stone column. The figure clearly shows that the settlement decreases as the angle of friction increases while

keeping other parameters constant. It should be clear, however, that the reduction is not significant although the increase in the angle of internal friction is relatively high.

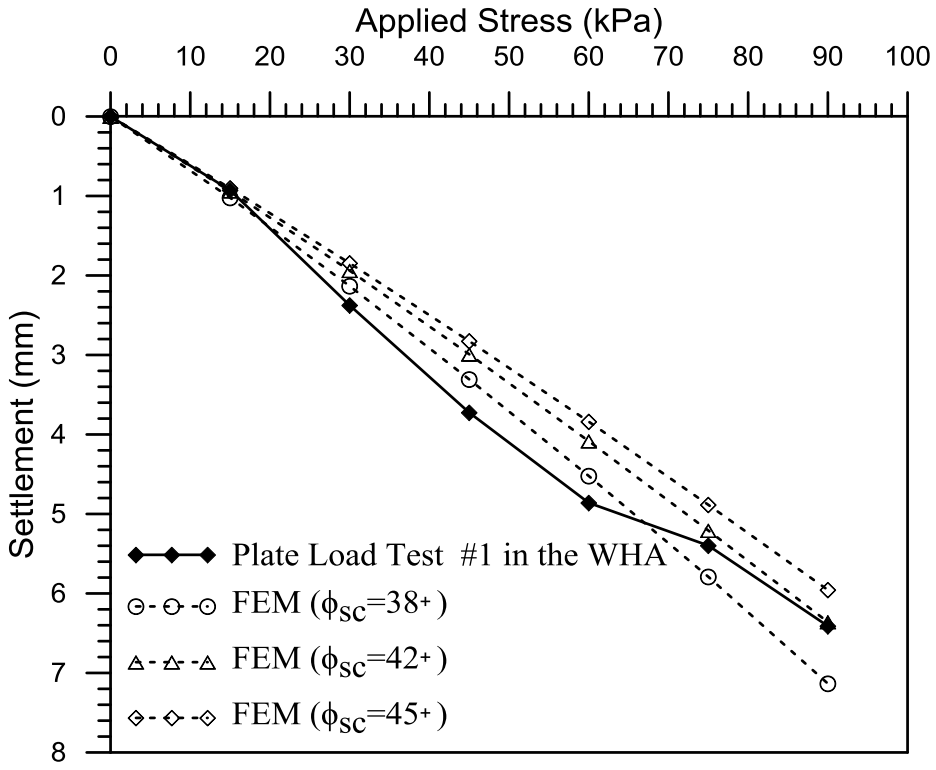

Figure 5-43: Effect of Angle Friction of Stone Column on Surface Settlement.

5.8.5 Effect of stone column Poisson's Ratio

Figure 5-44 shows a plot of settlement versus Poisson's ratio of the stone column. The figure shows that the settlement decreases as Poisson's ratio of the column increases. The figure illustrates the constant stone column parameters, the effect of Poisson's ratio is insignificant on vertical settlement. A value of 0.3 can be adopted for the stone column material.

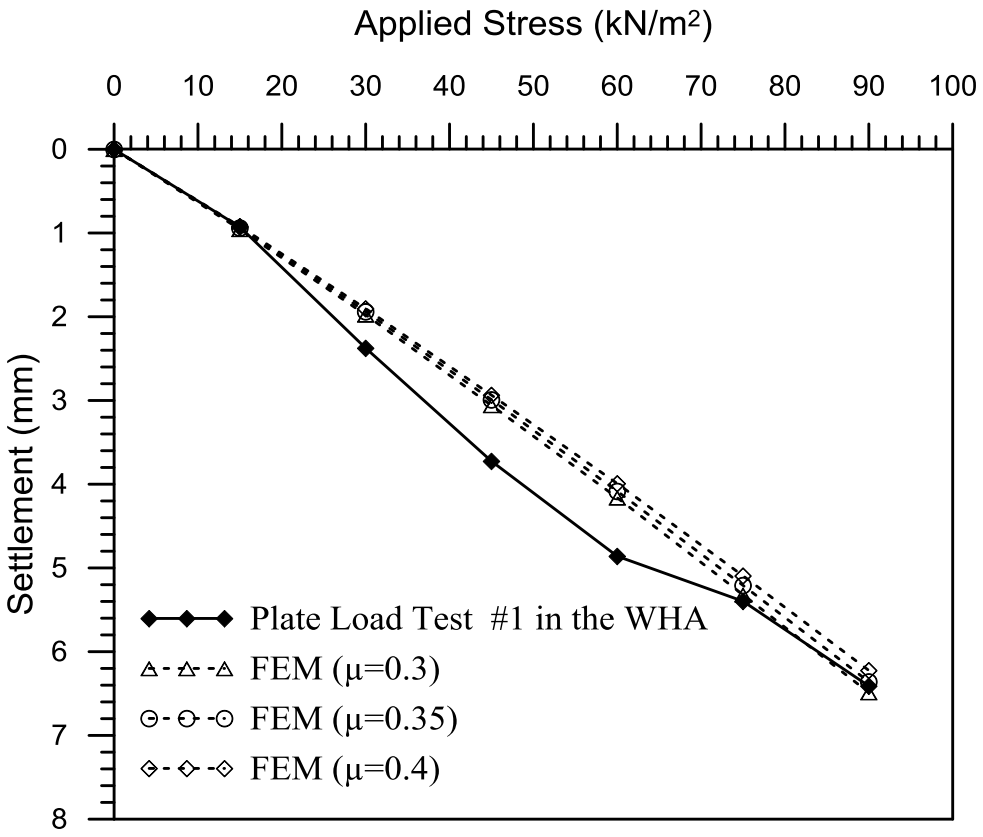

Figure 5-44: Effect of Poisson's Ratio of Stone Column on Surface Settlement.

CHAPTER 6

PERFORMANCE OF STONE COLUMNS IN SABKHA SOILS AFTER SABKHA CONSOLIDATION

6.1 Introduction

Numerical analysis provides a very useful tool for the investigation of the behavior of stone column reinforced ground. It is also utilized as a supplementary tool to the existing design methods especially in case of heterogeneous and anisotropic soil where current design methods normally adopt simplification and assumptions (Potts et al., 2001).

In addition to the high compressibility, sabkha soils exhibit very slow consolidation process. Stone columns are often used to strengthen the sabkha soils and work as a drainage influencing the consolidation time of sabkha surrounding the stone columns. However, there is no well-documented information on how the stone columns influence the consolidation time of sabkha.

In this Chapter, finite element analyses of consolidation have been performed to assess the performance of stone columns and the surrounding sabkha soils. The numerical results have been compared with the field data. The main features of stone columns, such as the reduction of surface settlement, the quick dissipation of excess pore pressures, and the stress concentration is studied.

6.2 Consolidation Modeling

The long-term behavior of sabkha soils under the applied loads in which excess pore pressure develops can be modeled using deformation consolidation analysis approach. In this method, the sabkha is assumed to behave in undrained manner during load application. Long-term settlements are determined by conducting a consolidation analysis taking into account the pore pressure dissipation. Mohr-Coulomb model is used for the determination and comparison of consolidation rate with field data. The stone columns and cohesionless soil are modeled as drained material.

6.3 Model Geometry

Full-scale plate load tests were conducted at the WHA as presented in Chapter 3. The loading test was performed on one stone column with static load intensity of 137 kN/m^2 using rigid concrete block for a period of 73 days. The stone columns were installed in a square grid arrangement at 2m spacing. The diameter of the stone columns was taken as 1 m and the length was considered to be 10 m, as per the construction reports. The ground water level was set at 1.7m below the ground surface, as indicated in the geotechnical investigation report. Due to the symmetrical conditions, only one quarter of the model has been considered in the simulations. The geometry of the adopted footing load test is shown in Figure 6-1.

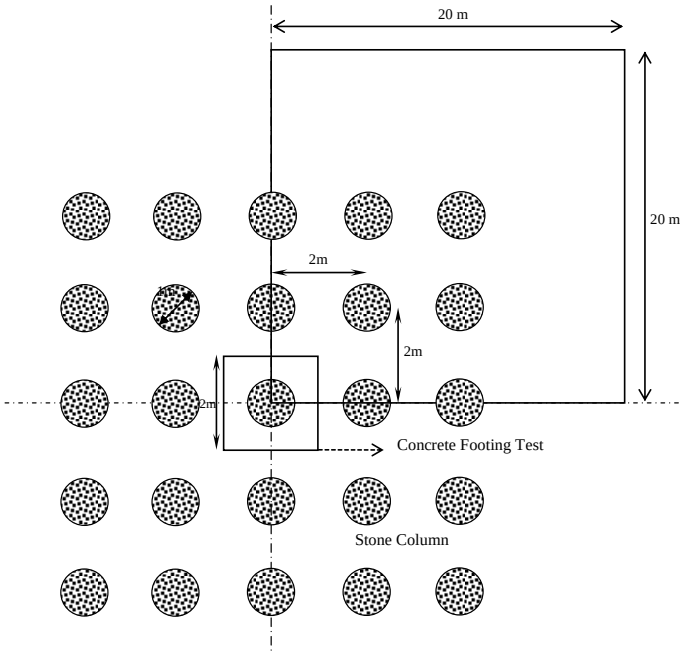

Figure 6-1: Geometry of FEM for Consolidation Test in the WHA.

The depth and width of the modeled region are selected to be large to avoid boundary conditions effects. The boundary conditions of consolidation have been accounted for in all construction stages.

It is important that a suitable mesh size is selected that it is fine enough to capture the real behavior of the model while the analysis time is kept reasonable. The global mesh coarseness was selected in the fine range, but the critical areas were refined to be finer. The created geometry of the model and the generated mesh used in analyses are presented in Figure 6-2.

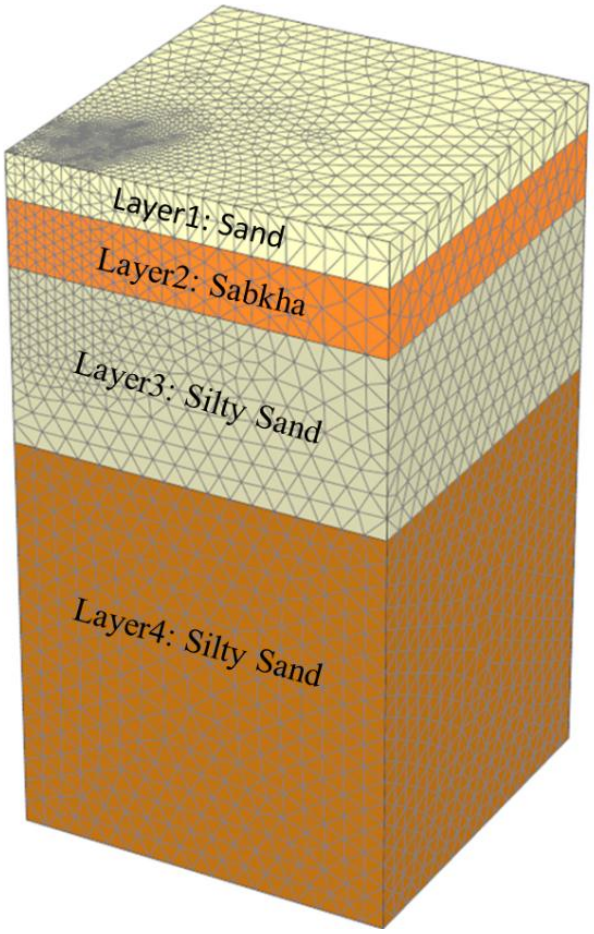

Figure 6-2: FEM Mesh of the PLAXIS 3D Consolidation Model.

6.4 Material Parameters

The soil profile was calculated based on the field data presented in Chapter 3. Strength parameters for soil layers are typically adopted using the approach develop in Chapter 4. Both stone column and soil layers were modeled using Mohr-Coulomb (MC) soil model. SPT and CPT tests around plate load test are shown in Figure 6-3. Material properties adopted for consolidation model are given in Table 6-1. The material parameters for stone columns are those shown in Table 5-2.

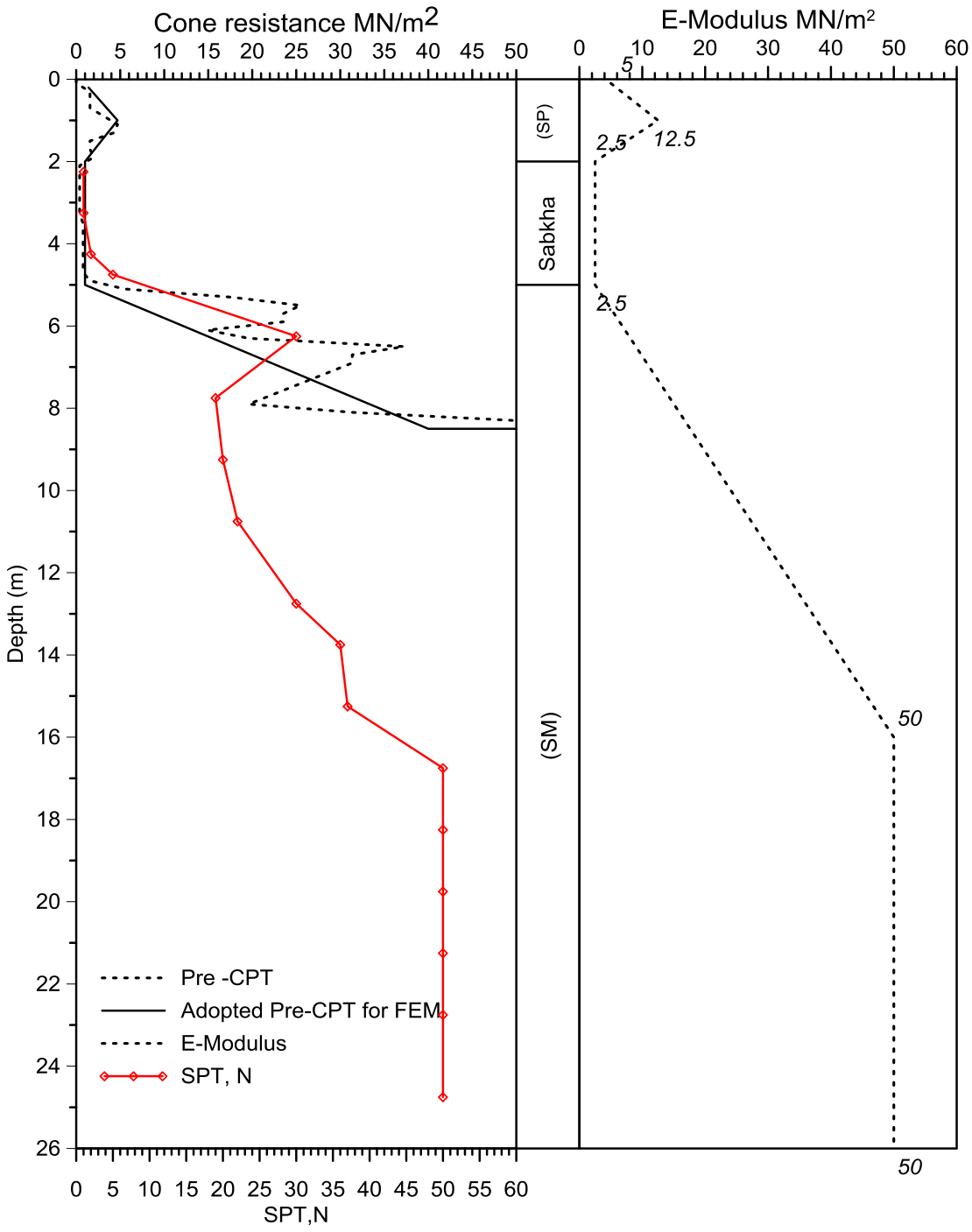

Figure 6-3: SPT, CPT Data and E-Modulus Adopted for the Consolidation Model.

Table 6-1: Soil Layer Properties after Installation of Stone Columns for Long-Term Plate Load Test.

Layer	Depth (m)	Dry/Sat. Unit Weight (kN/m^3)	Cohesion (kPa)*	Friction angle (°)	Dilatancy Angle (°)	Poisson Ratio
Layer1: Sand	0-2	17/19	1	32	2	0.3
Layer2: Sabkha	2-5.5	14 (saturated)	20	15	0	0.3
Layer3: Silty Sand	5.5-16	19 (saturated)	1	35	5	0.3
Layer4: Silty Sand	16-30	20 (saturated)	1	36	6	0.3

*: a cohesion value of 1 kPa is adopted for sands to improve the numerical stability.

The coefficient of consolidation (Cv) was determined directly from laboratory consolidation tests. Table 6-2 and Table 6-3 illustrate the summarized results for four different soil samples taken from bore holes located near the WHA. Coefficient of permeability (kv) can be calculated from the coefficient of consolidation (cv) and the coefficient of volume change (mv) using the following equation:

$$k_v = c_v \times m_v \times \gamma_w \quad (6\text{-}1)$$

The average value of the coefficient of consolidation is 1.23 m^2/day and coefficient of permeability is 1.20×10^{-2} m/day. The coefficient of permeability values for sand and stone columns were obtained from the relationships developed by many researchers, as outlined in Table 6-4.

Because of the migration of sabkha and cohesionless fine particles into the voids between stone column materials, a clogged zone could form within the stone column in the external shell of the soil-column interface. In addition, as a result of installation, a smear zone is developed in the soil adjacent to this interface. Relationships developed by Han and Ye (2002) and Wang (2009) are adopted to include the effect of these two zones on the coefficient of permeability (Han and Ye, 2002; Wang, 2009):

$$\frac{k_s}{k_h} = 0.1 \quad 6\text{-}2$$

Where

k_h: Horizontal permeability of soil before installation of the stone columns, and

k_s: Horizontal permeability of soil in the smear zones.

Table 6-2: Consolidation test No.1 in the WHA.

Sample Type	Sample Depth, m	Wet Density, g/cc	Initial Void Ration, e_0	Specific Gravity, G_s	Moisture Content, %
UDS	4.5-5	1.8	1.136	2.55	50.75

Pressure (KN/m^2)	Coefficient of Consolidation (Cv) m^2/day	Coefficient of compressibility m^2/kN	K m/day
0-25	2.8944	1.34×10^{-3}	3.80×10^{-2}
25-50	1.62432	5.35×10^{-4}	8.52×10^{-3}
50-100	1.23552	4.55×10^{-4}	5.51×10^{-3}
100-200	1.14912	3.34×10^{-4}	3.77×10^{-3}
200-400	0.79488	2.07×10^{-4}	1.61×10^{-3}
400-800	0.330912	1.64×10^{-4}	5.32×10^{-4}

Table 6-3: Consolidation Test No.2 in the WHA.

Sample Type	Sample Depth, m	Wet Density, g/cc	Initial Void Ration, e_0	Specific Gravity, G_s	Moisture Content, %
UDS	3.5-4	1.76	0.959	2.484	38.173

Pressure (KN/m^2)	Coefficient of Consolidation (Cv) m^2/day	Coefficient of Compressibility m^2/kN	K m/day
0-25	1.512	1.78E-03	2.64×10^{-2}
25-50	1.2096	1.48E-03	1.76×10^{-2}
50-100	0.438912	9.75E-04	4.20×10^{-3}
100-200	1.88352	5.13E-04	9.48×10^{-3}
200-400	0.9504	3.17E-04	2.96×10^{-3}

Table 6-4 : Summary of Permeability Coefficients for Different Soil Types.

Typical Soil	Value of k (cm/s)	Reference
Coarse gravel	$> 10^{-1}$	(Terzaghi and Peck, 1968)
Sand, fine sand	10^{-1} to 10^{-3}	(Terzaghi and Peck, 1968)
Silty sand, dirty sand	10^{-3} to 10^{-5}	(Terzaghi and Peck, 1968)
Silt, fine sandstone	10^{-5} to 10^{-7}	(Terzaghi and Peck, 1968)
Clean gravel and sand	10 to 10^{-3}	(Kézdi, 1980)
Fine sand, sandy silt, silt	10^{-3} to 10^{-7}	(Kézdi, 1980)
Well sorted gravel	10 to10^{2}	(Bear, 2013)
Well sorted sand or sand & gravel	10 to 10^{-3}	(Bear, 2013)
Very fine sand, silt, loess, loam	10^{-3} to 10^{-7}	(Bear, 2013)

6.5 Construction Stages

After the input of the material properties and generation of the mesh in the input phase of Plaxis software, initial stresses are built in the calculation step using K_o-procedure. Three methods were considered for examining the consolidation progress in the plate load test:

- Consolidation for the same field loading time of 73 days.
- Consolidation until full dissipation of the excess pore water pressures occurs; full dissipation is assumed when excess pore water pressure is less than or equal to 1 kPa.
- Consolidation until the soil has reached 90% degree of consolidation.

Figure 6-4 illustrates the calculation steps of modeling stone columns in sabkha soils during consolidation stages.

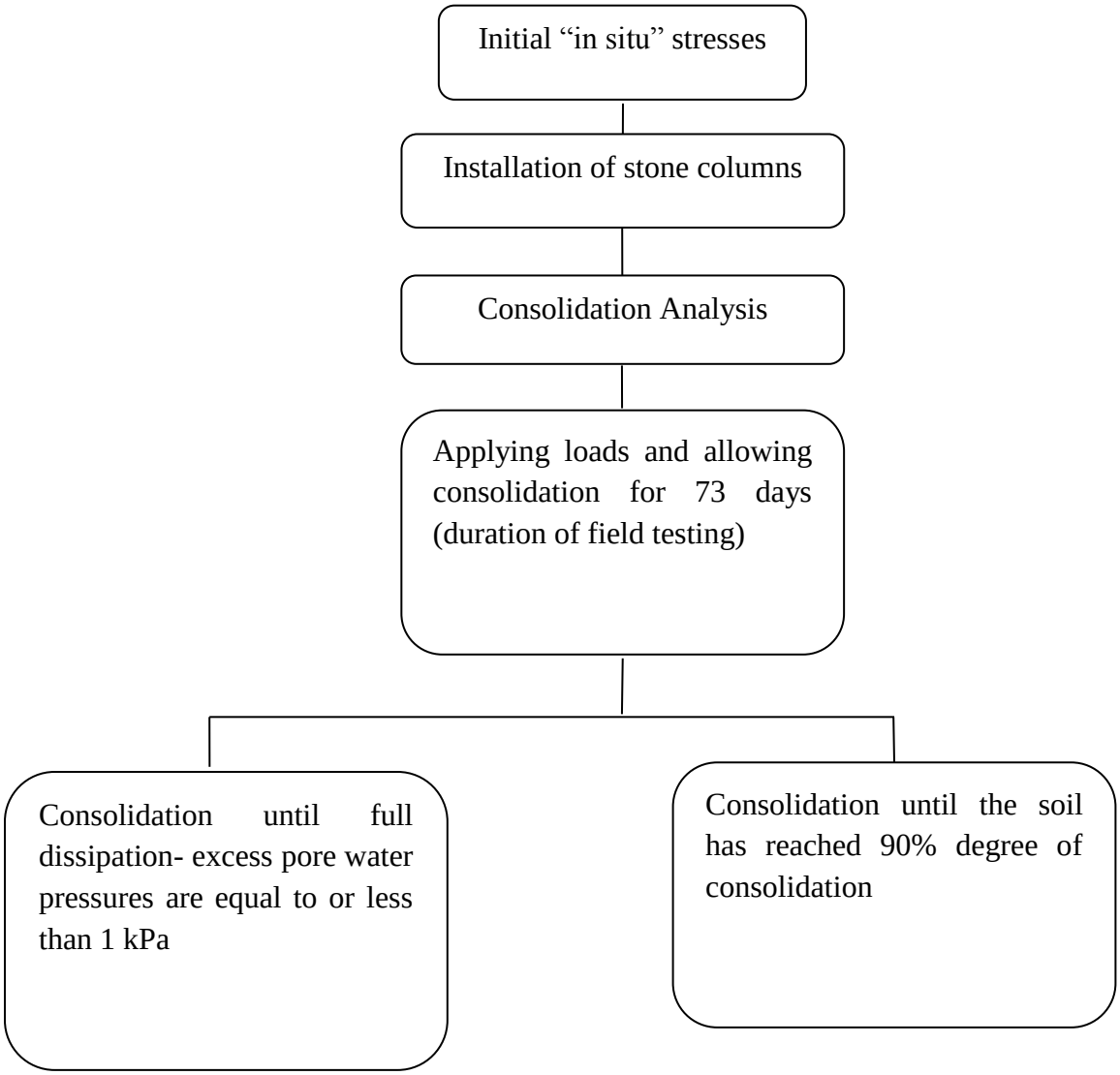

Figure 6-4: Numerical Simulations for the Consolidation Model.

6.6 Consolidation Modeling Results

The analysis of consolidation focused on the comparison of the time settlement (vertical) curves, horizontal displacement in stone column and the generated excess pore pressure.

6.6.1 Vertical Settlement

The rate of consolidation in terms of settlement at the top of the stone column is evaluated. Comparison between results from the finite element model and field results are presented in Figure 6-5. The comparison indicates that good agreement is achieved between the field and the finite element simulation. It is observed that the finite element results are slightly faster than the field results especially in the early phases. This could be attributed to the different assumptions used in finite element modeling.

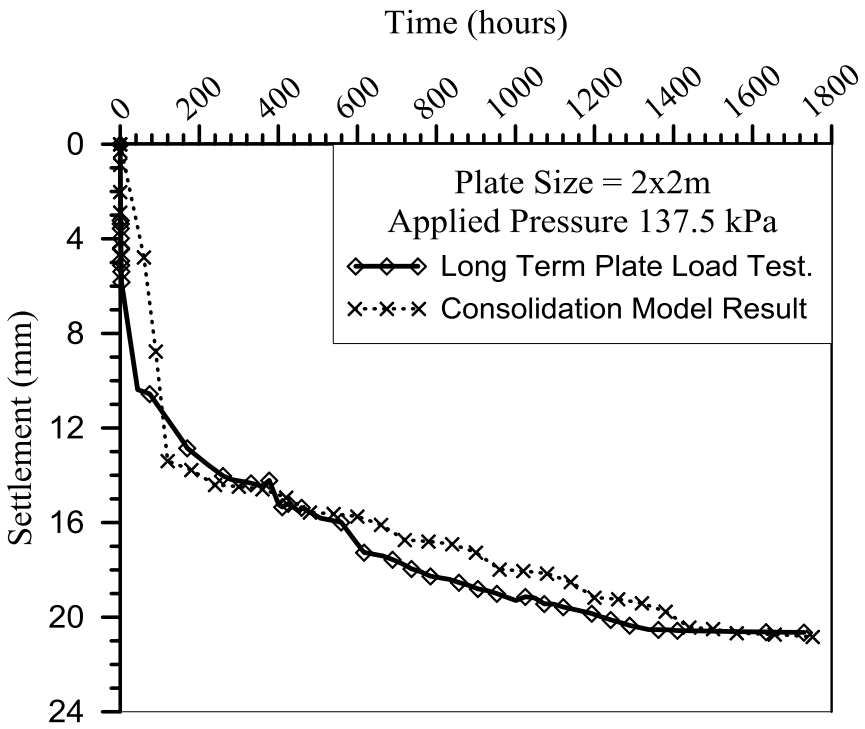

Figure 6-5: Comparison between Field and Numerical Consolidation Result for the 2x2m plate in WHA.

Figure 6-6 shows a slight increase in vertical settlement due to full dissipation of excess pore water pressures $\left|\mathbf{1\ kN/m^2}\right|$ or 90% degree of consolidation after 73 days.

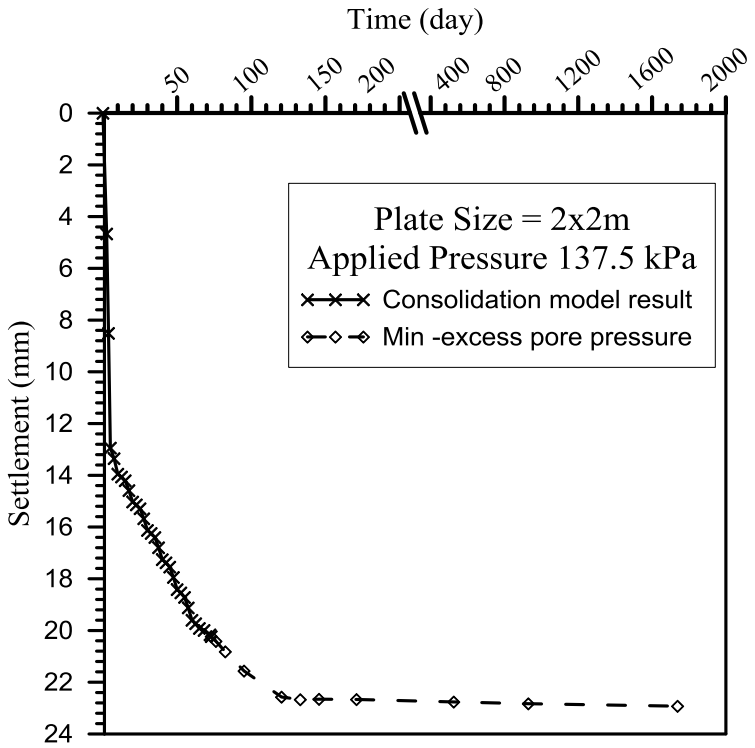

Figure 6-6: Increase in Vertical Settlement beyond the 73 Days Due to Full Dissipation, Excess Pore Water Pressures or 90% Degree of Consolidation.

6.6.2 Settlement versus Stone Column Depth

The literature reveals that stone columns might exhibit differnt modes of deformation such as punching, bulging and shearing. Figure 6-7 shows the relationship between settlement and stone column depth. It is clear that the maximum settlement occurred at the ground surface level and reduced gradually with depth till it becomes less than 2mm after sabkha layers. This promotes that the settlement takes place in a bulging mode and most of the bulging deformations occurred in the upper part of the stone column. This is expected due to the high stress concentration at the top of the stone columns and the lack

of lateral confinement. The results also indicate the punching deformation under stone column base resting on stiff layer, similar to this modeled case, can be neglected.

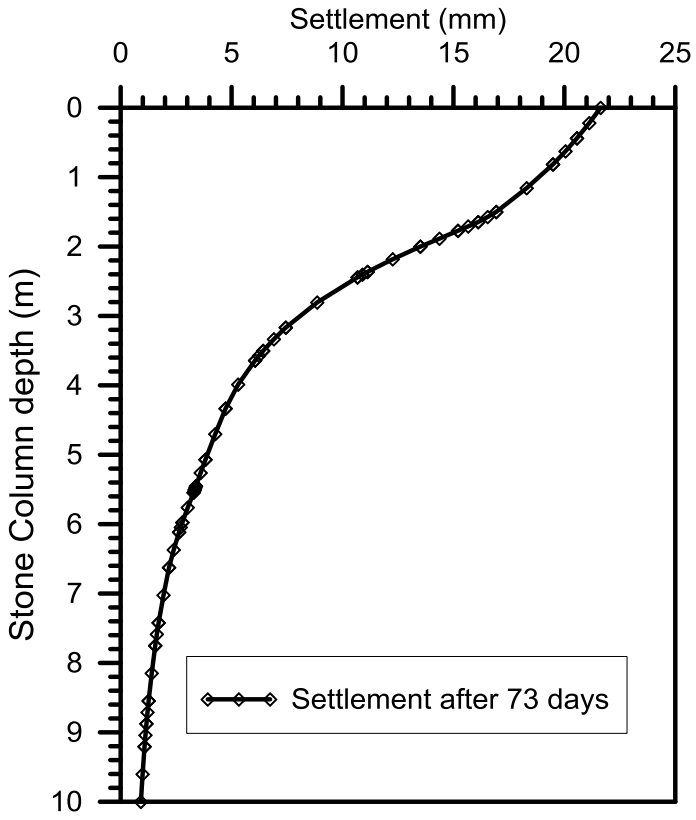

Figure 6-7: Variations of Settlement with Stone Column Depth.

6.6.3 Excess pore water pressures

In order to better understand the variation of excess pore water pressure dissipation, different areas in the treated and untreated finite element model were examined. The excess pore pressure dissipation at different ground locations and surface settlement profile adjacent to the stone column area and outside the stone column area were selected and excess pore pressure dissipation was studied. Figure 6-8 shows the numerical results of excess pore water pressure in treated case at line across section A-A, 0.75 m from

center of stone column, which extent from ground surface to a depth of 9 m. It can be seen that the amount of excess pore water pressure decreased with time proceed.

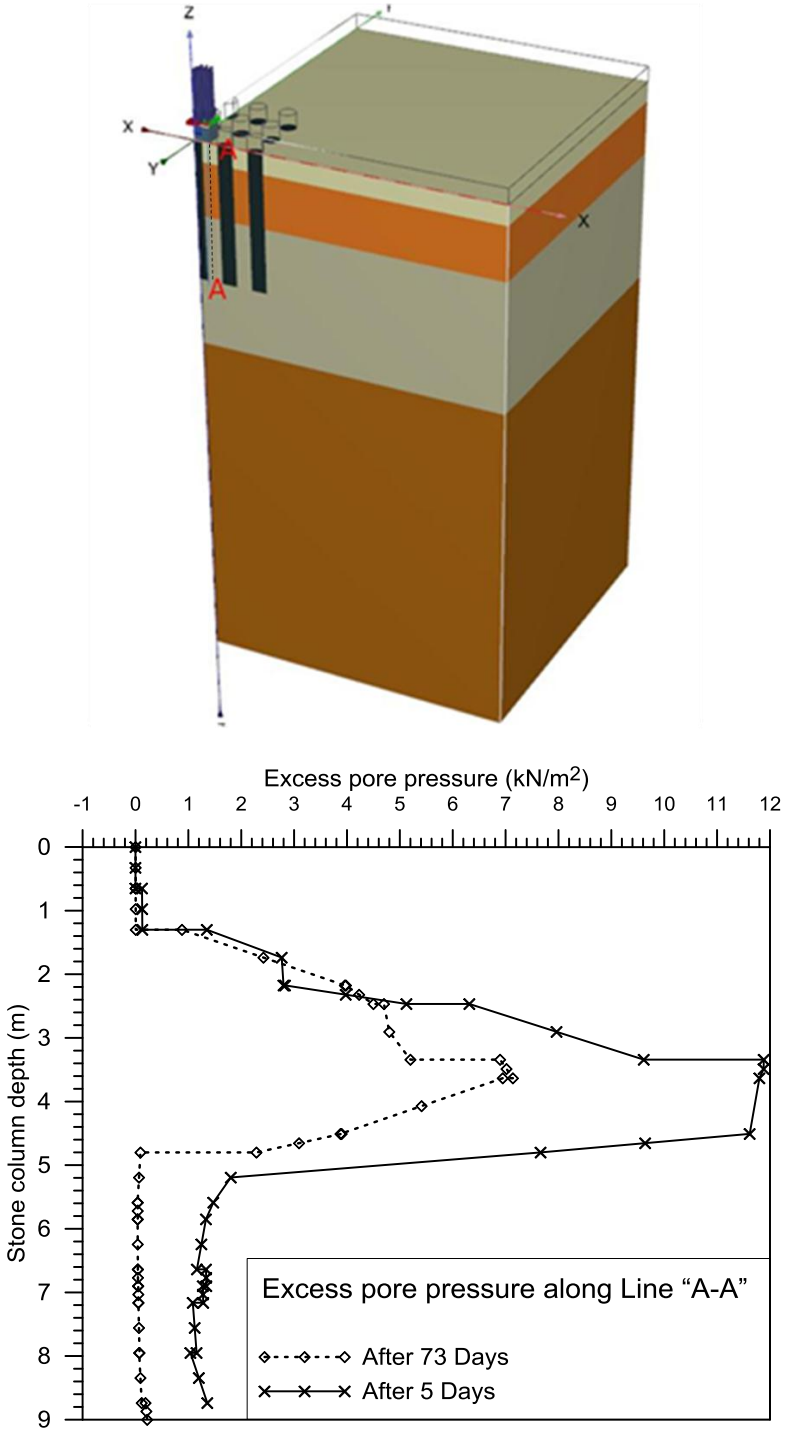

Figure 6-8: Excess Pore Pressure with Depth along Line "A-A".

6.6.4 Stress Distribution

It is obvious from Figure 6-9 that, after installation of stone column, the vertical stress concentration in the stone column is more than stresses in the surrounding soil. In addition, stress concentration is slightly increased with consolidation time. The stress concentration factor "n" changes with some parameters including the relative stiffness between the column and soil materials, stone column length, area ratio and the characteristics of the loading type placed over the stone column. When a load is applied over stone columns, it causes stress increase in stone columns much more than the stresses in the surrounding soils. This is mainly due to the higher stiffness of the stone columns and quick dissipation of excess pore pressure compared to the surrounding soils. The deflection of the two materials, stone and soil, is approximately the same, so the stress in the stiffer stone column material should be greater than in the surrounding soil for equilibrium considerations.

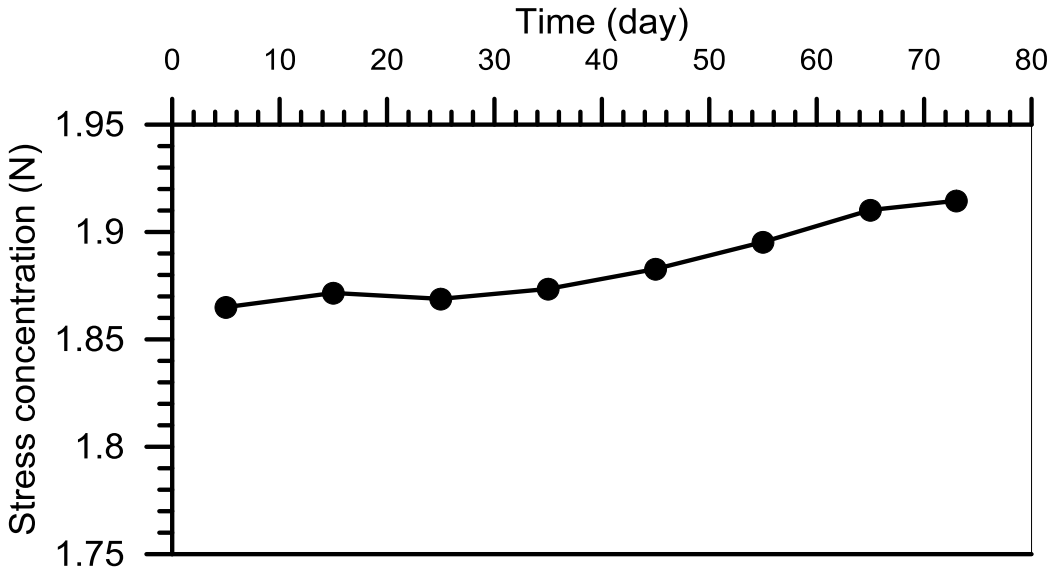

Figure 6-9: Stress Concentration Versus Time.

6.6.5 Effect of Stone Column Length

The stone columns are installed below the foundation to a depth below the bottom of the soft compressible strata. Stone columns provide drainage path, which will accelerate the dissipation of pore water pressure, therefore it is a function of consolidation settlement. Thus, the stone columns should be carried through the entire depth of major compressible strata where the stress increases due to significant applied load. Figure 6-11 shows the relationship between the magnitude of settlement and stone column length. The settlement has slightly increased with reduction in stone column length.

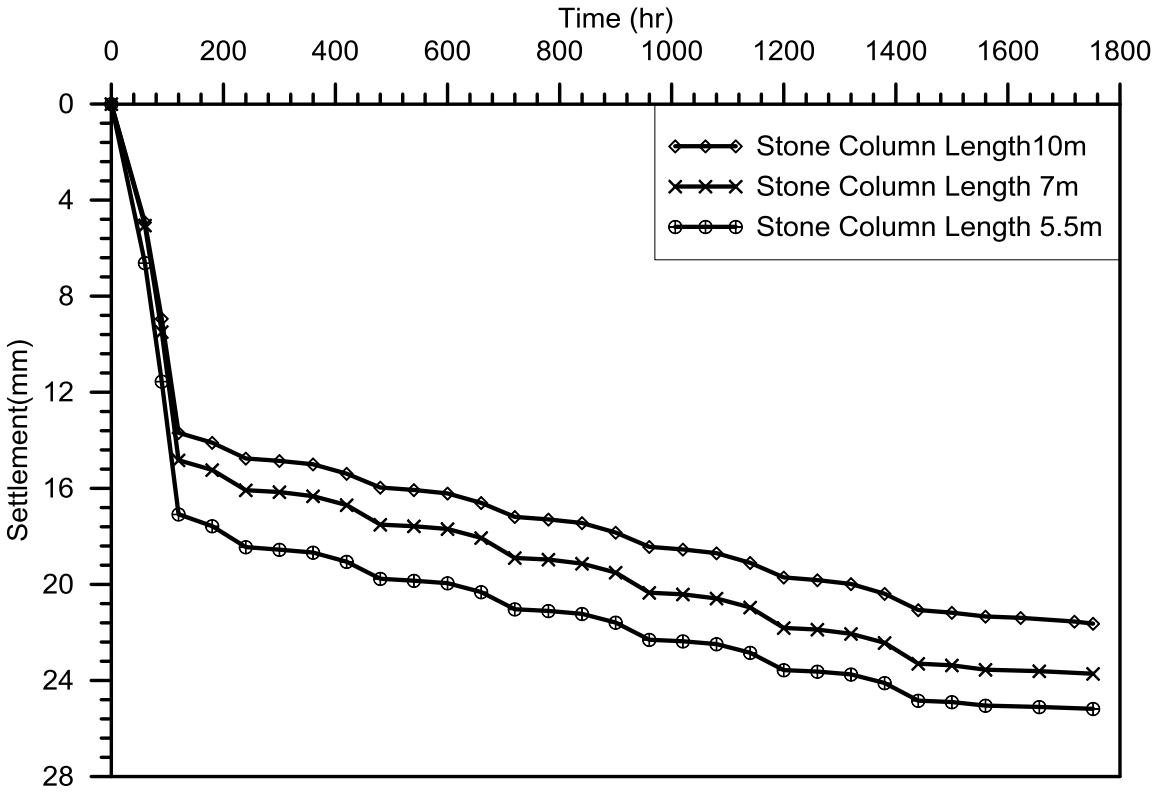

Figure 6-10: Settlement under different stone column lengths.

6.6.6 Bulging

Figure 6-11 shows the relationship between the magnitude of loading and bulging value along the stone column. As, the maximum bulging occurs at 2.2 times the diameter of the

stone column, bulging started from the top of the stone columns, increasing gradually and then reached a maximum value at a depth/diameter (D/D) ratio of 2.2. The bulging stops approximately at a depth of 6 D/D, which passes the sabkha bottom. The lateral resistance of soil increases with depth. This fact coupled with the application of the load from the top of the column means that bulging is most likely occurring in the upper part of the column, although in the case of longer columns bulging may be observed over the upper part of stone column length.

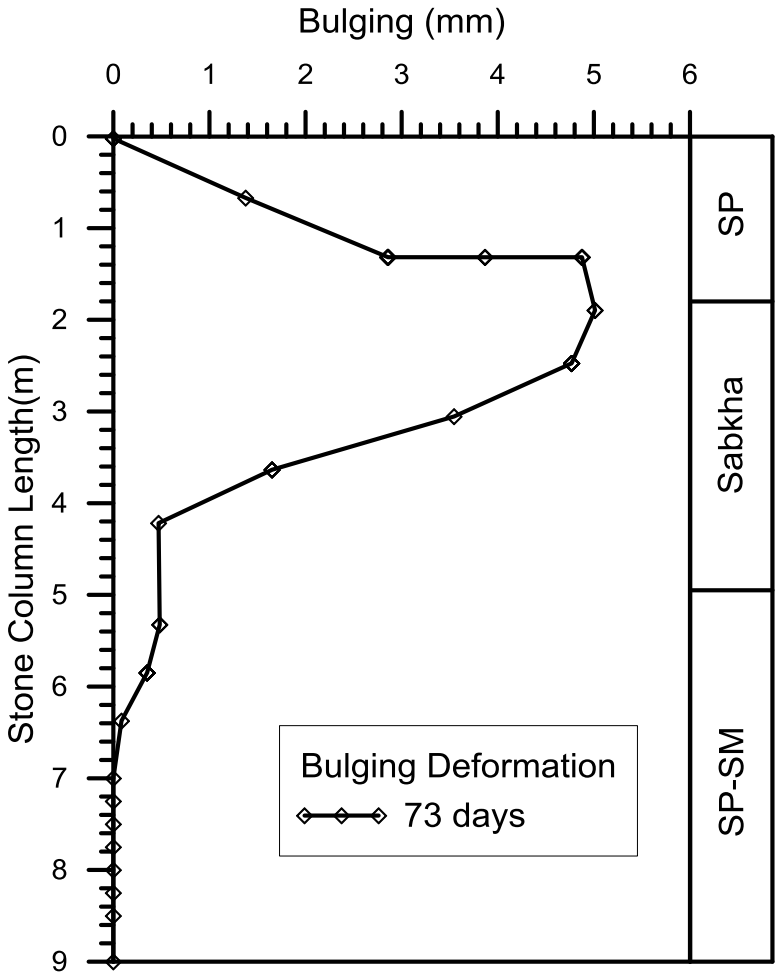

Figure 6-11: Bulging Deformation along Stone Column at Different Times**.**

CHAPTER 7

SIMPLIFIED METHOD TO PREDICT SETTLEMENT

7.1 Introduction

The use of stone columns as one of the effective method to improve sabkha soils has increased in construction practice to fulfill the industry demand for transmitting larger loads through foundations especially for low rise building and structures that can tolerate some settlements. Nevertheless, the ability to predict settlement of foundations resting on sabkha reinforced with stone columns is very limited and this issue has not been studied thoroughly. The available design methods for predicting settlement depend on Priebe (1995) method. This method was developed for the case of homogenous soft clay surrounding stone column. The method assumes unit cell idealization (Priebe, 1995).

Allowable loads on stone column reinforced foundation are normally derived from the settlement performance rather than the ultimate bearing capacity (Balaam and Booker, 1981; Barksdale and Bachus, 1983; Mitchell and Huber, 1985; Priebe, 1995). A new simplified design method of stone columns that accounts for area replacement ratio, stone column material properties and soil layers characteristics is proposed here based on a series of parametric studies. The results obtained from the simplified method are compared with the field results. This chapter demonstrates the advantages of the proposed method despite its simplicity.

7.2 Design Considerations

Column diameters typically range between 0.7m and 1.1m and spacing ranges between 1.5m and 2.5m. Column lengths depend on soils encountered on site but typically range between 6m and 20m (Raju et al., 1997). In order to assess the applicability of Vibro stone columns for a given site and foundation system, it is necessary to evaluate the performance of the unimproved ground and then determine if the stone columns will achieve the desired objectives in terms of settlement reduction. In the simplest terms, the preliminary design of stone columns can be accomplished as follows:

- Estimate the settlement for the proposed loading conditions for the unimproved ground using conventional settlement calculations.
- Determine the stone column length, diameter and spacing.
- Determine the area replacement ratio (stone column area divided by the tributary area of the stone column) necessary to provide the required settlement reduction.
- Determine the reduction of settlement that is required to meet the design requirements. This reduction factor is expressed as a ratio of the amount of settlement of the unimproved soils to the amount of settlement of the improved soils and is referred to as “settlement ratio,” or “improvement factor”.

7.3 Design Parameters

Once the finite element model was calibrated using the field data, as presented in previous chapters, the next step is to carry out a parametric study using this finite element model to investigate the effect of geometrical parameters and material characteristics on

the settlement improvement factor. Figure 7-1 shows the basic geometry utilized to develop the simplified method. Four different area replacement ratios (A_R = 0.35, 0.2, 0.155 and 0.125) were used for the stone column under different loading for each. The unit cell utilization was used to apply loading on one stone column as shown in Figure 7-1. Four different thickness of the sabkha layer were tried; specifically 10m, 7m, 5m and 3m for each different area ratio. Different foundation pressure values, q, were tried to include range from low to high stress; the selected values are 25, 50, 75, 100, 125, 150, 175, 200, 225, 250, 275 and 300 kPa. The pressure is applied assuming flexible footing conditions, because after installation of stone column the upper loose, at least 300 mm layer, is removed and replaced with compacted backfill materials. This procedure increases strength parameter for upper soils layer and stone column, and thus the relative stiffness of foundation material compared to concrete footing and this justifies the assumption of flexible footing condition.

The thickness of the top cohesionless layer was varied to cover thickness of 1m, 2m and 3m. The strength and deformation modulus values of the soil layers are shown in Table 4.1. The stone column properties are presented in Table 5-2.The model was used to study the performance and calculate the settlement improvement factor in two stages, the evaluation of settlement before installation of stone columns and then after installation of stone columns.

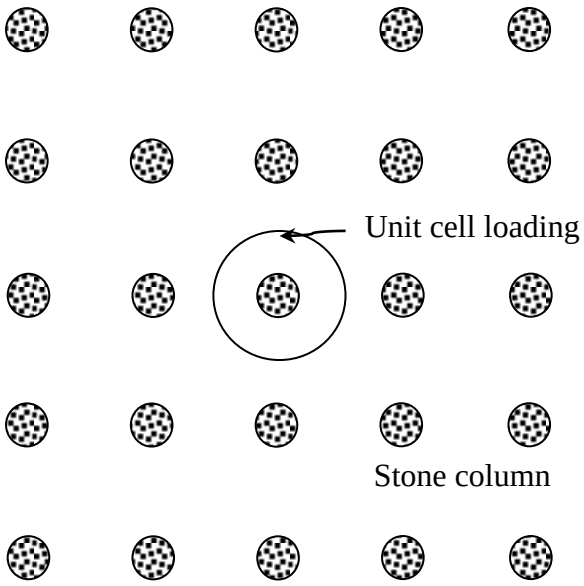

Figure 7-1: Schematic Representation of a Typical Stone Column Arrangement and Soil Layering.

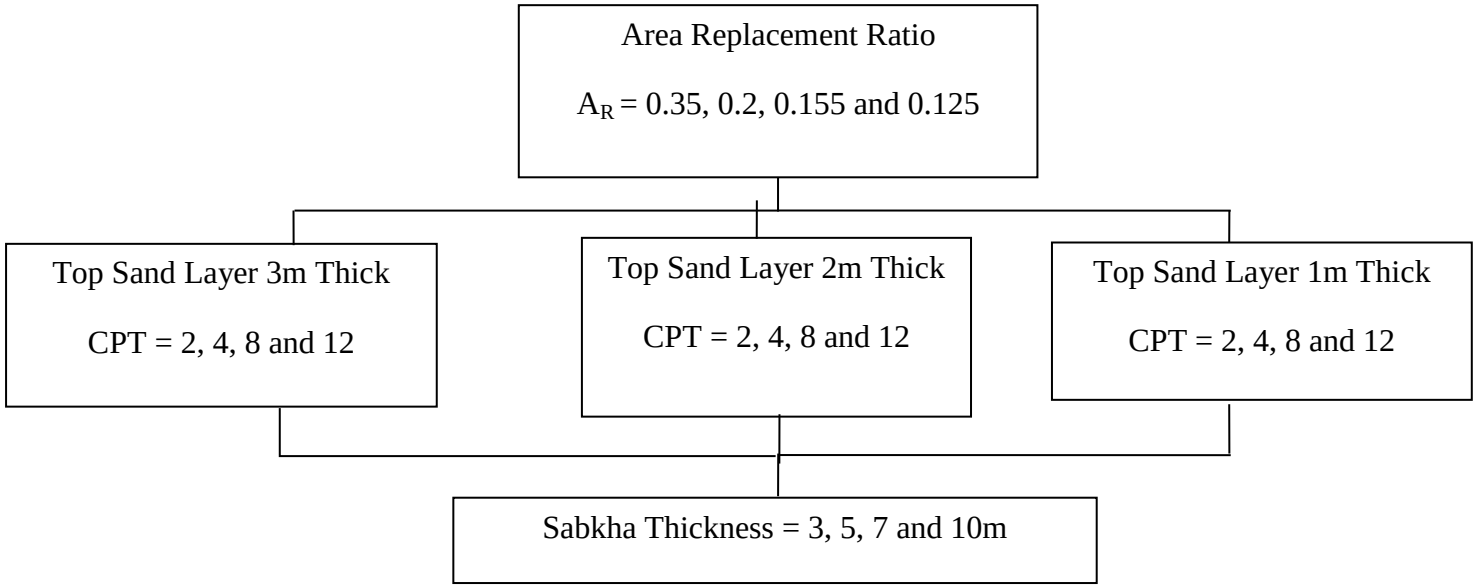

Figure 7-2: Design Parameters Adopted in the new Simplified design/Analysis Method.

7.4 Simplified Method to Predict Settlement

The numerical models offer the flexibility to account for many variables that control the performance of stone columns. Based on the parametric study in Chapters 5, 6, and the current chapter, a new design method is proposed for the stone column reinforced sabkha. These relationships are presented in the form of graphs to show the variation of the settlement with the change of soil/stone column parameters. The basic settlement reduction factors are derived from the end bearing stone column results for different area replacement ratios.

Comprehensive three-dimensional finite element modeling was used to study all main parameters affecting both the mechanisms of load transfer from stone columns to sabkha and the settlement performance. For each case, first the untreated case is analyzed by modeling the uniformly loaded unit cell area. Next, the load is applied on the unit cell area having one stone columns and the analysis was repeated. The soil layers and stone columns were modeled using Mohr-Coulomb model. The modeling was conducted assuming 120 days of consolidation, which is enough period for long-term deformation in composite area, according to the findings of Chapter 6.

Once the settlement values for the untreated and treated case are estimated, settlement reduction factors (R_{IF}) are calculated as follows:

$$R_{IF} = \frac{S_{treated}}{S_{untreated}} \quad (7\text{-}1)$$

Where:

R_{IF}: Settlement reduction factor.

$S_{untreated}$: Settlement of untreated soil.

$S_{treated}$: Settlement of treated soil with stone columns.

A simple design equation relating settlement reduction factor, applied pressure, CPT value for upper cohesionless layer and area ratio is developed as follows:

$$R_{IF} = F_{loading} \times F_{Area\ ratio} \times F_{CPT} \quad (7\text{-}2)$$

Where

$F_{loading}$: Settlement reduction factor due to applied pressure on 0.35 (base case) area replacement ratios.

$F_{Area\ ratio}$: Effect of area ratio variation between stone column and surrounding soil according to unit cell idealization.

F_{CPT}: Effect of CPT variation for top cohesionless layer.

The above equation is an interesting and useful finding, which allows designers to evaluate the settlement of end bearing stone column in sabkha soils by knowing applied pressure, CPT value for upper cohesionless layer and replacement area ratio.

7.4.1 Relationship between Settlement Reduction Factor and Applied Stress

The lines of best fit between the settlement reduction factor and applied pressure, for different top sand layer thicknesses, are shown in Figure 7-3 to Figure 7-5. These curves were developed from the case of area replacement ratio (0.35) and CPT of 2kN/m^2 for top layer. It is clear from the plots that the improvement factor values decrease as the top sand layer thickness increases. This is attributed to the increased stiffness of the top layer as the thickness increases and that reduces the load transferred to the columns. On the other hand, the improvement factor reduces with increase in sabkha thickness. This is attributed to the low stiffness of sabkha and thus the improvement is not very efficient.

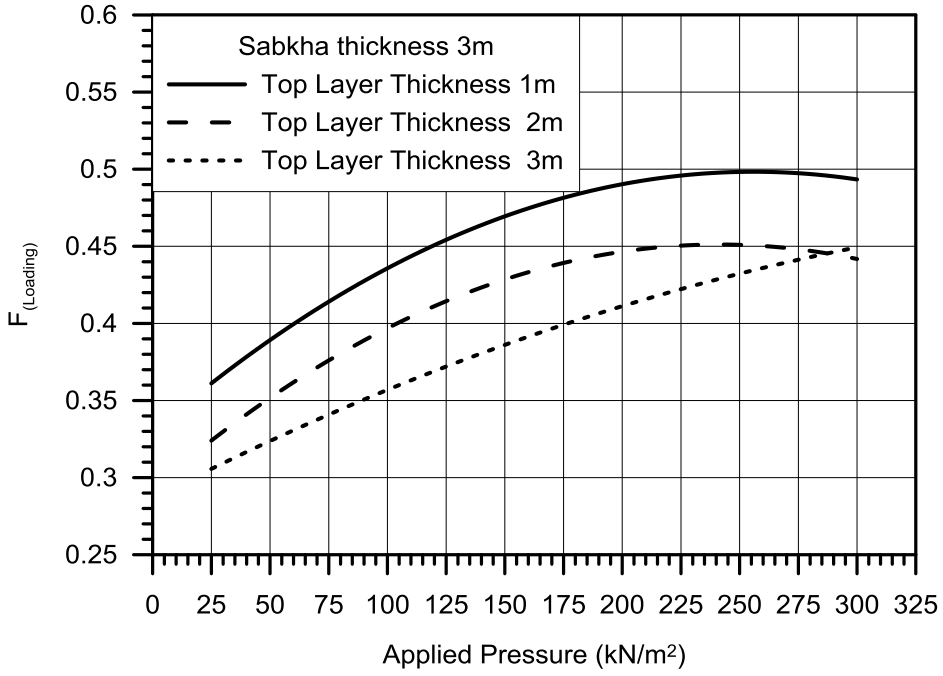

Figure 7-3: Variations of Improvement Factor with the Applied Stress for the Case of 3m Sabkha Layer Thickness.

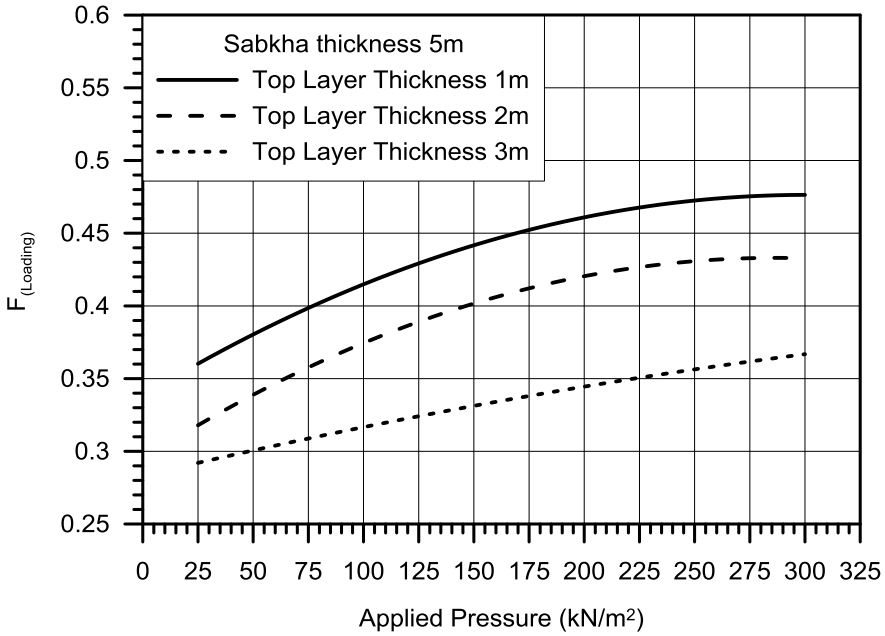

Figure 7-4: Variations of Improvement Factor with the Applied Stress for the Case of 5m Sabkha Layer Thickness.

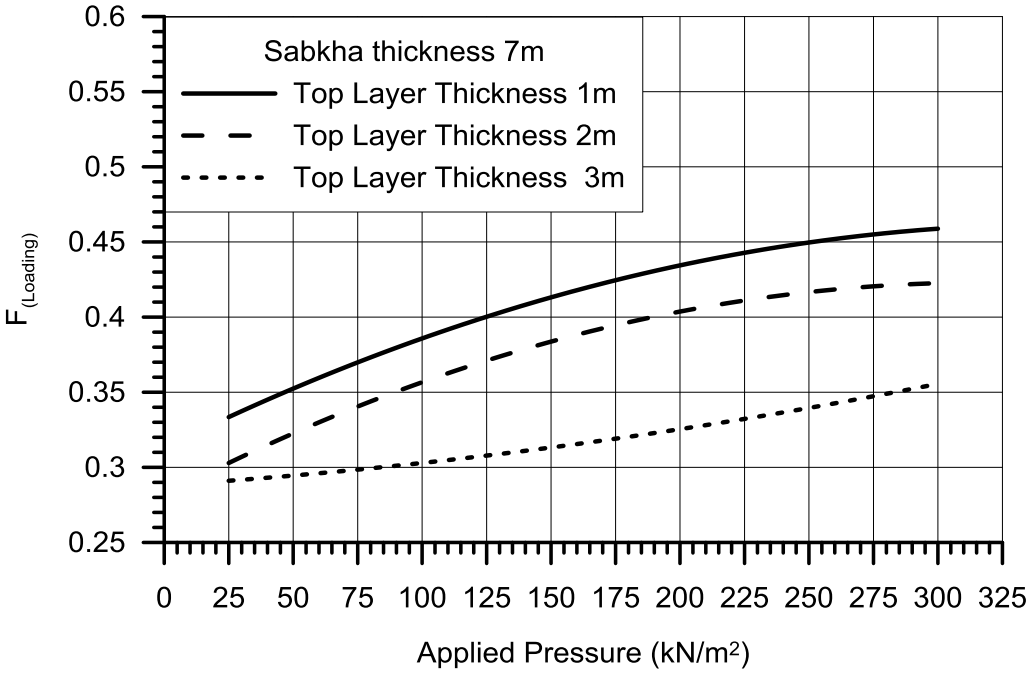

Figure 7-5: Variations of Improvement Factor with the Applied Stress for the Case of 7m Sabkha Layer Thickness.

7.4.2 Effect of Area Replacement Ratio

The results presented in the previous chapters show that the settlement performance (reduction) of stone columns improved significantly at high area replacement ratios. This is attributed to the increased levels of lateral confinement. Therefore, a significant densification occurs for soil layers surrounding stone columns at high area replacement ratios. The influence of area replacement ratios on the settlement improvement factors are plotted in Figure 7-6.

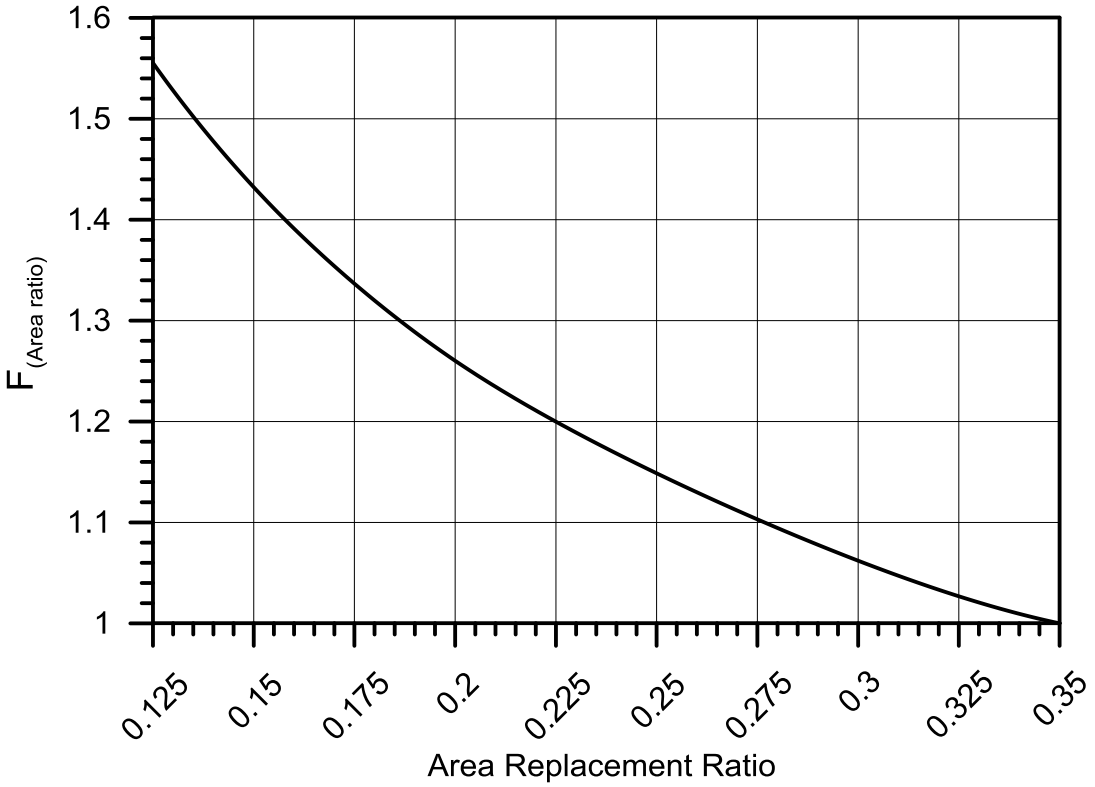

Figure 7-6: Effect of Area Ratio on Settlement Reduction Factor.

7.4.3 Effect of Increase in CPT Value for Top Layer

The stiffness of the top layer above sabkha tends to confine columns near the surface, where columns are subject to the lowest overburden stress and hence are most susceptible to bulging. Therefore, the presence of the stiff top layer enhances the load-carrying capacity of columns and reduces deformations. The effect of increase in CPT value for top layer is plotted in Figure 7-7 to Figure 7-9.

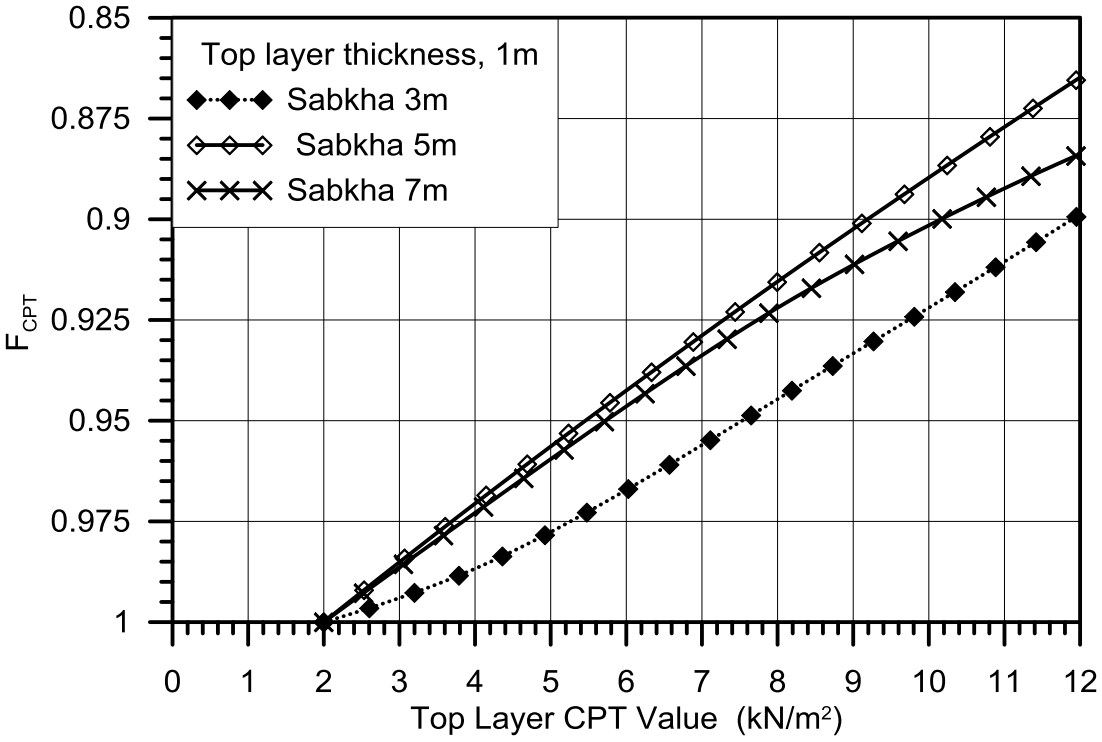

Figure 7-7: Effect of increase in CPT value for Top layer thickness, 1m.

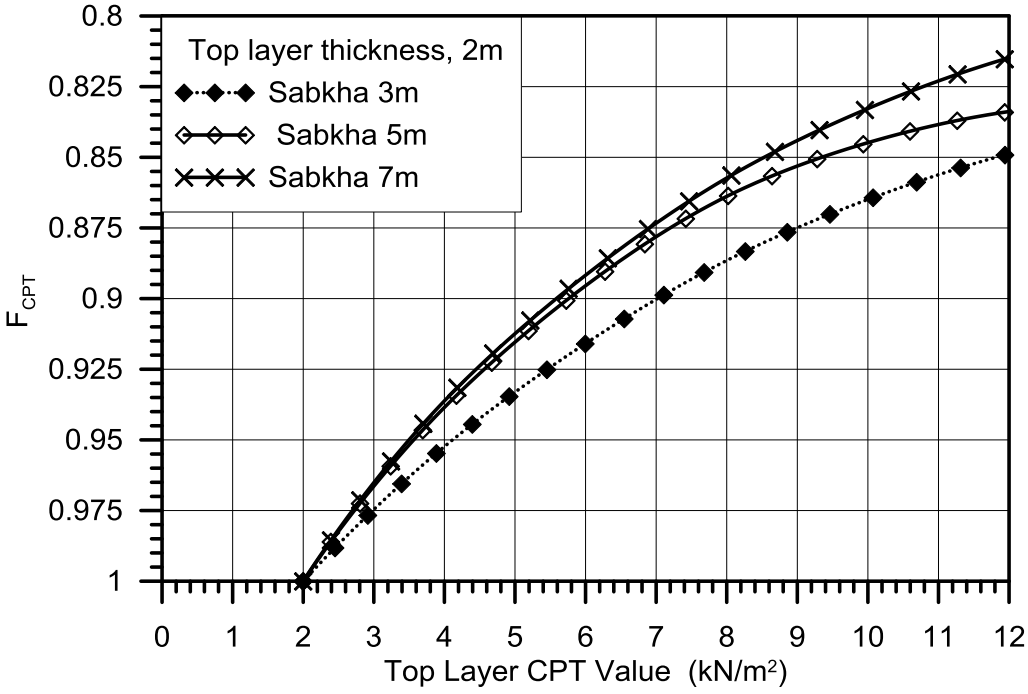

Figure 7-8: Effect of increase in CPT value for Top layer thickness, 2m.

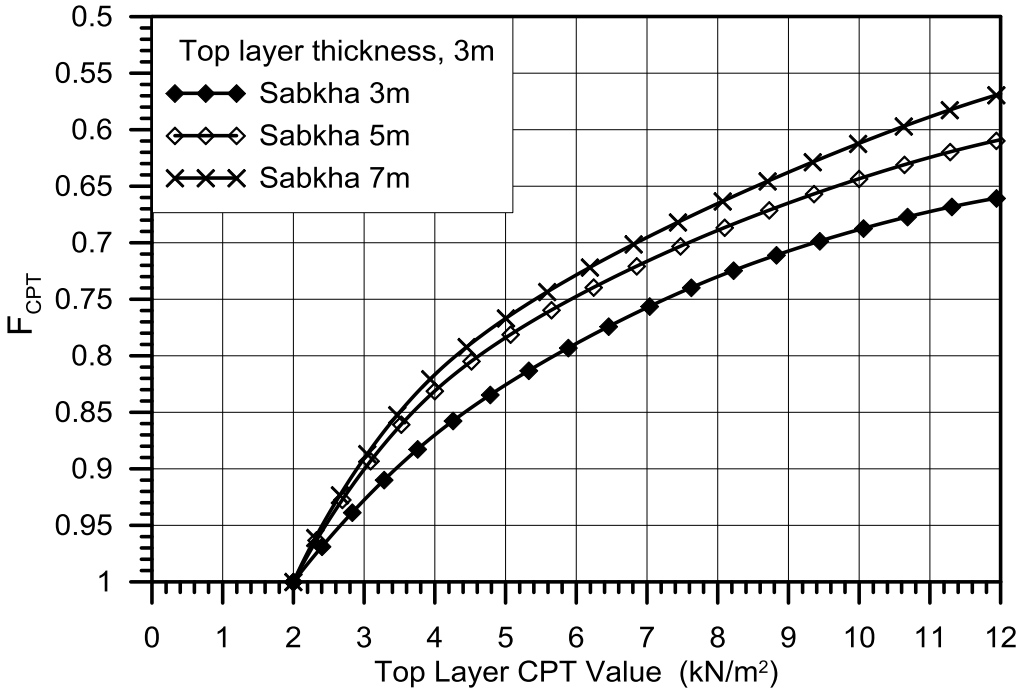

Figure 7-9: Effect of increase in CPT value for Top layer thickness, 3m.

7.4.4 Influence of column length

The findings from FEM indicate that small punching occurs at the base of end bearing stone columns resting on soil layer with elastic modules greater than 30MN/m^2. Therefore, in this study the effect of stone column length is neglected since in all cases sabkha located over stiff layer.

7.5 Comparison of Improvement Factors with Conventional Methods

The settlement improvement factors calculated from the simplified method and described in this Chapter are compared with field results data as shown in Table 7-1and Table 7-2. The results obtained from the simplified method are producing good correlation with field data. This demonstrates the advantages of the proposed method despite its

simplicity. Such proposed method can be used to design stone columns in sabkha in an optimum and accurate manner.

Table 7-1: Comparison of settlement between Simplified Method Field data in EWT.

Stone column configuration 1.7x1.7m in EWT	
Applied stress	190kN/m^2
Numerical settlement after 120 days consolidation	58 mm
$F_{(Loading)}$	0.42
$F_{(Area\ ratio)}$	1.05
$F_{(CPT)}$	0.85
R_{IF}	0.37
Settlement using Simplified method	21.6 mm
Field settlement in EWT	19 mm
% Difference	13.7

Table 7-2: Comparison of settlement between Simplified Method Field data in WHA.

Stone column configuration 2x2m in WHA	
Applied stress	60kN/m^2
Numerical settlement after 120 days consolidation	54
$F_{(Loading)}$	0.37
$F_{(Area\ ratio)}$	1.28
$F_{(CPT)}$	0.88
R_{IF}	0.42
Settlement using Simplified method	23 mm
Field settlement in EWT	21mm
% Difference	9.5

CHAPTER 8

CONCLUSIONS AND RECOMMENDATIONS

8.1 Conclusions

Based on the interpretation of the results presented in this research, the following main conclusions can be drawn:

- Literature search suggests that the field data on stone columns in sabkha soils are rather limited compared to stone columns in soft clays.
- Cone Penetration Test (CPT) is a useful tool for quality assurance and quality testing of ground improvement works before and after stone columns installation.
- The short and long term settlement performances of stone columns at typical working loads in sabkha soils can be accurately modeled using PLAXIS 3D.
- Simulating column installation effects by increasing the lateral stress coefficient cannot be accurately implemented in a FE program. However, an alternative approach to simulate column installation effects is to upgrade soil properties surrounding stone columns to reflect the effects of lateral earth pressure increase and soil densification.
- The presence of a relatively dense sand layer above sabkha has a significant influence on the settlement performance of stone columns. Such layer provides confinement to the columns, which reduces the stone columns bulging. Thus,

bulging is noticed to be higher in deeper soft sabkha layers due to lack of additional confinement. Such lateral restraining in the sand layer is enhancing the columns' load carrying capacity.

- In the absence of dense sand layer on top of sabkha, bulging generally occurs near the ground surface where lateral stresses/restraining for the sabkha are relatively low.
- By comparing the results from the treated (with stone columns) and untreated sabkha, it is obvious that the stone columns are very effective in accelerating the rate of sabkha consolidation.
- The deformational behavior of stone columns reinforced sabkha layer, having a cohesionless layer above the sabkha, is governed by the replacement area ratio and properties and thickness of the upper sand layer. This is an important finding, which was utilized in the development of the simplified design method.
- Significant improvement occurs in the sand layer above sabkha due to installation effect of Vibro-stone columns, especially for cases of very loose and loose condition (Pre-CPT< 4 MN/m^2). In case of medium relative density condition (Pre-CPT between 4 to12 MN/m^2), the data show slight increase in CPT values for the majority of points while few points show little decrease.
- Assessment of soil compressibility prior to the compaction work, resulting from the installation of stone columns, provides the opportunity to determine whether and to what degree soils are densified due to vibration when installing the stone columns. This feature may be used to optimize the design of stone columns in sabkha soils, which, in general, do not seem to be compactable using vibration.

- Results have shown that the vertical stresses on the top of stone columns increases significantly compared to the sabkha soil. However at the bottom of the 10m long stone columns, there is no substantial increase (increase within 15% only) in stress in the stone column, compared to adjacent soil, due to load application. This proves that stress is not transmitted through stone column to end bearing stratum. In such cases there may not be a need for long stone columns but his requires further studies.
- New approach to assess sabkha parameters before and after installation of Vibro-stone columns was suggested. The approach is based on linking field and laboratory values from geotechnical report and published data.
- Depending on the behavior of top sand layer (within 3m depth) above sabkha, improvement factor to predict the Post-CPT was developed. This factor is limited only to cases of cohesionless layer above sabkha soils and can be used as one of the quality control tools after installation of Vibro stone columns. It should be clear, however, that the top 600mm may not be densified in any stone column installation due to lack of confinement.
- A new simplified design method for stone columns, in sabkha soils, that accounts for area replacement ratio, stone column material properties as well as soil layers characteristics is proposed based on a series of parametric studies. The settlement predictions of the proposed method are very comparable with the filed data and the difference did not exceed 14 % for the two case presented.

8.2 Recommendations for future research

The performance of stone column sabkha behavior presented in this research is based on limited field observations and finite element studies. Certainly, more research is needed in the form of full-scale experiments and model studies for varieties of sabkha soils with different stone column characterizes (spacing, configuration, material, size, depth, installation method, etc …) and to assess the behavior of such system under different conditions.. The following specific recommendations can be made:

- Perform field testing on a properly instrumented full scale stone column-sabkha system. The instrumentation should include pore water pressure, lateral and vertical stresses, vertical and lateral deformation measurements at different distances from the stone columns and various depths.
- Perform more parametric analysis utilizing different strength values of the sabkha and sand backfilling thickness.
- Simulate a full-scale, well-documented and long-term behavior of stone columns sabkha system such as the EWT. This requires a 3-D FE package that has no limitations on mesh size.
- Perform parametric study to evaluate the length requirement of stone columns based on the stress transfer upon loading.

References

Abduljauwad, S. N., Al-Amoudi, O. S. B., 1995. Geotechnical Behaviour of Saline Sabkha Soils. Geotechnique 45, pp. 425–445.

Aboshi, H., Ichimoto, E., Enoki, M., Harada, K., 1979. The Compozer—a Method to Improve Characteristics of Soft Clays by Inclusion of Large Diameter Sand Columns, in: Proceedings of International Conference on Soil Reinforcement. pp. 211–216.

Abu-Taleb, M. G., Egeli, I., 1981. Some Geotechnical Problems in the Eastern Province of Saudi Arabia, in: Proceedings of the Symposium on Geotechnical Problems in Saudi Arabia, pp. 799–811.

Adalier, K., Elgamal, A., 2004. Mitigation of Liquefaction and Associated Ground Deformations by Stone Columns. Eng. Geol. 72, pp. 275–291.

Aiban, S. A., Field Testing, 2009, Design Optimization and Construction Supervision of Stone Columns in Sabkha Soil, Saudi Kayan Petrochemical Complex, Jubail, Saudi Arabia, Unpublished Summary Report.

Aiban, S. A., Al-Abdul Wahhab, H. I., Al-Amoudi, O. S. B., 1998. Identification, Evaluation, and Improvement of Eastern Saudi Soils for Construction Purposes, Final Report. Riyadh Saudi Arab. King Abdulaziz City Sci. Technol. KACST AR-14-61.

Aiban, S. A., Asi, I. M., Al-Amoudi, S. B., 1995. Stabilization of Ras Al-Ghar Sabkha soil with lime. Fourth Saudi Engineering Conference Vol. II, pp. 401-407.

Aiban, S. A., Bin Husain, A. and Al-Basri A., 2010, Foundations, Ground Improvement and Road Design Optimization: Saudi Kayan Experience, proceedings and presentation, SABIC Technical Exchange Meeting No. 9 (STM-9).

Akili, W., 1981. On Sabkha Sands of Eastern Saudi Arabia, in: Proceedings of the Geotechnical Problems in Saudi Arabia Symposium. pp. 775–793.

Al-Amoudi, O. S. B., 1995. Soil Stabilization and Durability of Reinforced Concrete in Sabkha Environments. Proceedings, 4th Saudi Engineering Conference, King Abdulaziz University, Jeddah, Vol. II, November 1995, pp. 313-338.

Al-Amoudi, O. S. B., 1994. Chemical Stabilization of Sabkha Soils at High Moisture Contents. Eng. Geol. 36, pp. 279–291.

Al-Amoudi, O. S. B., 1992. Studies on Soil-Foundation Interaction in the Sabkha Environment of Eastern Province of Saudi Arabia. Ph.D. Thesis, King Fahd University of Petroleum and Minerals, Dhahran, Saudi Arabia.

Al-Amoudi, O. S. B., Asi, I.M., EI-Naggar, Z.R., 1995. Stabilization of an Arid, Saline Sabkha Soil Using Additives. Q. J. Eng. Geol. Hydrogeol. 28, pp. 369–379.

Al-Guwaizani, A. S., 1994. Sedimentology and Geochemistry of Qurayyah Sabkha, M. S. Thesis. King Fahd University of Petroleum & Minerals, Dhahran, Saudi Arabia.

Al-Mousa, A., 2011. Investigation of Pile Foundations in the Al Hasa Area, Saudi Arabia. Ph.D. Thesis, University of Portsmouth, England.

Ambily, A. P., Gandhi, S. R., 2007. Behavior of Stone Columns Based on Experimental and FEM Analysis. J. Geotech. Geoenvironmental Eng. 133, pp. 405–415.

Ambily, A. P., Gandhi, S. R., 2004. Experimental and Theoretical Evaluation of Stone Column in Soft Clay. ICGGE-2004, pp. 201–206.

Andreou, P., Frikha, W., Frank, R., Canou, J., Papadopoulos, V., Dupla, J.-C., 2008. Experimental Study on Sand and Gravel Columns in Clay. Proc. ICE-Ground Improv. 161, pp.189–198.

Babu, M. D., Nayak, S., Shivashankar, R., 2013. A Critical Review of Construction, Analysis and Behaviour of Stone Columns. Geotech. Geol. Eng. 31, pp. 1–22.

Bachus, R. C., Barksdale, R. D., 1989. Design Methodology for Foundations on Stone Columns, in: Foundation Engineering@ Current Principles and Practices. ASCE, pp. 244–257.

Balaam, N. P., 1978. Load Settlement Behaviour of Granular Piles. Ph.D. Thesis. University of Sydney, Australia.

Balaam, N. P., Booker, J. R., 1981. Analysis of Rigid Rafts Supported by Granular Piles. Int. J. Numer. Anal. Methods Geomech. 5, pp. 379–403.

Barksdale, R. D., Bachus, R. C., 1983. Design and Construction of Stone Columns Volume I, Washington, D.C: FHWA/RD-83/026, Federal Highway Administration.

Baumann, V., Bauer, G. E. A., 1974. The Performance of Foundations on Various Soils Stabilized by the Vibro-Compaction Method. Can. Geotech. J. 11, pp. 509–530.

Baumann, V., Bauer, G. E. A., 1974. The Performance of Foundations on Various Soils Stabilized by the Vibro-Compaction Method. Can. Geotech. J. 11, pp. 509–530.

Bear, J., 2013. Dynamics of Fluids in Porous Media. Courier Dover Publications.

Bell, A. L., 2004. The Development and Importance of Construction Technique in Deep Vibratory Ground Improvement. Ground Soil Improvement, pp. 103–111.

Bergado, D. T., Anderson, L. R., Miura, N., Balasubramaniam, A. S., 1996. Soft Ground Improvement in Lowland and other Environments. American Society of Civil Engineers. 427, pp. 26-30.

Bergado, D. T., Asakami, H., Alfaro, M. C., Balasubramaniam, A. S., 1991. Smear Effects of Vertical Drains on Soft Bangkok Clay. J. Geotech. Eng. 117, pp. 1509–1530.

Black, J. A., Sivakumar, V., Madhav, M. R., Hamill, G. A., 2007. Reinforced Stone Columns in Weak Deposits: Laboratory Model Study. J. Geotech. Geoenvironmental Eng. 133, pp. 1154–1161.

Bolton, M. D., 1986. The Strength and Dilatancy of Sands. Geotechnique 36, pp. 65–78.

Bowles, J. E., 1988. Foundation Analysis and Design. 4th .Ed. McGraw-Hill Book Co

Brinkgreve, R. B. J., Engin, E., Swolfs, W. M., 2012. Plaxis 3D. Material Models Manual 2012. Hol. Plaxis Bv.

Brinkgreve, R. B. J., Engin, E., Swolfs, W. M., 2011. Plaxis 3D 2011 Manual. Delft University. Technol. PLAXIS Bv Neth.

Brown, D. F., 1989. Evaluation of the Tri Star Vibrocompaction Probe. M. A. Sc. Thesis, University of British Columbia, Vancouver, Canada.

Brown, R. E., 1977. Vibroflotation Compaction of Cohesionless Soils. J. Geotech. Eng. Div. 103, pp. 1437–1451.

Brown, R. E., Glenn, A. J., 1976. Vibroflotation and Terra-Probe Comparison. J. Geotech. Eng. Div. 102, pp. 1059–1072.

Butler, G. P., 1969. Modern Evaporite Deposition and Geochemistry of Coexisting Brines, the Sabkha, Trucial Coast, Arabian Gulf. Journal of Sedimentary Research. 39, pp. 70-89.

Canetta, G., Nova, R., 1989. A Numerical Method for the Analysis of Ground Improved by Columnar Inclusions. Computers and Geotechnics. 7, pp. 99–114.

Casagrande, L., Poulos, S., 1969. On the Effectiveness of Sand Drains. Canadian Geotechnical Journal. 6, pp. 287–326.

Castro, J., Karstunen, M., 2010. Numerical Simulations of Stone Column Installation. Canadian Geotechnical Journal. 47, pp. 1127–1138.

Castro, J., Sagaseta, C., 2009. Consolidation around Stone Columns. Influence of Column Deformation. International Journal for Numerical and Analytical Methods in Geomechanics. 33, pp. 851–877.

Datye, K. R., Nagaraju, S. S., 1975. Installation and Testing of Rammed Stone Columns, in: Proceedings, 5th Asian Regional Conference on Soil Mech. and Found. Eng., Bangalore, India. pp. 101–104.

Deb, K., 2008. Modeling of Granular Bed-Stone Column-Improved Soft Soil. International Journal for Numerical and Analytical Methods in Geomechanics. 32, pp. 1267–1288.

Domingues, T. S., Borges, J. L., Cardoso, A. S., 2007. Parametric study of stone columns in embankments on soft soils by finite element method, in: Proceedings of the 5th International Workshop on Applications of Computational Mechanics in Geotechnical Engineering V, Guimaraes. pp. 281–291.

Dove, J. E., Boxill, L. E., Jarrett, J. B., 2000. A CPT-Based Index for Evaluating Ground Improvement, in: Advances in Grouting and Ground Modification. ASCE, pp. 296–310.

Elshazly, H., Elkasabgy, M., Elleboudy, A., 2008. Effect of Inter-Column Spacing on Soil Stresses due to Vibro-Installed Stone Columns: Interesting Findings. Geotechnical and Geological Engineering. Eng. 26, pp. 225–236.

Elshazly, H., Hafez, D., Mossaad, M., 2006. Back-Calculating Vibro-Installation Stresses in Stone-Column-Reinforced Soils. Proceedings of the ICE-Ground Improvement. 10, pp. 47–53.

Etezad-Borojerdi, M., 2007. Geotechnical Performance of Group of Stone Columns. Ph.D. Thesis, Concordia University. Montreal, Quebec, Canada.

Evamy, B. D., 1973. The Precipitation of Aragonite and its Alteration to Calcite on the Trucial Coast of the Persian Gulf, in: The Persian Gulf. Springer, pp. 329–341.

Gäb, M., Schweiger, H. F., Kamrat-Pietraszewska, D., Karstunen, M., 2008. Numerical Analysis of a Floating Stone Column Foundation Using Different Constitutive Models. Geotechnics of soft soils—focus on ground improvement. Edited by Karstunen and Leoni 1, pp. 137–142.

Goughnour, R. R., Bayuk, A. A., 1979. Analysis of Stone Column-Soil Matrix Interaction under Vertical Load. Coll. Int. Renforcements des Sols, pp. 279–285.

Greenwood, D. A., 1970. Mechanical Improvement of Soils below Ground Surface, in: Inst Civil Engineers Proc, London, UK, pp. 11-22.

Guetif, Z., Bouassida, M., Debats, J. M., 2007. Improved Soft Clay Characteristics due to Stone Column Installation. Computers and Geotechnics. 34, pp. 104–111.

Han, J., Ye, S. L., 2002. A Theoretical Solution for Consolidation Rates of Stone Column-Reinforced Foundations Accounting for Smear and Well Resistance Effects. The International Journal Geomechanics. 2, pp. 135–151.

Hansbo, S., 1994. Foundation Engineering. Amsterdam. Elsevier Science B. V.

Hassen, G., Buhan, P. de, Abdelkrim, M., 2010. Finite Element Implementation of a Homogenized Constitutive Law for Stone Column-Reinforced Foundation Soils, with Application to the Design of Structures. Computers and Geotechnics. 37, pp. 40–49.

Hird, C. C., Pyrah, I. C., Russel, D., 1992. Finite Element Modelling of Vertical Drains Beneath Embankments on Soft Ground. Geotechnique 42, pp. 499–511.

Holtz, R. D., Kovacs, W. D., 1981. An Introduction to Geotechnical Engineering. Prentice Hall, Inc, Englewood Cliffs, N. J.

Huang, J., Han, J., Oztoprak, S., 2009. Coupled Mechanical and Hydraulic Modeling of Geosynthetic-Reinforced Column-Supported Embankments. Journal of Geotechnical and Geoenvironmental Engineering. 135, pp. 1011–1021.

Hughes, J. M. O., Withers, N. J., 1974. Reinforcing of Soft Cohesive Soils with Stone Columns. Ground Engineering. 7, pp. 42-49.

Hughes, J. M. O., Withers, N. J., Greenwood, D. A., 1975. A Field Trial of the Reinforcing Effect of a Stone Column in Soil. Geotechnique 25, pp. 31–44.

Hussin, J. D., Ali, S., 1987. Soil Improvement at the Trident Submarine Facility, in: Soil Improvement. ASCE 12, pp. 215–231.

Hu, W., 1995. Physical Modelling of Group Behaviour of Stone Column Foundations. Ph.D. Thesis, University of Glasgow, Scotland, UK.

Indraratna, B., Basack, S., Rujikiatkamjorn, C., 2012. Numerical Solution of Stone Column–Improved Soft Soil Considering Arching, Clogging, and Smear Effects. Journal of Geotechnical and Geoenvironmental Engineering. 139, pp. 377–394.

Ismael, N. F., 1993. Laboratory and Field Leaching Tests on Coastal Salt-Bearing Soils. Journal of Geotechnical Engineering. 119, pp. 453–470.

Jacobs, P., 2004. Cone Penetration Testing (CPT), Simplified Description of the Use and Design Methods for CPTs in Ground Engineering. Fugro Engineering Services Ltd., Oxfordshire, UK.

Jaky, J., 1944. The Coefficient of Earth Pressure at Rest. Journal of the Society of Hungarian Architects and Engineers. 78, pp. 355–358.

Juillie, Y., Sherwood, D. E., 1983. Improvement of Sabkha Soil of the Arabian Gulf Coast, in: Eighth European Conference on Soil Mechanics and Foundation Engineering, pp. 781-788

Kézdi, Á., 1980. Handbook of Soil Mechanics. Vol. 2. Soil Testing. Elsevier Scientific Publishing Company.

Kirsch, F., 2006. Vibro Stone Column Installation and its Effect on Ground Improvement, in: Numerical Modelling of Construction Processes in Geotechnical Engineering for Urban Environment. pp. 115–124.

Kirsch, F., Sondermann, W., 2003. Field Measurements and Numerical Analysis of the Stress Distribution Below Stone Column Supported Embankments and Their Stability, in: International Workshop on Geotechnics of Soft Soils-Theory and Practice. pp. 17–19.

Lamb, T. W., Whitman, R. V., 1979. Soil Mechanics, SI Version. Wiley, New York.

Lee, J. S., Pande, G. N., 1998. Analysis of Stone-Column Reinforced Foundations. International Journal for Numerical and Analytical Methods in Geomechanics. 22, pp. 1001–1020.

Lo, S. R., Zhang, R., Mak, J., 2010. Geosynthetic-Encased Stone Columns in Soft Clay: a Numerical Study. Geotextiles and Geomembranes. 28, pp. 292–302.

Mackiewicz, S. M., Camp, W. M., 2007. Ground Modification: How Much Improvement, in: Soil Improvement, GSP No.172, ASCE, pp. 1–9.

Madhav, M. R., 1996. Granular Piles-Construction, Design and Behaviour, 12th SEAGC, Kuala Lumpur, pp 285-289.

Madhav, M. R., Van Impe, W. F., 1994. Load Transfer Through a Gravel Bed on Stone Column Reinforced Soil. Geotechnical Engineering. 25, pp. 47-62.

Madhav, M. R., Vitkar, P. P., 1978. Strip Footing on Weak Clay Stabilized with a Granular Trench or Pile. Canadian Geotechnical Journal. 15, pp. 605–609.

Malarvizhi, S. N., Ilamparuthi, K., 2004. Load Versus Settlement of Clay Bed Stabilized with Stone and Reinforced Stone Columns, in: 3rd Asian Regional Conference on Geosynthetics, Seoul. pp. 322–329.

Massarsch, K. R., 2002. Effects of Vibratory Compaction, in: TransVib 2002–International Conference on Vibratory Pile Driving and Deep Soil Compaction. Louvain-La-Neuve. Keynote Lecture. pp. 33–42.

Massarsch, K. R., 1991. Deep Soil Compaction Using Vibratory Probes, in: American Society for Testing and Material, ASTM, Symposium on Design, Construction, and Testing of Deep Foundation Improvement: Stone Columns and Related Techniques, Philadelphia. Edited by RC Bachus. ASTM Special Technical Publication, STP. pp. 297–319.

Massarsch, K. R., 1985. Deep Compaction of Sand Using Vibratory Probes, in: Proceedings of the Third International Geotechnical Seminar, Soil Improvement Methods. pp. 9–17.

Massarsch, K. R., Broms, B. B., 2001. New Aspects of Deep Vibratory Compaction. Proceedings, Material Science for the 21st Century, JSMS 50th Anniversary Invited Papers, Vol. A, The Society of Material Science, Japan. pp. 172–179.

Massarsch, K. R., Fellenius, B. H., 2014. Use of CPT for Design, Monitoring, and Performance Verification of Compaction Projects, 3rd International Symposium on Cone Penetration Testing, Las Vegas, Nevada, USA. pp. 1187-1200.

Massarsch, K. R., Fellenius, B. H., 2002. Vibratory Compaction of Coarse-Grained Soils. Canadian Geotechnical Journal. 39, pp. 695–709.

Mayne, P. W., 2007. Cone Penetration Testing. Transportation Research Board.

McCabe, B. A., McNeill, J. A., Black, J. A., 2007. Ground Improvement Using the Vibro-Stone Column Technique, in: Joint Meeting of Engineers Ireland West Region and the Geotechnical Society of Ireland, NUI Galway. pp. 1–12.

McKelvey, D., Sivakumar, V., Bell, A., Graham, J., 2004. Modelling Vibrated Stone Columns in Soft Clay. Proceedings of the ICE-Geotechnical Engineering. 157, pp. 137–149.

McKenzie, J. A., 1981. Holocene Dolomitization of Calcium Carbonate Sediments from the Coastal Sabkhas of Abu Dhabi, UAE: A Stable Isotope Study. The Journal of Geology. 89, pp. 185–198.

Mitchell, J. K., Huber, T. R., 1985. Performance of a Stone Column Foundation. Journal of Geotechnical Engineering. 111, pp. 205–223.

Moseley, M. P., Kirsch, K., 2004. Ground Improvement. CRC Press.

Murugaiah, S., 2004. Numerical Simulation of the Performance of Sand Columns. M. Sc. Thesis, Washington State University. United States.

Murugesan, S., Rajagopal, K., 2006a. Geosynthetic-Encased Stone Columns: Numerical Evaluation. Geotextiles and Geomembranes. 24, pp. 349–358.

Navfac, D. M., 1982. Design Manual for Soil Mechanics, Foundations, and Earth Structures. US Dep. Navy Wash. DC.

Nayak, N. V., 1982. Recent Innovations on Ground Improvement by Stone Columns, in: Symposium on Recent Developments in Ground Improvement Techniques, Bangkok.

Paskkaran, K., 2004. Centrifuge model studies on set-up due to single sand compaction pile, M. S. Thesis, National University of Singapore.

Patterson, R. J., Kinsman, D. J. J., 1982. Formation of Diagenetic Dolomite in Coastal Sabkha along Arabian (Persian) Gulf. AAPG Bulletin. 66, pp. 28–43.

Patterson, R. J., Kinsman, D. J. J., 1981. Hydrologic Framework of a Sabkha along Arabian Gulf. AAPG Bulletin. 65, pp. 1457–1475.

Poorooshasb, H. B., Meyerhof, G. G., 1997. Analysis of Behavior of Stone Columns and Lime Columns. Computers and Geotechnics. 20, pp. 47–70.

Potts, D. M., Zdravkovic, L., Zdravković, L., 2001. Finite Element Analysis in Geotechnical Engineering: Application. Thomas Telford.

Priebe, H. J., 1995. The Design of Vibro Replacement. Ground engineering. 28, pp. 31-37.

Priebe, H. J., 1991. Vibro-replacement–design criteria and quality control. Deep Foundation Improvements: Design, Construction, and Testing, ASTM STP 1089, pp. 62–72.

Priebe, H. J., 1991. Vibro-Replacement–Design Criteria and Quality Control. Deep Foundation Improvements: Design, Construction, and Testing, ASTM STP. 1089, pp. 62-72.

Pulko, B., Majes, B., Logar, J., 2011. Geosynthetic-Encased Stone Columns: Analytical Calculation Model. Geotextiles and Geomembranes. 29, pp. 29–39.

Raju, V. R., 1997. The Behaviour of Very Soft Cohesive Soils Improved by Vibro Replacement. Ground Improvement Geosystems–densification and reinforcement, Thomas Telford, pp. 253–259.

Raju, V. R., Wegner, R., Krishna, Y. H., 2004. Ground Improvement Using Vibro Replacement in Asia 1994 to 2004, 5th International Conference on Ground Improvement Techniques. Kuala Lumpur, Malaysia.

Robertson, P. K., Campanella, R. G., 1983. Interpretation of Cone Penetration Tests. Part I: Sand. Canadian Geotechnical Journal. 20, pp. 718–733.

Robinson, D. M., 1995. Concrete Corrosion and Slab Heaving in a Sabkha Environment: Long Beach–Newport Beach, California. Environ. Eng. Geosci. 1, pp. 35–40.

Sanford, W. E., Wood, W. W., 2001. Hydrology of the Coastal Sabkhas of Abu Dhabi, United Arab Emirates. Hydrogeology Journal. 9, pp. 358–366.

Schaefer, V. R., White, D. J., 2004. Quality Control and Performance Criteria for Ground Modification Technologies. Geotechnical Engineering for Transportation Projects. ASCE. 2, pp. 1936-1942.

Schmertmann, J. H., 1978. Guidelines for Cone Penetration Test.(Performance and design). U.S. Department of Transportation.

Schweiger, H. F., Pande, G. N., 1986. Numerical Analysis of Stone Column Supported Foundations. Computers and Geotechnics. 2, pp. 347–372.

Siddiqi, Z. U., 2000. Effects of geotextiles on the load-carrying capacity of Pavements on Sabkha. King Fahd University of Petroleum and Minerals. Dhahran, Saudi Arabia.

Six, V., Mroueh, H., Shahrour, I., Bouassida, M., 2012. Numerical Analysis of Elastoplastic Behavior of Stone Column Foundation. Geotechnical and Geological Engineering. 30, pp. 813–825.

Terzaghi, K., Peck, R. B., 1968. Soil Mechanics in Engineering Practice: 2d Ed. J. Wiley.

Van Impe, W., 1983. Improvement of Settlement Behaviour of Soft Layers by Means of Stone Columns, in: Proceedings, 8th European Conference on Soil Mechanics and Foundation Engineering: Improvement of Ground. pp. 309–312.

Vesic, A. S., 1972. Expansion of cavities in infinite soil mass. J. Soil Mech. Found. Div 98.

Vesic, A. S., 1972. Expansion of cavities in infinite soil mass. Journal of Soil Mechanics & Foundations Div. 98.

Wang, G., 2009. Consolidation of Soft Clay Foundations Reinforced by stone Columns Under Time-Dependent Loadings. Journal of geotechnical and geoenvironmental engineering. 135, pp.1922–1931.

Wang, J. G., Leung, C. F., Ichikawa, Y., 2002. A Simplified Homogenisation Method for Composite Soils. Computers and Geotechnics. 29, pp. 477–500.

Weber, T. M., Springman, S. M., Gäb, M., Racansky, V., Schweiger, H. F., 2008. Numerical Modelling of Stone Columns in Soft Clay under an Embankment. Geotechnics of soft soils-focus on ground improvement. Taylor & Francis, London. pp. 305–311.

Wood, D. M., Hu, W., Nash, D. F. T., 2000. Group Effects in Stone Column Foundations: Model Tests. Geotechnique 50, pp. 689–698.

Yechieli, Y., Wood, W. W., 2002. Hydrogeologic processes in saline systems: playas, sabkhas, and saline lakes. E Earth-Science Reviews. 58, pp. 343–365.

Zahmatkesh, A., Choobbasti, A. J., 2010. Settlement Evaluation of Soft Clay Reinforced by Stone Columns, Considering the Effect of Soil Compaction. International Journal of Research & Reviews in Applied Sciences.3, pp. 158-166.

Vitae

Name : Hassan Ali Mohamad Abas

Nationality : Sudanese

Date of Birth :1/1/1977

Email : hassankfupm@gmail.com

Address : House NO.93, Hantoub, Wad Madni, Sudan

Educational Qualification:

- PhD (Geotechnical Engineering)

  King Fahd University of Petroleum and Minerals, Dhahran, Saudi Arabia, 2015.
- MSc (Construction Engineering)

  Sudan University of Science and Technology, Khartoum, Sudan, 2007.
- BSc Civil Engineering

  Sudan University of Science and Technology, Khartoum, Sudan, 2001.